# Optimization of 5G Second Phase Heterogeneous Radio Access Networks with Small Cells

**Bahram Khan**

Tese para obtenção do Grau de Doutor em

**Engenharia Eletrotécnica e de Computadores**

(3º ciclo de estudos)

Orientador: Prof. Doutor Fernando José da Silva Velez

**Julho de 2023**

**Provas públicas realizadas em 25 de julho de 2023**

**Composição do júri**

**Presidente**

**Doutor António João Marques Cardoso**
Professor Catedrático da Universidade da Beira Interior

**Vogais**

**Doutor Mário Marques Freire**
Professor Catedrático da Universidade da Beira Interior

**Doutora Ana Garcia Armada**
Professora Catedrática da Universidade Carlos III de Madrid, Espanha

**Doutor Luis Manuel de Jesus Sousa Correia**
Professor Catedrático do Instituto Superior Técnico da Universidade de Lisboa

**Doutor Fernando José da Silva Velez**
Professor Auxiliar da Universidade da Beira Interior

# Declaração de Integridade

Eu, Bahram Khan, que abaixo assino, estudante com o número de inscrição D2577 de Engenharia Eletrotécnica e de Computadores da Faculdade Engenharia, declaro ter desenvolvido o presente trabalho e elaborado o presente texto em total consonância com o **Código de Integridades da Universidade da Beira Interior**.

Mais concretamente afirmo não ter incorrido em qualquer das variedades de Fraude Académica, e que aqui declaro conhecer, que em particular atendi à exigida referenciação de frases, extratos, imagens e outras formas de trabalho intelectual, e assumindo assim na íntegra as responsabilidades da autoria.

Universidade da Beira Interior, Covilhã 26/07/2023

(assinatura conforme Cartão de Cidadão ou preferencialmente assinatura digital no documento original se naquele mesmo formato)

# Acknowledgements

The completion of this study could not have been possible without the expertise of Prof Dr. Fernando José da Silva Velez, my beloved dissertation supervisor. He has not only supported me from a research point of view but also provided all other supports. I value the insights and guidance he provided.

I am indebted to my parents (Moor Gwalono & Ghat Dada) and especially to my grandmother, Moor G, and my uncle Prof Dr. Mohammad Nisar (Shaal) for supporting me during the studies.

I would like to express my deepest gratitude to all the TeamUp5G supervisors for providing the trainings, conferences and all the learning opportunities from academia to industries.

I had the pleasure of working with Professor Wagen Jean Frederic (Haute école d'ingénierie et d'architecture de Fribourg, Switzerland ) and Dr. Slawomir Pietrzyk, Mr. Adam Flizikowski, Mr. Hatem OdetAlla (ISW Poland ) and Professor Dr. José Morgado.

I am also thankful to my lab mates Dr. Rui R. Paulo, Mr. Emanuel Teixeira and Mr. Rooderson M Andrade for their supports.

I acknowledge the excellent resource provided by Institute de Telecomunicações during my PhD, as they not only equipped me with a state-of-the-art laboratory but also fostered an enriching environment for my research.

This work funded by (TeamUp5G), it is the European training network, under the umbrella of Marie Skłodowska-Curie Innovative Training Networks (MSCA ITN) of European Commission's Horizon 2020 agenda.

TeamUp5G has received funding from the European Union's Horizon 2020 research and innovation program under the Marie Skłodowska-Curie ETN TeamUp5G, grant agreement No.813391. Discussions within the COST CA 20120 INTERACT are acknowledged.

Furthermore this work was partially supported by FCT/MCTES through national funds and when applicable co-funded EU funds under the project UIDB/50008/2020, ORCIP (22141-01/SAICT/2016).

# Abstract

Due to the exponential increase in high data-demanding applications and their services per coverage area, it is becoming challenging for the existing cellular network to handle the massive sum of users with their demands. It is conceded to network operators that the current wireless network may not be capable to shelter future traffic demands. To overcome the challenges the operators are taking interest in efficiently deploying the heterogeneous network. Currently, 5G is in the commercialization phase. Network evolution with addition of small cells will develop the existing wireless network with its enriched capabilities and innovative features. Presently, the 5G global standardization has introduced the 5G New Radio (NR) under the 3rd Generation Partnership Project (3GPP). It can support a wide range of frequency bands (<6 GHz to 100 GHz).

For different trends and verticals, 5G NR encounters, functional splitting and its cost evaluation are well-thought-out. The aspects of network slicing to the assessment of the business opportunities and allied standardization endeavours are illustrated. The study explores the carrier aggregation (Pico cellular) technique for 4G to bring high spectral efficiency with the support of small cell massification while benefiting from statistical multiplexing gain. One has been able to obtain values for the goodput considering CA in LTE-Sim (4G), of 40 Mbps for a cell radius of 500 m and of 29 Mbps for a cell radius of 50 m, which is 3 times higher than without CA scenario (2.6 GHz plus 3.5 GHz frequency bands).

Heterogeneous networks have been under investigation for many years. Heterogeneous network can improve users service quality and resource utilization compared to homogeneous networks. Quality of service can be enhanced by putting the small cells (Femtocells or Picocells) inside the Microcells or Macrocells coverage area. Deploying indoor Femtocells for 5G inside the Macro cellular network can reduce the network cost. Some service providers have started their solutions for indoor users but there are still many challenges to be addressed. The 5G air-simulator is updated to deploy indoor Femto-cell with proposed assumptions with uniform distribution. For all the possible combinations of apartments side length and transmitter power, the maximum number of supported numbers surpassed the number of users by more than two times compared to papers mentioned in the literature. Within outdoor environments, this study also proposed small cells optimization by putting the Pico cells within a Macro cell to obtain low latency and high data rate with the statistical multiplexing gain of the associated users.

Results are presented 5G NR functional split six and split seven, for three frequency bands (2.6 GHz, 3.5GHz and 5.62 GHz). Based on the analysis for shorter radius values, the best is to select the 2.6 GHz to achieve lower PLR and to support a higher number of users, with better goodput, and higher profit (for cell radius u to 400 m). In 4G, with CA, from the analysis of the economic trade-off with Picocell, the Enhanced multi-band scheduler EMBS provide higher revenue, compared to those without CA. It is clearly shown that the profit of CA is more than 4 times than in the without CA scenario. This means that the slight increase in the cost of CA gives back more than 4-time profit relatively to the ”without” CA scenario.

# Keywords

5G Second Phase, Hetnet, Carrier Aggregation, Standardization, 5G Wave Forms, eCPRI, Functional Splitting, Open RAN, Centralized RAN, Cost Revenue Trade-off.

# Resumo alargado

Devido ao aumento exponencial de aplicações/serviços de elevado débito por unidade de área, torna-se bastante exigente, para a rede celular existente, lidar com a enormes quantidades de utilizadores e seus requisitos. É reconhecido que as redes móveis e sem fios atuais podem não conseguir suportar a procura de tráfego junto dos operadores. Para responder a estes desafios, os operadores estão-se a interessar pelo desenvolvimento de redes heterogéneas eficientes. Atualmente, a 5G está na fase de comercialização. A evolução destas redes concretizar-se-á com a introdução de pequenas células com aptidões melhoradas e características inovadoras. No presente, os organismos de normalização da 5G globais introduziram os Novos Rádios (NR) 5G no contexto do 3rd Generation Partnership Project (3GPP). A 5G pode suportar uma gama alargada de bandas de frequência (<6 a 100 GHz).

Abordam-se as divisões funcionais e avaliam-se os seus custos para as diferentes tendências e verticais dos NR 5G. Ilustram-se desde os aspetos de particionamento funcional da rede à avaliação das oportunidades de negócio, aliadas aos esforços de normalização. Exploram-se as técnicas de agregação de espetro (do inglês, CA) para pico células, em 4G, a disponibilização de eficiência espetral, com o suporte da massificação de pequenas células, e o ganho de multiplexagem estatística associado. Obtiveram-se valores do débito binário útil, considerando CA no LTE-Sim (4G), de 40 e 29 Mb/s para células de raios 500 e 50 m, respetivamente, três vezes superiores em relação ao caso sem CA (bandas de 2.6 mais 3.5 GHz).

Nas redes heterogéneas, alvo de investigação há vários anos, a qualidade de serviço e a utilização de recursos podem ser melhoradas colocando pequenas células (femto- ou pico-células) dentro da área de cobertura de micro- ou macro-células). O desenvolvimento de pequenas células 5G dentro da rede com macro-células pode reduzir os custos da rede. Alguns prestadores de serviços iniciaram as suas soluções para ambientes de interior, mas ainda existem muitos desafios a ser ultrapassados. Atualizou-se o 5G $air - simulator$ para representar a implantação de femto-células de interior com os pressupostos propostos e distribuição espacial uniforme. Para todas as combinações possíveis do comprimento lado do apartamento, o número máximo de utilizadores suportado ultrapassou o número de utilizadores suportado (na literatura) em mais de duas vezes. Em ambientes de exterior, propuseram-se pico-células no interior de macro-células, de forma a obter atraso extremo-a-extremo reduzido e taxa de transmissão dados elevada, resultante do ganho de multiplexagem estatística associado.

Apresentam-se resultados para as divisões funcionais seis e sete dos NR 5G, para 2.6 GHz, 3.5GHz e 5.62 GHz. Para raios das células curtos, a melhor solução será selecionar a banda dos 2.6 GHz para alcançar PLR (do inglês, PLR) reduzido e suportar um maior número de utilizadores, com débito binário útil e lucro mais elevados (para raios das células até 400 m). Em 4G, com CA, da análise do equilíbrio custos-proveitos com pico-células, o escalonamento multi-banda EMBS (do inglês, Enhanced Multi-band Scheduler) disponibiliza proveitos superiores em comparação com o caso sem CA. Mostra-se claramente que lucro com CA é mais de quatro vezes superior do que no cenário sem CA, o que significa que um aumento ligeiro no custo com CA resulta num aumento de 4-vezes no lucro relativamente ao cenário sem CA.

# Palavras-chave

Segunda Fase da 5G, Rede Heterogénea, Agregação de Espetro, Normalizaação, Formas de Onda 5G, eCPRI, Divisões Funcionais, Open RAN, RAN Centralizada, Equilíbrio Custo-proveito.

# Contents

# List of Figures

# List of Tables

# Acronyms

| | |
|---|---|
| 1G | First Generation |
| 2G | Second Generation |
| 3G | Third Generation |
| 3GPP | Generation Partnership Project |
| 4G | Fourth Generation |
| 5G | Fifth Generation |
| 5G NR-U | Unlicensed 5G NR |
| 6G | Six Generation |
| ACLR | Low Adjacent Channel Leakage Ratio |
| AI | Artificial Intelligence |
| AM | Amplitude Modulation |
| AMBR | Aggregated Maximum Bit Rate |
| AMF | Access and Mobility Management Function |
| AP | Access Points |
| AR | Augmented Reality |
| ARQ | Automatic Repeat Request |
| B5G | Beyond 5G |
| BB | Base Band |
| BBF | Broadband Forum |
| BBU | Base Band Unit |
| CB | Channel Bonding |
| BH | Backhaul |
| BMBS | Basic Multi-Band Scheduler |
| BPSK | Binary Phase-Shift Keying |
| BS | Base Station |
| BW | Bandwidth |
| CA | Carrier Aggregation |
| CAPEX | Capital Expenditure |
| CC | Component Carrier |
| CCS | Cross-Carrier Scheduling |
| CDMA | Code-Division Multiple Access |
| CFP | Contention Free Period |

| | |
|---|---|
| CIF | Carrier Indicator Field |
| CIRN | Collaborative Intelligent Radio Network |
| CoMP | Coordinated Multi-point |
| COTS | Commercial-Off-The-Shelf |
| C-Plane | Control Plane |
| CP | Cyclic Prefix |
| CPRI | Common Public Radio Interface |
| C-RAN | Centralized Radio Access Network |
| CRAN | Cloud RAN |
| C-RNTI | Radio Network Temporary Identifier |
| CSP | Communications Service Provider |
| CST | Communication Service Template |
| CU | Centralized Unit |
| CV | Compensation Value |
| CWF | Carrier Weight Factor |
| D2D | Device-to-Device |
| DC | Dual Connectivity |
| DCI | Downlink Control Information |
| DFS | Dynamic Frequency Selection |
| DL | Downlink |
| DQS | Disjoint Queue Scheduler |
| D-RAN | Distributed RAN |
| DU | Distributed unit |
| DWDM | Dense Wavelength Division Multiplexing |
| eCPRI | Enhanced Common Public Radio Interface |
| EESM | Exponential Effective SNIR Mapping |
| E2E | End to End |
| eLAA | Extended LAA |
| eMBB | enhanced Mobile Broadband |
| EMBS | Enhance Multi-Band Scheduler |
| eNode | Evolved Node B |
| EPS | Evolved Packet System |
| eRE | eCPRI Radio Equipment |
| eREC | eCPRI Radio Equipment Control |

| | |
|---|---|
| ETSI | European Telecommunications Standards Institute |
| E-UTRA | Evolved Universal Mobile telecommunications |
| FBMC | Filter Bank Multicarrier |
| FCAIS | Fault Configuration Accounting Performance and Security |
| FCC | Federal Communications Commission |
| FDD | Frequency Division Duplex |
| FDM | Frequency Division Multiplexing |
| FFT | Fast Fourier Transform |
| FG | Focus Group |
| FH | Fronthaul |
| FHI | Fronthaul Interface |
| f-OFDM | Filtered-OFDM |
| FPGA | Field Programmable Gate Arrays |
| F-RAN | Fog RAN |
| GBR | Guaranteed Bit Rate |
| GFDM | Generalized Frequency Division Multiplexing |
| GMBS | General Multi-Band Scheduler |
| gNB | Next Generation Node B |
| GPP | General Purpose Processing |
| GSMA | Global System for Mobile Communications Association |
| GST | Generic Network Slice Template |
| GTP-U | General Packet Radio Service Tunnelling Protocol |
| HARQ | Hybrid Automatic Repeat Request |
| HD | High-Definition |
| HetNet | Heterogeneous Network |
| HRAN | Heterogeneous Cloud RAN |
| HSPA | High-Speed Packet Access |
| ICI | Inter Carrier Interference |
| IETF | Internet Engineering Task Force |
| IEEE-SA | Institute of Electrical and Electronics Engineers Standards Association |
| IFFT | Fast Fourier Transform |
| IGP | Integer Programming |
| IMT | International Mobile Telecommunication |
| IMT Advanced | International Mobile Telecommunications-Advanced |

| | |
|---|---|
| IoE | Internet-of-Everything |
| IoT | Internet of things |
| IP | Internet Protocol |
| IQ | In-phase and Quadrature |
| ISGs | Industry Standardization Groups |
| ISI | Inter Symbol Interference |
| ISW | IS-Wireless |
| ITU-T | International Telecommunication Union - Telecommunication |
| JQS | Joint Queue Scheduler |
| KPIs | Key Performance Indicators |
| LAA | Licensed Authorized Access |
| LFSR | Linear Phase Shift Registers |
| LPA | Linear Power Amplifier |
| LSA | Licensed Shared Access |
| LTE | Long Term Evolution |
| LTE-A | Long Term Evolution-Advanced |
| MAC | Media Access Control |
| MEC | Mobile Edge Computing |
| METIS | Mobile and wireless communication Enablers Information Society |
| MH | Midhaul |
| MIMO | Multiple-Input Multiple-Output |
| ML | Machine Learning |
| M-LWDF | Modified Largest Weighted Delay First |
| mMTC | massive Machine Type Communication |
| mmW | Millimetre Wave |
| MNO | Mobile Network Operator |
| MOOC | Massive open online course |
| MTC | Machine-Type Communications |
| NETCONF | Network Configuration |
| NF | Network Functions |
| nFAPI | network Functional Application Platform Interface |
| NFV | Network Functions Virtualization |
| NG-RAN | Next Generation RAN |
| NGMN | Next Generation Mobile Networks |

| | |
|---|---|
| NOMA | Non-orthogonal multiple access |
| NR | New Radio |
| NRT | Near-Real-Time |
| nRT | non-Real-Time |
| NS | Network Slicing |
| NSST | Network Slice Subnet Template |
| NST | Network Slice Template |
| N-SDO | National SDO |
| NTN | Non-Terrestrial Networks |
| O-CU-CP | OpenRAN Central Unit Control Plane |
| O-CU-UP | OpenRAN Central Unit User Plane |
| O-RAN | OpenRAN Alliance |
| O-RU | Open Radio Unit |
| OAI | Open Air Interface |
| OFDM | Orthogonal Frequency Division Multiplexing |
| ONAP | Open Network Automation Platform |
| ONF | Networking Foundation |
| OoBE | Out of Band Emission |
| OpenRAN | Open Radio Access Network |
| OPEX | Operational Expenditure |
| OQAM | Offset Quadrature Amplitude Modulation |
| PAPR | Peak to Average Power Ratio |
| PCA | Packet Scheduling Algorithms |
| PCC | Primary Component Carrier |
| PCell | Primary Cell |
| PDCCH | Physical Downlink Control Channel |
| PDCP | Packet Data Convergence Protocol |
| PDSCH | Physical Downlink Shared Channel |
| PDUs | Protocol Data Units |
| PF | Proportional Fair |
| PFCP | Packet Forward Control Protocol |
| PHY | Physical |
| PLFS | Physical Layer Frequency Signals |
| PLR | Packet Loss Ratio |

| | |
|---|---|
| PNF | Physical Network Function |
| PO | Professional Organization |
| PoP | Point-of-Presence |
| PPN | Poly Phase Network |
| PRB | Physical Resource Block |
| PRACH | Physical Random Access Channel |
| PTP | Precision time Protocol |
| PUCCH | Physical Uplink Control Channel |
| PUSCH | Physical Uplink Shared Channel |
| QAM | Quadrature Amplitude Modulation |
| QCI | Class Identifier |
| QoS | Quality of service |
| QPSK | Quadrature Phase Shift Keying |
| RAM | Random-Access Memory |
| RAN | Radio Access Network |
| RAT | Radio Access Technology |
| RB | Resource Block |
| RE | Resource Element |
| RF | Radio Frequency |
| RH | Remote Head |
| RIC | RAN Intelligent Controller |
| RIS | Reconfigurable Intelligent Surfaces |
| RLC | Radio Link Control |
| RoE | Radio over Ethernet |
| RRC | Radio Resource Control |
| RRH | Remote Radio Head |
| RRM | Radio Resource Management |
| RRU | Remote Radio Unit |
| RSRP | Reference Signal Received Power |
| RSRQ | Reference Signal Received Quality |
| RTT | Round Trip Time |
| RU | Radio Unit |
| SC | Secondary Cell |
| SC-FDMA | Single-Carrier Frequency Division Multiple Access |

| | |
|---|---|
| SCC | Secondary Component Carrier |
| SCell | Secondary Cell |
| SD | Service Descriptor |
| SDD | Supplementary Division Downlink |
| SDAP | Service Data Adaption Protocol |
| SDN | Software- Defined Networking |
| SDO | Standard Development Organizations |
| SDR | Software-Defined Radio |
| SDU | Service Data Unit |
| SG | Scheduling Grant |
| SINR | Signal to Interference & Noise Ratio |
| SLA | Service Level Agreements |
| SMF | Session Management Function |
| SNR | Signal-to-noise ratio |
| SON | Self-Organizing Networks |
| SPS | Semi-Persistent-Scheduling |
| SR | Sample Rate |
| srsLTE | Software Radio Systems LTE |
| SSH | [Secure SHell] |
| SyncE | [Synchronous Ethernet] |
| TCP-IP | [Transmission Control Protocol/Internet Protocol] |
| TDD | Time Division Duplex |
| TDM | Time Division Multiplexing |
| THz | TeraHertz |
| TPC | Transmit Power Control |
| TTI | Transmission Time Interval |
| TTM | Time-to-Market |
| UAV | Unmanned Aerial Vehicle |
| UDN | Ultra Dense Network |
| UE | User Equipment |
| UL | Uplink |
| uMTC | Ultra-Reliable Machine Type Communication |
| UFMC | Filtered Multi-Carrier |
| UP | User Plane |

| | |
|---|---|
| UPF | User Plane Function |
| URLLC | Ultra-Reliable and Low Latency Communications |
| V2X | Vehicle-to-Everything |
| vBBU | Virtual BBU |
| vC-RAN | Virtualized-C-RAN |
| VI | Video |
| VI+BE | Video plus Best-Effort |
| VM | Virtual Machine |
| VR | Virtual reality |
| vRAN | Virtualized Radio Access Network |
| Wi-Fi | Wireless Fidelity |
| WSN | Wireless Sensor Network |
| xMBB | extreme Mobile Broadband |
| WDM | Wavelength Division Multiplexing |

# List of Symbols

| | |
|---|---|
| $\alpha$ | Codes orthogonality factor |
| $\delta_i$ | Delay probability |
| $B$ | Number of sub-bands |
| $C_fi$ | Fixed terms of the costs |
| $C_b$ | Cost per BS |
| $c$ | RF velocity |
| $C_{RRH}$ | Cost of the RRH |
| $C_{Bh}$ | Cost of the Backhaul |
| $C_{BBU+FH}$ | Cost of the BBU plus fronthaul |
| $C_{inst}$ | Installation cost of the BS |
| $C_{M\&O}$ | Maintenance and operation cost |
| $D_{\mathrm{HOL},i}$ | Head-of-line |
| $d'_{BP}$ | Break point distance |
| $dB$ | decibel is written dB |
| $d$ | Distance between the user and base station |
| $F$ | Noise figure |
| $f_c$ | Center frequency |
| $f$ | Scaling factor |
| $G_{Rx}$ | Receiver gain |
| $G_{Tx}$ | Transmitter gains |
| $h_{BS}$ | eNb height |
| $h_{UE}$ | Height of the user |
| $H_b$ | Average budling height |
| $H_M$ | Macro-cell height |
| $I$ | Interference computed |
| $i^{\mathrm{th}}$ | Number of flow |
| $k$ | Subcarrier index |
| $k^{\mathrm{th}}$ | Number of frame |
| $(k, l)p,$ | Resource element |
| $l$ | Side length |
| $L_b^{MAX}$ | Maximum threshold for preselected frequency band |
| $M_{symb}^{layer}$ | Per layer the number of modulations |

$N_{hex/\mathrm{km}^2}$ Hexagonal areas

$N_{\mathrm{year}}$ Project's lifetime

$N_0$ Noise spectral density

$N_{SC}^{RB}$ Subcarriers per resource block

${N_{symb}}^{subframe,\mu}$ OFDM symbols

$N_f$ FFT size

$n_T$ Total number of interfering neighbors Femto-cells

$OH^{(j)}$ Overhead

$P_{ownFemto}$ Own Femto-cell recived power

$P_{nhFemto}$ Neighboring Femto-cells interference

$P_{noise}$ Thermal noise power

$P_{RX,i,j}$ Recived power

$P_Tx$ Transmitter power

$p$ Antenna port

$PL$ Path loss

$Q_m^{(j)}$ Number bits per symbol

$R_{UE}$ Rate of user equipment

$\bar{R}_i$ Average transmission rate

$R(CQI_{\mathrm{b,u}})$ Throughput

$RCQI_{b,u}$ Maximum throughput that the network offer

$r_{i,j}$ Instantaneous available rate

$R_i(k)$ Throughput achieved in each flow

$R_i(k-1)$ Throughput for the previous TTI

$R_{max}$ Maximum code rate

$R_v/cell$ Revenues per cell

$R_{(b-sup)}$ Throughput per BS

$S_{rate}$ Throughput of the requested service

$\tau_i$ Threshold

$T_c$ Sampling time

$T_s$ Sampling time

$T_{bh}$ Duration of busy hours

$u$ Subcarrier spacing

$v$ Supporting layer

$W_{\mathrm{b,u}}$ Normalized metric

$X_{\mathrm{b,u}}$ Allocated UE in band $u$

# Chapter 1

# Introduction

## 1.1 Motivation and Approach

The Mobile and wireless communication Enablers Information Society (METIS) 5th Generation (5G) system concept is highly flexible and configurable in order to adapt to the large deviation in 5G requirements (e.g., data rate, latency, number of devices connectivity) that exist in diverse scenarios. The METIS 5G concept has three scenarios service trends: extreme mobile broadband (xMBB), massive Machine Type Communication (mMTC), and ultra-reliable Machine Type Communication (uMTC), as shown in Figure 1.1. The first one (xMBB) provides services like increased data rates but also improved Quality of Experience (QoE) through reliable provisioning of moderate rates. As the number of users increases, the performance gracefully degrades data rate and latency, whereas mMTC provides connectivity for a very large number of devices. The third one (uMTC) is a time-critical service category that addresses applications such as vehicle-to-vehicle communications and industrial control. The main objective of this services is high reliability when the total number of devices and required data rates are fairly low compared to mMTC [1].

In the above-defined services, there are several 5G design and optimization challenges that need to be well-thought-out, as network would become complex, costly and inefficient by designing a distinct radio system for the above-mentioned service categories to meet heterogeneous network requirements. On the one hand, it is difficult to design a composite radio frame structure that fulfils the requirements for the entire types of services. For example, mMTC may require large symbol duration to support massive delay tolerant devices. On the other hand, xMBB required reliability and latency, so symbol duration must be shorter. Hence, there is a trade-off between subcarrier spacing and symbol duration to accomplish the requirements [2].

A new 5G waveform candidate must have the following characteristics to realize the demands of future mobile networks: low Out of Band Emission (OoBE), Relaxed Synchronization and Flexibility. Low OoBE not only reduces the guard band to a smaller value to acquire spectrum efficient transmission [3], but also offers a basis for supporting many types of services, with a special frame structure existing in the base band, with almost negligible interference [4].

In a second scenario, a huge total number of users are estimated to be supported in 5G mMTC, particularly for Internet of Things (IoT), which makes synchronization tough. Therefore, a new waveform must support asynchronous communications which lead to simplified transceiver processing [5]. Wireless communication systems do not have infinite radio resources and demand effective management [6]. Hence, wireless communications network design should be flexible, for example, on the basis of the variation of the Signal-to-noise Ra-

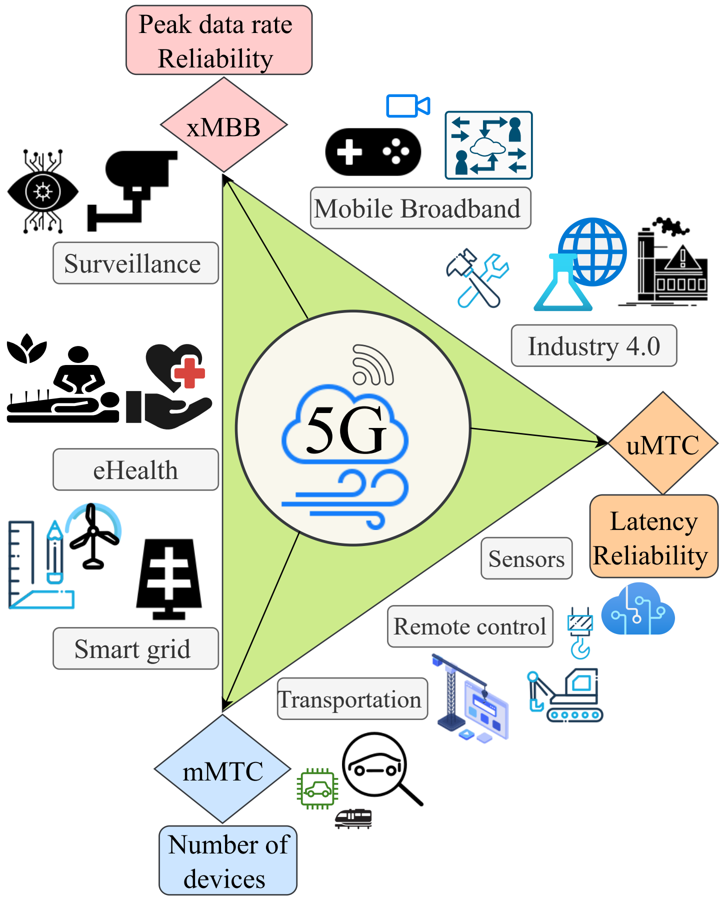


Figure 1.1: In the perspectives of METIS the three generic 5G services emphasize different 5G requirements, adapted from [1].

tio (SNR) and application data requirements, users require a flexible architecture to support their needs. One of the possible solutions is to design the modulation parameters (e.g., symbol period and subcarrier bandwidth) independently, which is simply possible over flexible architectures. Several techniques (Frequency Division Multiple Access, FDMA, Code Division Multiple Access, CDMA, or Time Division Multiple Access, TDMA) have been proposed in the above mentioned architectures to facilitate independent design of modulation parameters, with their own pros and cons [7].

To fulfil the requirements of the 5G vision of "everything everywhere and always connected", a new waveform must contain the features to support a large number of users, on high data rate. Although Orthogonal Frequency Division Multiple Access (OFDMA) has been widely used in the 4th generation (4G), 5G vision may encompass improvement, and many waveforms have been more recently proposed to cope with new challenges.

Mobile user traffic and its more sophisticated broadband services are solidly rising, and pushing the limit of the existing standards of mobile, to offer better integration among high speed wireless technologies. With the support of Heterogeneous Networks (HetNets), 5G and beyond are foreseen to provide a wide convergence for the high-speed user, with mobile networking. This trend is prominently termed as the "Mobile Internet" through HetNets. The sophisticated services, with high mobile device capabilities, escalate the power requirements. To overcome power issues, "Green communications" will play an important role in 5G evolution, with the adoption of cost-effective strategies. In this context, small cells get the attention as an enabler of high-speed wireless internet with low power requirements.

The vital Femto-cells signify the indoor version of the small cell solutions, while Pico-cells provide coverage for outdoor environment, it is possible to break the exiting mould of Femto applications and outspread the Femto-cell availability to outdoor communications. The massification of small cells, by deploying Macro-cells overlaid with several small cells, Pico, relays or Femto-cells is also known as HetNets [8]. Heterogeneity increases the network capacity and coverage, eliminates coverage holes and provides coverage in indoor and outdoor areas. However, different techniques such as massive Multiple-Input Multiple-Output (MIMO), coordinated multipoint, Carrier Aggregation (CA), interference management/cancellation techniques and authorized shared access can meet at the very best 1000-fold increase in data traffic.

In our everyday life, zones that are widely known to have a hotspot, for example, music concerts, popular spots, crowded stadiums, shopping malls, and public parks attract huge crowds whose traffic demand is massive. Because of the enormous traffic volumes of the traffic and a lot of connection requests, it may not be easy to place or receive a simple phone call, as well as text.

To resolve this issue, terrestrial small cells can be deployed in these areas by using CA for high data rate demand inside the Macro-cell. Small cells with CA will burst the traffic demands by achieving non-contiguous statistical multiplexing gain through the simultaneous use of inter-band resources, i.e., extra bandwidth. Base stations (BSs) will offload high amounts of traffic to small cells with CA, either in static spectrum assignment, or shared licensed and unlicensed spectrum scenarios.

Moreover, small cell networks come with various advantages, such as small size with CA, energy saving, affordability in price, portability because of the small size, as well as deployment flexibility, thus showing advantages of the small cell network technology. To ensure efficient provision of services, an operator might increase the capacity of the system by deploying more base stations. Small cell deployment comes with various benefits, such as the increase of the capacity or the enhancement of the coverage service, increasing the ability of the system, as well as the integration of multiple radio access technologies to provide wireless services.

Deploying Macro-cells overlaid with small cells implies a variety of benefits improvements, as mitigation of traffic congestion, and quality of the signal both in indoor and outdoor environments. Whereas the deployment of Macro-cells requires a lot of physical space together for the setup, and involves consuming a lot of energy to serve a wide area, the small cell deployment (with CA), utilizes small physical space, enables high data rate, efficient use of spectrum and is energy-saving, mainly when remote site operation is enabled. Hence, the deployment of small cells with CA within the Macro-cell is a promising and economical solution to improve the performance of the entire system.

The evolution of the mobile and wireless networks sector enabled by emerging 5G New radio (NR) technologies, and massively connected devices, supports a significant increase in data traffic demand. As a result, new business models and services are available, e.g., supported by ultra-low latency and ultra-high throughput networks. The need for diverse applications and seamless connectivity implies supporting on-demand services and involves critical requirements.

With the roll-out of 5G wireless networks, Network Slicing (NS) evolved as a fundamental feature to facilitate segmented layers of networks, in addition to the base network architecture [9]. In reality, NS provides a paradigm shift from the conventional approach towards novel traffic and network management strategies [10]. It allows virtual logical network layers to enable all the functionalities of a shared physical network. Furthermore, it sub-divides the network into several isolated virtual networks leading to a dedicated channel to provide resources to serve the user demands.

Thus, NS empowers conventional networks to support a wide range of use cases and business models. Additionally, while enabling enhanced service quality, NS supports tailor-made user-specific solutions. For instance, the latency requirement for emergency services is more stringent than for agriculture-based applications (to maintain the crops health). Hence, it will make current networks dynamic, flexible and scalable whilst accommodating growing demand, from various applications, with diverse requirements.

Unlike conventional networks, 5G networks are enabled with NS, and its evolution opens up the support of many services and use cases. New physical networks are not required anymore to facilitate dedicated services. As proposed by the 3rd Generation Partnership Project (3GPP), the introduction of NS is established in the framework of Release 15 [11] and is regularly updated for the required technical details and enhancements. 3GPP has specified that, for Communications Service Providers (CSPs), NS is significant for creating new services and generating new business models. NS allows CSPs to create multiple virtual slices to encompass colossal traffic increase and specific user requirements. As a consequence of this evolution, Working Groups from various Standard Development Organizations (SDOs) entered into force to support a multi-vendor landscape that develops NS specifications and guidelines.

CSPs further benefit from NS by implementing network orchestration, the automated communication among various entities on and across the network, to meet network and user requirements. It sets structured guidelines to establish connections through the network while offering services with the associated ambitious Service Level Agreements (SLAs).

## 1.2 Objectives

The Radio Access Network (RAN) architecture evolves with different generations of mobile communication technologies, and forms an indispensable component of the mobile network architecture. The main component of the RAN infrastructure is the BS, which includes a Radio Frequency unit and a Baseband Unit (BBU). The RAN is a collection of base stations connected to the core network to provide coverage through one or more radio access technologies. The advancement towards cloud-native networks has led to centralizing the baseband processing of radio signals. There is a trade-off between the advantages of RAN centralization (energy efficiency, power cost reduction, and the cost of the fronthaul), and the complexity of carrying traffic between the data processing unit and distributed antennas as consequence. 5G Advanced networks hold high potential for the centralized architecture to reduce maintenance costs while reducing deployment costs and improving resilience, reliability and coordination.

This research has been developed within the framework of the New RAN Techniques for 5G Ultra-dense Mobile networks - TeamUp5G, MSCA ITN/ETN, who's Early Stage Research seven (ESR 7) goals from the analysis of Centralized RAN (C-RAN), its functional splits and networks slicing to spectrum management, a vision toward standardization of 5G advanced and beyond, optimization of small networks with Femto-cells and Pico-cells by considering different packet scheduling strategies, and the consideration of multi band scheduling to support inter-band CA.

The detailed set of research objectives is as follows:

- **Incorporating the concept of virtualization, and C-RAN architecture** that enables to meet the overall requirements for both the customer and Mobile Network Operator. Functional splitting is one of the key enablers for 5G networks. It supports C-RAN, virtualized Radio Access Network, and the recent Open Radio Access Networks. This thesis provides an extended survey on this area whilst presenting an overview of the functional splitting, its requirements and possible solutions for implementation, underlying algorithms, and required tools. A vision on beyond 5G second phase is described. This part of the research provides a comprehensive tutorial on the paradigms of the RAN architecture evolution, its key features, and implementations challenges. It provides a thorough review of the 3GPP functional splitting complemented by associated challenges and potential solutions.

- **Providing an overview of the advances in NS** from the perspective of the business opportunities and associated standardization activities. Standardization is critical in research as it intends to maintain interoperability among multi-vendor hardware in telecommunication companies. The technical facets of slicing within the business implementation and industry standardization process are highlighted. Additionally, addressing the application of Artificial Intelligence (AI) and Machine Learning (ML) to NS enabled future networks deployments, a set of use cases and the underlying specific requirements challenges are discussed as well.
- **Addressing the requirement and vision of Beyond (B5G)**, as The 6G inherit the concept of 5G technologies and partially its standards, which are opening several innovative opportunities. The concepts of the mandatory standards to reach a fully practical and inter operable 6G era are added. Various use cases and KPIs, highlighting and enabling technologies for B5G are explored. To address the concerning challenges in the perspective of the spectrum management, underlying solution, and suggestions are studied.
- **Application of multi band scheduling and performance evaluation of HetNets with small cells applying inter band CA** - With the growing demand for a new blend of applications, the usage of the Internet is increasing daily. Mobile Internet users are giving more attention to their experience, especially regarding communication reliability, high data rate and service stability, on the move. This increase in the demand is causing saturation of existing radio frequency bands. To address these challenges, CA is one of the recent innovations which seems to fulfil the demands of the future spectrum. CA was one of the essential features for Long Term Evolution - Advanced. To get the upcoming International Mobile Telecommunication Advanced mobile requirements, i.e., 1 Gb/s peak data rate, CA is presented by 3GPP to achieve considerable statistical multiplexing gain, while sustaining a high throughput by using widespread frequency bandwidth, up to 100 MHz. To address the technical issues containing the aggregation structure, its implementation, deployment scenarios, control signal technique and challenges for CA technique in LTE-Advanced, considering backward compatibility. Performance evaluation in Pico cellular scenarios with low-complexity multi-band schedulers through a simulation approach will determine service quality and system capacity enhancement.
- **Modelling and optimization of Femto-cells in heterogeneous network for 5G and Beyond** - Femto-cells cover smaller indoor coverage areas, and are served by inexpensive, low-power base stations in residential and business enterprise environments. Shorter coverage lengths could cause a higher Signal-to-Interference-plus-Noise Ratio (SINR), while enhancing the goodput and service quality. The optimization of Femtocell deployments involves a perpetual periodical redimensioning in the

upcoming years while addressing the impact of the 5G New Radio SINR trade-off, not only in theoretical terms but also via a simulation approach. An updated version of the 5G-air simulator is being considered, where the frame level scheduler and maximum-largest weighted delay first scheduler will be tested in the indoor scenario

- **Briefly reviewing new waveform candidates**, e.g., Filter Bank Multicarrier (FBMC), Generalized Frequency Division Multiplexing (GFDM), Universal Filtered Multi-Carrier Modulation (UFMC), and Filtered-Orthogonal Frequency Division Multiplexing (F-OFDM), based on complexity and hardware design, to investigate 5G NR indoor Femto-cell deployment scenarios, within HetNets, while examining its supported number of users and achievable goodput to satisfy customers requirements.
- **Examining the cost revenue trade-off results** while comparing the architecture without implementing splitting with either the consideration of split six or seven (7.2) by determining the system capacity (obtained through simulation, for given target values of the PLR and average delay). The explored approach consists of addressing the discussed splits 6 and 7 (7.2) of 3GPP, in an implementation with sub-6 GHz wave-bands. The simulations (with the 5G-air simulator) consider NR operating bands (2.6 GHz, 3.5 GHz, and 5.62 GHz), reuse pattern three ($k$=3) and assumes scenarios that support either Video (VI) or Video plus Best-Effort (VI+BE), with the Proportional Fair (PF) packet scheduler,as an example. The split 6 is ideal for small cell deployment in region with low density of laying fiber optics, while split seven, mainly splits sub split 7.2, requires high fiber capacity, which increases the price of the fronthaul.
- **MOOC about Ultra-dense networks for 5G and its evolution** - The research spans from aspects of communication technologies to use cases, prototyping and the future ahead, not forgetting issues like interference management, energy efficiency or spectrum management. The aim of the MOOC is to fill the gap in graduation and post-graduation learning on content related to emerging 5G technologies and its applications, including the future 6G. Addressing the existing gap is beneficial for Early-stage Researchers and established researchers within TeamUp5G. So, it is worthwhile to share the high-level vision over the 5G mobile network with University students and younger researchers, while exploring the beyond enabling technologies, and underlying technical aspects.

  It was identified the need for a creative method for knowledge sharing over the future mobile networks to get the effective result in taking the young researchers into a proper understanding of 5G and beyond networks. Resulting form this effort, the team contributed to the production of the TeamUp5G Massive open online course (MOOC) package on ”Ultra-dense Networks for 5G and its Evolution”. It thoroughly covers the high-level vision and dig into the technical perspective over the topic.

  Indeed, after looking more closely at the scope of the necessary roadmap, one needs to understand the target technologies and their evolution, impacting the telecom roadmap, identified the gaps that could be covered through our MOOC series. This would support the young students and practitioners on getting deep knowledge on 5G Advanced.

So, the produced visionary MOOC series material targets knowledge transferring in a crystal-clear technical language within the defined boundaries of high-level 5G and beyond roadmap vision. After well developing an understanding of the vision for the audience, shared the technical perspective of each key technology player in a smooth manner.

It would enable the audience to get the readiness for understanding the latest state of under-develop roadmap and therefore enhance their mind creativity readiness for contributions in their future career.

## 1.3 Contributions

The out come of the research towards completing the writing of this thesis give the following contribution toward the journal papers publishing.

### 1.3.1 Papers in Journal Papers

- [12] Bahram Khan, Nidhi, Hatem Odetalla, Adam Flizikowski, Albena Mihovska, Jean-Frederic Wagen and Fernando J. Velez, "Survey on 5G Second Phase RAN Architectures and Functional Splits," submitted for possible publication to IEEE Surveys and Tutorials, July 2023.
- [13] Nidhi, Khan, B., Mihovska, A., Prasad, R. and Velez, F.J. Trends in Standardization Towards 6G. Journal of ICT Standardization, pp.327-348. Dec. 2021.
- [14] Paulo, R.R., Velez, F.J. and Khan, Bahram. Study of Indoor Small Cell Deployments. Journal of Mobile Multimedia, pp.329-344, Feb, 2021.
- [15] Khan, B. and Velez, F.J. Deployment of Beyond 4G Wireless Communication Networks with Carrier Aggregation. World Academy of Science, Engineering and Technology International Journal of Electronics and Communication Engineering Vol:15, No:2, 2021, Online. World Academy of Science, Engineering and Technology, 2020, July.

### 1.3.2 Envisaged Journals

- Rui R. Paulo, Bahram Khan, Emanuel B. Teixeira and Fernando J. Velez, "5G Service Quality and Fairness in the Line of Site Urban Micro UMi_A Cellular Scenario," submitted for possible publication to IEEE Transactions on Wireless Communication, July 2023.
- Bahram Khan, Rui R. Paulo, and Fernando J. Velez, "Modelling and Optimization of Femtocells in 5G and Beyond Heterogeneous Networks," to be submitted for possible publication to IEEE Access, July 2023.
- Bahram Khan, Rui R. Paulo, Emanuel B. Teixeira and Fernando J. Velez, "Cost/Revenue Trade-off in Energy-efficient Heterogeneous Open RAN with Small Cells operating with Carrier Aggregation," (to be submitted for possible publication to IEEE Access,

July 2023.

### 1.3.3 Papers in Conferences

- [16] Bahram Khan,Nidhi, Albena Mihovska, Rui R. Paulo and Fernando J. Velez, "Cost Revenue Trade-off for the 5G NR Small Cell Network in the Sub-6 GHz Operating Band,“ accepted for the publication in WPMC 2022: Wireless Personal Multimedia Communications, Aarhus University, Herning, Denmark, October 2022.
- [17] Nidhi, Bahram Khan, Albena Mihovska, Ramjee Prasad, Vladimir K. Poulkov and Fernando J. Velez, "Dynamic Resource Block Allocation and Isolation in Network Slicing,“ in proceedings of 12th Symposium on COmmunications, Navigation, SENsing and SErvices (CONASENSE) 2022 CONASENSE 2022, Munich, Germany, June 2022.
- [18] Manuel J. Lopez Morales, D. Alejandro Urquiza Villalonga, Diego Gonzalez Morin, Nidhi, Bahram Khan, Farinaz Kooshki, Ahmed Al Sakkaf, Leonardo Leyva, Hamed Farkhari, Daniele Medda, Ilias Nektarios Seitanidis, Ayman Abu Sabah, Joseanne Viana, Pedro Cumino, Victor P. Gil Jimenez, Maria J. Fernandez Getino Garcia, Máximo Morales-Cespedes, Ana Garcia Armada and Fernando J. Velez, Innovation in the Development of the MOOC on "Ultra dense Networks for 5G and its Evolution," (in Portuguese) in proceedings of the CNaPPES.22, Coimbra, Portugal, July 2022.
- [8] Manuel J Lopez-Morales, D Alejandro Urquiza-Villalonga, Diego Gonzalez Morin, Nidhi, Bahram Khan, Farinaz Kooshki, Ahmed Al Sakkaf, Leonardo Leyva, Hamed Farkhari, Daniele Medda, Ilias-Nektarios Seitanidis, Ayman Abu Sabah, Joseanne Viana, Pedro Cumino, Victor P Gil Jimenez, Maria J Fernandez Getino Garcia, Máximo Morales Cespedes, Ana Garcia Armada and Fernando J Velez, "Massive Online Open Course (MOOC) on 'Ultra dense Networks for 5G and its Evolution'," in proceedings of the EAEEIE 2022 31st Annual Conference of the European Association for Education in Electrical and Information Engineering, Coimbra, Portugal, July 2022.
- [19] Nidhi, Bahram Khan, Albena Mihovska, Ramjee Prasad and Fernando J. Velez, "A Study on Cross-Carrier Scheduler for Carrier Aggregation in Beyond 5G Networks," in proceedings of 3rd URSI AT AP RASC, Gran Canaria, Spain, June 2022.
- [20] Bahram Khan, Nidhi, Albena Mihovska and Fernando J. Velez, "Overview of Network Slicing: Business and Standards Perspective for Beyond 5G Networks," in Proc. of 2021 IEEE Conference on Standards for Communications and Networking (CSCN) Track on Softwarization, Slicing, Automation and Network Management, the Thessaloniki Greece (Virtual Conference), Dec. 2021.
- [21] Bahram Khan and Fernando José Velez, "Multi-carrier Waveform Candidates for Beyond 5G," in Proc. of 2020 12th International Symposium on Communication Systems, Networks and Digital Signal Processing (CSNDSP), Porto (online), Portugal, Jul. 2020.

### 1.3.4 Book Chapter under Preparation

- Víctor P. Gil Jiménez, David Alejandro Urquiza Villalonga, Manuel José López Morales, Daniele Medda, Ilias-Nektarios Seitianitis, Ahmed Gaafar Al-Sakkaf, Bahram Khan, M. Julia Fernández-Getino García, Ana García Armada, Periklis Chatzimisios, Athanasios Iossifides, Máximo Morales Céspedes and Fernando J. Velez, "MOOC as a Way of Dissemination, Training and Learning of Telecommunication Engineering," Chapter in the book Sam Goundar Massive Open Online Courses - Current Practice and Future Trends, IntechOpen, Jan. 2023, doi: 10.5992/intechopen.1000574, ISBN 978-1-83769-523-2, https://www.intechopen.com/online-first/1122974.
- Bahram Khan,Nidhi,Daniele Medda,Fernando J. Velez, "Spectrum sharing and carrier aggregation, Chapter in the book Máximo Morales Cespedes and Fernando J. Velez, Ultra-dense networks for 5G communications and beyond, River Publishers, Gistrup, Denamark, 2023 (under review).

### 1.3.5 Conference, Seminars, and Workshops

The following presentations and talks were given in the conference, seminars and workshops.

- B. Khan, presentation on "Business and Standards Perspective for Beyond 5G Networks", Seminars, University of Aveiro, 01-06-2022.
- B. Khan, R. R. P. Paulo, E.S.B.Teixeira Teixeira, F. J. Velez, "System Capacity and Fairness of 5G Urban Pico-cells in the sub-6 GHz Frequency Bands", Seminars, 31st Seminar of the Mobile Communications Thematic Network (RTCM), 01-02-2022.
- B. Khan, Overview of Network Slicing: "Business and Standards Perspective for Beyond 5G Networks", Seminars, IEEE Conference on Standards for Communications and Networking, 30-11-2021.
- B. Khan, Li-Fi, poster presentation about "Spectrum Sharing and Carrier Aggregation in Heterogeneous Networks with Small Cells", Seminars, European Researchers' Night, Museu Nacional de Historia Natural e da Ciencia da Universidade de lisboa., 31-08-2021.
- B. Khan, 29th Seminar of "RTCM – Portuguese thematic Network on Mobile Communications", Seminars, Instituto de Telecommunication/UBI, 31-01-2021.
- B. Khan, "Getting involved in IEEE standardization introducing IEEE COM/NETSOFT standards committee", Tutorial, IEEE Communications Society CommSoft TC Webinar, 31-01-2021.
- B. Khan, Tutorials Day on "Simulation Tools for 5G New Radio", Tutorial, ointly organized by TeamUp5G MSCA ITN/ETN from Instituto de Telecommunication, RTCM, IEEE VTS Portugal Chapter and ConfTele, 31-01-2021.
- B. Khan, Teaching of two modules in Massive Online Open Course (MOOC) on topic "Ultradense Networks for 5G and its Evolution", Spain, Madrid, 06-2021.
- B. Khan, "1st Post-IRACON Meeting", Brussel Belgium University Catholique de Lou-

vain, Seminars, 1st Post-IRACON Meeting, 01-09-2020.

- B. Khan, "Reference Scenarios and Key Performance Indicators for 5G Ultra-dense Networks", Seminars, 12th International Symposium on Communication Systems, Networks and Digital Signal Processing (CSNDSP), 01-07-2020.
- B. Khan, TeamUp5G: "A Multidisciplinary Approach to Training and Research on New RAN Techniques for 5G Ultra Dense Mobile Networks," in Proc. of 2020 12th International Symposium on Communication Systems, Training Course, 12th International Symposium on Communication Systems, Networks and Digital Signal Processing (CSNDSP), 01-07-2020.
- B. Khan, Deployment of "Beyond 4G Wireless Communication Networks with Carrier Aggregation", Seminars, ICEEE 2020: 14. International Conference on Electronics and Electrical Engineering, Toronto, Canada, 30-06-2020.
- B. Khan, RTCM 28th SEMINAR of the "Mobile Communications Thematic Network" Universidade Nova de Lisboa, January 22nd, 2020, Seminars, Portugal Universidade Nova de Lisboa, 01-01- 2020.
- B. Khan, "IRACON 12th MC meeting and Final workshop". Brussel Belgium Universit Catholique de Louvain, Seminars, Brussel Belgium Universit Catholique de Louvain, 01-01-2020.
- B. Khan, Li-Fi, poster presentation about "5G waveform candidate", RTCM 28th SEMINAR of the Mobile Communications Thematic Network Universidade Nova de Lisboa, January 22nd, 2020, Seminars, Portugal Universidade Nova de Lisboa, 01-01- 2020.
- B. Khan, "Multicarrier Waveform Candidates for Beyond 5G", Seminars, 12th IEEE/IET International Symposium on Communication Systems, Networks and Digital Signal Processing- CSNDSP,Portugal, 31-12-2019.
- B. Khan, Poster presentation "Winter school UC3M", Spain, Training Course, Madrid Spain UC3M, 01-11-2019.

### 1.3.6 TeamUp5G Work Packages

The following contributions were given to the different work packages of the TeamUp5G MSCA ITN ETNs:

- **Work Package 1, D 1.3-** Final report on scenarios, user and system requirements and project vision.
- **Work Package 2, Deliverable 2.1-** Initial set of PHY/MAC protocols for small cells
- **Work Package 2, Deliverable 2.2-** New waveforms, interference cancellation and massive multiple input multiple output techniques for small cells.
- **Work Package Deliverable 3.1-** Conception of centralized/decentralized spectrum and resource sharing and spectrum availability detection techniques.
- **Work Package Deliverable 3.2-** Advanced algorithms for carrier aggregation in heterogeneous network: modelling and performance evaluation.

- **Work Package Deliverable 4.2**- Advanced energy efficient radio resource management for heterogeneous network with small cells.
- **Work Package Deliverable 5.1**- Specification and design of the TeamUp5G proof of concept.
- **Work Package Deliverable 5.2**- Proof of concept of TeamUp5G: simulations and measurements.
- **Work Package Deliverable 6.3**- Initial contributions to standardization activities/-groups.

### 1.3.7 Thesis Structure

This thesis is form by a set of seven Chapters and three appendices. The thesis begins with the introduction and motivation and heads to the contribution and objectives of the work.

The contributions sections contain the publications and envisages papers detail, the attended winter and summer schools, training, presented talks and the contribution to different work packages deliverable of TeamUp5G.

Chapter 2 of the thesis is the literature review of the thesis. The Chapter begins with a summary of NS and sheds light on enabling technologies for 5G. The centralized and decentralized concepts are elaborated. Beyond aspects of centralized base band units are highlighted. The spectrum requirement perspective for 5G and Sixth Generation (6G) are explained, and it's the spectrum management. Heterogeneous network and 5G use cases and different perspectives of 5G standards and their standardization are overviews. Standardization activities on NS and its opportunities for service providers, and challenges, are explained accordingly. Finlay, at the end of the Chapter, the 5G to 6G road map (standardization) is researched.

Chapter 3 is a comprehensive set of literature review elements on 5G Second Phase RAN Architectures and Functional Splits, which explain the evaluation of a 4G radio access network to 5G and beyond. The Chapter describes the current research status on functional splits. It explains each split in detail while summarizing the essential aspects, from theory to implementation, algorithms, and tool (simulator/ emulator) requirements. The later sections of the Chapter address ongoing research on fronthaul and explain the move from Common Public Radio Interface (CPRI) to Enhanced Common Public Radio Interface (eCPRI). The Chapter also presents a detailed overview of recent advancements in RAN architectures, including virtualized Radio Access Network (vRAN) and OpenRAN conceptual architectures. It also describes the main implementation challenges and opportunities.

Chapter 4 is about aspects of CA. It discusses the underlying challenges and road map of 3GPP releases with CA. An overview of different deployment scenarios is followed by description of the functionalities and terminology, including specificities of the protocol stack, radio resource management, configuration of different types of user equipment, primary versus secondary cell management, and the illustration of 4G User Equipment (UE)/Evolved Node B (eNB) implementation. Performance evaluation is explored with CA only between Picocells, considering bands 2.6 GHz and 3.5 GHz frequency bands. The simulations are run in the LTE-Sim Frame work.

Chapter 5 provides a very brief overview of the 5G New Radio (NR). The first part of the Chapter discusses the 5G NR features, their benefits, and deployment moods of 5G. The most important introduction to the spectrum is added. The mathematical modeling of the new radio grid, its variable sub-carrier spacing, and the frame structure are entirely explained. To understand and implement the 5G NR data rate calculation, the mathematical formulas are investigated as well. The later section of the Chapter gives the research and implementation of indoor Femto-cells in heterogeneous networks by updating the 5G-air-simulator. The results for goodput, packet loss ratio and updated path loss models are well thought out by considering the schedulers(FLS and M-LWDF).

Chapter 6 address cost revenue trade-off for the 5G NR small cell networks in the sub-6 GHz operating band. The Chapter considers the assumption on open RAN and functional splitting from Chapter 3 and while addressing the cost revenue trade-off for functional split options 6 and 7, it discusses the achieved results for given cost and prices for the traffic, followed by the cost/revenue and profit analysis. Chapter 7 is presents the conclusion and future work.

The appendices are added at the end. Appendix A evaluates different waveform candidates for 5G and beyond. It contains comprehensive introduction to various waveform candidates and underlying literature review. A comparison of the hardware complexity between candidate wave forms is addressed, following by a comprehensive comparison of the characteristics among the possible wave forms. The best candidate among them were analyzed at the end of appendix A . Appendix B explains the real time outdoor analysis of small cell operating at 3.5 GHz, explains our real-time implementation of the 5G NR signal transmission in an outdoor flat environment with asphalt near the data centre in Covilhã Portugal. The setup was used to experimentally verify the two slope UMi_A loss line of sight propagation model. Appendix C is the updated code for the indoor Femto-cell scenario in a heterogeneous network within a 5G-air-simulator, where we put our updated user distributions and required path loss model. Appendix C addresses how to get our results from the data and contains the code of it. Appendix D provides the code and information how to set the inputs.

# Chapter 2

# Literature Review on B5G Requirements, Network Slicing and Standardization Toward 6G

## 2.1 Summary

The deployment of fifth-generation wireless communication networks brought a significant difference in the data rate and throughput to the wireless systems. It ensures ultra-low latency and high reliability. In particular, NS, one of the enablers for the 5G phase-II and beyond, has opened enormous opportunities for the CSPs. NS allows CSPs to create independent virtual networks in the same physical network to guarantee high service levels.

Since the beginning, mobile communication has been a significant part of digital society. Academia combined with industry work to enhance future wireless technologies. The 6G use case and KPIs have elevated the bar. 6G is developing to support the desired infrastructure for several services and devices. 6G will inherit the 5G technologies and their required, acceptable standards, creating more opportunities for innovations. This Chapter adds the requirements for B5G, its vision and the standardization that reaches the 6G era. Its KPIs are highlighted together with enabling technologies for B5G [13]. In detail, the initiatives, activities of standardization and related challenges concerning spectrum utilization are discussed.

One provides literature of the advances in NS from the perspective of the business opportunities and associated standardization activities [20]. Standardization is critical in research as it intends to maintain interoperability among multi-vendor scenarios in telcos, emphasize highlighting the technical facets of slicing within the business implementation and industry standardization process. Additionally, one addresses the application of AI and ML to NS-enabled future networks deployments. Underlying specific requirements challenges are discussed as well. Finally, future research directions are addressed in detail road map for 6G is presented at the end.

With the growing demand for a new blend of applications, users' dependency on the internet is increasing day by day. Mobile internet users are giving more attention to their own experiences, especially in terms of communication reliability, high data rate, and service stability on the move. This increase in demand is causing saturation of existing radio frequency bands. As an answer to challenges, researchers are investigating the best approaches. CA is one of the newest innovations, which fulfill the future spectrum's demands; CA is also one of the essential features for 5G and beyond. For this purpose, to get the upcoming International Mobile Telecommunications-Advanced (IMT-Advanced) mobile requirements (1 Gb/s peak data rate), CA is proposed by 3GPP, which would sustain a high data rate using widespread frequency bandwidth up to 100 MHz. Technical discussion such as aggregation structure, its implementations, and control signal techniques, with consideration of backward compatibility, are highlighted [15].

The deployment of 5G wireless communications networks brought a significant difference in the data rate and throughput to the wireless systems. It ensures ultra-low latency and high reliability. In particular, NS, one of the enablers for the 5G phase-II and beyond, has opened enormous opportunities, as it allows CSPs to create independent virtual networks in the same physical network while guaranteeing high service quality levels.

## 2.2 Introduction

Since 1981, telecommunication technology has evolved from first generation (1G) mobile technology to 5G and beyond. This communication technologies evolution as generally shows that a new generation of mobile communication subsists every decade while offering users new services. Predictably, 6G will develop around 2030 [22]. These generations proposed enhancements in costs, data speed, reliability, power consumption efficacy, available network functions, latency, system performance communicating the sim card and roaming, diverse services and coverage. With these enhancements, disruptive technologies are seen with a different generation. For example, in the case of 2nd Generation (2G) addition of narrow band, inclusion of wide band in 3rd Generation (3G), the involvement of ultra-broadband in 4G, presently the world wide web in 5G and terrestrial wide band expected in 6G. Also, the needed modifications in bandwidth and data transmission are realized.

1G technology started with the analog assembly that twisted to 25 MHz of bandwidth utilization for both 2G and 3G, and the bandwidth went up to 5 times that is 100 MHz in 4G networks [23]. As we can see from the 5G requirements, its use cases are set in the 30-300 GHz spectrum bands for communication. Predictably, it seems that 6G would require higher bandwidth, higher than 300 GHz, further up to some THz levels [24]. The speedy growing data-centric intelligent systems, with futuristic scenarios, networks, and applications have imposed challenges to the currently 5G networks deployments [25]. The crucial differentiating characteristic of 5G is low latency, particularly guaranteed end-to-end latency, combined with reliability and exactness that future use cases need. However, 5G is currently minimal by deployment in some typical scenarios, like access in remote areas villages or motorways, which are not satisfactorily covered. Terrestrial 5G NR will not support some applications that contain actual driver less vehicles and only 5G phones and 5G advanced will allow for full functionality. Satellite communication networks are needed, which can improve the coverage as compared to terrestrial networks. Unmanned Aerial Vehicle (UAV) communication networks are essential for quick response in strict and challenging environments. High-quality communication services can be provided to ships by maritime communication networks. Applications such as virtual reality, the mix of Virtual Reality (VR), high quality three-dimensional as well as VR and augmented reality will require Tbps, due to this, and sub-Terahertz, Terahertz and optical frequency bands can be candidate bands. Although 5G New Radio is a tremendous evolution step, it will not fulfill all the future network requirements (2030) [26]. The networks of the next generation are likely to assist in several deployment scenarios for different applications, such as coverage from space-air to ground-sea, communications coverage, high-mobility, vehicle to everything, robotic machine, integrating communication, sensing, computing, and high touch virtual reality. 6G is expected to provide nearly 100% geographical coverage, millisecond Geo-location update rate, and sub-centimeter Geo-location accuracy to fulfill use cases' requirements and support an enormous amount of data generated because of heterogeneous networks, wide bandwidths, large number of antennas, and diverse communication scenarios [25, 26]. 6G networks are expected to completely shift the existing communication networks to new extreme network capabilities, which cater to the demands of the future data-driven society.

The majority of KPIs of the 5G are valid for the 6G. It is expected that 6G, will require per link peak throughput to reach Tbps. Some use cases like factory automation will be needed, ultra-high reliability and ultra-low latency and as well as high accurate synchronicity, almost around 1 μs in 6G, it is expected that in 1 billion bit there will be just one erroneous bit, which reaches the industrial control at the top. Security and privacy are also essential KPIs of 6G, and associated with hyper security high-end user and industrial control. A wider radio bandwidth will be required under the sub-THz and THz bands. Therefore, it is essential to determine how the research community is investigating and focusing on the 6G wireless communication networks. The use of the spectrum involves many challenges, but at the same time, it is an opportunity for future networks. These high-frequency bands will provide a significant role in the overall network. Cost and battery limitations will be challenging in many exiting Internet of Things (IoT) scenarios. However, in 6G, will provide contextual battery support from the network. On path loss, $CO_2$ molecular absorption has a significant impact, particularly at a lengthier distance. Penetration through different materials and reflection from the surface are factors to study while classifying the radio spectrum. Although these KPIs must be investigated in more detail, a basic set of the KPIs are comprehensively presented in Figure 2.1 [13].

Whether they are open or not, standards are the key to smoothen the journey towards 6G networks in time. It helps to have a unified approach throughout the pre-development and development phases. In addition, it helps to join forces against obstacles en route and accelerate innovation. Many standardization bodies are currently working in similar directions, in similar or different areas. There are huge overlaps and intersections; thus, it is essential to facilitate the idea of cross-research. Furthermore, these standard bodies work to identify the right time to initiate actions concerning work on pre-standards or full-standards.

In the remaining of thesis Chapter is structured as Section 2.3, enabling technologies for 6G and beyond are discussed. In Section 2.4 centralized and decentralized concept are elaborated. In Section 2.5 centralized baseband units for 5G are highlighted. The foreseen spectrum requirements for 5G and 6G are explained in Section 2.6, and its spectrum management is addressed in Section 2.7. Heterogeneous network and 5G use cases are well described in Section 2.8 network and 2.9. According to different foreseen of 5G standards, and future perspectives on standardization are in Section 2.10. There, its standardization activities on network slicing are mentioned in 2.11. Section 2.12 and 2.13 shed the light on opportunities

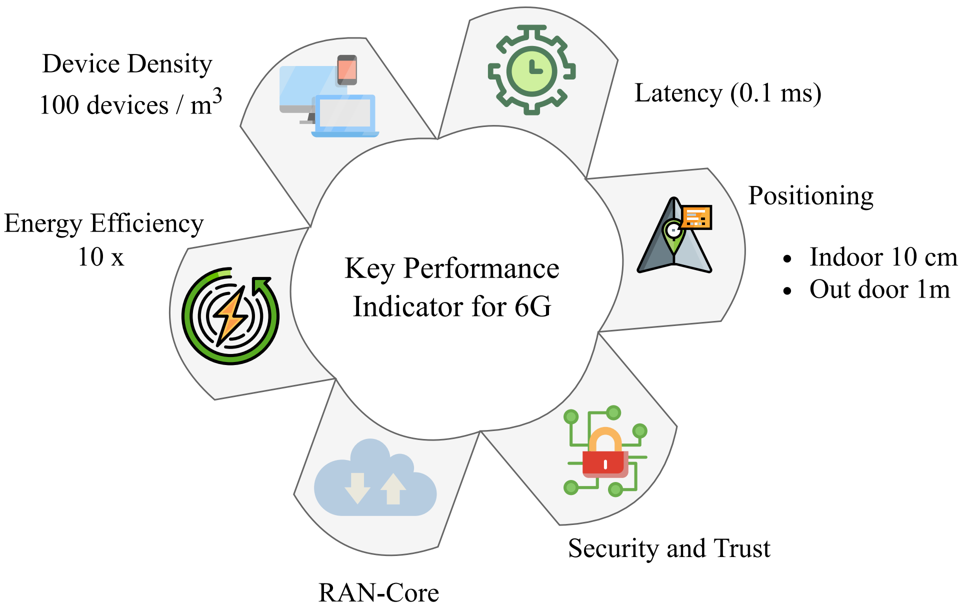


Figure 2.1: A set of key performance indicators for 6G.

and challenges for service providers. The road map (standardization) from 5G to 6G and conclusion are added at the end of the Chapter.

## 2.3 Enabling Technologies

To enable 5G Advanced and 6G use cases, and its required services, the enhanced technology of the previous generation (1G to 5G) must be added. The enabling technologies that can support the 6G services contain satellite communication, above 6 GHz, Terahertz communications, AI, cell-free, CA, multi-band scheduling and other technologies. Some of the enabling technologies are discussed below:

- Carrier Aggregation CA is one of the enablers technologies. It can improve the reuse of the spectrum with proper converge. Further, it can provide high data rate and fairness among the user, system capacity and better user experiences. As today's users require a high data rate and service quality, CA will allow the user to fulfil its requirements. The CA was added in Release 10 of 3GPP, LTE advance, where it is possible to aggregate five carriers, which can utilize the 100 MHz bandwidth (20 MHz each). In Release 13 [27] of 3GPP, the maximum number of aggregated carriers advanced from 5 to 32.

  In Release 16, the number of rate-matching patterns available in new radio has been increased to allow spectrum sharing when CA is used for LTE. Besides, Release 16 reduces latency for setup and activation of CA/Dual Connectivity (DC), leading to improved system capacity and the aptitude to achieve higher data rates. Unlike Release 15, where measurement configuration and reporting do not take place until the UE comes into the fully connected state, in Release 16, the connection can be resumed after periods of inactivity without the need for extensive signalling for configuration and reporting [28]. Additionally, Release 16 introduces a periodic triggering of channel state information reference signal transmissions in case of the aggregation of carriers with different numerology. In the Release 17 eMBB trend, the NR frequency range will be extended to allow for exploiting more spectrum (above 52.6 GHz), including the 60 GHz unlicensed band, while defining new Orthogonal OFDM numerology and channel access mechanism to comply with regulatory requirements applicable to unlicensed spectrum. This enhanced framework will also be useful for Licensed Authorized Access (LAA) operation in unlicensed spectrum where large blocks of spectrum are available [29].

- Communication with large intelligent surfaces, MIMO will be strong candidate for 6G, to enable energy efficiency and better spectral. With the innovative environments and intelligent surfaces it will backing massive wireless communications surfaces [26, 30].
- Wireless power transfer, due to the high data rate demanding applications, the users use more power, and wireless devices may need wireless power transfer to proven by their batteries. Until now, wireless power transfer has been under development. In 6G, it is expected that the user will be served wirelessly (wireless energy transfer) by the base stations. Using RF, power harvesting techniques can get energy from nearby energy providers. Getting wireless energy from neighbouring energy providers can be environment-friendly [31].
- Terahertz frequency band, the THz band is from 0.1 THz to 10 THz. It will work an important role in 6G, and will be able, with the support of the THz band, to use more bandwidth with enhanced capacity. Beside, it will provide high energy efficiency, terabit-per-second link capacities, and secure transmission [32].
- Cell-free communication, cell-free massive is the evolution of the classical cellular communication architecture. The cell-free control of the irregular scattered access points through the central processing unit. It requires more than one central processing unit when the coverage area is larger. With the addition of UAV, it is very important to provide full converge with no dead zones. 6G is expecting that it will provide full dense network with multiple options. For avoiding dead zones cell free communication will be use associated with satellite communications. The user will connect to the entire network to avoid the coverage and handover problems.
- AI and ML, to automate industries and other businesses, AI and ML will be used in 6G. From the perspective of the communication network, it will control resource allocations, network selection, positioning and handovers. Also, it will predict (future events based on the past and present values) on the several parameters for future activities.
- Integrated terrestrial, drones, and satellite communication, in 6G, the terrestrial and satellite communication will be used in coordination to avoid coverage issues. Further, the drones will be used as base stations and reuse the bandwidth opportunistically to support more users in sudden dense traffic. This coordination will enhance the user's service with expected high throughput.

## 2.4 Centralized and Decentralized concept

The main difference between the centralized and decentralized communications is shown in Figure 2.2 is control of the overall network. A centralized network or system contains a singular main administrator, which control all the facets of the throughout system or network. The administrator is actually employed through a central server that runs all data and authorizations. While decentralized is different, it works in a distributed manner. Every point (base station, node) in the network is a distinct authority with self-governing administrative, and is able in about how to cooperates with other systems independently.

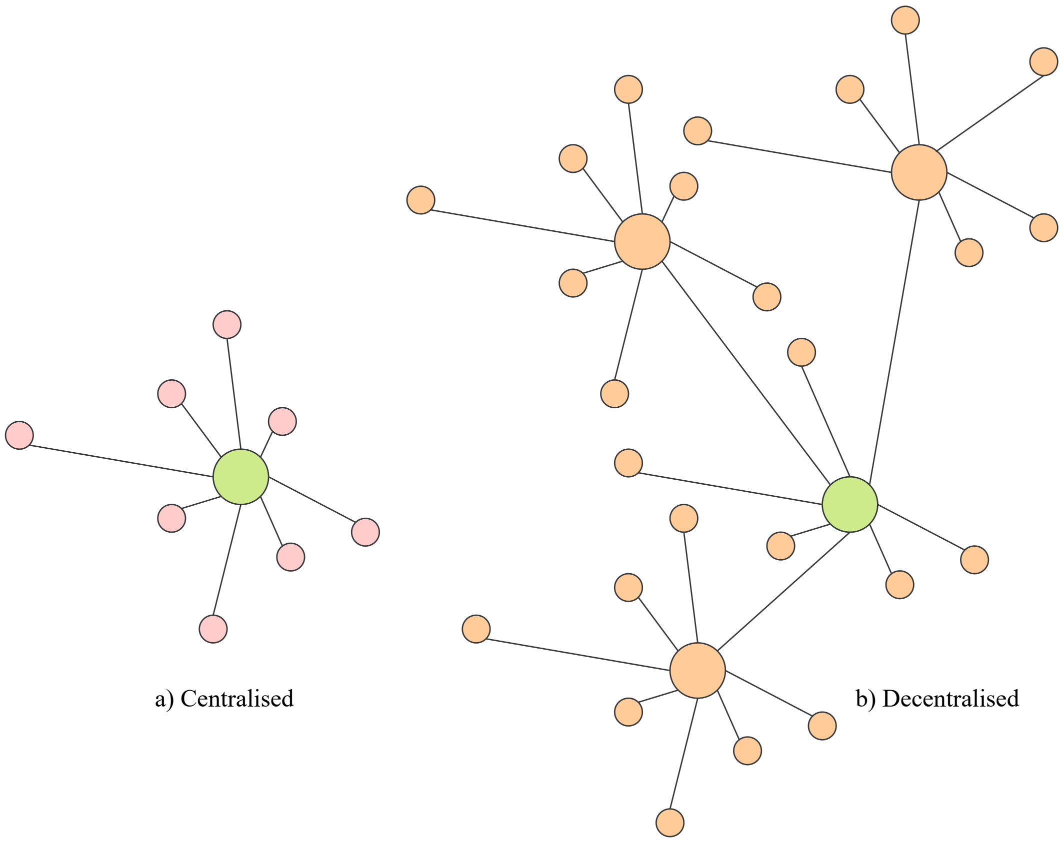


Figure 2.2: Centralized and decentralized concept.

## 2.5 Centralized Baseband Units in 5G and beyond

It is expected that the demand for wireless services will increase by at least 1000 times over the next decades, stimulated by new applications and a push towards the Internet of Things [33]. To provide intermittent or always-on hyper-connectivity for Machine-Type Communications (MTC), covering diverse services, such as connected vehicles, connected homes, moving robots, smart parking, and industrial monitoring, with sensors that must be supported in an efficient and scalable manner. More applications rely on data collected by Wireless Sensor Networks (WSNs) that is sent over the telecom infrastructure. Besides, traffic offloading to fixed networks through Wireless Fidelity (Wi-Fi) in unlicensed frequency bands has become widespread. To enhance the network capability and optimize its usage, the operators are deploying more localized capacity, in the form of small cells (e.g., Pico and Femto-cells and remote radio units connected to centralized baseband units by optical fiber) [34]. Virtualization of wireless nodes based on Software-Defined Radio (SDR) principles, to allow them to support multiple heterogeneous transmission technologies, together with techniques for optimal resource sharing according to application requirements.

## 2.6 6G Spectrum Requirements

To boost 6G research accomplishments, in 2019, the Federal Communications Commission (FCC) suggested a new between 95 GHz and 3 THz to be considered for research, termed as "far frontier of spectrum policy". 6G is in the direction of witnessing high bandwidths, and adapting to preform in ultra-high frequencies. Hence, some challenges arise, especially in the propagation modelling. The technologies over viewed in the following will be of fundamental importance in 6G.

### 2.6.1 Spectrum Associated with 5G

The three trends proposed by International Telecommunication Union (ITU) (in IMT 2020) are Ultra-Reliable and Low Latency Communications (URLLC), enhanced Mobile Broadband (eMBB), and massive Machine Type Communications (mMTC). The eMBB scenario is for applications requiring more bandwidth, such as remote surgery, high-quality telepresence, and telemedicine. It includes Multi RAT, CA and MIMO Technologies. The MTC required high-volume, fast-growing applications include, for example, asset tracking, smart metering and smart cities. These applications need almost have low complexity, low cost and low power.

URLLC supports applications that provide services that are mission critical, for example, healthcare, autonomous vehicles, and industrial automation. Its requirements are low latency, ultra-reliability, and strong security. The 5G spectrum allocation is centred on application services, as shown in Table 2.1. The spectrum availability and its scarce resources are challenging. It needs to reuse the present spectrum bands in 6G to obtain and fulfil bandwidth demands. In the upcoming years, the standardization activities of exploiting unlicensed and licensed bands will be crucial for service providers.

### 2.6.2 Beyond THz Spectrum

Investigation of new spectral bands is required considering terrestrial and (Non-Terrestrial Networks) (NTN). The aim can be to advance channel models and propagation conditions and inter-node communications. Under the umbrella of terrestrial applications, the 6G ecosystem, will use the 100 GHz spectrum and above, while, for NTN, beyond 50 GHz frequency bands are excepted, and even THz frequency bands will be used. NTN is assembled with free-space optical communication (that consider higher frequency bands), for example, from 150 to 300 THz. The evolutionary architecture of NTN systems will support efficient, low-cost network configuration with flexible typologies. It will be a reusable infrastructure among

Table 2.1: 5G spectrum allocation

| Frequency Bands | Range | Application |
|---|---|---|
| Low bands | 2 GHz | eMBB, URLLC mMTC applications |
| Mid bands | 2-8 GHz | |
| High bands | 24 GHz | eMBB and URLLC applications |

the NTN and terrestrial networks. In a 6G network, the UAVs will perform as flying nodes, capable of processing, and supporting communication and computing functionalities.

### 2.6.3 Associated Challenges

The devices operating in the heterogeneous and homogeneous network are vastly diverse. The homogeneous network not only operates in licensed bands but also works in unlicensed bands. The key challenges and the underlying aspects of their design are discussed below:

- The need for efficient spectrum design and its sharing algorithms while studying complex network scenarios;
- The positioning of User Equipment (UEs), and its handovers in the ultra-dense network with spectrum sharing;
- 5G and 6G reliable varying size of data transmission, with required advanced spectrum sharing techniques to maintain the time-varying data needs;
- Designing the algorithms that can coordinate and work collaboratively between different multiple Access Points (APs) and Base Stations (BSs) within heterogeneous networks.

## 2.7 Spectrum Management

Spectrum management strategies facilitate the efficient use of the spectrum. In the history of communications, several arrangements have been considered to utilize the spectrum in an efficient way [35]. This management contains effective management of spectrum allocation, allocation scheme, licensing mechanism, and administrative approaches. Although, the research on 6G and its spectrum is still not matured, predictably, 6G will be deployed in the Terahertz (THz) frequency bands range assigned to mobile communication systems [36]. The spectrum bands (2G, 3G, 4G and 5G) that different countries currently use, will also be considered in 6G, where applicable. Such 6G frequency bands include the lower, mid, and higher ones.

As it is challenging to manage the 6G spectrum, one possible solution is to use AI services to tackle it. The set of operations that AI can handle will be dynamic operation, combined sensing, i.e., the radio environment sense the medium and will adopt it in actual situations [37]. With fundamentals properties, the available 5G and 6G frequency bands are given in Table 2.2.

Table 2.2: Characteristics of the spectrum bands for 5G and 6G.

| Frequency Band | 0.3-3 GHz | 3-30 GHz | 30-300 GHz | 0.3-3 THz | 3-30 THz |
|---|---|---|---|---|---|
| Wavelength | Wavelength | Wavelength | Wavelength | Wavelength | Wavelength |
| Dominant Propagation Mechanism | LoS, Reflection, Direction, Scattering, Penetration | LoS, Reflection, Direction, Scattering, Penetration | LoS, Reflection | LoS, Reflection | LoS, Reflection |
| Dominant Attenuation Effects | Free Space Loss | Free Space Loss -Transmission Loss Through Materials High at Upper Band | Free Space Loss/ Molecular Absorption -$O_2$ @60 GHz -$H_2O$ > 24 GHz | Free Space Loss/ Molecular Absorption -High $H_2O$ Peaks | Free Space Loss/ Molecular Absorption -High $H_2O$ Peaks |
| Supported Link Distance | 10 km | 1000 m | 100 m | <10 m | <1 m |
| Tx Power Limiting Factor | Regulation | Regulation | Technology | Technology | Technology |
| Approximate System Bandwidth | Up to 100 MHz | 400 (or 800) MHz | Up to 30 GHz | Up to 300 GHz | > 100 GHz |

### 2.7.1 Carrier Aggregation with Millimetre Wavebands

For 5G and beyond, Millimetre Wave (mmWaves) bands are considered the capable contender that can provide the opportunities to fulfil the spectrum shortage in a wireless network. It became the redeemer of 4G/5G mobile operators. It will suit its coexistence with the LTE network [38]. mmWave bands and CA scenarios are broadly investigated in [39,40]. The research of these papers address low computational complexity and channel state information to enhance CA while improving the energy efficiency in 5G environments. Sub-6 GHz and mmWave aggregation is needed for the network. Aggregation enables to achieve massive capacity with a multi-Gigabit rate for customers and enterprises. Combine allocation of spectrum resources would make it possible to achieve a wired broadband rate wirelessly.

### 2.7.2 5G Networks with Unlicensed Spectrum

Suggested deployment modes for 5G NR-U to enhance LAA with Release 16 contains (i) Standalone, (ii) CA, and (ii) Dual Connectivity (DC). In DC and CA modes, the 5G NR-U band amplifies user-plane capacity in DL. NR-U supports Uplink (UL) in DC mode compared to Down Link (DL). The CA deployment is based on LTE-LAA, while DC deployment is built on extended LAA (eLAA). In any case, these deployment Control Plane (C-Plane) data are associated with licensed bands. Standalone mode relies independently on unlicensed bands for user and C-Plane operations. It would allow the 5G to avoid depending on the licensed Mobile Network Operators (MNOs). NR-U is predicted, will offer more opportunities for better spectral efficiency with further enhancements. Table 2.3, shows the available globally and under-review unlicensed spectrum bands grounded by Release 16.

### 2.7.3 Licensed plus Unlicensed Bands within Small Cells

An assorted network operator deploys small cells with unlicensed bands. These small cell networks are considered to be the updated version of that LTE-Advance (LTE-A) technology, and is used within microcells, which happens to exit in Wi-Fi systems. LTE-A provides supporting the use of CA in both 2.4 and 2.5 GHz frequency bands, because they are flexible and enhance the utilization of the available bandwidth. There are different variants and sizes for the component carriers, with bandwidths of 1.4, 3, 5, 10, 15, or 20 MHz.

The best proposal for the scheme is to consider that the licensed band is provided by the suitable carrier. Then, its Primary (user) Component Carrier (PCC) provides the opportunity to the licensed band aggregation, which can certainly provide the next level of the component carrier, due to the use these components carriers, or to be included as Secondary Component Carriers (SCC's) in the unlicensed bands. Moreover, there are unlicensed bands which are cast off as "on demand", a connotation associated with the trivial cells that have vigorous consumers, and are able to communicate in the unlicensed band (and do not communicate at all at additional spectrum intervals). These configurations are conceivable as a compulsory "anchor" in the certified band. There are two important disposition techniques that helps gathering unlicensed band: the first one is Supplementary Downlink (SDL) mode while the other one is the Time-Division Duplex (TDD) mode, as follows:

- Supplementary Downlink - In the SDL method, i.e., Division Downlink or SDD mode, unlicensed bands will merely be combined with the related downlink, as data rates and sizes will be significantly amplified in the downlink.
- Time-Division Downlink or TDD mode - in the TDD mode, gathering of unlicensed band is required for both the downlink and uplink, similarly to the classic LTE-TDD structure. The operation just occurs according to the typical LTE-TDD accumulation of the carrier. The benefit here is the tractability to amend the amount of asset among the downlink and the uplink. Besides, when the 5G ban is exploited by the CA, to guard detectors by means of the 5 GHz band, it is a compulsory supervisory constraint to use Transmit Power Control (TPC). One may call it either TPC or Dynamic Frequency Selection (DFS).

### 2.7.4 Using Wi-Fi inLicensed plus Unlicensed Bands

Presently, Wireless Fidelity (Wi-Fi) is applied sub optimally aiming for wireless communication. There is challenges for deployment of licensed and unlicensed spectrum groups, CA transversely (using Wi-Fi) is consider one of the best technique by the network operator, to communicate combine with licensed and unlicensed spectrum. When CA is exploited crosswise an unlicensed band, a user's PCC is continuously in licensed band and befitting from unlicensed spectrum band.

Table 2.3: Unlicensed spectrum bands in 3GPP [41]

| Countries | 1-7 GHz Mid-Bands (sub 7GHz) | Status | 24+ GHz High-Bands (mmWave) | Status |
|---|---|---|---|---|
| United States | 5.2 – 5.8 GHz | Available Now | 57 – 71 GHz | Under Study/ Review |
| | 5.9 – 7.1 GHz | Available Now | | |
| Canada | 5.2 – 5.8 GHz | Available Now | 57 – 71 GHz | Under Study/ Review |
| EU except (Germany, France & Italy) | 5.2 – 5.9 GHz | Available Now | 57 – 71 GHz | Under Study/ Review |
| | 5.9 – 6.4 GHz | Under Study/ Review | | |
| United Kingdom | 5.2 – 5.9 GHz | Available Now | 57 – 71 GHz | Under Study/ Review |
| | 5.9 – 6.4 GHz | Available Now | | |
| Germany | 5.2 – 5.7 GHz | Available Now | 57 – 71 GHz | Under Study/ Review |
| France | 5.2 – 5.7 GHz | Available Now | 57 – 71 GHz | Under Study/ Review |
| Italy | 5.2 – 5.7 GHz | Available Now | 57 – 71 GHz | Under Study/ Review |
| China | 5.2 – 5.3 GHz | Available Now | 59 – 71 GHz | Under Study/ Review |
| | 5.7 – 5.8 GHz | Available Now | | |
| South Korea | 5.7 – 5.8 GHz | Available Now | 57 – 64 GHz | Under Study/ Review |
| | 5.9 – 7.1 GHz | Under Study/ Review | | |
| Japan | 5.7 – 5.8 GHz | Available Now | 57 – 64 GHz | Under Study/ Review |
| India | 5.2 – 5.5 GHz | Available Now | 57 – 66 GHz | Under Study/ Review |
| | 5.7 – 5.9 GHz | Available Now | | |
| Australia | 5.2 – 5.8 GHz | Available Now | 57 – 66 GHz | Under Study/ Review |

### 2.7.5 Cell Dormancy

Release 16 of 3GPP initiated the idea of small-cell dormancy, enhancing power utilisation in CA scenarios. If the cell is considered a dormant cell, its connected devices stop observing the physical downlink control channel, whereas considering beam management and measurements of channel state information [42]. Regarding the dormant cell, not completely deactivating it from the network, but reasonably, with less activities, it can save power. Deactivation is an alternative to save energy, but this approach doesn't support providing channel state information reports. Further, the activation of small cell it returns longer duration than dormancy [43].

### 2.7.6 Intelligent Spectrum Management

Spectrum sharing is a technique which allows the cooperative utilization or the simultaneous use of spectrum resources [44] with different self-determining entities in a specific geographical area. Spectrum sharing by Multi-tier, using Licensed Shared Access (LSA) [45] to support operative utilization of white spaces or the under-utilized portions of the spectrum. To obtain the climbing outcome of these techniques, it has been mentioned by Spectrum Collaboration Challenge (SC2) in [46]. Collaborative Intelligent Radio Networks (CIRNs) and Al-based autonomous wireless radio technologies. Which interchange obvious information to get the solution cooperatively with collaboration, and can reuse spectrum through coordination and guarantee protection [44].

### 2.7.7 Application Machine Learning and Artificial Intelligence

The exponentially growing demand for connectivity is raising concerns about massive operations and maintenance requirements. ML and AI applications at various levels of the network can provide scalable and flexible solutions to manage complex generations of communication. For instance, AI can identify patterns in enormous datasets and thus can significantly reduce the prediction and decision time for processing tasks. In addition, AI can administer MNOs in determining demand and reconfiguring the network. In CA-enabled networks application of ML algorithms can determine the Component Carriers (CCs) to select based on the available spectrums. Moreover, it guarantees fairness in selecting the carriers from both available licensed and unlicensed spectrums [47].

### 2.7.8 Scheduling Techniques

#### 2.7.8.1 Cross-Carrier and Self-Scheduling

In CA-empowered scenarios, UE operates with more than single CCs. It can be from a different or the same cell (small/Macro cell). Resources are scheduled based on Scheduling Assignments (SA) and Scheduling Grants (SG) corresponding to data. The decisions for each carrier are the scheduler's responsibility and assign the SA for individual transmits. So, the UE receives several Physical Downlink Control Channels (PDCCHs). When SA and SG transmit through the same cell as data, it is called self-scheduling, and if the SA and SG transmit over different cells is called Cross-Carrier Scheduling (CCS).

For CCS, the Downlink Control Information (DCI) accommodating the SG for a carrier is received on a different carrier. When a UE is in search mode, the Carrier Indicator Field (CIF) value affects the DL control channel and defines the carrier for SG. In the Primary Cell (PCell) configuration, CIF-Presence-r10 indicates the availability of CIF in PDCCH DCI. A CIF value of 0 indicates PCell, while another indicates the Secondary Cells (SCs). To support 32 CCs enhancements for CA with the latest 3GPP releases [28], the CIF length increased from 3 to 5 bits.

#### 2.7.8.2 Packet Scheduling Schemes

Packet Scheduling Algorithms or (PCA) time domain algorithms have a significant role in resource management [48]. It handles how and when to allow the transmission of specified resources. In Figure 2.3, the packet scheduling classifications are presented. In CA scenario efficient PCA has given requirements [49];

- Acceptable to provision of multi-CCs situation,
- High QoS,
- High system throughput,
- Optimized fairness,
- Lower complexity.

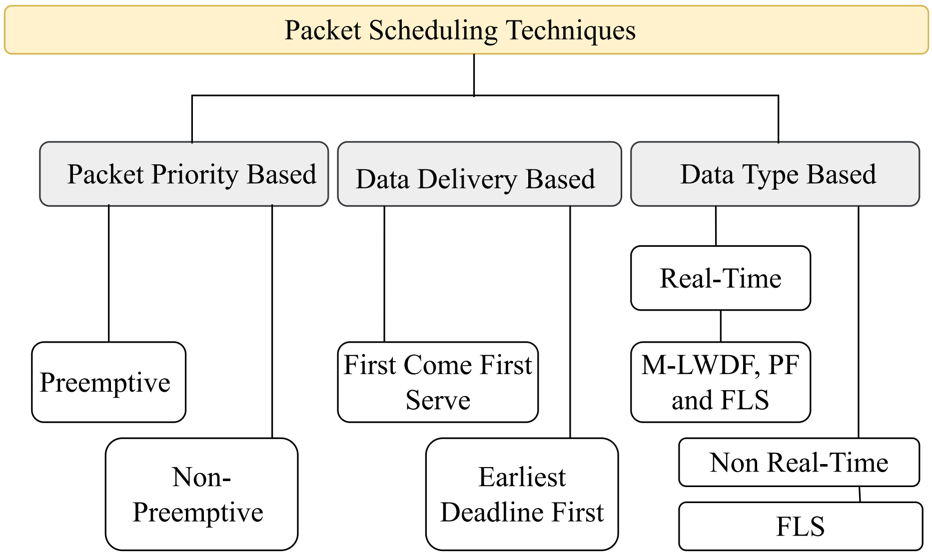

Figure 2.3: Classification taxonomy for packet scheduling schemes.

#### 2.7.8.3 Multi Band Scheduler Structure for CA

Multiband scheduling or the scheduling based on frequency domains contains the allocation of frequency domain resources to the scheduled time domain UEs or more specifically a subset of the time-domain defined group of authorised UE [48]. It aims to allocate frequency-domain resources for different UE, in a technique with which UE can utilize the subset of the frequency domain, to obtained furthermost favourable channel conditions [48]. The condition of the channel could be different for in frequency domain for each UE as function when frequency domain UEs are allocated.

For the allocation of RB in the CA environment, the Next Generation Node B (gNB) requests UE for the carrier specifications, including Quality of Service (QoS). gNB takes calls for carrier activators and PCell assignments for the UE and indicates through the PDCCH signals for fixed time slots. In case of time slots which are larger spotted delay. With the UE, the scheduler response time is challenging to manage the delay, and required throughput trade-offs in CA scenario [50]. Author from [48,50,51], defined schedulers with an optimized time slot to obtain the QoS for UE.

#### 2.7.8.4 Disjoint Queue Scheduler

In Disjoint Queue Scheduler (DQS), individual users have independent traffic queues on each CCs. Therefore, this scheduler operates in a two-step model to allocate the RBs. At the first level, the scheduler allocates the traffic packets on each CC and waits for their turn to transmit. Then, at the second level, schedulers present at each CC allocate the RBs and map the packets to the user. The schedulers at both levels can use the same or separate scheduling algorithms. However, this approach offers little efficiency and high complexity with large packets as the user packet, CC, and the associated RBs are mapped one-to-one.

#### 2.7.8.5 Joint Queue Scheduler

In Joint Queue Scheduler (JQS), the users have a shared/joint queue to access the CCs, resulting in a single-layer scheduling platform. The scheduler allocates the traffic packets to all the CCs with the RBs. Thus, the user packet uses all the available Resource Blocks (RB) on different CCs. This scheduling structure offers higher efficiency and a higher frequency selective gain than the DQS, as the mapping is one-to-many but not successful with high traffic densities. In addition, together with a priority-based scheduling scheme, JQS can mitigate long waiting queues.

## 2.8 Heterogeneous network

5G and beyond wireless networks require high data rate, to obtained high data rate network densification is considered one of the important mechanisms in the evolution of cellular networks. This densification results in higher spectral efficiency and reduces power consumption by replacing Macro cells with small cells. Network densification also improves the network capacity and coverage. The simultaneous distribution and operation of Macro-cell, micro cell, Pico-cell and Femto-cells in a network are termed HetNets [52] as shown in Figure 2.4. Different requirements and details for different cells are presented in Table 2.4.

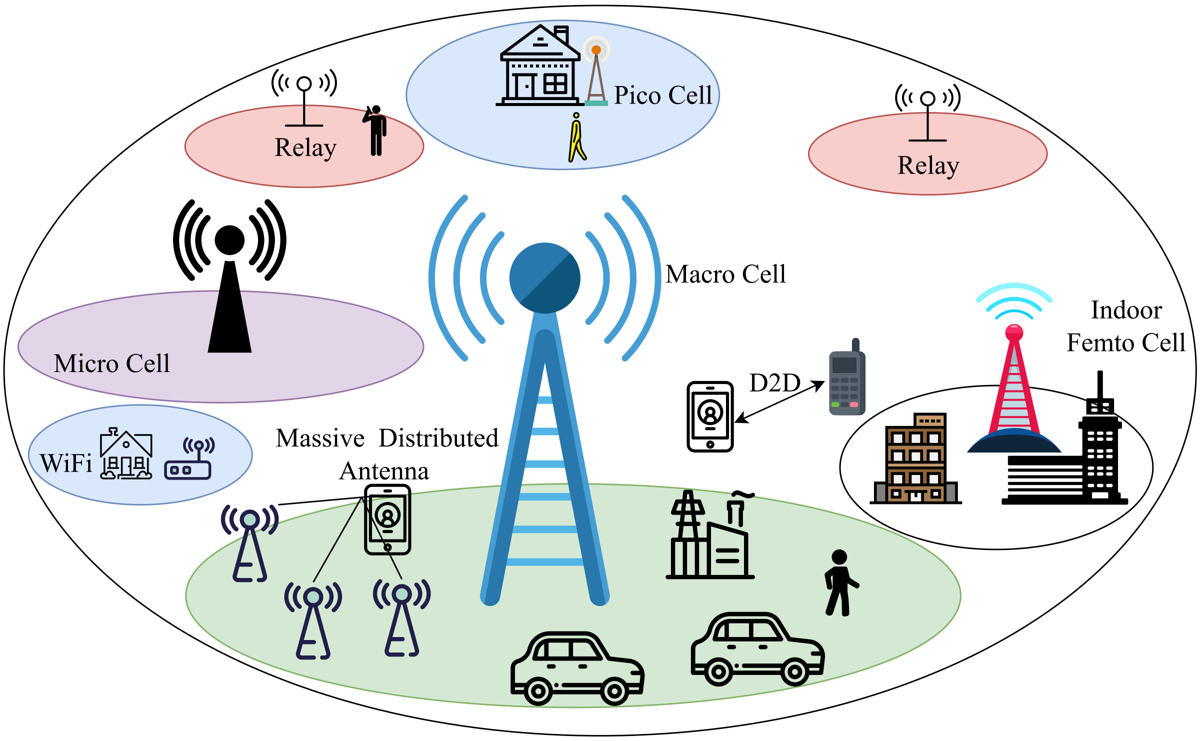


Figure 2.4: 5G ultra-dense heterogeneous networks.

Table 2.4: Comparison between different types of cells in a heterogeneous network [53].

| Specification | Macrocell | Microcell | Picocell | Picocell |
|---|---|---|---|---|
| Transmit Power | 45 dBm | 30 dBm | 30 dBm | 20 dBm |
| Power Consumption | High | Moderate | Low | Low |
| Coverage distance | Several kilometres | Less than 500 m | Less than 100 m | Less than 30 m |
| Deployment | Outdoor | Outdoor and Indoor | Indoor and Outdoor | Indoor |
| Backhaul connectivity | Microwave, Fiber | Microwave, Fiber | Microwave, mm | DSL, cable, fiber |
| Installation | Operator | Operator | Operator | User |

## 2.9 5G Use Cases

### 2.9.1 Autonomous Vehicles

Autonomous vehicles, self-driving vehicles, or robotic vehicles incorporate vehicular automation, which could be efficient without human intervention. With the human-provided input, it will sense the environment using sensors and AI. It required full coverage with low latency. The details of the uses case are given bellow.

#### 2.9.1.1 Context

This use case is concentrated on the slicing of the 5G network, ranging from vehicle services to everything, licensed and unlicensed spectrum sharing, LTE side link, cell-free, CA, with the infrastructure as well as infrastructure and any entities of communication for better fluidity of transport, safety, as well as road relaxation. Explanation of slicing includes the partition(s) of the core network, RAN resources, and vehicular end-device functionality configuration. Furthermore, it is extended to URLLC, involving ultra-reliable low-latency and/or strong communication links and mMTC.

#### 2.9.1.2 Motivation For The Need of 5G Networks

Autonomous vehicles or vehicle-to-everything are considering one of the most foreseen 5G applications. Autonomous vehicle forthcoming is completely dependent on Vehicle technology that's why it is advancing rapidly to sustenance it. To emerge a completely autonomous vehicle future, various diverse improvements in-vehicle technology, network speed, data throughput must approach organized. Due to the considerably reduced latency of 5G, it will be an immense enabler for autonomous vehicles, whilst vehicles will be capable to answer 10-100 times above the existing cellular networks. The eventual aim is a Vehicle-to-Everything

(V2X) communication network, which will allow vehicles to automatically answer to objects and changes across them almost immediately. As the vehicle will be capable to send and receive information's in milliseconds in directive to brake or shift directions in reaction to road signs, people crossing the street, and hazards.

For example, compare the latency of 4G and 5G, assume a car is going up the road at speed of thirty miles per/hour and required to receive a signal which can escape striking an object. Presently with 4G, it has a latency of approximately a hundred milliseconds, a car would travel about four feet or one point two meters. While With 5G latency approximately ten milliseconds, the vehicle would only have travelled five inches or twelve centimetres.

#### 2.9.1.3 Description

In recent years the idea of "connected car" has arisen, which has the capability to drivers a recent scope of services through cordless communications, that are well-thought-out as being among the furthermost distinct designs of the coming generation vehicles.

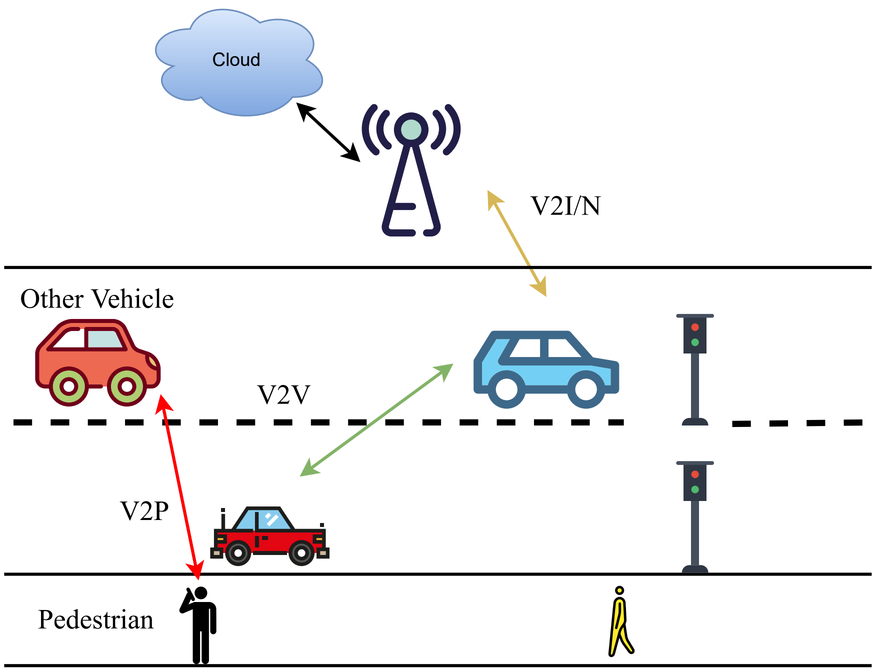


Figure 2.5: Types of V2X services.

These wireless connected vehicles with pedestrians and each other's within contiguity can recognize the possibility of a collision by sharing the information, for example, the direction and speed of their location. Similarly, the vehicle that is linked with network infrastructure can transmit to the device that is controlling the traffic that will in return warn of any anonymous fatal hazards along the road or route to ensure optimal flow of traffic and guidance on the speed. Because of LTE air interface of high spectral efficiency, it can support numerous Vehicle-to-Everything (V2X) services, also it is able to upkeep diverse categories of communications from transmissions of one device to many devices or one device to another device, and from usual downlink and uplink cellular communications to Device-to-Device (D2D) direct over-the-air communications.

#### 2.9.1.4 Initial Scenario

On the system of LTE-based V2X, two air interfaces will be helpfully worked one D2D interface utilizing sidelink, and the other one cell interface dependent on UL/DL and will choose to deliver to the need of each V2X administration. The D2D and cell correspondence is the fragment of LTE-based V2X, which will introduce great operational favourable position proficient use of the range. By and large, the canny transportation framework has four kinds of substance; focal workers' keen transportation framework, side of the road unit, vehicles prepared with an installed team, conventional street clients, for instance, bike riders and people on foot. These characterized substances can speak with one another utilizing D2D or cell-based correspondence. V2X, which depends on Device 2 Device (D2D), uphold low inactivity, and give short-range parity even to out-of-network inclusion, while equality, which depends on cell correspondence, is for a wide-region post with a high limit.

The transportation framework substance side of the road unit that can act in eNB or a standing client terminal, it offers numerous administrations dependent on the data of neighbourhood geography procured from close by weak clients, focal shrewd transportation framework worker, and sensors, for instance, acceptance circles and cameras. With installed units, when a restricted check of vehicles is prepared, at the fundamental phase of V2X administration dispatch, the side of the road unit conveys nearby geography information gotten by the side of the road sensors rather than V2V correspondence. On the off chance that a predominant eNB can fill in as a side of the road unit, the rapid development of the V2X market may be assessed. Indeed, even in the development stage, a side of the road unit can require more extensive geography information with high dependability. For the street, administration data, and all different substances just as traffic, the focal smart transportation framework give the incorporated control to them. The focal smart transportation framework can be sent externally to the organization of LTE by the transportation industry, for instance, the division of transportation. The range is either assigned to D2D or cell.

To offer the sufficient capacity for the cellular-based V2X, the LTE spectrum and infrastructure can be reused, which is operating by different operatives with several LTE carriers in a particular region, which belongs to the Figure 2.6 scenario A. at the point when the client hardware utilizing the range of its administrator for commonly kinds of connections, the uniform coverage have the option to be pushed off for the two links. In this condition, it is fundamental to think about how to convey the essential nature of administration (QoS) for the V2X interchanges through client hardware's going to particular administrators where tight coordination and quick information move couldn't continually be assumed. Because of the recurrence portion rule, it is practical that another committed range is allotted to D2D-based V2X.

An LTE transporter for D2D activity isn't authorized to an administrator. In such kind cases, therefore, ultimately, the D2D activity for V2X continues habitation in the committed D2D range as appeared in situation B, and the matter of between administrator activity is confined to the cell connect. The administrator may be utilized in such a case cell interface for V2X administrations standing nearly low inertness in order to decipher for the inactivity brought about by the between administrator activity. However, for the D2D connecting use, its administrations required short idleness and restricted short inclusion. For radio boundary enhancement, clog control, radio asset distribution, security, and validation, the organization control will be created. On the off chance that no LTE inclusion is offered for certain particular territories, at that point for the V2X, the D2D connection will be utilized without taking such organization control as in situation D. Every one of those boundaries that are constrained by an organization will be set to predefined ones, which may be led to decently non-streamlined activity. On the off chance that strategic administrations are supported by cell based V2X, the submitted range for the whole V2X can have benefits in relation to limit and (QoS) control. In terms of this situation, a specific administrator in every particular region and RAN sharing activity among administrators is estimated as operational decisions with little arrangement charge.

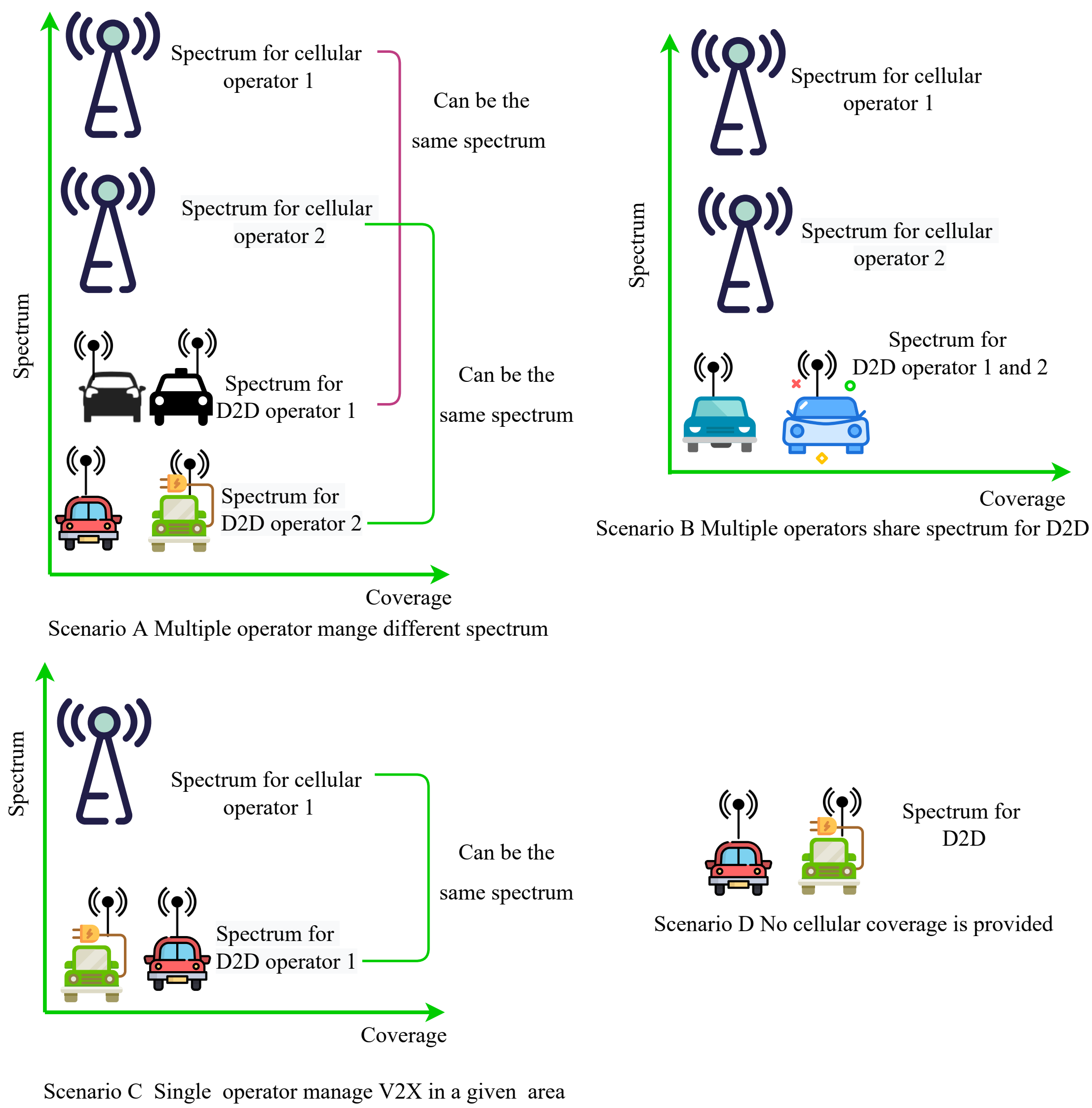


Figure 2.6: Spectrum options for V2X operation in a given area.

#### 2.9.1.5 Step By Step Scenario

**Efficiency in safety and traffic** The event-driven and periodic messages of a vehicle to vehicle / vehicle to pedestrian (V2V/V2P) taking the position and its kinematics parameters of the car which is using as a transmitter to permit other vehicles and exposed road users to feel the nearby situation and upkeep applications such as a warning of a forward collision which notifies a driver of an impending rear-end collision through a vehicle upfront, for sharing the same path a cooperative adaptive cruise control is exercising which is permitting the cluster of a vehicle in proximity.

- **Autonomous driving** Autonomous driving conditions are additional narrower than those in V2V safety applications; because it might be at a higher speed relatively, 200km per hour, and will be very close to each other. Furthermore, it requires complete road network coverage to be driver less in all geographies, with that network condition that can support communications with high vehicle density. In certain situations, video/-data interchange throughout V2N links may supplementary improve the autonomous driving efficiency and safety.
- **Vehicular Internet and soft news** For the browsing, social media approach content, applications download, and High-Definition (HD) video streaming for travellers are measured a "must-have" for the latest cars and would become even extra related with enlarged penetration of self-driving vehicles, in which also the driver might be involved in media utilization.
- **Remote diagnostics and management** A V2X application server maintained through a car producer or a diagnostic centre for vehicles can save communication occasionally directed by cars that are in V2N mode to locate their position for easy problem solving.

**Final Scenario**

To support safe drive and connect with application by digital high speed data.

**Summary how our work is related to the scenarios**

In the scenario of autonomous vehicles, it is possible to support the slicing of the 5G network ranging from vehicle services to everything, usage of licensed and unlicensed spectrum sharing, side-link, cell-free and CA. This scenario comprises communications between infrastructure and any entities of communication for better fluidity of transport, safety, as well as road relaxation.

### 2.9.2 6G Use Cases

The identified KPIs of the 5G 2nd phase handhold the significance in 6G. It is further adapted based on 6G requirements. A rich blend of use cases that explore 6G features can be identified [32]. The 6G use cases concerted on energy efficiency, latency, positioning, device density and peak data rate.

The following defined use cases range from human twins to manufacturing units (smart factory plus). The use case human twin needs low latency while required a high data rate. Thoughtful factory plus needs tighter security. The main aim of 6G communication is to transfer the world to a global village. The identified 6G use cases are as follows:

- Digital Twin of Human

  With the cooperation of medical sciences and 6G evaluation, the body of humans can be virtually designed. It can appear far away, where the patient can be monetized from that digital twin. It will be possible to check the health data, for example, blood pressure and other required measurement, in real-time from the digital twin of the human body.

- Internet on Air

  6G will be providing high-data internet for air users, and this could be possible with the support of satellite communication. It is expected that the cost will be high, and nowadays, some airlines provide air internet, but it's still not advanced and is limited to text and other services.

- Smart Cities with AI and Sensors

  The 6G heterogeneous network will be befitted from AI and many other sensors, which will provide the integrated service which is the requirement of smart city. For example, AI will be used to sense the hazards using high speed internet connected with cameras. Furthermore different sensors will be mounted outside the building and outside to complete several task without human support.

- Autonomous System and Robots

  Due to high-speed internet and security the 6G will enhanced the robots and autonomous business. For example, the driver-less car will be supported by satellite which will reduce the accident chance, the traveller can enjoy the trip with out driving. The 6G will enable the UAVs communication between UAVs and other ground controllers. The autonomous vehicles has demands it will not only provide comfort in travelling only, but it will also support other businesses, for example agriculture, which will use autonomous machinery, that will properly harvesting and also reduced the human mistakes.

- XR (Extended Reality) Based on Holographic Communication

  Due to high data rate reequipment and technology advancement by 2030, it is expected that the 6G will support Augmented Reality (AR)/VR to Extended Reality (XR). The users will be enjoying holographic communication and holographic display. It will be possible to enable hearing, taste, and sight using XR. Further, it can boost entertainment bossiness, for example, concert and sports.

- Emergency Internet Services

  6G will support unmanned aerial, and its network will be benefited from satellite communication. This service will help restore the internet in floods and other natural disasters. For example, in the case of earthquakes, the terrestrial transmission will be replaced by satellite or unmanned aerial networks.

- Smart Factory Plus

The 6G service will not only restricted to support only factory application but will assure full connection and stability, security to the entire production cycle. It will quickly and flexibly connect intelligent devices that require to be connected inside the factory, will provide dynamic adjustment according to the requirement of the production line using AI. Through the 6G network, Smart Factory PLUS will add an end-to-end closed loop. It is expected that the 6G Ecosystem creates opportunities for new businesses by implementing these use cases in real-time. According to the Finnish 6G Flagship [54], these innovations can enhance the use of the networks in a very innovative way.

## 2.10 5G Standards Perspective

The evolution of the mobile and wireless networks sector enabled by emerging 5G NR technologies and massively connected devices supports a significant increase in data traffic demand. As a result, new business models and services are available, e.g., supported by ultra-low latency and ultra-high throughput networks. The need for diverse applications and seamless connectivity involves critical requirements and implies supporting on-demand services. With the roll-out of 5G wireless networks, NS evolved as a fundamental feature to facilitate segmented layers of networks in addition to the base network architecture [9].

In reality, NS provides a paradigm shift from the conventional approach towards traffic and network management [10]. It allows virtual logical network layers to enable all the functionalities of a shared physical network. Furthermore, it sub-divides the network into several isolated virtual networks leading to a dedicated channel to provide resources to serve the user demands. Thus, slicing empowers conventional networks to support a wide range of use cases and business models. Additionally, while enabling enhanced service quality, NS supports tailor-made user-specific solutions. For instance, the latency requirement for emergency services is more stringent than for agriculture-based applications (to maintain crop health). Thus, it will make current networks dynamic, flexible and scalable whilst accommodating growing demand, from various applications, with diverse requirements.

Unlike conventional networks, 5G networks are enabled with networking slicing. 5G evolution opens up many services and use cases. New physical networks are not required anymore to facilitate dedicated service. As proposed by the 3GPP, the introduction of NS is established in the framework of Release 15 [11] and is regularly updated for the required technical details and enhancements. 3GPP has specified that, for CSPs, NS is significant for creating new services and generating new business models. NS allows CSPs to create multiple virtual slices to encompass colossal traffic increase and specific user requirements. As a consequence of this evolution, Working Groups from various Standard Development Organizations (SDOs) entered into force to support a multi-vendor landscape that develops NS specifications and guidelines.

CSPs benefit by implementing network orchestration, the automated communication among various entities on and across the network to meet network and user requirements. It sets guidelines to establish connections through the network while offering services with the associated SLAs [55].

A network slice (often referred to as "5G Slice") incorporates the Network Functions (NF) and settings that encompass the supported use case or applications being served. It facilitates resources on-demand by incorporating existing virtualization and computing techniques. Slices make the resources modular while introducing flexibility into the network. In [56], authors have defined different layers of 5G slices, as shown in Figure 2.7.

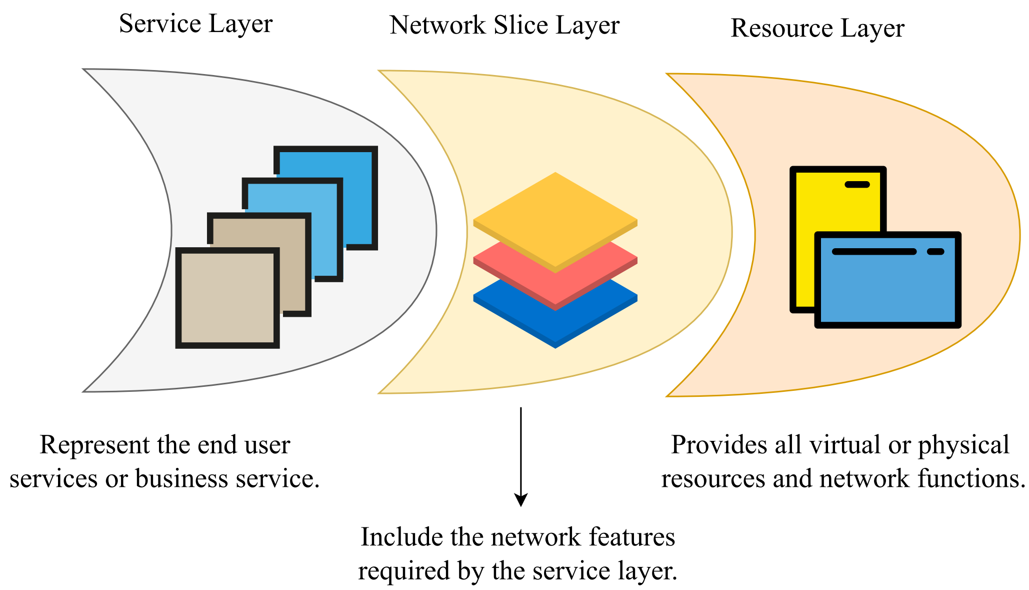


Figure 2.7: Different layers of network slicing.

The two key enablers of Network Slicing are described as follow:

- Virtualization Technologies, Virtualization facilitates resource sharing on the 5G Slice and removes dedicated hardware dependency. As the resources are independent of the physical hardware, slices are easy to deploy and manage as a modular block on a 5G network; [56]. Interfacing the independent modules of resources is critical and needs assistance for resource allocation purposes;
- Management and Orchestration; Automated orchestration and management techniques help regulate and manage many network slices in a complex environment. Besides, according to [57], it facilitates network slice management functions.

### 2.10.1 What are Standards and Standardization's Bodies

The final result of specified research is the set of standards for operation. It can be defined that the desires and specifications for services, products and processes [13]. Further, it can be defined as an accepted pattern with considered quality assurance [13]. Standard is the acknowledged pattern with a quality guarantee. It is the regulations which aim for its usage. It is ruled to do things which can provide benefits.

With the development of technologies, the need for standards is increasing. It Is essential to have standard and different filed, has various standardization organizations. Information and Communication Technology (ICT) standardization procedure for telecommunication is itself vast and critical [58]. Both the hardware and software companies are considering the standards to make the national and international completability of standards between different vendors. Different forums, organizations and alliances are developing the standards. Different products pass through standardization before getting into the market.

### 2.10.2 Standards Development Organizations

Forums, organizations, and alliances develop the SDOs and ensure their regulations. The SDO can be formed by different manufacturers, verticals, providers and regulators. To set standards, industries and academia play fundamental roles and provide convincing opinions to make a standard. They also led down regulations to ensure a legitimate development process. Based on different classifications, there are different SDOs. The classification of different SDOs with accordance to European Telecommunications Standards Institute (ETSI) [58] are shown in Figure 2.8.

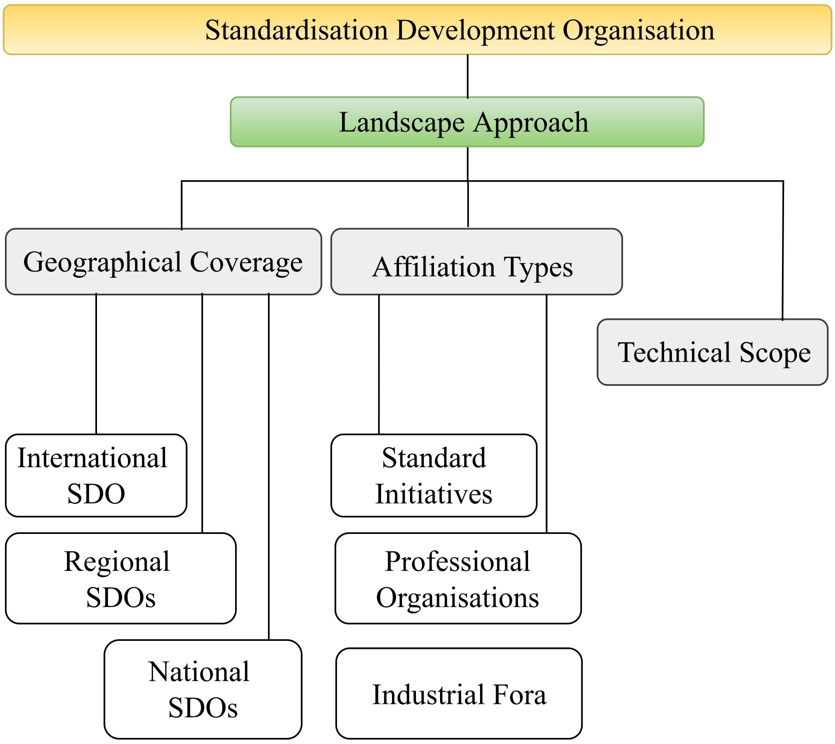


Figure 2.8: Types of standardization organizations.

SDO represents the members nationally and globally. Globally the standard bodies are ITU, IEC (International Electrotechnical Commission), etc., while in regional SDO it contains the academia and industries, and national SDOs developed from different countries. For example, African Organization for Standardization, formerly ARSO. If the standard belongs to a specific country, the national SDO collaborates with the international SDO.

The SDO is taking the initiative to set up the groups. For example, 3rd Generation Partnership Project (3GPP), oneM2M. They make it able to coordinate and collaborate with standardization efforts through distinctive matters. Independent professionals are connected by

Professional Organizations (POs) to encourage better approaches in the context of innovation. The Institute of Electrical and Electronics Engineers Standards Association (IEEE-SA) and Internet Engineering Task Force (IETF) are examples of it.

### 2.10.3 5G-PPP and NGMN Architectural Vision

Next Generation Mobile Networks (NGMNs) vision is to enhance their flexible softwarization. The NGMN architecture is subdivided into three layers, as follows: i) business application, ii) infrastructure resource, and iii) its business enabling [9]. It is characterized by an End-to-End (E2E) scope encompassing the Radio Access Network (RAN) and core networks [59]. 5G Infrastructure Public-Private Partnership (5G-PPP) elaborates on roles and relationships among different parts of the 5G network. It generally shares the NGMN perspective that the 5G architecture must flexibly support softwarization for different use cases. Besides, it is worthwhile to note that the NGMN 5G-PPP architectural proposal is divided into five layers, namely service, infrastructure, business function, network function, and orchestration layers [60].

### 2.10.4 ETSI NFV MANO Management Architecture Evolution

Network Function (NF) Virtualization (NFV) enables broadening the upgraded capabilities of communication networks. These capabilities are flexible enough to instantiate the NFs where needed, e.g., in the data centre or network, and provide elasticity in allocating extra resources to these NFs. However, management and orchestration functions require new algorithms that handle essential resources and control the VNFs life cycle. To manage the VNF life cycle and resource allocation, the ETSI has added an NFV Management and Network Orchestration (MANO) architecture. It primarily provides the management and orchestration of network services, VNF, and all resources in a data centre (virtual machine resources, networking, computation, and storage) [57]. The three functional blocks of NFV MANO are i) the NFV orchestrator, ii) the VNF manager, and iii) virtualized infrastructure manager [61].

### 2.10.5 Slice Creation and Isolation

Depending on use cases requirements, 5G heterogeneous network nature allows for designing different network slices. For example, an ultra-low-latency slice will be supported irrespectively of general network requirements if the use case requires short delays.

Slice isolation consists of creating slices and then distinguishing them by considering the assisted use cases. Thus, it facilitates the simultaneous coexistence of multiple slices in the same network without affecting their performance. In fact, in-built security and privacy will be induced in the design by isolating the slices over the shared infrastructure [62].

## 2.11 Standardization Activities on Network Slicing

Standards are the guiding force behind research, development, innovation, policy establishment, and industries. It regulates the execution of productive tasks and implementation of the products while assuring quality [63]. In addition, standards ensure interoperability among research techniques or products.

There are different types of SDOs working towards proposing standards within various verticals. In the context of 5G New Radio, it is essential to have collaborative standardization in E2E network slicing architectures [64], as it includes widespread coverage domains and application areas and is opening up new research opportunities. Therefore, SDOs and academia, together with industries, need to collaborate on standardization efforts to facilitate interoperability [63].

### 2.11.1 Worldwide Standardization Approaches on 5G Network Slicing

Different telecommunications standardization bodies and industries are shown in Figure 2.9 together with their efforts on network slicing. Global System for Mobile Communications Association (GSMA) and NGMN contribute to the investigation of high-level requirements and architecture, as well as to the creation of the concepts of E2E 5G network slicing and business initiatives [65]. Currently, the industry focuses on investigating network slicing requirements while analyzing their influence on different network layers, e.g., core network or RAN. Different SDOs have been defined as technical specifications for many domains, as follows:

- GSMA is a global organization that develops a unified mobile ecosystem that supports research and innovation in the mobile communications industry sector while integrating industry solutions, including network slicing. For example, the recently published white paper on ”E2E Network Slicing Architecture” [64] describes industries, operators, and vendors’ requirements and the need to collaborate in standardization activities to achieve a unified solution for the NS architecture. The white paper further explains E2E NS architecture, high-level requirements, and ongoing initiatives from various SDOs.
- 3GPP, one of the main standardization bodies, encompasses several active working and study groups to support 5G network slicing. For example, the SA1 group of 3GPP focuses on use cases and requirements. The SA2 working group defines the architecture selection to support network slicing [65]. The SA3 working group addresses security while SA5 addresses slice management [66]. The NS concept was introduced in 3GPP’s Release 15 [11] and has further been enhanced within Releases 16 [67] and 17 [68]. Release 16 added authentication and authorization controls, enhancements to network automation, and service-based architecture to the 5G slicing. Release 17 adds enhancements for phase 2 of the NS architecture and outlines support to the GSMA defined Generic Network Slice Template (GST) attributes. It also addresses simultaneous usage of network slices in 5G-assisted networks.

- The ETSI activities for 5G network slicing address the optimization of 5G services, configuration, delivery, and assurance of deployment, enabling complete automation. It also provides a solution for computing and storage [57].
- The Internet Engineering Task Force (IETF) standardization activities address the general requirements and development of the 5G network slicing architecture. Besides, they consider the orchestration mechanisms and network slice management. Their latest work includes gateway function for network slicing, the applicability of abstraction, and control of traffic-engineered networks to network slicing.
- The Broadband Forum (BBF) involves the activities to term the slicing management architecture for transport networks. Moreover, the BBF standardization activities contain the sharing of broadband network infrastructure between different service providers while providing resource control support [69].

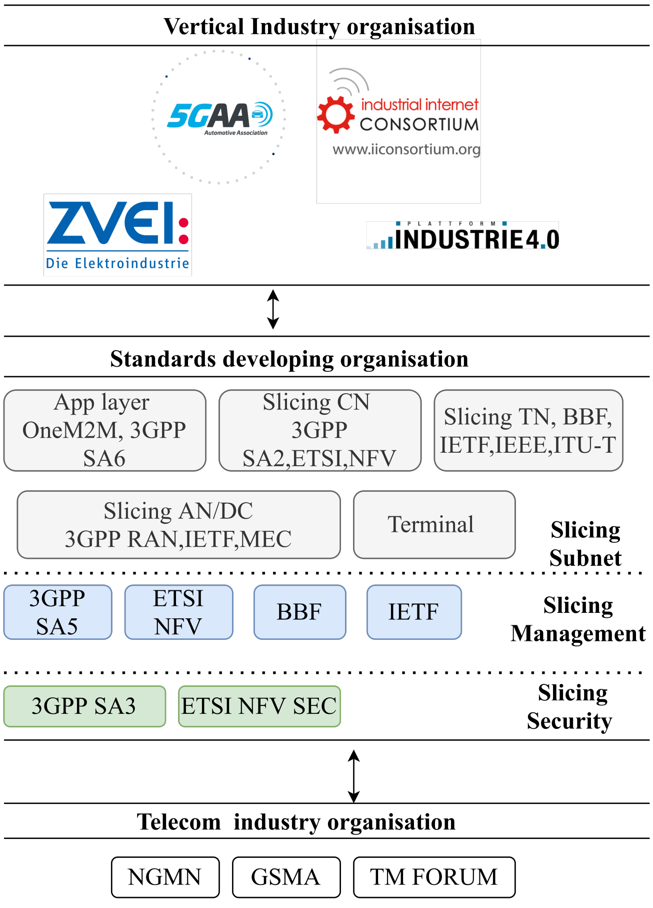


Figure 2.9: Standardisation groups and SDOs for network slicing [70, 71].

- The International Telecommunication Union - Telecommunication (ITU-T) encourages different functionality of E2E network slicing to provide reliability to customers. ITU-T functionality contains softwarization, network capability exposure, requirements of mobility, and diverse End to End (E2E) QoS with distributed nature, the support of edge cloud, control, and user plane separations. ITU-T Study Group 13 (SG13) [72] works in orchestration, network management, and horizontal slicing standardization activities. It also addresses the data plane programmability and defines high-level network softwarization. An ITU-T SG13 Focus Group (FG) on ML for future networks, including 5G (FG-ML5G) [73], has catalogued its deliverable, which had specific requirements that include details for interfacing, network architectures, protocols, algorithms, and data formats. Deliverables related to network slicing and ML are as follows [73];

  - ITU-T Y.3172 [74]: Architectural Framework for Machine Learning in Future Networks including IMT-2020;
  - ITU-T Y.3176 [75]: ML Marketplace Integration in Future Networks including IMT-2020;
  - Requirements, Architecture and Design for Machine Learning function orchestrator;
  - Serving Framework for ML models in Future Networks including IMT-2020;
  - Machine Learning Sandbox for Future Networks including IMT-2020: Requirements and Architecture Framework;
  - Machine Learning-based End-to-End Network Slice Management and Orchestration;
  - Vertical-assisted Network Slicing based on a Cognitive Framework.

- The Open Networking Foundation (ONF) studies network slicing connectivity for high bandwidth 5G services by considering low latency and secure virtual subsets of the network [76].
- The Open Network Automation Platform (ONAP) [77] is an open community by operators for next-generation network automation platforms. It focuses on unifying standards and open source activities while promoting cross-organizational collaborations. Recently, ONAP has published a series of white papers related to technical challenges associated with 5G slices. It emphasized the following four design goals:
  - Communication Service Template (CST) to collect SLA requirements by users;
  - Service Descriptor (SD) records the user requirements collected by CST and facilitates slice creation by converting them into network requirements;
  - Network Slice Template (NST) describes the deployment information of slice instances;
  - Network Slice Subnet Template (NSST) deploys slice subnet instances.

### 2.11.2 Network Slicing and ML/AL

ML and AI have recently become very important in different fields of activity. It makes the system intelligent so that human intervention can be avoided. For example, Telecommunications operators use ML in analyzing the customer experience, network automation, and business process automation [71]. ML and big data are also needed to facilitate intelligent capabilities and integration for network slicing. Besides, ML and AI can be the best solution for self-optimization, self-configuration, and fault management functionalities, as well as network security and malware detection [78]. Table 2.5 presents different techniques considering ML/AI applied to the implementation of network slicing available in the literature.

## 2.12 Opportunities for Service Providers

MNOs consider network slices as an isolated independent network segment self-sufficient in resources and provides services at approved QoS. MNOs can implement slicing while maintaining transparency with the end-users. NS ensures connectivity tailored-made service delivery. MNOs maintain SLAs to administer the offered services, data rate, QoS, latency, reliability, and security. MNOs can implement either single or multiple slices in the network to offer services to varied requirements of different genres. Some of the prominent industries that can benefit from 5G slicing are the following ones:

- Logistics;
- Media & Entertainment (Augmented/Virtual Reality);
- Automotive;
- Industrial Internet;
- Financial Sectors;
- Health & Wellness;
- Smart Cities.

To meet the diverse service requirements and demands, conventional business models are evolving as well. Therefore, new use cases are being defined. The underlying market ecosystem is divided into three categories, as follows [9].

- Asset Provider: performs infrastructure leasing to the third party;
- Connectivity Provider: facilitates essential connectivity delivery at high-speed to meet QoS requirements, including latency ;
- Partner Service Provider: enables enhanced communication services to end-users &/or to third-parties.

## 2.13 Challenges and Open Research Areas

Network slicing is a promising paradigm for 5G and beyond networks, but its introduction faces various challenges [10].

In [56], NGMN has explained that sharing the resources between slice tenants is the most challenging issue for network slicing. Resource sharing can be either by static partition or by elastically dynamic sharing. One of the major open problems for resource sharing is standardizing a proper scheduling mechanism that can allocate radio resources among different slices while providing computational resource sharing and slice isolation mechanisms. Besides, network reconstruction is required in 5G and beyond, as the resulting ultra-dense network will comprise cooperative Macro-cells and small-cells networks while addressing the slicing demands (high transmission throughput, fairness, short delay, and reliability).

Table 2.5: Papers with concepts using ML/AL for network slicing.

| **Papers** | **Algorithms covered in different papers using ML/AI considering Network Slicing** |
|---|---|
| [79] | Cellular and IoT networks resource management techniques using ML |
| [80] | Implementation of deep learning neural network, considering the network availability and network-load efficiency. |
| [81] | Network-slicing for the vehicle-to-everything service, intelligent network architecture that influences the recent ML techniques. |
| [82] | Resource mapping algorithm for 5G network slicing using deep reinforcement learning. |
| [83] | A deep reinforcement learning optimization model for slice configuration. |

Today, we lack on integrating network slicing with NFV and C-RAN to facilitate supporting point-to-point connections among radio equipment controllers and physical radio equipment. To fill this gap, network slicing requires cooperation with other 5G technologies, such as mobile cloud engineering, broadband transmission and NFV.

Designing new virtualization mechanisms is required to make the sharing of resources efficient and give strong support for implementing radio access network slicing. In addition, with multi-domain infrastructure, security issues turn out to be more complex. Therefore, defining security mechanism policies between several infrastructure domains is required.

Resource scheduling in RAN slicing is challenging due to performance isolation, diversified service requirements, and network dynamics (including user mobility and channel states).

Although different service providers and operators work on industrial solutions for network slicing and its management [84], some open management challenges include NS activation and deactivation at the service level, QoS maintenance at the network level, intra-slice resource sharing, and load balance.

NS creates separate logical networks on a shared physical infrastructure specific to use cases, realizes automation across various operational, management and business processes, and scales up the business without increasing Operating Expense (OPEX). The commercial usage of network slicing in industries, intelligent configuration, SLA guarantees, and integration with vertical industries needs improvement. 3GPP defines the NF parameter for the slice and slice-subnet management accompanied by the related interfaces. However, it still needs further research to manage the automatic and intelligent closed-loop controls and SLA requirements. 5G network slice coordination is critical to guarantee high QoE. Use-cases and business requirements need to be considered by operators to enable new approaches that result in easy maintenance of the networks.

The open areas for future research activities include support for HetNets for availing intelligent services in IoE scenarios, in addition to support for various kinds of realities (augmented, virtual, extended), connected autonomous systems or drone-based networks. The management and orchestration requirements vary indistinctively in drone-based networks and conventional networks. ML and AI capabilities enable intelligent radios to support various new services while incorporating fast and efficient training and tuning ML models. Besides, there is a need to develop novel meta-learning models for ML-enabled network slicing, an open research area.

## 2.14 6G Standardization Map

5G is commercialized in many countries. Currently, the expedition is beyond the 5G ecosystem. Several studies groups drafted their initial standards based on KPIs and use cases. In 2023 the 3GPP expects to suggest and publish the requirements for 6G [85]. According to the current trend and approaches of the researchers toward 6G, from now in decades, 6G systems will be fully matured. Academia and industries are focussed on different technologies, for example, Communications, mmWave, Reconfigurable Intelligent Surfaces (RISs), AI and ML intervention, and holographic communications. In May 2019, ITU, IMT 2030 perception was added to explain B5G with a hybrid network.

Different industries, for example, Facebook (Meta now), QUALCOMM, and AT&T work collaboratively for 6G standardization in deployment and R&D sectors. On another side, Next Generation Alliance [86], working on 6G rollout in different perspectives, contains R&D, manufacturing standardization and deployment. China has formed alliances to initiate early 6G research [87].

With the support of European Union (EU) member states and the European Commission (EC), European Commission Radio Spectrum Policy Group (RSPG) [88] is working on 6G developments and recommends 6G initiatives. It opens opportunities for efficient utilization of the EU spectrum and possible usage of the new THz band to support wireless backhauling, and wireless access [87]. 6G Flagship is a project at the University of Oulu (Finland), contributing to 6G technologies [54]. Vodafone announced its 6G development and research facilitation in Germany at Dresden. “Hexa-X” is a project funded by the EU and led by Nokia investigating future technologies in the context of 6G use cases.

NTT Docomo Japan is spending vast funds on 6G research in the direction of 6G infrastructure with a target to get ready the 6G specifications by the year 2025. To mark their presence for 6G initiatives, Samsung (South Korea) added a 140 GHz wireless link for digital beamforming solution, spectrum band of Terahertz [89]. The R&D sector of institute NIIR [90] contracted with Ericsson test 5G technology.

In Release 18 of 3GPP, new capabilities and features are defined for 5G. This release will probably be permitted by 2023. It will expectedly be focused on B5G and 6G specifications. Roadmap of 5G NR NTNs with products available and completion of Release 17 is expected by 2023. Beyond THz and 50 GHz, bands will be applicable by 2025 for NTN systems. The 6G development and road map are presented in Figure 2.10, [13].

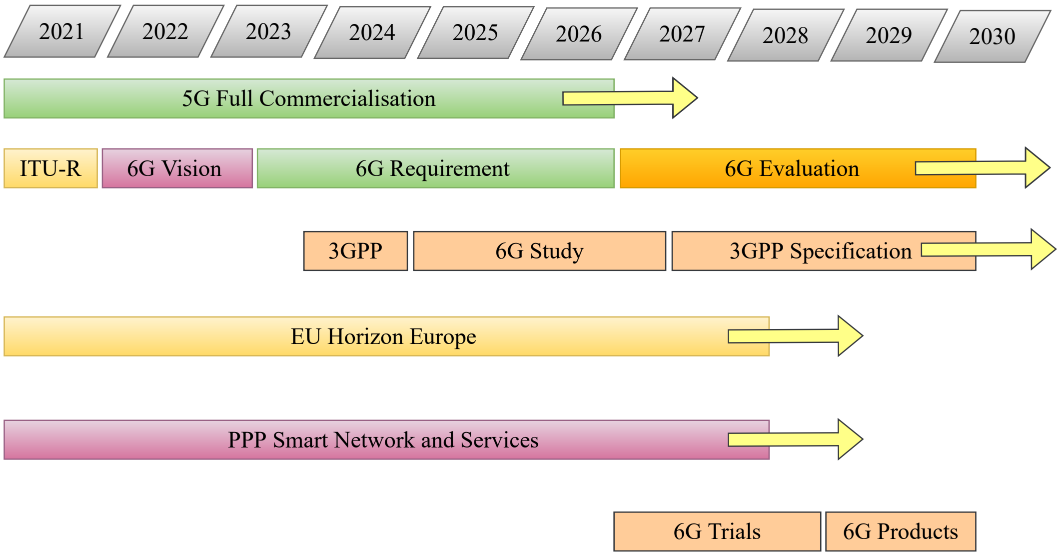


Figure 2.10: EU 6G development road map.

## 2.15 Summary and Conclusions

In this study, we provided a research-based overview of the current and ongoing work on Network Slicing within different Standard Development Organizations. It includes a detailed study on application/use cases, requirements, and challenges for network slicing in the light of standardization.

In 5G phase-2 and future communication generations, network slicing is expected to be one of the most influential technologies and provide solutions tailored to specific end-users, varying from residential to industrial or corporate. It can evolve and shift the telecommunication industry to the next level by allowing more flexible and reliable design. It is required to enhance network infrastructure and incorporates virtualization and softwarization to make the best use of services provided by network slices. It will allow operators to offer premium services to their customers. Moreover, NS will enhance the business opportunities in many sectors, which will gain attraction by increasing revenues. It is worth noting that network slicing supports the economic model and service differentiation that meets the end-user Service Level Agreements. Finally have identified some open issues [77] that require standardization, e.g., cross-domain inter-working, as well as SLA assurance, intelligence and automation.

6G, in the context of a technology perspective, will offer several opportunities to the customers and MNOs to explore different use cases and services. The new spectrum will provide comprehensive support for various services but will have different challenges. In this part of the research, different perspectives of 6G are presented, also its enabling technologies and associated services. The requirements in future prospective with KPIs and its standardization initiatives are addressed. It is concluded that technology development and standards need to be broadened to offer future ecosystems with technological development with exponential growth. The product design must comply with standards to assist full capabilities for upcoming networks. Currently, many organizations provide their standardization and specifications requirements with scenarios for 6G, considering the 6G plans, like 100x throughput and latency in a millisecond compared to 5G.

Specific considerations are needed to develop technologies and standards for the next generation. Firstly, the SDOs need to spread their scope to the communication ecosystem to provide new prospects. Secondly, there are needs for scalability and re-usability, like standards evolution must support these needs. Thirdly, universal global standards are needed to overcome limitations in SDOs, that is, to avoid replications of standards. Further, the market and industry must motivate the competitive development of existing and new solutions to certify and secure the global supply chain without disruptions

# Chapter 3

# Survey on 5G Second Phase RAN Architectures and Functional Splits

## 3.1 Introduction

Each generation of mobile communication technologies (1G, 2G, 3G, 4G and 5G first phase) has enabled the telecommunications operators to upgrade their network and renew its infrastructure to fulfil service provision and their customer's demands. However, decreasing costs, reducing energy consumption and improving the service have been limiting network operation. A shift towards novel radio access technologies is thus in order.

Fifth Generation contributions are gradually going through the commercialization phases. With the 3rd Generation Partnership Project (3GPP) Release 16 [67], the second phase of 5G is introduced to define the transformation and evolutionary features and capabilities of Radio Access Network (RAN). The second phase of 5G intends to enhance the battery life, performance and support multitude of applications and services. While the first phase of 5G Networks is already commercialized globally, there are still few customers with 5G User Equipment's (UEs). Meanwhile, operators have not yet solved many outstanding issues, for example, adopting a cost-effective architecture that effectively addresses the current ultra densification issue that hinders every Mobile Network Operator (MNO) [91].

With the evolution of 5G applications and services, new RAN architectures and protocols are emerging. Network densification is among the potential contenders for increasing the network capacity [92], [93]. The introduction of virtualization is transforming the communication networks and the RAN architectures including the Radio Units (RU) and the Base Band Units (BBUs) which were usually at the cellular BSs.

The 3GPP [94] has defined the idea behind virtualization of network functions and functional splitting in order to promote RAN centralization by while reducing the total cost of densification. In the new RAN architecture, the functionalities of 5G BBU are split into several functional blocks, such as the Centralized Unit (CU), the Distributed Unit (DU) and the RU, forming the key building blocks of the Next Generation RAN (NG-RAN). The idea is to support flexible, cheap, energy efficient and straight forward Remote Radio Heads (RRHs) that provide extensive benefits, such as joint processing of radio signals, load balancing, network extensions, and power reduction. Figure 3.1 presents the NG-RAN concept. The splitting up of the functionalities at the BBU significantly reduces the transport rate requirements. Enhanced Common Public Radio Interface (eCPRI) protocol in the fronthaul transport should provide a cost-efficient enhancement of the performance [92].

Since the beginning of 4G deployments, there are many works describing and analyzing the various functional split options. In 2018, Larsen et al. [95] gave "*an overview of where the*

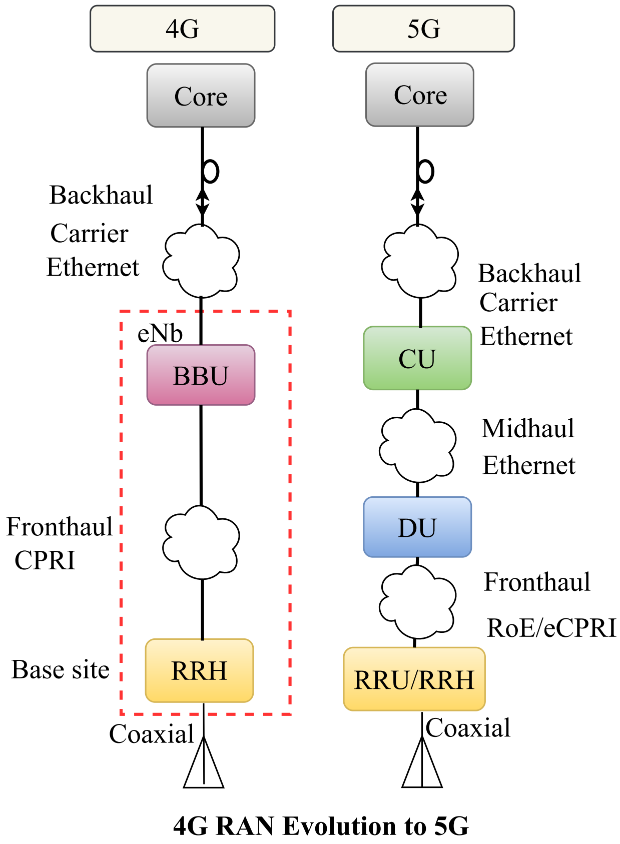


Figure 3.1: The evolution of 4G RAN to 5G.

*most effort has been directed in terms of functional splits, and where there is room for further studies*". This contribution aimed to provide an update while being self-contained. The contribution exposes recent tools, emulators, simulators, and analysis of the impact of functional splitting. Furthermore, some detailed comparisons of these splits are reported together with the discussion of and their pros and cons with within different use cases are reported.

This work addresses tools that enable to analyze and choose the best functional split options according to their own requirements. Comparative graphs are provided, and it is shown how many researchers are using these tools. The published real-time implementations of the functional splits are also identified. An analysis and our vision on the RAN fronthaul, midhaul and backhaul evolution are included.

The remaining Chapter is organized as in Section 3.2 starts with several definitions and then presents our current overview of the RAN terminology from 3GPP, Open RAN and other sources. Section 3.3 describes the current research status on the functional split, and explains each split, in detail while summarizing the essential aspects, from theory to implementation, algorithms, and tools (simulators or emulators) requirements. Section 3.4 addresses ongoing research on front/mid/backhaul and explains the move from CPRI to the eCPRI. Section 3.5 presents a detailed overview of recent advancements in RAN architectures. We discuss vRAN and Open Radio Access Network (OpenRAN) conceptual architectures in detail and how they evolved, and address the main implementation challenges and opportunities in Section 3.6.

Finally, conclusions are drawn in Section 3.7.

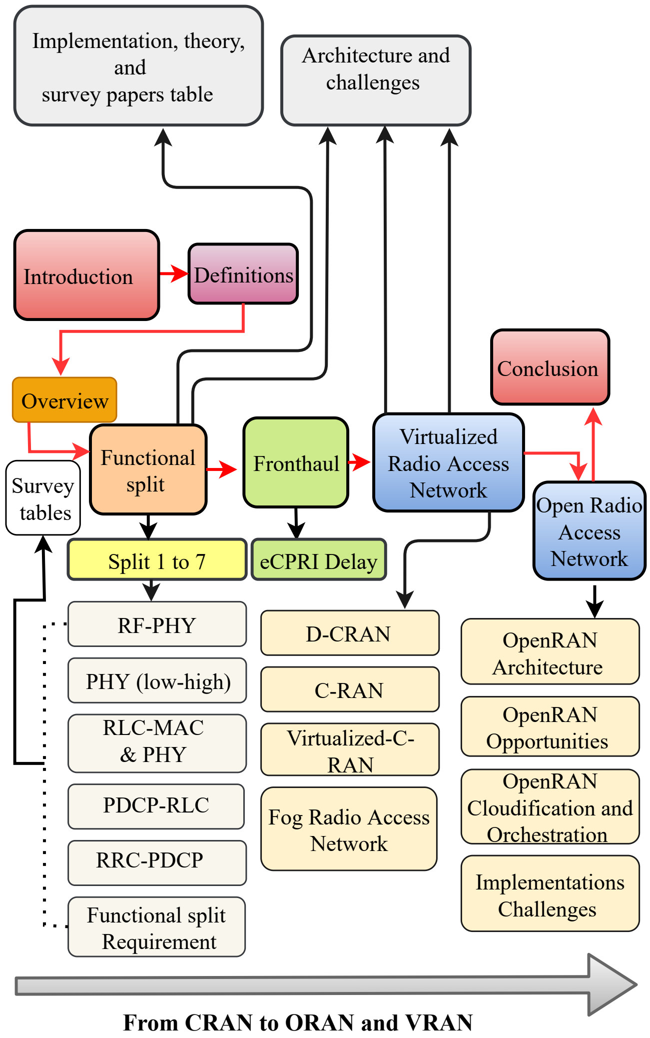


Figure 3.2: Overall structure of Chapter 3, with details of sub sections.

## 3.2 Overview

### 3.2.1 Overview of O-RAN Fronthaul

Fronthaul indicates the connection between the multiple RRHs and the centralized BBUs, facilitating a more expansive coverage range and faster data transmissions. As defined by the Open RAN Alliance (O-RAN) fronthaul specification [96], the fronthaul interface is defined as Open Fronthaul when it acts as an interface between the multi-vendor DU and RU by the defined signaling and control formats [97]. The Open Fronthaul architecture defines the Open RAN Distribution Unit (O-DU) and the Open RAN Radio Unit (O-RU) entities as logical nodes for accommodating RLC/MAC/High-PHY layers and Low-PHY with RF processing based on lower layer functional splits respectively.

#### 3.2.1.1 Operational Planes

The O-RAN Fronthaul defines four different operational planes, as shown in Figure 3.3(a) [96–98].

- **Control Plane (C-Plane):** It establishes the control between the DU and RU, in real-time, and transmits messages defining the scheduling information, data transfer coordination requirements, FFT size, length of the cyclic prefix, subcarrier spacing, beamforming and downlink precoding configurations, among other functionalities.
- **User Plane (U-Plane):** It characterizes the frequency domain's In-band and Quadrature (IQ) sample data transfer between the DU and RU in the frequency domain. The U-Plane transmits messages containing Downlink (DL)/ Uplink (UL) user data (PDSCH/ PUSCH), DL/UL control channel data (PDCCH/ PUCCH), and Physical UL PRACH (connection request purpose) data, among other, to the RU, before the transmission initiates. Additionally, The U-Plane also supports data compression and DL data precoding.
- **Synchronization Plane (S-Plane):** It is responsible for synchronizing and aligning the time, frequency, and phase clocks between the DU and the RU. S-Plane uses different synchronization profiles like the IEEE 1588 PTP packets, Synchronous Ethernet (SyncE), Physical Layer Frequency Signals (PLFS), among other to control the timing and synchronization aspects.
- **Management Plane (M-Plane):** It manages the RU, and facilitates functionalities for fault, configuration, accounting, performance, and security (FCAPS) required by the other operational planes, and supports C/U Plane IP and delay management. M-Plane eliminates dependency on the vendor's RU to support a multi-vendor OpenRAN infrastructure.

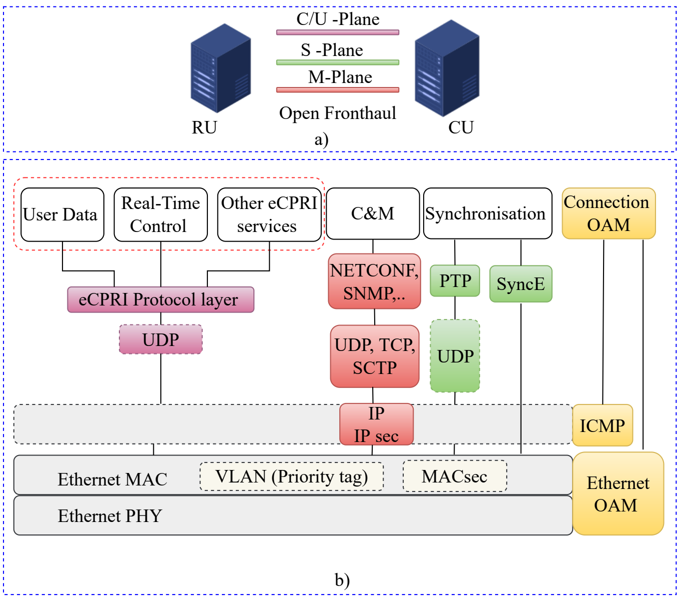


Figure 3.3: Typical fronthaul protocol stack considered by the O-RAN ALLIANCE and eCPRI to support: user and C-Planes, other eCPRI services, Control and Management (C&M), synchronization (PTP or SyncE over UDP or directly over Ethernet) and operation and maintenance [99]. This survey focus on the user and C-Planes.

#### 3.2.1.2 Protocol Stack

The O-RAN Fronthaul (FH) specifications [96] enlist guidelines and blueprint for implementing the four operational planes: Control, User, Synchronization, and Management planes. Figure 3.3(a) and (b) illustrate the O-RAN FH protocol stack for the 4 different operational planes. The functions of the operational planes are explained in the above section. The O-RAN Fronthaul Interface (FHI) library [97] supports IQ sample transmissions, O-RAN packets generation, appending IQ samples in the packet payload, and extracting IQ samples from O-RAN packets for split 7.2x based O-RAN architecture [97] [98].

The O-RAN FHI library constitutes of (i) O-RAN specific packet handling functionality (src), (ii) Ethernet and the supporting functionality (ethernet), and (iii) Set of header files to support external functions and structures. The C/U-Plane transmits eCPRI or Radio over Ethernet (RoE) essential data over the Ethernet or the UDP/IP protocol stack. The S-Plane transmits the Precision Time Protocol (PTP) and SyncE essential data over the Ethernet. The Management-Plane (M-Plane) transmits Network Configuration (NETCONF) signals over Ethernet with TCP/IP with Secure SHell (SSH).

### 3.2.2 Definitions

Essential definitions of the RAN architecture and functional splitting are as follows:

- **Backhaul:** It is the connection to the internet or the core [100].
- **BBU:** It is baseband unit transports a baseband frequency or a unit that processes baseband [101].
- **Core network:** It offers different services to the customers who are interconnected by the access network, or it is the site among the external networks and radio network [102].
- **CPRI:** It Common Public Radio Interface is the interface specification for the fronthaul, i.e., between the radio equipment and radio equipment control of radio base stations, considers for wireless cellular networks.
- **CU and DU:** It is the 5G gNodeB (gNB) is divided into two physical entities CU and DU, generally CU provide support to higher layers and DU provides support for the lower layers [103].
- **eCPRI:** It enhanced CPRI, for the interface specification be radio equipment and radio equipment control of radio base stations, considered for wireless cellular networks. While the eCPRI is the enhanced version of CPRI and its connecting enhanced radio equipment and enhanced radio equipment control through fronthaul transport network and is used for 5G systems [104, 105].
- **Functional split:** It is the set of techniques proposed by 3GPP, that divide the network functions to different part to improve overall system performance [106].
- **Fronthaul:** It is commonly the link among the controller and the radio head or small cell. Also, it is the link between the radio head and UE device. It is considered as the

end link [100].

- **Midhaul:** It is the link between the controller the radio head that provides information to the next link [107].
- **Network Function Virtualization:** NFV facilitates the virtualization of the network services, such as routers, firewalls, and load balancers, packaged as VMs to enable that allow the mobile service providers may run their network on standard servers instead of proprietary hardware solutions [108].
- **RAN:** It is the mobile network part connecting the end-user devices by sending information via radio waves over the Internet. It performs complex processing and handle the increasing demand based on the user-specific services [109].
- **Virtualized RAN (vRAN):** It is virtualized RAN virtualizes the RAN functions to promote agility in RAN deployment and management offered by the service providers. vRAN eliminates the dependency on proprietary solutions and enhances flexibility in hardware, software and system integration [110].
- **Remote radio head:** It is the remote radio transceiver which maintain the connection to radio base station unit via electrical or wireless interface [111].
- **Software-defined network:** It facilitates network service management and faster configuration based on the software. It separates the CU and DU and centralizes the network control and configurations [112].
- **Virtual Machines:** It is the computing-enabled resource virtualization of a physical systems to execute and deploy programs and applications [113].
- **OpenRAN:** It defines interoperability of open hardware, software, and interfaces for the wireless cellular networks. OpenRAN disaggregates the RAN to facilitate an open user and C-Plane with incorporated synchronization and management plane [114].

### 3.2.3 Introduction to RAN functional splits

Among many organisations contributing to the xG cellular mobile telecommunication standards, the ITU and 3GPP are instrumental. The increasing complexity of the RAN and its management, the virtualization of network functions, the hope to deploy Artificial intelligence (AI) powered distributed networks, the benefits of open interfaces, and the potential to propose innovative connectivity-based services led many organisations and companies to push toward open RAN standard, including, maybe unsurprisingly to some readers, Facebook and Google.

Late 2020, the 2018-founded O-RAN ALLIANCE and the 2006-founded Next Generation Mobile Networks (NGMN) Alliance signed a cooperation agreement to *decompose* the RAN. As explained in the next paragraphs, RAN decomposition, radio network dis-aggregation, base station dis-aggregation and RAN functional splits are somewhat similar terms used when addressing the challenges of 4G and beyond RANs.

The NGMN Alliance is formed by service providers and has defined and developed many RAN topologies to model demand-service-cost-performance statistics. Distributed RAN (D-RAN) and C-RAN are dominant examples of the newly defined topologies based on the requirements. D-RANs demonstrate the lowest latency using Baseband Unit (BBU) at the cell site while requiring usually acceptable transport capacity. The C-RAN solutions propose centralized BBUs and thus require a high-performance transport layer. The C-RAN eliminates the requirement of configuring the individual cell site based on BBU's capacity [115, 116]. The C-RAN architecture is shown in Figure 3.4. The C-RAN consists of the Remote Radio Heads (RRHs) at cell sites connected via a FH network to BBUs in a BBU Pool (Farm or Hotel depending on the authors). The BBU Pools are connected to the Core Network via the backhaul (BH) network. The C-RAN topology eases the load balancing among the BBU computing resources [116].

Each RRH carries out radio functions, mainly at the physical layer, and is located at the cell site defining the mobile service coverage area. The BBUs are remotely located in BBU Pools and are responsible for processing the radio signal [117]. A BBU is executing and processing radio functions, for example, modulation, channel estimation, Fourier transforms, and error correction. The FH network should provide a low-latency high bandwidth transport for user and control data and synchronization, unless satellite-based synchronization at each cell site is preferred. Besides, it should also provide control and management of the radio equipment.

The CPRI and eCPRI standards specify the fronthaul connecting the BBU and RRHs (Figure 3.4).

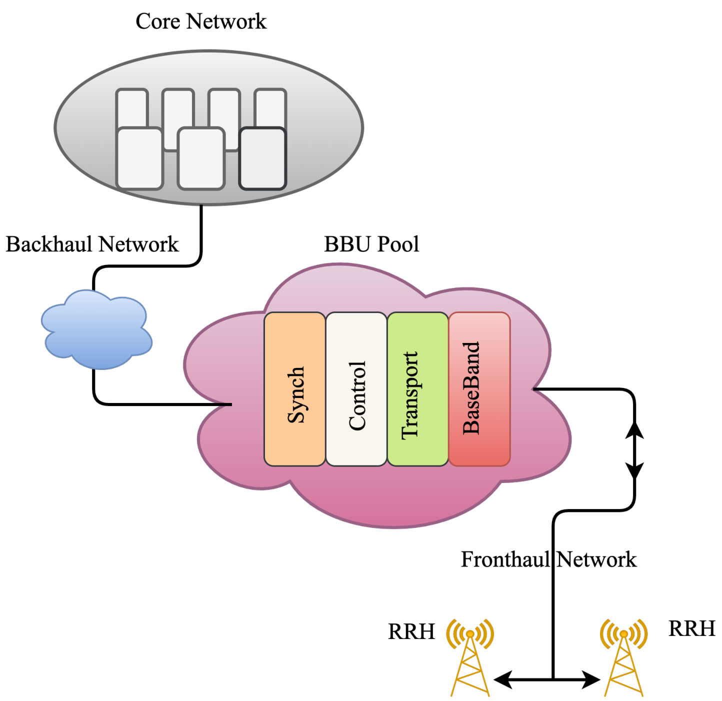


Figure 3.4: C-RAN architecture: the BBU and RRH are connected through the fronthaul while BBU and core network are connected through backhaul.

Most 2G and 3G cellular sites were deployed with a base station hosting both the BBUs and the Radio Units (RU), also called Radio Heads (RH) near the cell site mast and with coaxial cables to link the RUs and the antennas on the mast. The concept of separating the BBUs and RRHs with a point-to-point radio transmission or an optical fiber was first introduced in 3G. The BBU-RRH links are called the fronthaul (FH) links. In 2003, several equipment manufacturers defined the open CPRI specifications to transport, over the FH, I/Q user data, synchronization data and Control & Management data. The CPRI v7.0 was specified in 2015 [118]. The CPRI signals can be transported over an electrical cable but are usually transported over an optical fiber less than 2 km although the link could be as long as 20 km [119,120]. The CPRI line bit rate ranges from 1.288 Gbps to 24.3302 Gbps supporting one to twenty four (20 MHz 4G LTE signal). CPRI is a constant bit rate Time Division Multiplex (TDM) stream. Synchronization and accurate timing can be insured using global navigation satellite system, e.g., GPS, Galileo, QZSS, NavIC, and BeiDou, or via the CPRI link using the synchronous property of TDM signal, or PTP (IEEE 1588v2) or SyncE (ITU-T G.826x). All details can be found in the CPRI specifications [118]. Note that eCPRI, presented next, is replacing CPRI for the 4G and 5G FHs.

In 2017, the enhanced CPRI (eCPRI) [121,122] specifications started to be designed to enable 5G FHs to be carried using a continuous bit rate over dark fiber, WDM, and even Ethernet. In 2019, Ericsson, Huawei Technologies, NEC and Nokia updated the eCPRI specification enabling flexible deployments of FHs. The eCPRI allows splitting the physical layer to allow data FH bit rate raising from the CPRI maximum bit rate of 25 Gbps to any available bit rate, e.g., 100 Gbps [123]. The eCPRI also enables to analyze and prioritize traffic. The eCPRI splits are denoted A to E and the mapping to 3GPP splits is given in Figure 3.5 [122].

Despite the efficiency of the eCPRI, massive MIMO will impose high line rates requiring the use of Dense Wavelength Division Multiplexing (DWDM) if the processing for each MIMO antenna is kept at the BBU. In an experimental setup in 2020, Le et al. [124] demonstrated that *"an aggregated [5G] radio bandwidth of 25.6 GHz was transmitted on a single optical wavelength over 40 km without fiber chromatic dispersion compensation"*. Note that the distance of 40 km leads to a latency of 133 $\mu$s, below the maximum latency of 250 $\mu$s on the eCPRI fronthaul [72].

The C-RAN architecture was introduced for 4G. C-RAN places the BBUs in a centralized BBU pool (hotel or farm) [95]. Some advantages of the centralized radio signal processing of C-RAN are as follows:

- To share the BBUs resources on-demand depending on the traffic load on the attached RRH in the served cells: in the simplest scheme, BBUs can be launched or turned off as needed, and more complex schemes could optimize the resources allocated to BBUs while reducing energy consumption using AI techniques;
- To simplify or enable radio processing features requiring cooperation between cell sites, such as advanced interference management, fast handover, Coordinated Multi point (CoMP) transmission and reception;
- To virtualize some or all functions required from the BBUs;
- To simplify upgrades.

The C-RAN architecture with its BBUs and RRHs shown in Figure 3.4 is identified as one of the 5G enablers. Nevertheless, it is challenging to reach the high-capacity requirement of the FH network when centralizing the base band units for multiple antennas, especially for MU-MIMO. Some challenges have been addressed by the CPRI discussed in the next subsection. To reduce the load over the fronthaul, researchers are investigating techniques to maintain the benefits of the C-RAN and further reduce the burden on the FH link. Heterogeneous C-RAN (HCRAN) and Fog RAN (F-RAN) have been described to mitigate some C-RAN challenges [125–127]. Some details will be provided in the following sections. It is recalled that, in 5G and beyond, the Base band Units (BBUs) functionalities are split between Control Units (CUs) and Distributed Units (DUs) as shown schematically in Figure 3.1.

#### 3.2.3.1 3GPP, CPRI and eCPRI Functional Splits

3GPP has defined eight functional split options. They include further sub-splitting possibilities in the lower and higher physical layer [128]. DU's functions are highly near to the user and will be placed at the antenna side. The functions in the CU will benefit from the centralization processes as well as from the high processing powers within a data center. The functional splits proposed by 3GPP and eCPRI, Small Cell Forum and NGMN are presented in Figure 3.5 [122]. To improve the CPRI requirements, several higher-layer functional splits are proposed in the literature [129]. The proposal from [128] shifts the radio processing responsibility from the BBU to the RRH while reducing the burden of the FH. According to our research, the most beneficial and popular split is the option seven Physical (PHY) layer, and its underlying intra splits. Besides, split seven has further sub-splits that involve moving Inverse Fast Fourier Transform (IFFT), resource mapping, pre-coding, and cyclic prefix addition, functionalities to RRH, which efficiently reduce the load over the FH.

Split six is the Media Access Control (MAC) split, known as MAC-PHY split. It moves the RF and PHY and other functionalities to the RRH. Split option two is the split between the Packet Data Convergence Protocol (PDCP) and Radio Link Control (RLC). In this split, the network layer/PDCP functionality is kept in the BBU while all the other processing functionalities (RLC, MAC, PHY, and RF) shift to the RRH. Option 1 to option 6 are well-thought-out to comprise the higher layer splits [91].

Different splits have been defined in the eCPRI specification [131]. eCPRI has introduced splits named A, B, C, D, $I_D$, $II_D$, $I_U$, and E [130].

When presenting the split, the DL is usually considered first and the split is said to be between higher layer functions at the CU and lower layer at the DU. A single split defines: (1) a BH between the Core and combined CU/DUs, and (2) a FH between each CU/DU and RUs. Double split introduces a Midhaul (MH) between each CU and the DUs. A very good overview from Huber&Suhner show the detailed architecture and the elaborate terminology related to functional splits [132].

The mapping between eCPRI and (3GGP) splits is as follows:

- eCPRI A (3GPP 1), between user Data (IP in 4G) or Radio Resource Control (RRC) and Packet Data Convergence Protocol (PDCP);

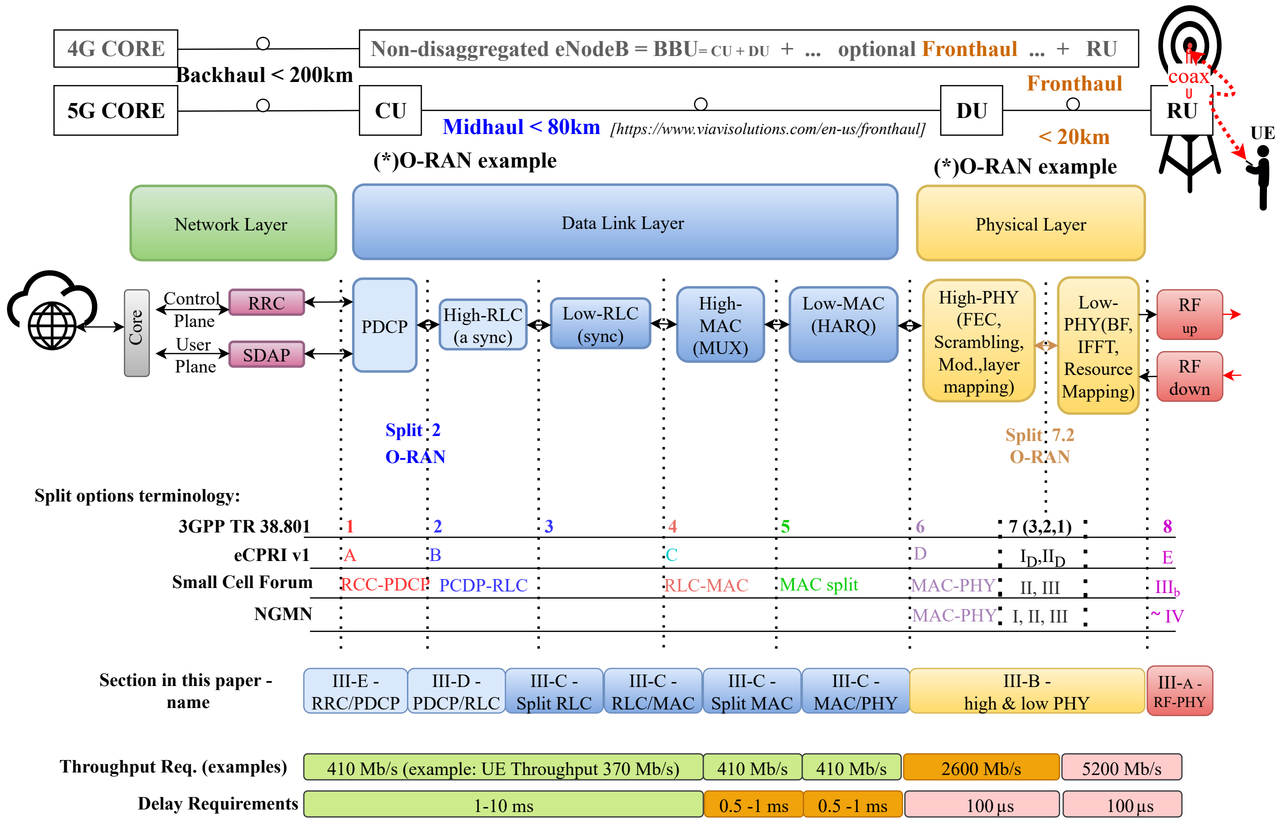


Figure 3.5: Different functional splits proposed by 3GPP [122], eCPRI, Small Cell Forum and NGMN [130] with different names.

- eCPRI B (3GPP 2), between PDCP and RLC (Radio Link Control);
- no eCPRI split for the 3GPP split 3 separating the RLC high and low (segmentation);
- eCPRI C (3GPP 4), between the RLC and MAC (Medium Access Control), i.e., the multiplexing controlled by a scheduler;
- no eCPRI split for the 3GPP split 5 separating the MAC multiplexing and MAC HARQ (in 5G NR, HARQ is asynchronous in DL and UL but in 4G/LTE, HARQ is asynchronous in the DL and synchronous in the UL);
- eCPRI D (3GPP 6), between the MAC (HARQ) and MAC-PHY (Forward Error Correction, Rate Matching and Scrambling, all bit processing before/after modulation/demodulation);
- eCPRI $I_D$ (3GPP 7.3) for the DL only (subscript $D$) between Scrambling and Modulation/Layer Mapping/Precoding;
- eCPRI $II_D$ (3GPP 7.2) for the DL only between the Precoding ($N$ symbols per antenna) and the Resource Element Mapping to each sub-carrier and beam forming Port Expansion (if any); for the UL: the corresponding eCPRI split is called $I_U$ between the Resource Element Demapping and the channel estimation and other received signal processing steps before demodulation;
- no eCPRI split for the 3GPP split 7.1 between the signal and the iFTT (for OFDM pro-

cessing) and addition of the Cyclic Prefix (to mitigate the multi path effects), in the DL;

- eCPRI E (3GPP 8) between the Cyclic Prefix insertion or removal and the RF (Radio Frequency) transmission in the DL or UL, respectively.

More details are provided in the next section.

As discussed in [133], data link layer splits (3GPP 1 to 6) offer gains in performance concerning CoMP, interference mitigation, scheduling and Radio Resource Management (RRM), and resource sharing, as more functionalities are centralized in the CU. Moreover, the CU can be connected to many DUs, controlling various cells in a reasonably large area.This change in the classical architecture improves and advances RRM and scheduling algorithms. However, this solution increases the complexity of the fronthaul interface and implies a potentially considerable increase in the latency and throughput. As a consequence, OpenRAN provides split option 7.2 (precoding/Resource Ethernet, RE, Mapper) only while avoiding split option 8 (digital/analog IQ symbols), e.g., tens of Gbps at mmWaves transmission transported for, say, 64 antennas would be very challenging to be carried on the fronthaul as terabits per second might be required. However, a Macro-cell site with some micro cells could be served using centralized BBUs.

According to 3GPP, there is market demand for two somewhat different split option opportunities. On the one hand, the first one consists of options 6, 7, and 8 (low level). It it targets the operators with sufficient fiber FH transport. On the other hand, options 1, 2, 3, and 5 (high level) splits may be deployed by operators that do not have fiber fronthaul transport yet or need to postpone investment in fiber transport.

#### 3.2.3.2 Open Radio Access Functional Splits

The introduction in 2016 of the open standards for RAN formed the basis for implementing functional splits [134, 135]. The split options rely on the available transport links and network services. Hence, using open standards makes the implementation and assignment of network functions flexible. Open Radio Access Network (OpenRAN) has been proposed to transform traditional communication systems towards an open, intelligent, virtualized and fully inter-operable RAN [136]. The OpenRAN Alliance (O-RAN), created in 2018, is a group aiming at enabling RAN key solutions based on general-purpose hardware and software-defined technology that can be open from different perspectives [137].

The main aim of the O-RAN openness is to break the vendor lock-in, proprietary execution of the software, underlying hardware, by launching open standard RF interfaces that increase operational savings using vRAN and C-RAN. The RAN openness will provide flexible deployment and access of BBUs, CUs, DUs and RRHs from different vendors to shape adaptable and scalable RAN networks. OpenRAN made network architecture flexible by adding FH and MH transport by offering alternatives to service providers.

OpenRAN concepts intend to enable any split to create flexible RAN architecture. In 2021, the O-RAN ALLIANCE defined a low-level split option 7.2x, between 7.2 and 7.1, i.e., be-

Table 3.1: Number of split options proposed by 3GPP.

| Split Number | Split Name | Covered in section 3.3 |
|---|---|---|
| 8 | RF-PHY | 3.3.2 |
| 7 | High-Low PHY Split | 3.3.3 |
| 6 | RLC-MAC, and PHY Split | 3.3.4 |
| 5 | | |
| 4 | | |
| 3 | PDCP-RLC | 3.3.5 |
| 2 | | |
| 1 | RRC-PDCP | 3.3.5 |

tween the 1-sub carrier by 1-symbol resource element de-mapper and the beam forming port reduction-expansion. Split 7.2x include fronthaul de-compression techniques of IQ signals.

## 3.3 3GPP Functional Splits

### 3.3.1 Naming Conventions

This section provides a detailed overview of the conceptual aspects of the 3GPP functional splits by analyzing and explaining the algorithms associated with each split. For the sake of of understanding and cross-reference, we provide a naming convention for the 3GPP-defined splits in Table 3.1. Detailed charts and tables are added for comparison among different simulators. Moreover, simulators/emulators that are frequently considered for functional splitting implementation are discussed. Tables 3.2, 3.3, 3.4 and 3.5 show specific simulators/emulators/analytical approaches.

### 3.3.2 RF-PHY Split (option 8)

Split eight was initially considered based on the traditional C-RAN design: the CPRI or another standard is used to link the BBU and Remote Radio Head or Unit (RRH/RRU) support [138]. Currently, the deployment of split option 8 is indeed still advantageous in some use cases.

Split option 8 is based on the CPRI industry-standard interface. CPRI provides the complete split-up of the Radio Frequency (RF) from the PHY layer to all-out virtualization gains. All the protocol layers from the PHY layer and above are centralized, resulting in a very compactly synchronized RAN, as shown in Figure 3.6. The placement of only the RF sampler and up-converter in the DU gives a precise and simple DU. This method enables the existence of several functions such as mobility and efficient management of the resources [139].

Bitstream over the FH link is continuously using split eight, and depends on the scales for the count of antennas [139]. This architecture moves New Radio (NR) functions from central to distributed structure. Its advantages are as follows [138]:

- It provides a flexible hardware implementation that supports scalable cost-efficient solutions;

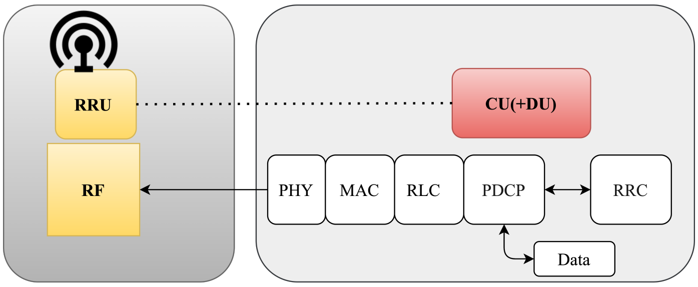

Figure 3.6: RF-PHY split architecture.

- The split between central and distributed units allows feature coordination, real-time performance optimization, and load management.

Moreover, the DU can assist multiple radio units in handling the digital signal processing and optimize the network traffic.

Field Programmable Gate Array (FPGA) is claimed to be one of the cheapest and possible selections for the implementation of split 8 [140], [141]. FPGAs consider the digital processing assignments in DU but they can correspondingly integrate analog sub-systems. gNodeB [142] from IS-Wireless (ISW) [143] is a software solution that can be deployed on either physical or virtual resources. ISW-gNodeB is a 3GPP-compliant implementation of the 5G-NR base station and enables any protocol stack cutting option. An ISW-gNodeB consists of independent Network Functions (NF), which implement 3GPP-compliant NR RAN protocols namely: PHY, MAC, RLC, PDCP, SDAP, RRC, NRAP. The ISW-gNodeB Network Functions can run together or independently and can be deployed on either physical (e.g., a small cell chipset) or virtual resources (e.g. dedicated COTS server or shared cloud resources).

Table 3.2 shows a set of characteristics for the RF-PHY split and indicates whether simulations, emulations, or analytical approaches have been conducted by researchers from the indicated reference.The PHY layer is shown in Figure 3.7.

### 3.3.3 High-Low PHY Split (option 7)

As shown in Figure 3.7, the physical layer is split in the High-PHY and Low-PHY. The low-PHY stays in the RUs while the high-PHY stays in the DUs, and handles the Forward Error Correction (FEC), among other functionalities.

The 3GPP option 7 split has centralization benefits through MIMO, Carrier Aggregation (CA), and Coordinated Multi-Point (CoMP) [157]. CoMP is seen as a significant candidate for 5G in terms of system performance improvement, and is separated into two classes: MAC sub-layer coordination and PHY layer coordination. CoMP include joint transmission and joint reception.

Figure 3.7 presents the functions of the PHY layer in the DL direction, and presents the data information that is exchanged between the different blocks. The transport block is the input to the PHY layer from the MAC sub-layer on the top. As we can observe, the PHY layer's overall procedures transform the transport block received from the MAC sub-layer into In-phase and Quadrature (IQ) symbols, as shown on the top of Figure 3.7. The transport blocks are en-

Table 3.2: Literature review on RF-PHY Split.

| **Concepts/Algorithm/Consideration** | **Simulator/Emulator /Analysis** |
|---|---|
| Encapsulating CPRI over Ethernet (CoE), stringent CPRI desires like delay jitter to make CoE a certainty, considered PHY RF split option 8 [140] | FPGA, MATLAB Simulink |
| Latency is mathematically analyzed using queuing theory, and closed-form formulas [144] | Mathematical analysis |
| Development of virtual network architecture while considering flexibility to choose the suitable functional split for respectively small cell [145] | MATLAB |
| Virtualized multi-layer cellular network [146] | Numerical model analysis |
| Real-time implementation of functional split among RRH and BBU, to balance the transmission throughput among RRHs and BBUs [141] | FPGA, MATLAB and Simulink |
| The software solutions offering 5G NR protocols to implement stack cutting of option 8 defined by 3GPP (between RU and DU) [142] | gNodeB (IS-Wireless) |
| Theoretical mathematical concepts on split 8 [147] [148] [149] [150] [139] [151] [152] [153] [154] [155] [156] | Analysis |

coded and segmented into block segments and then passed through the rate matching block. Next, the rate-matched codewords are scrambled. The scrambled codewords are then passed through the modulation mapper, where the bits are converted into symbols, according to the modulation order. Then, the layer mapping block takes the modulated symbols into account and maps them into one or various transmission layers [158]. The precoding block then precodes the symbols on each layer before transmission through the desired antenna ports occurs. The resource element (RE) mapper is responsible of mapping the antenna symbols into resource elements, converting them into subcarriers. These subcarriers pass through the IFFT block [159], which produces the IQ symbols in the time domain. Finally, the Cyclic Prefix is attached. This split is detailed in Table 3.3.

In the split 7 of the PHY layer, the IFFT transformations and the Cyclic Prefix insertion are computed in the DU [160]. Compare to split 7.1, the split 7.2 further reduces the bit rate over the FH by keeping two more functionalities at the DU: resource elements mapping and beamforming. Option 7.3 keeps even more PHY functionality at the DU, resulting in a complex DU and lower achievable bit rates: grey and blue functions in Figure 3.7. Each split has its benefits and drawbacks, as shown in Figure 3.8. The splits 7 are considered as the best compromises for the FH bit rate requirements versus advantages due to centralization. Hence, splits 7 are the strongest candidates to achieve high capacity in ultra-dense networks [161] and the FH bit rate is dropped to values comparable to eCPRI.

Splitting options 7.2, 7.3, 6 or below should be used to avoid considerable bit rates on the FH between the RU and DU. Table 3.5 contains additional details on the 7.x splits.

The PHY latency requirements are stringent due to the need for coordination from the upper layers. As elaborated in [162], the round-trip latency of 5 ms is required for Hybrid Automatic Repeat Request (HARQ), located in the MAC sub-layer. The comparison of PHY latency with

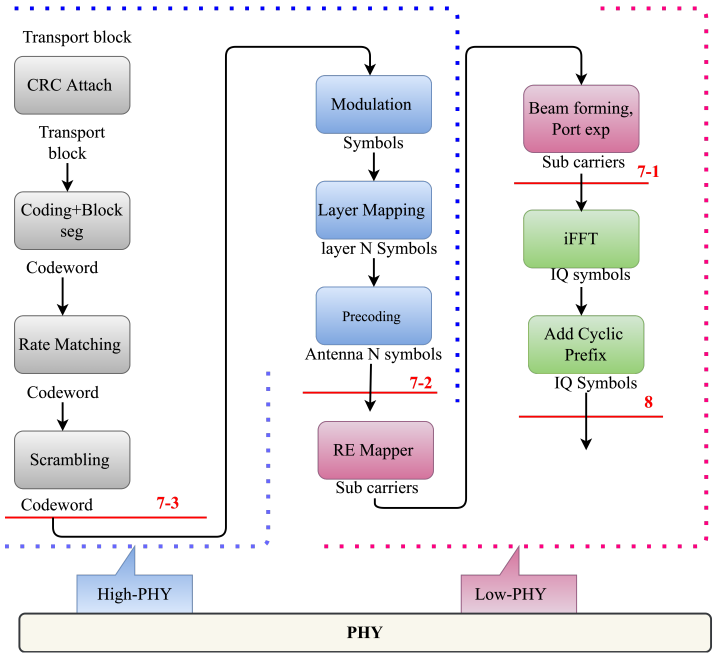


Figure 3.7: 3GPP split 7: detailed splits 7.3, 7.2, 7.1 and 8 in this (conventional although strange) order considering the downlink and the 4G/LTE protocol stack (5G NR is the same at this level of details).

the latency in splits from other layers is defined in [163]. These latency requirements limit the distance between CU and DU to 40 km of optical fiber [163], and from 15 to 20 km of dark fiber connectivity [164]. Note that splits 7.x requires the shortest CU-DU distances. Much longer CU-DU distances ($< 200$ km) can be achieved using for example split 2 as discussed later and shown in 3.5. More details are out of the scope of this introductory survey.

The one-way latency is defined in [129] by considering the PHY layer's ideal or near-ideal characteristics. Timing and other frame and subframe requirements are explained in [165]. Because of the automatic repeat request placement within CU, the PHY split options are reliable even with non-ideal transmission conditions. It is possible to relax the FH requirements in terms of latency and bandwidth, by considering the PHY and RF splits as the baseline. For example, to keep a processing FFT/IFFT block and subcarrier mapping/demapping at the DU reduces the FH bandwidth requirements by a factor of 2.5 [145]. By performing the IFFT/FFT function at DU, the cyclic prefix is removed from the Baseband signal, and only the received signals of the allocated Physical Resource Blocks (PRBs) are forwarded to the CU pool.

### 3.3.4 RLC-MAC, and PHY Split (option 6, 5 and 4)

The MAC sub-ayer, green box, in Figure 3.9 is an interface to the RLC layer: blue box. The MAC layer sends or receives the data from layer 1 using transport channels [180], while logical channel services provide the data transfer to or from the RLC sub-Low layer. There are 2 logical channels classified as traffic and control channels [181]. Data on a transport channel is organized into dynamic-sized transport blocks, whereas transport formats determine the configuration of the transport block.

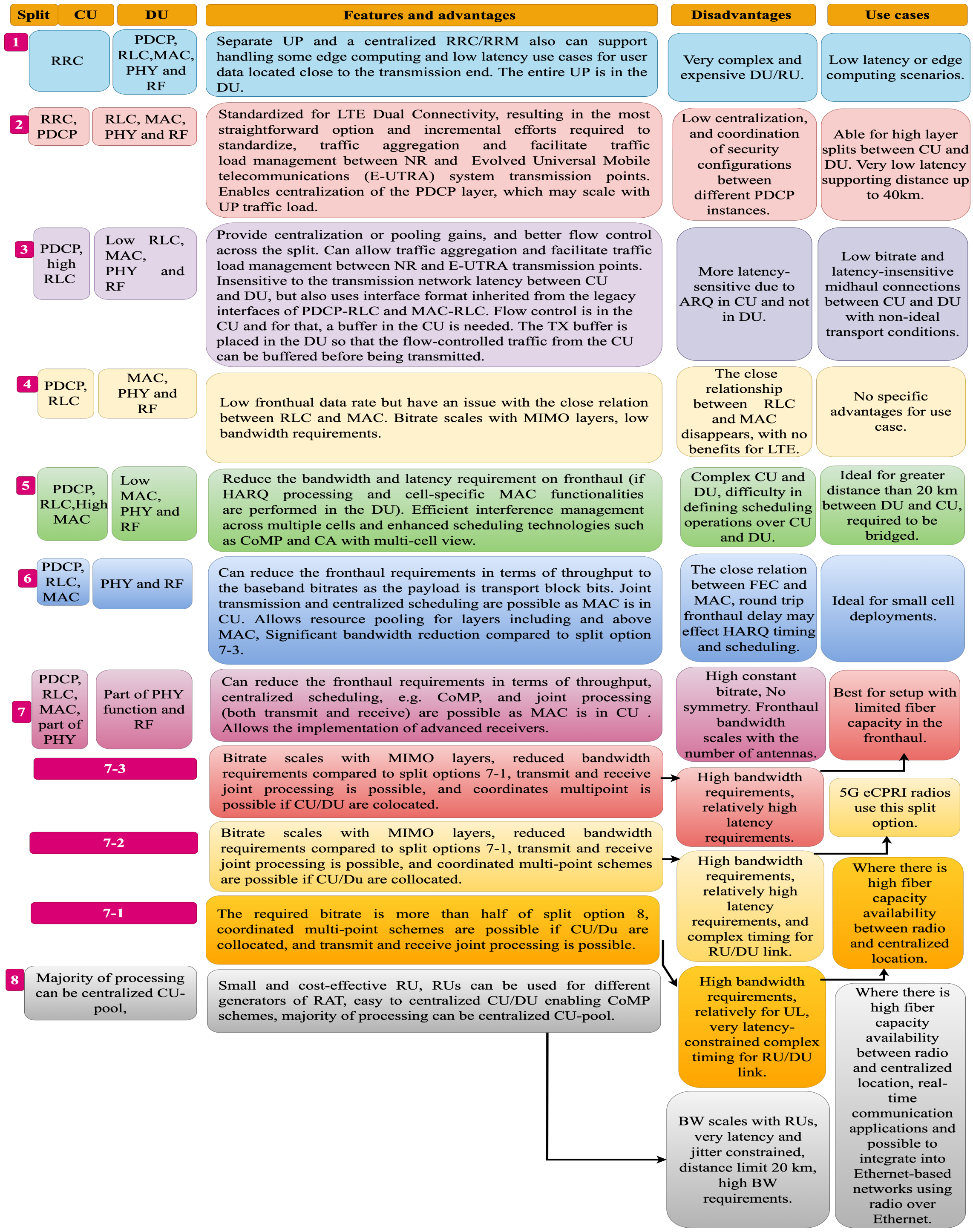


Figure 3.8: Advantages and disadvantages in the perspective of this survey.

Table 3.3: Literature review on the PHY (High-Low) split.

| Concepts/Algorithm/Consideration | Simulator/Emulator /Analysis |
|---|---|
| Exploited functional split at PHY utilize it to serve RAN in capacity-limited scenarios [166] [167] | MATLAB |
| Implementation of split 7 by using OAI considering NR [168] | OAI |
| Prototyping validation of a DU Lower PHY transmission chain, for 5G and NR [169] | FPGA, MATLAB and Simulink |
| Design of an adaptive RAN that switches between two different centralization options at runtime, switch from MAC-PHY to PDCP-RLC without service interruption [170] | B200 1 Gb/s Ethernet link |
| Spliting for efficient fronthaul, to enable the consumed bandwidth with cooperative radio, intra-PHY functional split C-RAN architecture and 7.1, 7.2 and 7.3 splits [161] | OAI |
| MAC-PHY split generation to find an amount of overhead traffic on the downlink [171] | srsLTE |
| 5G-NR DU CU, UL receivers implementation [172] | FPGA, MATLAB and Simulink |
| Complexity of the RRU with 5G NR considering functional split 7.2 [173] | FPGA |
| The software solution to implement stack cutting option defined by 3GPP at option 7 (between RU and DU) [142] | gNodeB (IS-Wireless) |
| Survey papers, theoretical mathematical concepts [161] [171] [172] [173] [174] [175] [176] [177] [145] [178] [179] | Mathematical theoretical analysis |

Based on the Protocol Data Units (PDUs) delivered from the RLC sub-layer towards the MAC, MAC Service Data Units (SDUs) are configured and later converted to MAC PDUs, which are provided later on in a form of transport blocks to the PHY layer. Each transport block is transmitted in a single transmission time interval in the MAC sub-layer. The MAC sub-layer details for multiple underlying UE MAC entities, are explained in [180]. The MAC sub-layer has a set of functionalities defined in [182]. The 3GPP sets rules for mapping the logical channel traffic to transport block are addressed in [182].

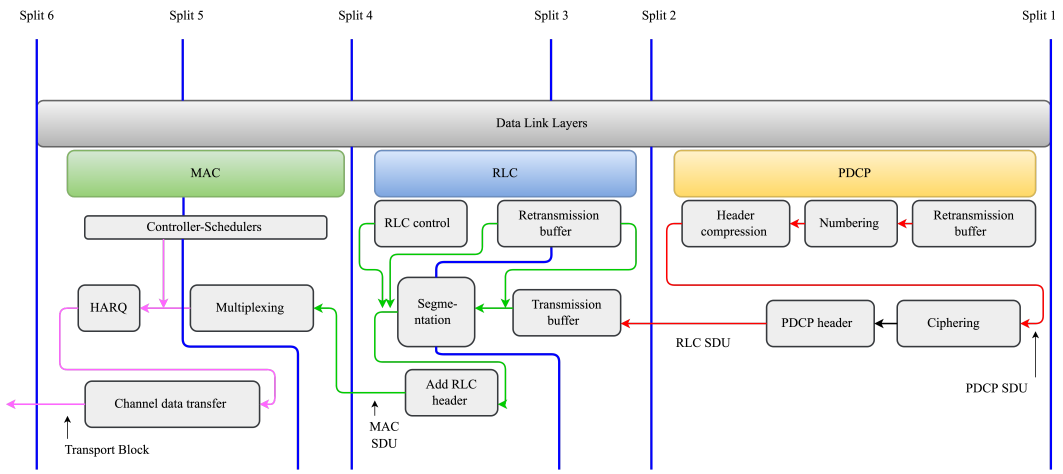


Figure 3.9: Architecture of split 1 to split 6 of the data link layer: from PDCP to RLC to MAC in the downlink.

The MAC sub layer handles the resource scheduling. It plays a fundamental role in the implementation of Carrier Aggregation (CA) techniques. The MAC Layer generates one transport block per transmission time interval (TTI) per component carrier. The MAC sub-layer shares the MAC packet data units and control elements over different component carriers. Each component carrier within the MAC sub-layer has its own HARQ entity. All the cells involved in CA within the cell group are under a single MAC entity. Authors in [15] and in [183], [184], [185] addressed the aspects of CA and Dual Connectivity (DC) with respect to the MAC sub-layer. Due to the execution per TTI, the MAC scheduler requires very low latency and low jitter [186]. The NGNM Alliance [187] warns that placing the MAC functions in a CU-pool (split 5 or 4) can limit the CoMP functions performance.

The functional split options 1 to 5 have relaxed latency requirements on FH, as the HARQ processing and other time-critical functions are placed in the DU close to the antennas. According to [151], setting the MAC in the CU pool will ease the use of LTE-Advanced in unlicensed bands.

With split 5, low and high RLC, PDCP and RRC will be in CU, and the low MAC (HARQ, multiplexing/scheduling) will be in DU. Functions like scheduling decisions can be performed at CU, for example, inter-cell interference coordination, CoMP. With split 5, the HARQ, a MAC time-critical processing tasks are computed at DU [188]. The split 5, with the High MAC containing multiplexing and scheduling decision at the CU, simplifies the MAC management by the mobile network operator [189].

The split 6 or MAC-PHY split and its resulting reduced FH bit rate requirements are addressed by 3GPP in [190, 191]. The split 6 (MAC-PHY) specifies the transport of MAC PDUs

Table 3.4: Literature review on split between MAC (High-Low) and PHY split.

| **Concepts/Algorithm/Consideration** | **Simulator/Emulator /Analysis** |
|---|---|
| To minimize the intercell interference the fronthaul bandwidth utilization by dynamically selecting the appropriate functional split considering PHY-MAC split [193] | MATLAB |
| Trade-off between bandwidth and RRU complexity for different split [173] | FPGA |
| Optimization of processing bandwidth resource usage, minimizing the overall energy consumption compared to i) cell-centric, ii) distributed and iii) C-RAN approaches [194] | OAI |
| Examine Ethernet as FH work in C-RAN, with focusing on the MAC and PHY split [195] | OAI |
| Theoretical mathematical concepts [165] [196] [197] [198] [199] [200] [201] [189] [202] [203] [204] [205] | Analysis |

instead of IQ-data blocks. The split 6 is advantageous compared to CPRI as it decreases the fronthaul capacity requirement: for example, [190] reported a fronthaul bit rate of about 137 Mbps for the split 6 while split 8 requires over a 100 times more: 14700 Mbps for 4G. For 5G: 7 Gbps (split 6) is required instead of 157 Gbps (split 8).

The Small Cell Forum favors the Split 6 to reduce costs of 4G and 5G small cell deployments. The Small Cell Forum publishes the so-called 5G network functional application platform interface (5G nFAPI). The 5G nFAPI extends for 5G the functional split between the MAC and PHY functions to enable virtualization of the MAC function. The nFAPI support communication between the Virtual Network Function (VNF) handling the MAC sub-layer in the DU and the Physical Network Function (PNF) in the RU. Note that the Small Cell Forum refers to S-DU and S-RU instead of DU and RU [192].

Table 3.4 provides a glimpse on several papers discussing the split 6 to 4, i.e., the MAC (High-Low) and PHY splits.

### 3.3.5 PDCP-RLC split (3GPP option 3 and 2)

The 3GPP defines the split 2 as the split between the Radio Link Control (RLC) in the DU and Packet Data Convergence Protocol (PDCP) in the CU [206]. The 3GPP Split 3 separates the RLC by keeping the segmentation (Low RLC) at the DU and the other RLC functions (High RLC) at the CU [206]. split option 3 is further studied in [206].

The PDCP maintains the real-time operation using a buffer at the RLC level. Every incoming packet from the U-Plane, i.e., the Internet Protocol (IP)+SDAP packet is processed by the PDCP. The PDCP handles packet buffering and retransmission, layer 2 numbering, header compression, ciphering, and integrity protection before the RLC in the downlink. The RLC handles bufferization, segmentation, and ARQ retransmissions.

According to [151], the PDCP centralization in the CUs, i.e., the 3GPP split 2, is a 5G enabler. The delay sensitive processing of ARQ retransmissions is kept at the DU which can be close

Table 3.5: Literature review on PDCP-RLC split

| Concepts/Algorithm/Consideration | Simulator/Emulator /Analysis |
|---|---|
| Different functional splits implementation in C-RAN [207] | OAI |
| The CU/DU C-plane split at the RRC/RLC [208] | OAI/SDR |
| Split buffering between the RLC PDCP layers. PDCP buffer with per-flow queues, and applied to the RLC buffer a new dynamic sizing mechanism that enforces the lowest queuing delay that is compatible with the existing configuration of the RLC connection [209] | OAI |
| C-RAN based architecture allows the selection dynamic switching of different hetnets in the RAN [210] | OAI |
| Software solution to offer NR RAN protocols such as PHY, MAC, RLC, PDCP, SDAP, RRC, NRAP in Option 2 (between DU and CU) [142] | gNodeB (IS-Wireless) |
| Surveys, theoretical mathematical concepts [211] [212] [213] [214] [211] [215] [216] [217] [218] [219] [220] [221] [222] [223] [224] | Analysis |

to the RU.

According to [207], one PDCP traffic flow is considered per radio bearer. The traffic Split 2 is organized into several flows. Each flow can be directed to various access nodes and support multiple types of connectivity. According to [129], split 2 keeps real-time support in the DUs, resulting in a relaxed CU-DU link requirement.

Figure 3.11 compares the bit rate among different functional spitting options in uplink and downlink. Table 3.5 contains additional details on the PDCP-RLC split (split 2).

The PDCP handles both the NAS/RRC messages for the C-Plane, and the IP/SDAP for the 5G U-Plane. Thus, the CU is composed of two logical components, one for the c-plane and one for the UP as defined in the context of Software Defined Network (SDN). Some authors use the term CU/c-plane split but this should not be confused with the functional splits discussed here. Based on the functional split requirements, all the network functions at the CU are organized as either part of the c-plane or UP [98].

In the RRC-PDCP (3GPP option 1) split, the whole processing for the control and U-Planes is placed in the DU. Split 1 is thus not very different from the usual Core-BBU-RRH. As the processing of the user data is now near the transmitter there is an advantage for caching. However, features like inter cell coordination are not supported in this split 1 option. Consequently, split 1 is not advantageous if many cells are connected to a CU pool [95], [225].

The control and U-Plane splitting are designed and implemented in [150]. The RRC in the DU handles the C-Plane functions in this split 1 while the U-Plane functions are handled by the new 5G Service Data Adaptation Protocol (SDAP) to handle new services beyond IP for 4G. Authors from [226] show that the split option 1 (also called PDCP/RRC) requires low C-Plane overhead, which benefits load balancing and mobility management using virtualization. In [227], complete and partial scheduling processes are performed at the RRC.

### 3.3.6 Functional Splits Requirements

The maximum latency requirement of each split option is shown in Figure 3.10. The splits 8 to 5 require a latency less than ms because more processing at DU . Split 3 and 2 requires a latency of 5ms or less which is higher as compared to split 8 to 4 because of less functions at CU . Split 1 has the less tight requirement, 10 ms.

The DL and UL data rate of different splits. Figure 3.11 compares data rates according to the Small Cell Forum. One can see that all the considered references suggest higher fronthaul bit rate between split options 5 to 8. High and low mm Wave band communications perform better for split option 7.1 and 7.2 compared to 5G/ band of less than 6 GHz. Overall the split options 8, 7.1 and 7.2 provide higher bit rate over the FH.

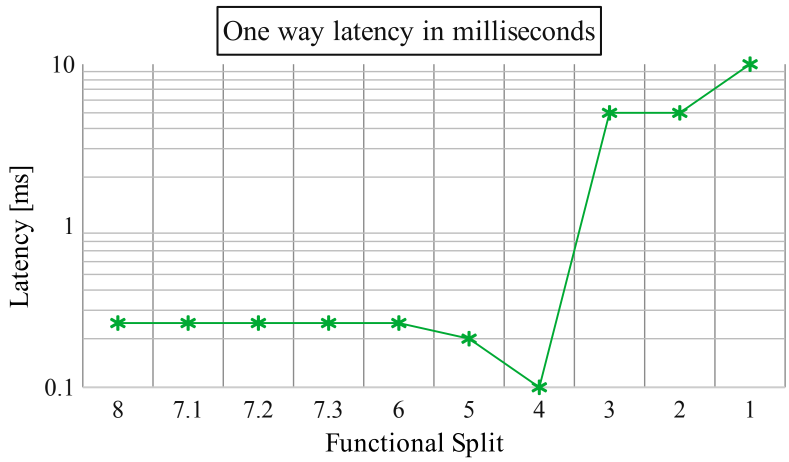


Figure 3.10: Latency for different functional splits [129] [228] [229].

Figure 3.12 presents a comparison of different simulators/emulators considered for the implementation of the splits by other researchers.

Mainly the Physical (PHY) layer split implementation is analyzed, and authors considered FPGAs (62%, i.e., 31 out of the 50 papers considered here) and MATLAB (60%) For overall split implementation and testing in different scenarios, Software Radio Systems (30%),(srsLTE, now srsRAN) and (20%) Open Air Interface (OAI) have been considered, among others. This analysis is based on the research papers listed in the tables from this survey.

## 3.4 Fronthaul

Figures 3.1 and 3.4 show the FH network link, usually formed by optical fibers or wireless connections, from the BBUs or DUs to the radio equipment (RRHs, RRUs or RUs) linked via coaxial cables to the antennas, as discussed in , e.g., [157]. The FH carries the data, control, synchronization and operation & maintenance signals. 5G developments challenges current

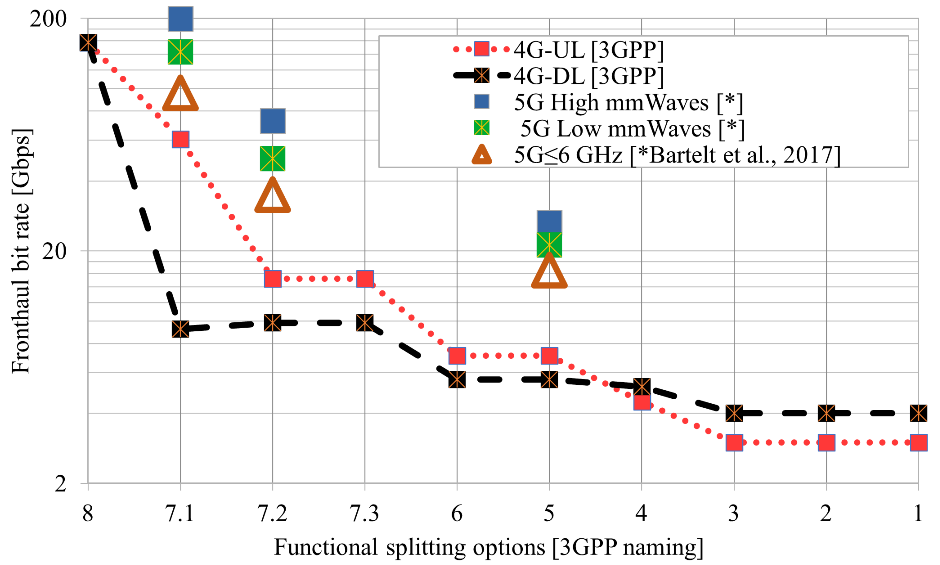


Figure 3.11: Fronthaul bit rate (log scale) for different split options according to 3GPP [228, 230], Small Cell Forum [129] and Larsen et al. [95] for 4G (lines), and according to Bartelt et al. for 5G sub 6 GHz (triangles) and near mm Wave bands (squares) [231].

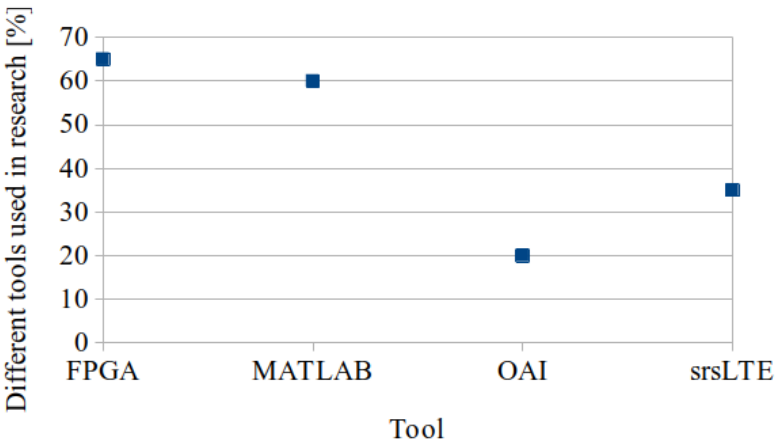


Figure 3.12: Different simulators used for implementing functional splits.

FH transport and next-generation FH interface, radio-over-fiber, and xHaul were investigated in [121, 232–234]. Some more details are mentioned in the next sub-sections.

### 3.4.1 Requirements and Standardization Bodies

The FH requires high data rate, low latency, low jitter, and low packet loss. The data rate for CPRI is 2.46 Gbps in LTE Networks while the eCPRI capacity reaches more than 10 Gbps [157, 235, 236].

The traditional approach for the transport layer is not expected to continue within 5G and beyond. Instead, next-generation networks require integrated BH and FH technologies that can minimize Operational Expenditure (OPEX) and Capital Expenditure (CAPEX). Authors from [233] present the architecture integrating FH and BH in a shared packet-based network defined as the Xhaul. In fact, the research community has shown that operators are getting more interest in the FH. In a survey of global operator 2020 [237], it is reported that 46% of FH support will be needed for functional split implementation.

Realistic functional split implementation require standards and virtualization. The European Telecommunications Standards Institute (ETSI) is one of the international bodies that is very active in standards related to virtualization and C-RAN concepts. According to ETSI, base stations are held in cloud computing centers. With virtualization, the BBU, usually located at the base station sites can be moved to data centers, providing the opportunity for easier load balancing. Virtualization of RAN functions facilitates the distribution and shift of the functions across data centers, providing enhanced load balancing and advanced cooperation between antenna sites.

### 3.4.2 Delay

The FH architecture must satisfy specific 5G end-to-end delay to offer time-critical 5G services, such as URLLC. Some envisioned 5G applications could require delays as low as 1 ms. The FH transport within the PHY layer corresponds to options D and E in eCPRI I [238], i.e., 3GPP split 6, 7 and 8. In this context, the HARQ protocol limits the maximum delay between the BBU (or DU) and RRH. For example, after transmitting three 1 ms sub frames, the UE sends a positive or negative acknowledgement in the fourth sub frame. All the processing at the BBU or DU must be finalized and the frame is created before three sub frames, i.e., 3 ms [239].

In [240], the suggested processing time of the BBU is 2754 $\mu$s. The 3 ms HARQ limit implies a FH path round-trip time of 246 $\mu$s. Thus, the maximum FH one-way latency is 123 $\mu$s, or about 24 km assuming, as usual, a propagation speed of 200 m/$\mu$s.

Other authors, such as [239, 241, 242] and IEEE 802.1CM, consider a slightly stricter requirements for the delay, i.e., 100 $\mu$s for one way communications. This 100 $\mu$s maximum delay results from a breakdown of the HARQ processing which ensures the best performance for the FH. Delays longer than this target would degrade the performance of the radio network [239]. In the transmission path using optical fiber, the delay is close to 5 $\mu$s/km. Consequently, the maximum distance must be less than 20 km to accomplish the 100 $\mu$s highest end-to-end one-way delay limit.

### 3.4.3 eCPRI

In LTE-Advanced, FH connections could use the CPRI protocols, while for 5G NR, eCPRI has been introduced [121]. Going toward the 2nd phase of 5G and beyond, more and more operators might consider the C-RAN architecture. With 4G, 5G NR and dual connectivity, the fronthaul network will carry an amount of traffic which is challenging the CPRI interface.

Currently, for 4G, several Telcos use the CPRI interface for their FH connections. CPRI is a point-to-point interface and considers that operators will use the same vendors at each end of the FH. In turn, the eCPRI interface is open and supports virtualization options, like software-defined network and network functions virtualization. eCPRI is claimed to provide more flexibility to operators to complement networks with shared equipment, improve bandwidth efficiency, and simplify deployments. However, unlike the CPRI, eCPRI neither supports end-to-end synchronization. eCPRI supports and recommends the PHY splitting. Besides, to reduce cost, eCPRI allows deployments using Ethernet transport technology.

In [243], the CPRI to eCPRI replacement have been implemented. Based on the specification of eCPRI, data has been encapsulated in eCPRI format to create eCPRI packets. The system in [243] supports the raw Ethernet header, in which the payload contains one eCPRI message.

#### 3.4.3.1 eCPRI Protocol Planes

The eCPRI specification defines three protocol planes between the eCPRI Radio Equipment (eRE): RU, RRU or RRH and eCPRI Radio Equipment Control (eREC): DU. The first is the U-Plane, the second is the control and management plane while the third is synchronization plane. Some details are provided as follows:

- The U-Plane data protocol deals with user data, the real-time control information and related eCPRI services depend on the functional split implementation for the user data;
- The control and management involve non-time-based data flows within eCPRI nodes;
- The synchronization plane carries time-critical information essential for frame and time alignment, utilizing protocols such as precision time protocol (PTP) and SyncE.

#### 3.4.3.2 eCPRI Frame

the eCPRI framing is supported by an Ethernet frame whose sections are transported by using separate layers of the Ethernet frames. The eCPRI message (header) contains four sections, while the reserved portion keeps the payload. Details are as follows:

- The eCPRI protocol revision contains 4 bits.
- C is one bit and shows the eCPRI concatenated message. If it is 0, it indicates that the alternative frame of the same group follows. Otherwise, if it is one, it shows the last frame of the concatenated group.
- The message type section contains 8 bits and the payload size contains 16 bits that follows the eCPRI (message) header. There are eight different payload types carried in the eCPRI frame payload, that includes IQ data transfer, bit sequence transfer, real-time control data, generic data transfer, remote memory access, one-way delay management, remote reset, and event indication. These message types are defined as follows [244]:
  - **eCPRI Message Type 0 - IQ Data Transfer** specifies the time/ frequency domain - IQ sample transfers between eREC (BBU) and eRE (RU), with the vendor-defined structure for the payload;
  - **eCPRI Message Type 1 - Bit Sequence Transfer** specifies the transfer of user data between eREC and eRE;
  - **eCPRI Message Type 2 - Real Time Control Data** specifies the vendor-specific

real-time control messages associated with user data (IQ samples, bit sequence) between eCPRI nodes (eREC and eRE);

- **eCPRI Message Type 3 - Generic Data Transfer** specifies the transfer of the U-Plane and control messages for generic data transfer and data synchronization;
- **eCPRI Message Type 4 - Remote Memory Access** allows read/write action from/to opposite eCPRI nodes at a specific memory address using remote units. This service facilitates different read/write accesses depending on the driver routines and hardware implementation;
- **eCPRI Message Type 5 - One-Way Delay Measurement** estimates the one-way delay between two eCPRI-ports, unidirectional. The local time is sampled by the sender, including a Compensation Value (CV), while the receiver, time stamps the message on arrival and reverts it to the sender with an internal CV;
- **eCPRI Message Type 6 - Remote Reset** is used when one eCPRI node requests a reset of another node. eREC sends the request to initiate an eRE reset;
- **eCPRI Message Type 7 - Event Indication** is used to inform the end of a link fault.

## 3.5 Virtualized Radio Access Network

This section first recalls some basics related to virtualization and discuss then virtualized RAN.

### 3.5.1 Network Functions Virtualization and Software-Defined Networking

NFV and Software-Defined Networking (SDN) is considered a key pillar of 5G. SDN and a key protocol called OpenFlow are promoted by the 2011-founded Open Networking Foundation (ONF). The operator-driven SDN & Open Flow proposal led to the creation within the ETSI of the NFV Industry Specification Group (ISG).

The 3GPP 5G architecture defines several core Network Functions (NFs), such as the Session Management Function (SMF) controlling the User Plan Function (UPF) via the N4 interface. By separating the SMF/controller from the UPF/packet forwarding element, the 3GPP 5G architectures follow the SDN concept of separating the control from the user traffic switching, a concept appropriately short named by 3GPP as CUPS (Control/U-Plane Separation). CUPS was introduced by 3GPP for 4G and 5G.

To satisfy mobility requirements in the core network, the controlling protocol running over the N4 interface between the C-Plane (SMF) and the U-Plane Function (UPF) is not OpenFlow but the Packet Forwarding Control Protocol (PFCP).

The RAN's Access and Mobility Management Function (AMF) are linked to the 5G base station (gNBs), forming the RAN via the N2 interface. The gNBs are interconnected via the Xn interface. Mainly for access and handovers, the protocols over N2 and Xn are NGAP and XnAP, respectively, for the C-Plane and GTP-U for the U-Plane. Additional RAN controls and the virtualization of the controllers are not standardized and led to initiatives from operators and vendors to improve the RAN.

Virtualization techniques can be adapted to perform RAN enhancements. Virtualization technology separates the software from the hardware, i.e., the network and computing resources from the physical resources. The primary purpose of virtualization is to incorporate scalable and flexible solutions like efficient resource and cost management, load balancing, automatic scaling, operation and control procedures, and, it is often claimed to enable the introduction of Artificial Intelligence and Machine Learning based control. Virtualization allows MNOs to engineer the network by centralizing the network equipment to high-volume industrial servers, switches, and storage, among others, so-called Commercial Off-The-Shelf (COTS) equipment such as x86 physical machines or P4-devices. The centralized units, BBU, CU or even DU in the context of RAN, may reside at the data centers, and/or at so-called Point-of-Presence (PoP) or at or near the users premises, e.g., in the case of Private 5G [245].

### 3.5.2 Distributed RAN and C-RAN

The D-RAN concept is presented to understand basic virtualization. Each cell site is composed of isolated RRU and BBU subsystems in a D-RAN architecture. The RRU unit is connected to the assigned BBU through the FH connection using CPRI. Cells are equipped with radio functions and connected to the core network via the backhaul. Figure 3.13 presents the basic D-RAN architecture. Depending on the network requirements, network resources are allocated dynamically by the BBU [246]. The BBU, or more realistically, some parts of the BBU, may run on virtual machines (VMs). VMs and co-locating the BBUs led to the C-RAN architecture presented below.

The fundamental of C-RAN architecture is to separate all BBUs from their RRU subsystems and move the BBUs to a centralized, shared, possibly virtual pool. The BBU subsystem is centralized in C-RAN. Each C-RAN cell site is composed of the antennas and the RRU subsystems. Figure 3.4 shows the basic C-RAN architecture. In C-RAN, network-related resources are kept at the edge, at the RRUs, and the core functionalities reside in the BBUs in the cloud. As a result, C-RAN networks are more flexible and, in some case, easier to deploy and maintain than the classic D-RAN if the fronthaul bit rate is supported.

C-RAN implementations are based in generic terms on Cloud Computing. Cloud Computing is the services provided by clusters of networked elements which may or may not be user-administered. In the context of cellular networks Cloud Computing allows Mobile Network Operators to store vast volumes of data generated by the devices and network and to insure cost effective sharing of required computing resources. In fewer words, C-RAN, like Cloud Computing, could ease on-demand availability of the networked data for RAN optimization. Sharing the COTS computing power and storage between BBU and end users seems obvious at first but might to very challenging to implement practically and securely.

C-RAN like Cloud Computing techniques present some challenges: increased latency, potential traffic congestion, increased data processing time if the computing resource in not available, and communication costs. To mitigate some challenges of Cloud Computing: Vir-

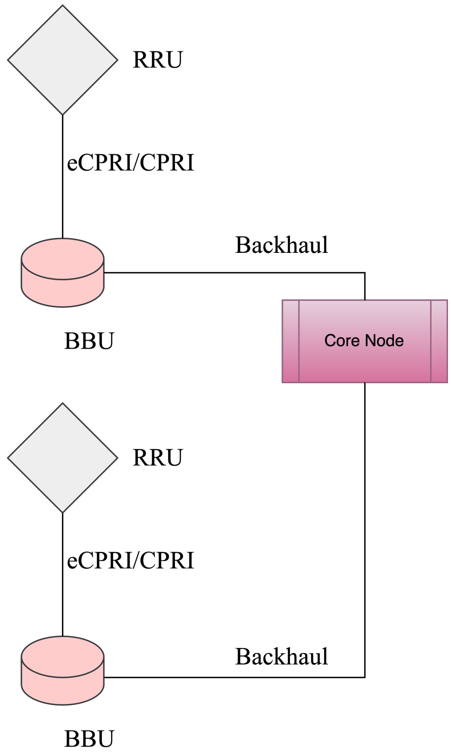


Figure 3.13: D-RAN architecture: the classical setup with the antennas, RRU and BBU at each base station site. The short RRU-BBU fronthaul link remains proprietary although CPRI is used. The backhaul is connected to a core node, usually over optical fiber or point-to-point microwave link.

tualization, Edge-Computing and Fog Computing could be presented as solutions.

### 3.5.3 Virtualized or Virtual RAN

MNOs migrate the data center to Mobile Edge Computing (MEC) to achieve high performance at the user end while supporting many devices. MEC reduces latency and offers high data capacity. They are incorporating NFV and SDN technologies with C-RAN to help virtualize the RAN functions and resources and are thus called “virtualized-C-RAN” or “vC-RAN”. vC-RAN implementation is related to specific characteristics of the wireless access network, like time-varying channel conditions, interference, UE distribution, and mobility.

Appropriate resource allocation, optimized interference management, etc., are challenging from the MNOs’ perspective. The author from [247] proposed the concept of the virtualized base station to facilitate the virtualization of the computing resources of a BS in vC-RAN. The virtualized BS executes multiple protocol stacks of a BS in software while sharing the radio equipment at the hardware end. MNOs have been implementing techniques to achieve enhanced energy efficiency and decreased OPEX, as discussed in [247].

The virtual RAN (vRAN) isolates the software from the hardware by implementing the network virtualization functions. vRAN separates the RRU from BBU on a General-Purpose Processing (GPP) unit and implements functionalities in software. vRANs are composed of centralized pools of BBUs, virtualized RAN control functions, and optimized service delivery protocols. vRAN could offer several advantages over conventional RAN deployments, such as scalability, flexibility, faster upgrade cycles, resource pooling gains, and centralized scheduling.

### 3.5.4 Fog Radio Access Networks

Centralizing the BBUs far from the base station sites might raise concerns about optimizing local RAN problems such as handovers, local interference, and services to static users.

Edge Computing and Fog Computing solutions have probably inspired the terms Mobile Edge Computing (MEC) mentioned earlier, and Fog-RAN (F-RAN) presented very briefly. Fog Computing forms a distributed computing environment that enables storage and data processing at the network edge [248]. The RAN architecture that enables fog computing is known as Fog-RAN, F-RAN, or F-RAN [249, 250]. F-RAN aims to facilitate the processing the generated raw data at the computing units at the user end or closest proximity. Hence, FRAN forwards processed data instead of raw data, resulting in a decreased requirement for high bandwidth and QoS enhancement [251]. Thus, F-RAN, C-RAN, HCRAN (Heterogeneous C-RAN) [126, 127, 252], and other cloud-based RAN will certainly be re-visited and further improved. In the evolution of the RANs, the OpenRAN has gained particular attention. OpenRAN is discussed in the following section.

## 3.6 Open Radio Access Networks

The terms Open RAN, OpenRAN, O-RAN, ORAN can all be found in the literature. However, we cannot claim to present a unique definitions for each of these terms. The industry-focused Telecom Infra Project (TIP) initiated an Open RAN MoU Group in 2020 to "supports the development of dis aggregated and inter operable 2G/3G/4G/5G NR Radio Access Network (RAN) solutions based on service provider requirements", quoted from [253]. The O-RAN ALLIANCE "has been founded in February 2018 by AT & T, China Mobile, Deutsche Telekom, NTT DOCOMO and Orange. It has been established as a German entity in August 2018. Since then, O-RAN ALLIANCE has become a world-wide community of mobile network operators, vendors, and research & academic institutions operating in the Radio Access Network (RAN) industry", quoted from o-ran.org. The TIP OpenRAN and O-RAN ALLIANCE are joining forces to promote Open RAN.

### 3.6.1 Working Alliances and Groups

The O-RAN ALLIANCE [136] specifies open industrial standards for RAN interfaces that support interoperability. The preeminent intention for supporting new OpenRAN and vRAN architectures is to detach individual base station components and facilitate independent interactions. OpenRAN assures inter operable RAN elements, both hardware, and software, from different vendors. Open RAN promotes 3GPP based vRAN architectures and provides MNOs with capabilities to overcome the challenges with proprietary hardware and software. The vRAN technologies aims to foster the development of OpenRAN standards by specifying open interfaces between the DU and CU and BBU. The DU/CU/BBU separation is based on the concept of the functional splits [254] and is claimed to enhance security, flexibility, and reduce CAPEX and OPEX costs. The DU/CU/BBU separation should provides MNOs with opportunities in the allocation of the functional blocks to maximize performance. OpenRAN will empower smaller MNOs and vendors to introduce their services and network customization based on requirements and needs [136].

Different working alliances towards OpenRAN are mentioned in Figure 3.14 [255–260]. The main purpose of these individual alliances and collaborations is to drive openness and interoperability in the RANs from 2G to 5G systems. The OpenRAN initiatives provide software and hardware solutions to support implementing an open and intelligent RAN. The O-RAN ALLIANCE specifications allows to build an open and modular RAN architecture based on 3GPP and dis-aggregated base station software. The O-RAN ALLIANCE has its own defined working groups to achieve the mission and vision of the Alliance. The different OpenRAN working groups are summarized in Figure 3.15 [261].

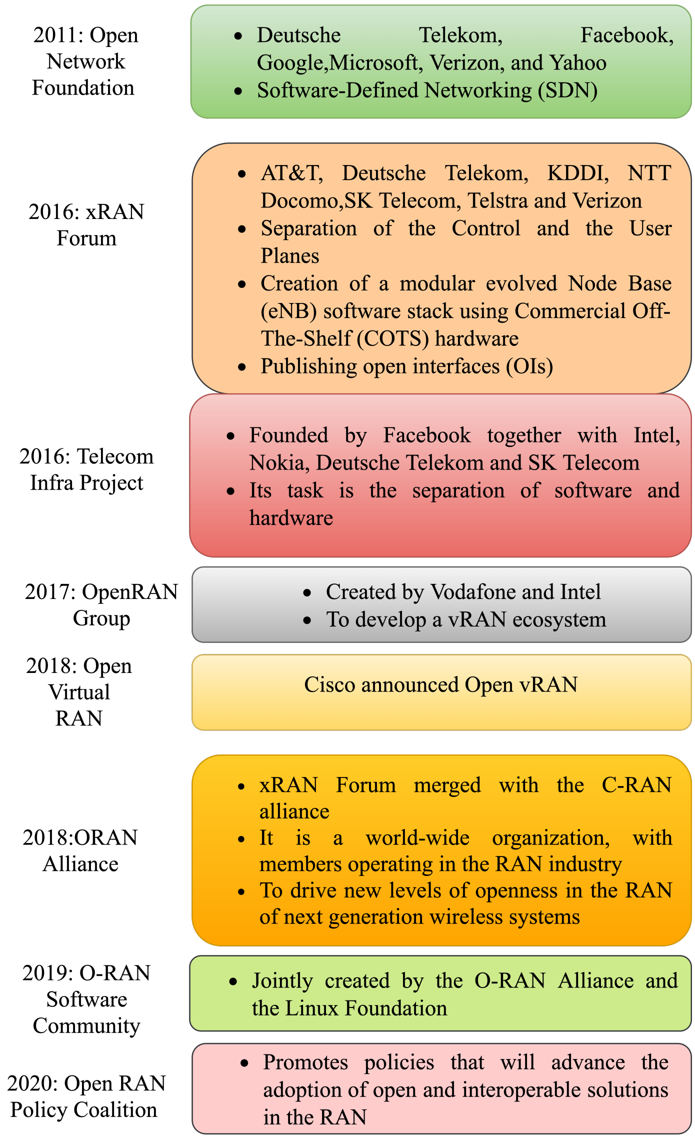


Figure 3.14: Summary of initiatives and organization working towards OpenRAN architecture and infrastructure.

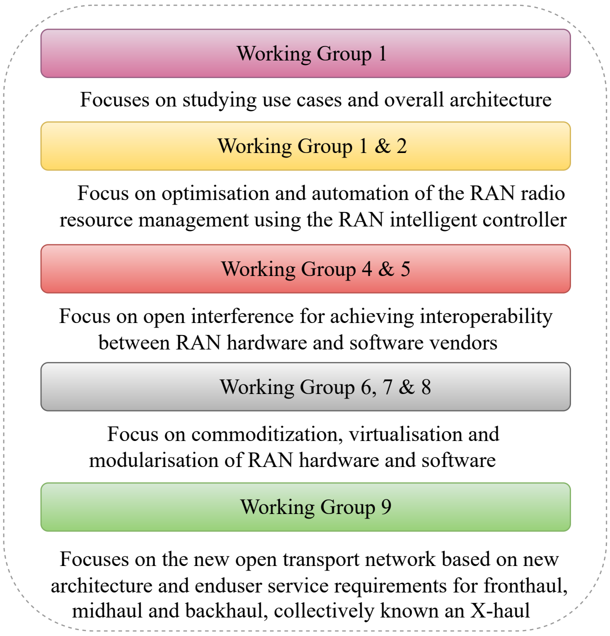


Figure 3.15: Different OpenRAN working groups and associated tasks for developing new RAN architecture.

### 3.6.2 OpenRAN Architecture

According to [262, 263], OpenRAN focuses on three specific areas, namely: (a) separating the CU RAN from UP, (b) creating a modular or dis aggregated base station software stack using COTS hardware and (c) Open Interfaces. OpenRAN mainly defines the concept of open architecture, enabled by well-defined interfaces between the different elements of the RAN. OpenRAN also defines the integration of machine learning and artificial intelligence techniques in the RAN [264]. All OpenRAN components must support the same Application Programmable Interface (API), allowing OpenRAN-based 5G deployments to integrate elements from multiple vendors and make it possible to utilize COTS hardware.

In March 2019, the O-RAN ALLIANCE defined the functional splits between the BBU and RRU to embed FH functional requirements. The O-RAN ALLIANCE defined a reference architecture, in order to support next-generation open virtual RAN infrastructures with intelligent radio [136]. The reference architecture describes well-defined interfaces to facilitate an open, inter operable supply chain ecosystem with respect to the 3GPP and other industry standards organizations. Figure 3.16 shows the reference OpenRAN architecture.

The splits of the O-RAN architecture are basically organized as follows:

- **For the fronthaul** - the 3GPP split 7.2 or Low Layer split between the so-called O-RU and O-DU (O for O-RAN);
- **For the midhaul** - the 3GPP split 2 or PDCP/split between the O-DU and O-CU. Note that the CU-c-plane and the CU-U-Plane are explicitly mentioned in the O-RAN architecture.

Similarly in essence to an SDN architecture, the forwarding elements (O-DU, O-CU-C-plane and O-CU-UP) are controlled by two so-called RAN Intelligent Controllers (RICs). Two RICs are needed to take into account two time scales required for efficient RAN functions, as fol-

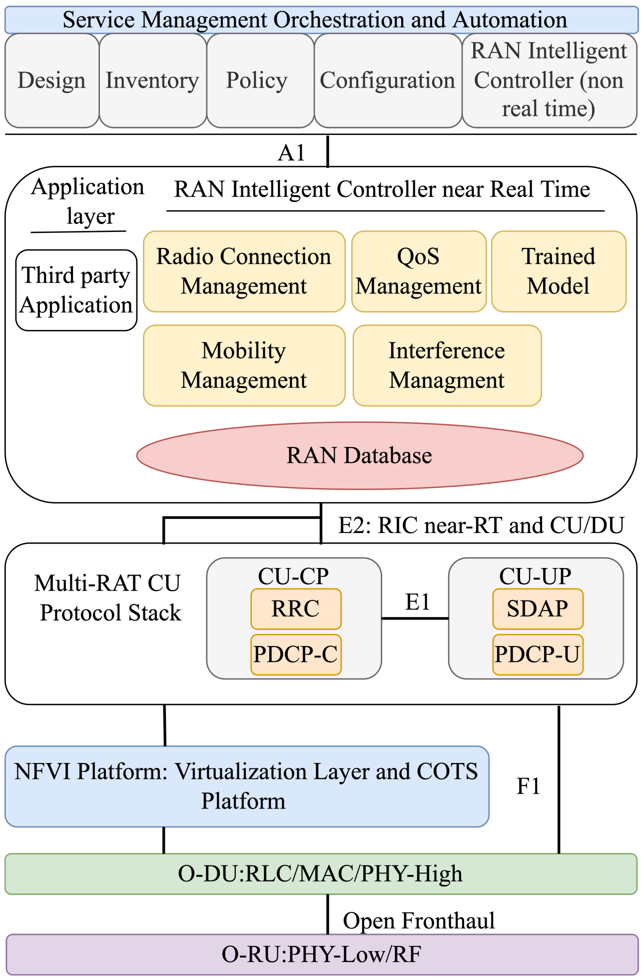


Figure 3.16: OpenRAN architecture as defined by the O-RAN ALLIANCE to achieve an OpenRAN infrastructure.

lows:

- A near-Real Time (near-RT) RIC to handle control from 0.1 to 1 second;
- A non-Real Time (non-RT) RIC to handle control above 1 second.

O-RAN ALLIANCE advocates the use of virtualization. Hence, specifies the so-called Service Management and Orchestration Framework which contains the non-RT-RIC function. The non-RT-RIC communicate with the near-RT RIC, with an interface called A1, and with the O-DU and O-CUs, via O1. The near-RT control and optimization of OpenRAN elements and resources is performed through compact data collection and control over a new E2 interface (not specified by 3GPP for the DUs and CUs). The non-Real Time RIC implements control and optimization of RAN elements and resources. The non-Real Time RIC is anticipated to incorporate specific AI/ Machine learning (ML) workflow, which involves training modules and provides policy-based guidance for applications in the non-RT-RIC [264].

The O-CU element handles the RRC for the C-Plane and the Service Data Adaption Protocol (SDAP) for the U-Plane and the PDCP. The O-CU-c-plane hosts the RRC and the control-plane part of the PDCP protocol, while the O-CU-UP hosts the SDAP protocol and the user-plane part of the PDCP protocol. The PDCP streams are exchanged to the O-DU via the MH which could be physically or virtually almost anywhere in the Open Cloud. MH distances up to 80 km have been reported earlier in this survey, but it remains to be seen how vendors, service providers and operators uses O-RAN for their use cases.

The O-DU contains the RLC/MAC/High-PHY layers. The O-RU contains the Low-PHY layer and RF processing based on a lower layer functional split. The fronthaul link (RU-DU link specified by the so-called LLS-C/U/S interface) should be less than about 20 km as reported in the first figure of this survey.

The virtualization platform, or Open Cloud, which hosts the O-DU, O-CU and RICs, should handle the multi-RAT CU protocol stack and support many protocol processing for 4G or 5G. The virtualization platform isolates the blocks and performs virtual resource allocation [136]. Obviously, a lot of work remains for the operators and vendors to implement and exploit the O-RAN ideas. Major operators and vendors are working hard to make intelligent RAN a reality.

### 3.6.3 OpenRAN Opportunities

OpenRAN benefits from the advancing RAN architectures toward interoperability and intelligence. OpenRAN holds enormous opportunities for both the user and the operators. OpenRAN defines new technical solutions and business models to tackle in- creasing costs, complex deployments, and many more by incorporating software and hardware dis aggregation through open interfaces [265]. In the white paper published by O-RAN ALLIANCE on use cases and deployment scenarios [266], an initial set of OpenRAN use cases is introduced, which benefits from the advances in open architectures and show high business value. The OpenRAN ecosystem utilizes AI and ML capabilities at the back-end blocks of the architecture to facilitate an open and intelligent multi-vendor network.

ML and AI algorithms are applied to manage and control RAN performance, configurations, and optimization, in real-time, for the envisaged use cases in target deployment scenarios. The use cases are categorized based on the application area and requirements [266].

Each use case has its focus area, well-defined purposes, and requirements [266]. The concept of white-box hardware as the base site will motivate an economical 5G deployment. The so-called white-box Base Stations focus on UL and DL processing, RF conversions, and gateways. Most of the use cases are defined based on the incorporated AI techniques, and cover a comprehensive range of applications, from traffic steering, Service Level Agreement (SLA), dynamic handover management for Vehicle-to-Everything (V2X) to enhanced user services and experiences through optimized resources. Within various Unmanned Aerial Vehicles (UAVs)-based use cases, applications are introduced envisaging OpenRAN and open interfaces. The context-based dynamic handover management for V2X use case focuses on supporting frequent handover requests in high-speed heterogeneous environments. A summary of the categorized use cases is presented in Figure 3.17. The O-RAN ALLIANCE web site hosts many impressive demonstrations of current and future OpenRAN capabilities [267].

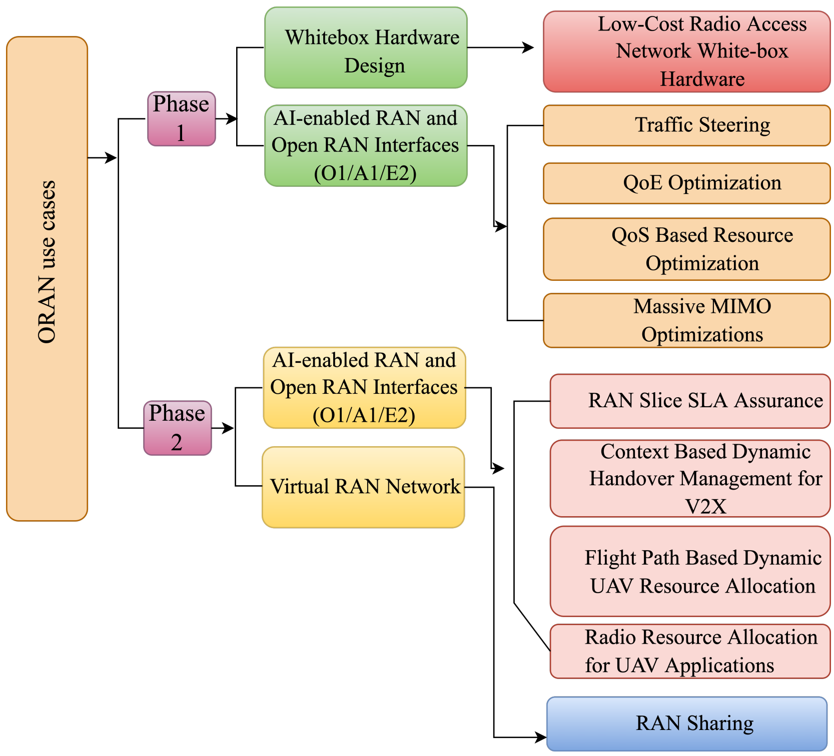


Figure 3.17: Summarized OpenRAN use cases criterion as defined by the ORAN ALLIANCE to validate OpenRAN development.

### 3.6.4 Open RAN Cloudification and Orchestration Platform

The O-RAN ALLIANCE has defined and sketched requirements for open cloud architecture and various deployment scenarios, as discussed in [266]. The so-called OpenCloud (OCloud) is an O-RAN cloudification and orchestration platform that classifies deployment options to expedite the cloudification of OpenRAN virtualized network elements. The OCloud provides a cloud computing platform encompassing physical nodes to execute applicable functionalities related to management and orchestration. The orchestration facilitates BBU resource pooling and cloudification, which should help maximize the operational improvement/cost ratio.

#### 3.6.4.1 OCloud Architecture

OpenRAN cloudification architecture is based on the reference architecture provided by ETSI NFV Architectural Framework [268], which includes appropriate COTS hardware that enables abstraction through virtualization. The ETSI NFV Architectural Framework implements VM on the servers that facilitate Virtual Network Functions (VNFs) in the cloud. The Virtual Infrastructure Manager (VIM) acts as the C-Plane in OCloud and manages different servers as a single distributed system [266]. The VNFs mainly provide the interfaces and virtualized open planes (O-DU, O-CU, NRT-RIC), along with the MEC applications and the 5G U-Plane Function (UPF).

#### 3.6.4.2 OCloud Deployment

OCloud defines a hierarchical deployment model comprising different modules, like regional cloud and edge cloud, hosted at independent or dependent levels. Figure 3.18 presents a hierarchical cloud deployment where each Edge Cloud, monitoring individual cell sites, is connected to the Regional Cloud (different traffic flows are represented by different colours). The VNFs are either implemented in the proprietary network element or on the OCloud component. Based on the different deployment scenarios in [266], the functionalities and hosting of O-DU and O-CU vary.

### 3.6.5 Implementation Challenges

One of the main challenges in O-RAN is to integrate the multi-vendor model and seamless interoperability between the services and the equipment they provide. The RAN virtualization can bring concerns about the capacity of the FH link in order to host several virtual BSs while maintaining the latency requirements between the RRH and BBUs. Implementing the functional splits can be challenging, affecting the FH network's bit rate and latency.

Open architecture also imposes several challenges on security aspects at various levels. The OpenRAN standards and 3GPP specifications have evolved in hand to facilitate RAN-functional splits resulting in RAN virtualization. At the deployment and implementation side, there is stil a gap on clearly defining vRAN specifications and on how the software and hardware parts are deployed [133].

RAN virtualization to support high data rate, low latency and high availability 5G and beyond requirements are certainly very challenging for researchers and practitioners.

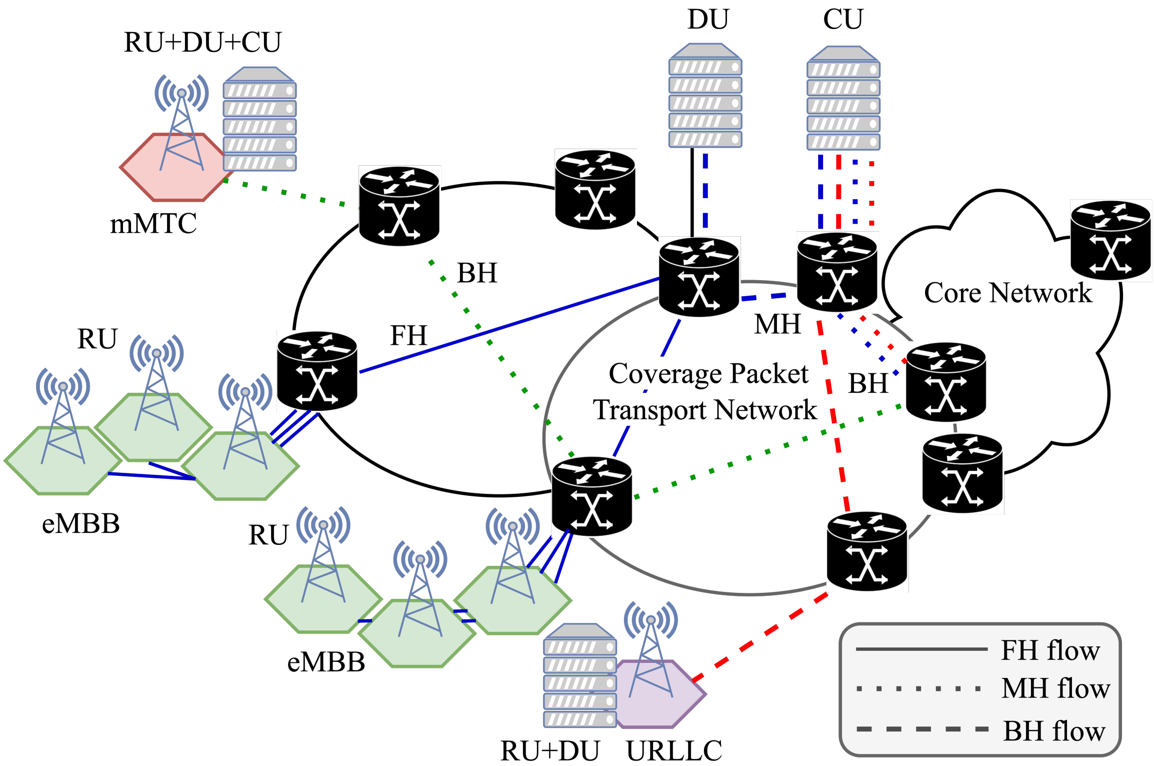


Figure 3.18: A typical layout of a RAN infrastructure [95, 269].

## 3.7 Summary and Conclusions

This survey [12] comprehends an extensive literature review on different functional splits proposed by 3GPP and the O-RAN ALLIANCE. A practical approach to the functional split requirements and implementation was provided. As a result of RAN splitting and virtualization, network deployments are more flexible and facilitate the creation of a multi-vendor marketplace for different radio and network components that are different from the traditional business models. By creating various interfaces between layers through splitting, new hardware and software products can be designed and fabricated while guaranteeing interoperability between elements produced by different manufacturers. The main advantages, disadvantages, and challenges are discussed. Each functional split is described in detail, and the underlying challenges are identified. Broadband access will be enhanced, and ultra-reliable low latency communications (URLLC) and massive Machine Type Communications will be supported. URLLC will enable applications like self-driving cars or coordinated autonomous UAVs, e.g., in a disaster-resilient swarm of coordinated drones participating in rescue missions. Expected 5G and beyond reliability and resilience are commonly cited to enable remote surgeries with physicians commanding high-precision robots from remote hospitals in real-time and to support high-speed nano-robot communications for in-body healthcare applications. More realistically, 5G and beyond will serve the needs of the industry 4.0 and beyond.

Moving the processing functionalities from the RRHs to the DUs and CUs may be advantageous as the RAN architecture evolve and leads to an economy of scale. Many functional splits, serving various use cases, have been devised but have limitations. For example, the 3GPP split option 8 requires a data rate much higher than the total user data rate and a distance between CU and DU lower than 20 km. The split option 7.2 has been preferred by the O-RAN ALLIANCE. Different splitting implies different data rates and latency requirements.

For example, to implement split option 6, the PHY and RF are in the DU, while the MAC is in the CU. The MAC layer performs functionalities like the computation/calculations and operations in CU considering software, whereas the RF (DU) takes care of the rest of the functionalities, resulting in high hardware costs.

Various standardization bodies are actively working to provide energy-efficient, reliable, and economic solutions by allowing BBUs to support multi-RF units.

The final part of the survey discussed the RAN evolution from C-RAN to OpenRAN. The virtualization functions have been examined. The O-RAN ALLIANCE architecture was discussed while addressing how it may serve future stakeholders for 5G and beyond RAN. The O-RAN ALLIANCE intends to support diversified 4G to 5G and beyond use cases by developing the specifications and architectures with new open interfaces to control the DU and CU with the so-called RAN Intelligent Controller. State-of-the-art technologies for incorporating various split options were discussed. Some relevant solutions allow splitting, such as split eight implementations using FPGA (hardware) [140, 141], gNodeB from ISW (software) [143] have been presented. The ISW-gNodeB consists of independent network functions to implement PHY, MAC, RLC, PDCP, SDAP, RRC, and NRAP protocols.

The survey shed light on the various RAN architectures and deployment scenarios, providing a vision of the functional splits, underlying opportunities, and evolution challenges. We provided detailed literature to justify the emergence of functional splits as an enabler for beyond 5G networks. In addition to the overview of functional splits, we also summarized the concept of virtualization and O-RAN ALLIANCE architecture. However, we did not address Massive MIMO, CoMP, and mm Waves, concerning functional splits in the scope of this survey.

Academia, industry, and research organizations are working toward an OpenRAN infrastructure to support RAN dis aggregation. The O-RAN ALLIANCE implements different intelligent processing algorithms to deploy flexible, and economic networks. Integrated access backhauling, edge processing with cloud and virtualized (also Fog) RAN are certainly open research areas that have the potential to incorporate intelligence into the network while supporting 5G second phase and 6G deployments.

# Chapter 4

# Deployment of Beyond 4G Wireless Communication Networks with Carrier Aggregation

## 4.1 Introduction

By 2025 the number of subscriptions that include mobile broadband, mobile portable computers, tablets, router, and IoT devices is expected to grow up to more than 9 billion plus [270], new applications and services will require even higher data rates. MIMO and OFDM are two base technologies that will be enablers for 5G and beyond. CA is a technique that can improve the coverage, throughput, resource reuse, system capacity, service quality, and user experience. The telecommunication industry has observed a high data rate application services, offering a high quality of services in a cost-effective way for mobile applications, which has become essential for operators to meet customer requirements. For this purpose, the international telecommunication union introduced a global standard initiative [270] , IMT-Advanced technique contains new capabilities for offering a wide range of services and applications for telecommunication.

For supporting service demand and enhanced user, IMT-Advanced recognized the peak data rate of 100 Mb/s for high-speed movement and 1 Gb/s for lower speed mobility. ITM-Advanced is upkeep for variable bandwidths with encouraging to support up to 10 MHz [271]. Similarly to 3GPP (LTE-A), IMT-Advanced can be supported by different spectrum bands, that justifying the need for the system to have the capability to support aggregation of a different carrier to provide high data rate, that is the demand of today users.

Based on the requirements and observations, the 3GPP has identified CA as a significant feature for achieving improved data rates. There are options in High-Speed Packet Access (HSPA) evaluation to aggregate up to four carriers for DL, up to two carriers for UL, and both the carriers are considered contiguous. In release 8/9 of 3GPP LTE, different carrier bandwidths of 1.4, 3, 5, 10, 15, and 20 MHz, support for several deployments, plus spectrum plans. Succeeding the desires of 100 MHz Bandwidth (BW) of system, Release 10 of 3GPP LTE has presented CA as one of the foremost vital LTE-Advanced structures to balance the bandwidth afar 20 MHz [15]. CA Release 10 described in [272], up to 100 MHz system bandwidth can be achieved by concurrently aggregating up to 5 CCs of 20 MHz, according to user equipment compatibility.

To acknowledge better network advancements, it is essential to guarantee backward compatibility for an LTE-Advanced design. Thus LTE Release 10 UE and LTE Release 8/9 might be sustained in the consistent carrier deployed by Release 10 eNBs. CA is very well-defined for Release 10 and establishes that every CC is companionable for LTE Release 8/9 [272] and one of BW expressed in Release 8/9. It has similarly permitted the reuse of RF in Release 8/9 schemes and implementation in UE and eNB. There was no option in release 10 to aggregate in UL, however in the downlink, just two CC might be aggregated; in Release 11, it was upgraded up to two CC in UL aggregation; Frequency Division Duplex (FDD) and TDD CA added in Release 12. In Release 13, the CC improved from count 5 to 32. The evaluation is still more relevant beyond Release 13. Release 16 introduced CA with different numerologies Figure 4.1. It will be a tremendous value for that, which expands a massive block of unlicensed spectrum in the 5 GHz band.

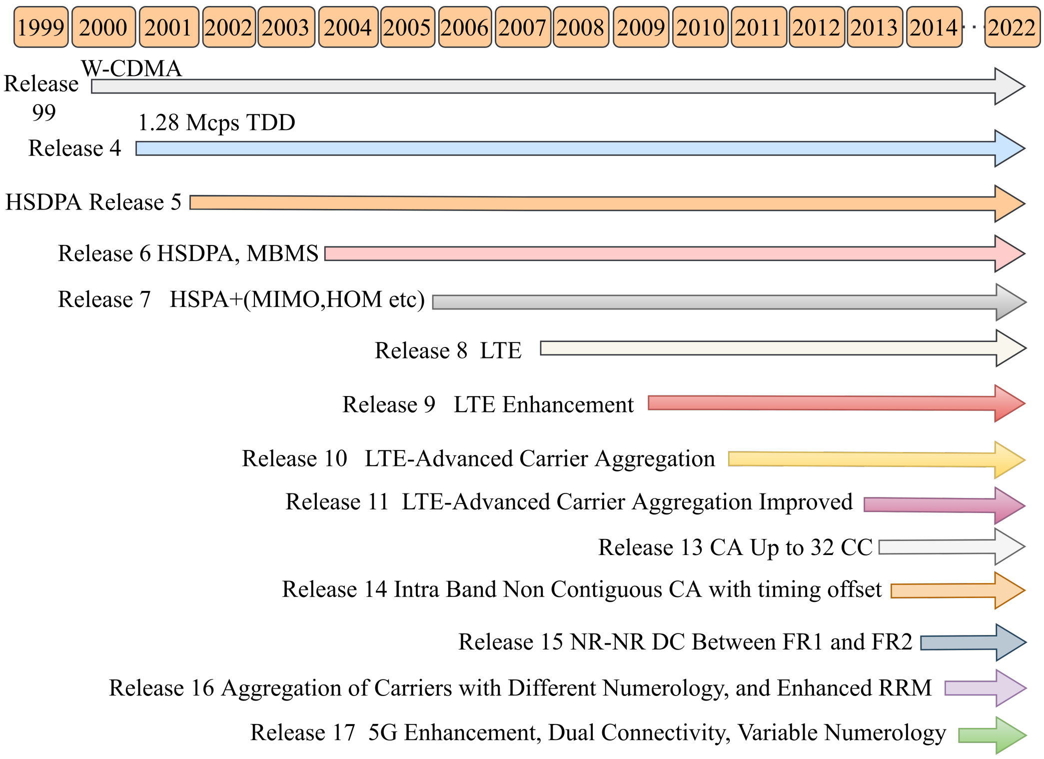


Figure 4.1: CA evaluation and enhancement with the period of time in different releases.

Furthermore, with CA, hardware circuitry is complex, not because the number of CC is more in CA, while in contrast, because receiving different frequencies, multiple signals produce intermodulation results that interfere with the required signals. Depending on the capabilities mobile terminal of UE can receive one or several CCs. Likewise, it is feasible to aggregate a different total of CC, ultimately of different BW in UL and DL, with the limitation that the number of CC in UL is not greater than the number of CC in DL. In each direction (UL, DL) using CA, one of the CC essential be nominated the Primary Primary (PCC), whereas the rest are named Secondary Component Carrier (SCC) shown in Figure. 4.2. Radio resource control connection will always be handle by the primary serving cell. In idle mode, the UE listens to system information block broadcast message through the primary serving cell and sends the uplink control information through the uplink control channel. PCC handles all the control signaling. Unlike PCC, there can be multiple SCC. The SCC can be adding or remove as require for UE, while the PCC is only changing at handover occurrence.

In the framework of a European 4G communications network scenario, e.g., available band-

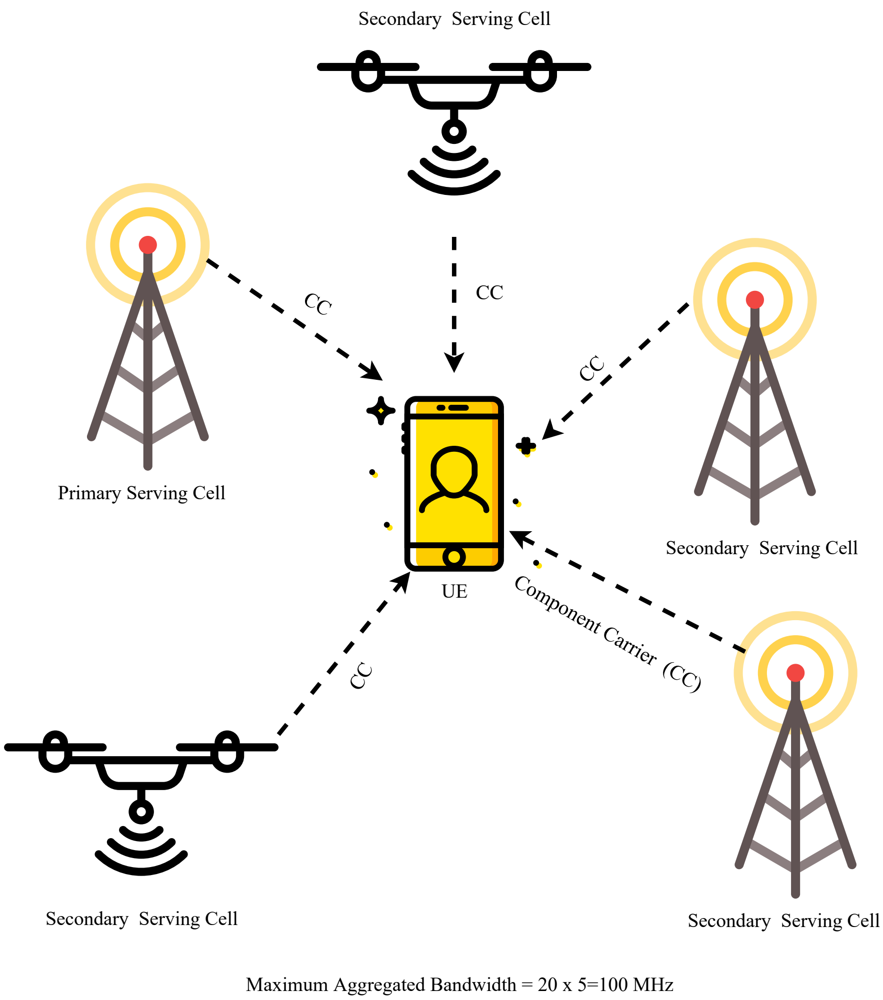


Figure 4.2: Basic understanding of CA in heterogeneous networks with small cells.

width and radio frequency bands for Portugal (2.6 GHz and 3.5 GHz), multi-band scheduling algorithms are explored to optimize average cellular capacity, service performance, and the users perceived quality. Compared to [273], [27], and [274], this work, considers a proper uniform distribution of users within the cell, and Mersenne Twister pseudo-random generator to generate genuinely random distributions, while obtaining simulation results for Packet Loss Ratio (PLR), goodput and average delay.

A sample of mobile user distribution produced by the LTE-Sim [275] during simulations is present in Figure. 4.3 for developers' code and in Figure. 4.4 after the code update from [276].

Figure 4.3 represents the deployment of 100 000 different locations for the users in the coverage area from an eNB with the original LTE-Sim code, where only the radial position of each user was generated by considering the uniform distribution. The old LTE-Sim versions were used to create most of the user's positions closer to the central eNB. In this work, aiming to obtain a truly uniformly random distribution of users within the cell, the simulator has been updated, as in [276], to generate the user's normalized distance to the cell-center the square root of a uniform distribution. Figure 4.4 presents a sample of the change in user positions resulting from this update in the LTE-Sim code. Further to updated (LTE-Sim code)

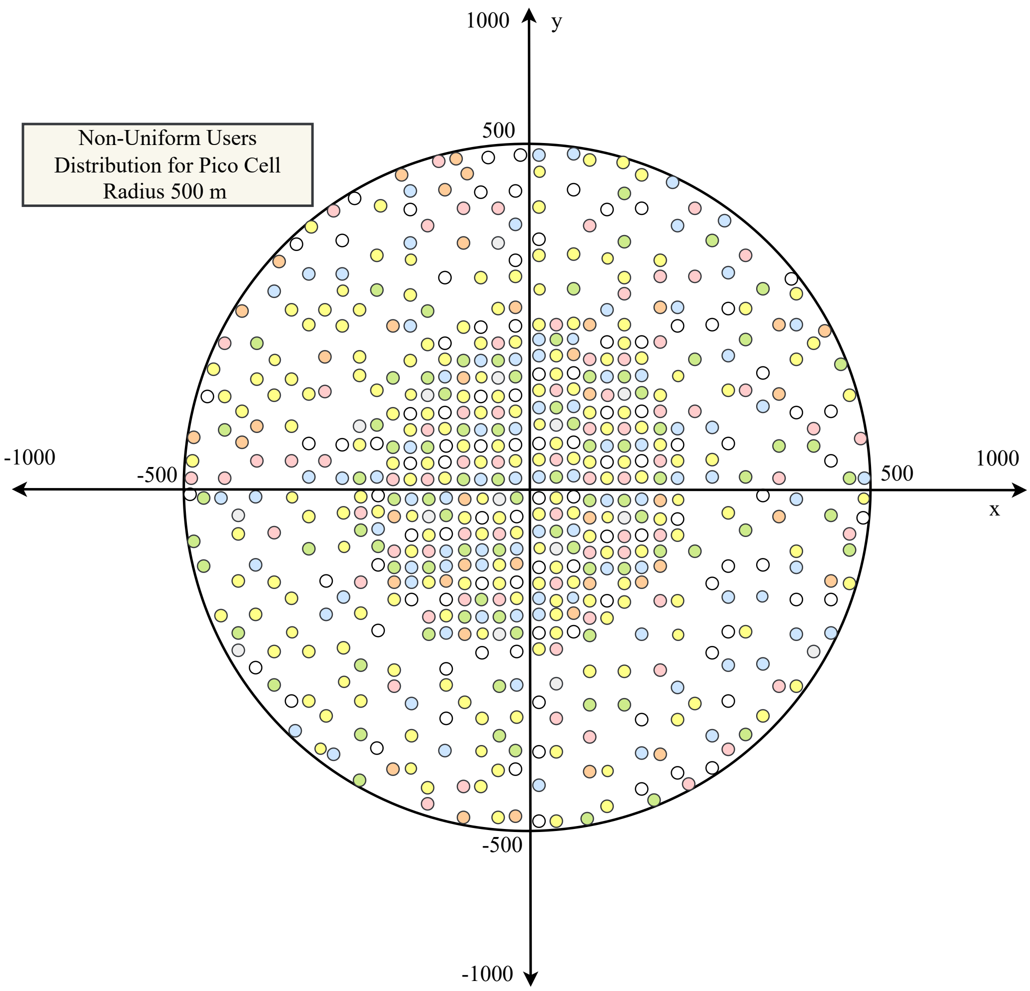


Figure 4.3: Original non-uniform distribution of users, where just the distance to cell centre for each mobile user was generated by considering the uniform distribution.

the path loss model from single slope to dual slope 2D urban Pico environment, to analyse the CA.

In Section 4.2, this work introduces aspects of CA and discusses the challenges in providing contiguous and non-contiguous CA. The discussion of the underlying deployment scenarios is followed by an overview of the functionality and terminology, which includes specificities of the protocol stack, radio resource management, and configuration of different types of user equipment, primary versus secondary cell management, as well as the illustration of UE/eNB implementation. In Section 4.3 performance evaluation of Pico-cell scenarios is explored through a simulation approach by considering Pico cellular scenarios implemented in LTE-Sim, path loss modelling are explored. The scenarios of the implementations are presented in sub Section 4.3.3. Simulations results are analysed in sub Section 4.3.4, results for PLR, good-put, fairness index and average delay are compared for CA (multi-band schedulers) and without CA (Frame level scheduler). Comparison of maximum supported goodput obtained through computations and simulations are presented in sub Section 4.3.5. The cost revenue trade-off for CA and with out CA scenario are given in sub Section 6.6. Conclusions and suggestions for further research are present at the end of the Chapter.

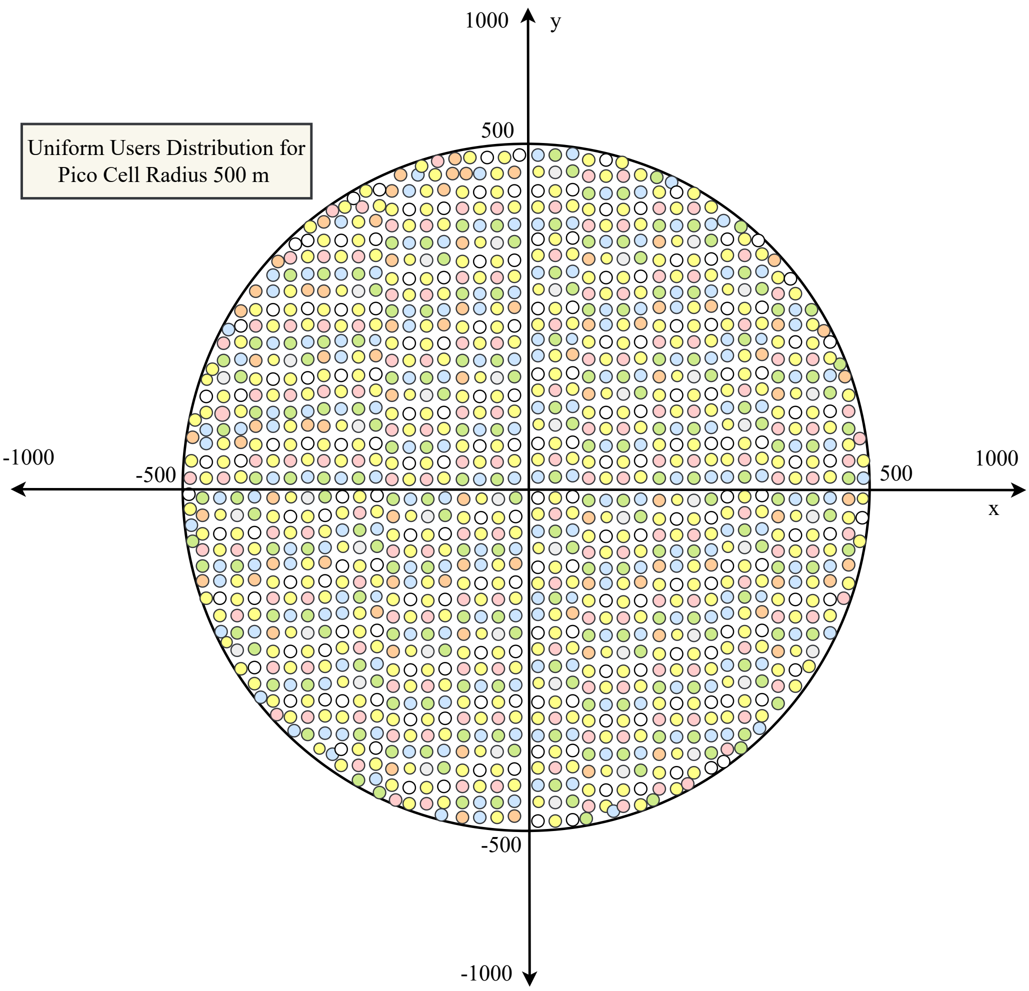


Figure 4.4: Truly uniform distribution of users in simulations.

## 4.2 Carrier Aggregation

According to the CC arrangement, two main types of CA are identified [277] [272]:

- Intra-band CA - It uses a single band, as shown in Figure. 4.5.a), and has two main types, intra-band contiguous and intra-band non-contiguous. In intra-band contiguous aggregation, the carriers are adjacent to each other. In this case, only one transceiver is required within the terminal or UE, where more is needed when the channels are not adjacent. The complexity of intra-band non-contiguous CA is higher, as it uses the carrier of the same band but not the adjacent one, because of this, the signal cannot be treat as a single signal that increases the complexity and cost of the system.
- Inter-band non-contiguous CA - This type of CA using different bands, as shown in Figure. 4.5.b), due to the existence of carriers from different operating bands, it is more challenging, as there is a need for multiple transceivers to receive or transmit the signal that enhances complexity, power requirement, cost, and creating space constraints.

The provision for contiguous and non-contiguous CA of CCs through distinctive BW provides substantial flexibility aimed at competent spectrum utilization and continuing changing of frequencies formerly used by other radio access schemes. According to physical layer perception, contiguous CA is simple to implement without making numerous changes to the structure of the physical layer of the LTE system [278]. Using a single Fast Fourier transform (FFT), it is possible to obtain contiguous CA for the LTE-Advanced UE block (also by using RF block). However, keeping the backward compatibility for LTE schemes, in the case of non-contiguous CA, several radio frequency and fast Fourier transfer modules will be required. For the UL, in LTE-Advanced, the focus is presently on non-contagious CA because of the challenges arising from the simultaneous transmission on various non-contiguous CCs and underlying device linearity limitations. In Release 10, these two cases, intra-band, and inter-band are considering in the DL. Nevertheless, the particular RF desires already develop in [279]. Usually, instead of spectral efficiency CA are amid to improve data rates.

Time domain scheduling for n number of users is defined in [48]. The author from [48] has formulated the frequency-domain scheduling as:

$$\max(R) = \sum_{n=0}^{N} R_{UE,n} \quad (4.1)$$

Where $n$ =(0,...., $N$) describes the frequency domain resources, for example RF spectrum.

Different scheduling algorithms investigated in literature [48]. Greedy allocation is the usual approach to get the maximum rate. It is also possible to use linear programming to provide an optimal solution. The best fit first or greedy allocation is simple heuristic algorithms. This algorithm finds probable utility in the matrix defined by user and n until all frequency-domain resources ($n$) are exhausted and/or all users are scheduled [48].

### 4.2.1 Carrier Aggregation Deployment Scenarios

Different deployment scenarios are showing in Figure. 4.6. These scenarios have been considered through the LTE-Advanced CA design, demonstrated using two CC denoted by frequencies F1 and F2. Usually, in many deployment scenarios, for different CCs, the eNB antennas are collocated and have consistent beam patterns/directions. In scenario 1 (identical coverage), if CCs belong to a similar band or frequency separation is short, almost equal coverage will be provided for all CCs. Scenario 2 (various coverage) corresponds to a larger frequency separation between CCs, providing different coverage. Similarly, in a similar band, CCs could be deployed at eNBs with diverse transmit power planes to offer various coverage footprints for inter-cell interference management commitments [272], the place where the coverage of CCs overlapping the CA allows higher user throughput to shift the beam across the carriers.

In the third scenario, different patterns or beam directions are used for different CCs to improve the throughput at the cell edge. Finally, in scenario 4, two frequency bands are considered; one is the lowest frequency, and the other is high frequency. One CC, typically in low frequency, offers macro coverage while another CC, which considers higher frequency,

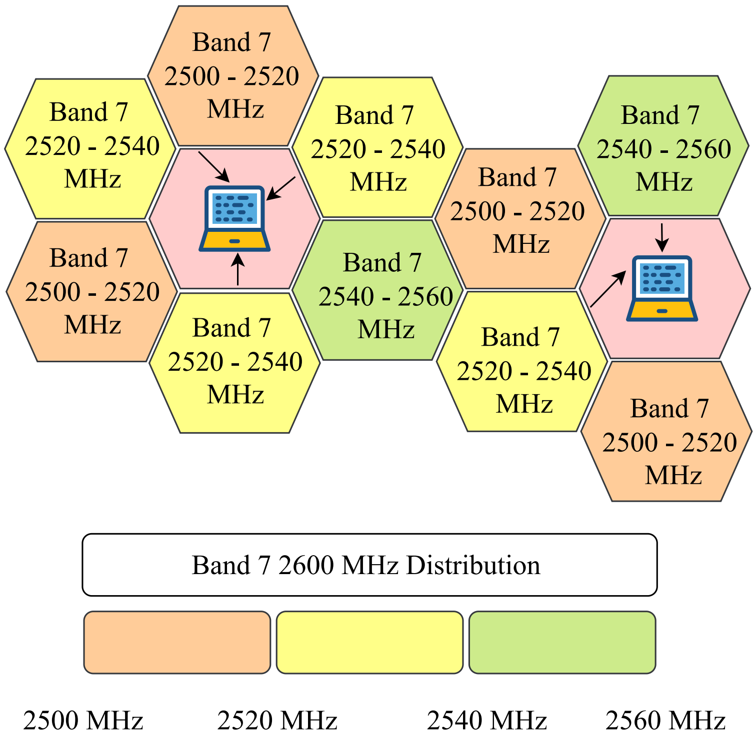


(a) Intra-band.

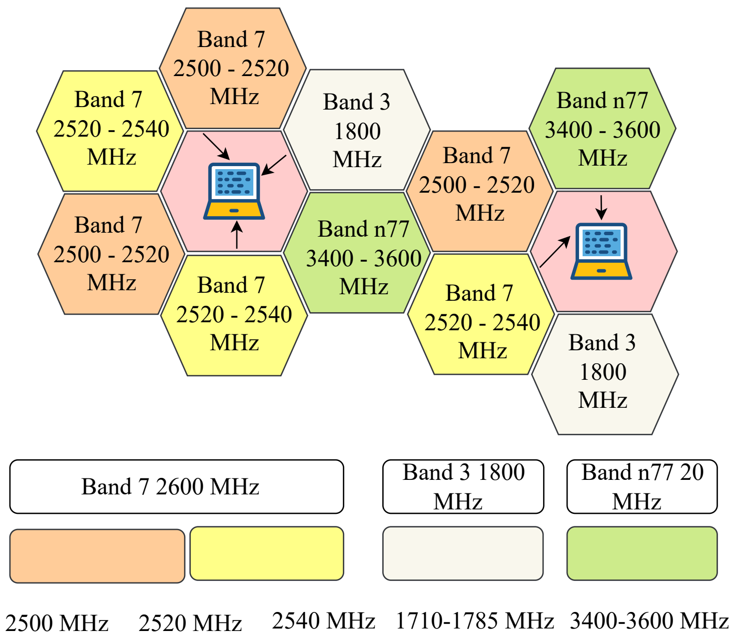


(b) Inter band.

Figure 4.5: Types CA and its band management.

uses RRH units to absorb traffic from a hotspot. Using optical fiber, the RRH is connected to eNB, thus permitting the aggregation of CCs among the macrocell and RRH cells based on the same CA framework for collocated cells. This type of deployment allows the operators to advance system throughput utilizing low-cost RRH devices [280]. Among different deployment scenarios, most efficient can be decided according to different factors, like either the service locations are rural, urban, or suburban, and where around there are hotspots in an area or not. A probable near possible scenario that presents deployment using legacy frequency band (e.g., 2.6 GHz) to offer adequate coverage through the service area, and new bands (e.g., 3.5 GHz) is used to assist traffic in an additional cost-effective way. It is estimated to use CA in a heterogeneous network for flexible spectrum use, varying with operator requirements [281]. In all CA cases, even inside a single eNB, different LTE-Advanced user equipment will be configured with various CCs [282]. The CCs, which will be part of the serving cell's configuring set, might be non-contagious or contiguous; it depends on the UEs deployment scenarios and UEs capabilities. Respectively one CC is configured for DL and UL when UE primary establishes or re-establishes Radio Resource Control (RRC) linking with eNB, which is referred to as PCC, which agrees to Primary Cell (PCell). The DL CC being titled is DL primary CC, and the resultant UL CC being titled is UL PCC. According to the traffic, load need the UE may be connecting with one or more CCs, which is the title as component carrier, SCCs for Secondary Cells (SCells), the DL and UL concern with it are termed as DL and UL secondary CCs of SCCs [277]. The handling of DL/UL SCCs through UE is moreover configurable using eNB.

The UE equipment served by the same eNB but the PCC and SCCs configurations are user-specific, which can be different for the different user equipment, as shown in Figure. 4.7. Different users may not be using the same carrier component as their PCC, In eNB it is clear that CC can be used as the PCC for one user equipment and assist as an SCC for another UE. The PCC can be considered anchor CC of UE and thus cast-off for fundamental functionalities, like radio link breakdown checking, etc. [283]. Dedicated signal information is sent through SCCs, the DL and UL resources can be scheduled on the SCCs using the control channel of PCC.This technique is estimated can be the best aimed at interference management for control channels regarding heterogeneous networks and permit load corresponding through diverse cell layers. DL and UL PCCs are most of the time rubout and can be select, such that it can provide the best signal feature, i.e., based on measurements of Reference Signal Received Power (RSRP) or Reference Signal Received Quality (RSRQ). The UE move in the area related to eNB, the PCC can happen change to the CC that can provide the best signal quality, the change of PCC is also can be performed by eNB keep in consideration load balancing [272].

DL SCCs can be dynamically activated and deactivated depending on carrier loading, buffered data amount, and quality of service. In LTE with FDD, considering the options frequency gap and bandwidth through system information signalling, DL and UL carriers are eternally paired. At the same time, the CA asymmetric of LTE-Advanced is accompanying in two-directions. That like the CCs for two directions can not be the same to improve the spectrum efficiency. As in this framework, UE configured CA might require cooperation with eNB on uneven figures of DL/UL CCs, hence the usage of UL SCCs of certain of the SCells is not configured. Unlike this is defined in LTE, the DL CCs might be linked to UL CCs with duplex gaps. The asymmetric CA might produce uncertainty in downlink CC collection since it is tough for LTE-Advanced eNB, distinguishing the CC to UE anchors in the downlink. In mode time division, duplex CA asymmetric can also be accomplished by changing the allocated time slots ratio for DL and UL transmission. This plan streamlines the resource allocation association among the DL and UL channels [278].

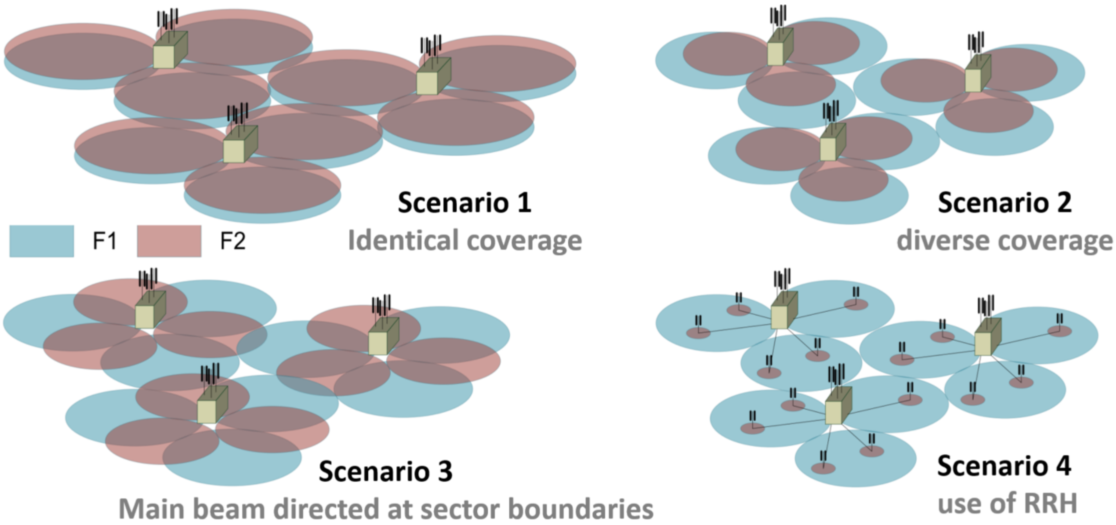


Figure 4.6: 3GPP CA deployment scenarios, adapted from [284].

### 4.2.2 Functionality and Terminology

**a) Protocol Stack**

The overview of the DL user plan protocol stack at the base station is shown in Figure. 4.8, Also, the mapping for furthermost important Radio Resource Management (RRM) functionalities for CA is presented. Every user has a minimum of only one barrier that is offered by the default radio bearer. Mapping the data to defaulting bearer depends on operator end policies that configure using the traffic flow template. Adding to the radio bearer, users can have further bearers configuration. The radio bearer has one PDCP and one RLC. The packet data convergence protocol containing functionalities like security, segmentation, robust header compression, and radio link control contain outer automatic repeat requests. The radio link control and packet data convergence protocol LTE-Release-8 are in paper [285].

The Interface among RLC and MAC indicated consistent channels. Every user has MAC using for control of multiplexing data that comes from a consistent channel to the user. It also controls how the data are transmitted on the accessible CCs. As shown, there is one Hybrid Automatic Repeat Request (HARQ) unit per CC. Each CC has a separate transport channel that means the interference among the MAC and physical layers. The transport blocks sending diverse CCs are transmitted using different coding schemes, modulation schemes, and MIMO coding schemes, these all should be independent. The latter permits that data per CC can be sent using open-loop transmit diversity. However, the data on alternative CC are transmitted by twin stream closed-loop pre-coding. The self-governing link adjustment for every CC to get an advantage from optimally corresponding the transmission through diverse CCs agrees to the experienced radio circumstances. The technique also uses different transmit power settings for CC thus, according to principle, they will have a level of coverage, which is also explained in [272]. The control plane stack of LTE Release-8 is also applied to LTE-Advanced with numerous CCs. Likewise, idle approach mobility techniques of LTE Rel-8 are similarly involved in a network deploying CA. They are further acceptable for the network to configure a single subset of CCs for idle mode camping.

**b) Radio Resource Management**

LTE-Advanced and LTE Release-8 have many similarities in regards to the RRM framework. The admission control process is accomplished at the BS prior to forming first-hand radio bearers and configuring related quality of service parameters. The LTE-Advance and LTE Release-8 service parameters for excellence are the same [286].

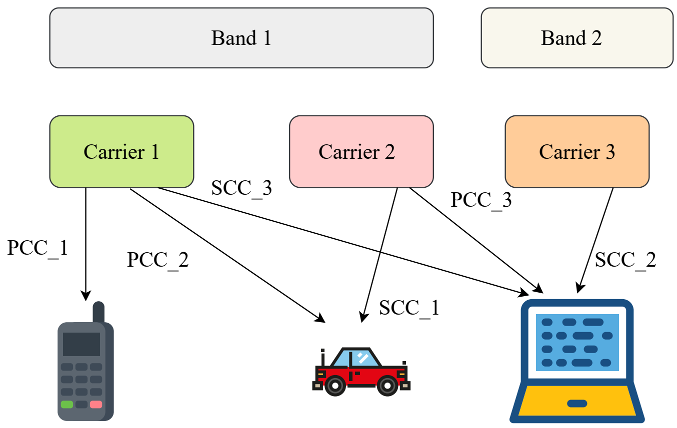


Figure 4.7: Configuration for different types of user equipment, adapted from [279].

The CC configuration block is an essential block in system performance optimization and for user's saving power consumption. For the best system performance approach, they must have the same load on diverse CCs, so own-cell load information is desirable as input. It assists the outstanding CC configuration and balancing of load [287]. LTE-Advanced users assist multiple CCs, Guaranteed Bit Rate (GBR), QoS parameters like the QoS and Class Identifier (QCI) to determine the required number of CCs for the user; the Aggregated Maximum Bit Rate (AMBR), QCI and GBR provide useful information. For example, a single carrier component will be allocated to a user with a single call or streaming connection but can still satisfy its QoS necessities. The aggregated maximum bit rate can be used for the top effort traffic to evaluate almost the best CC by considering their size. By allocating only one CC to this type of usage, the user benefits that terminal power utilization is sustained lesser than the case wherever the user has assigned more CC set. The proper CC configuration algorithm is under Base Station (BS) vendor specification. As shown in Figure. 4.8, packet scheduling and additional functionalities are tightly coupled for dynamically deactivating CCs configured as SCells for different users. It has also further anticipated supplementary control means to reduce the user's power utilization additionally.

Accordingly, the user may be schedulable only on activated CCs but not on deactivated CCs. Besides, the user cannot provide Channel State Information (CSI) for deactivated CCs when required for a base station for frequency domain packet scheduling and radio-channel-aware link adaptation [285]. Via MAC signalling the SCell is activated and deactivated autonomously [272]. Furthermore, it is also possible to set the timer for deactivation. Hence, the activated SCell spontaneously gets deactivated without sending a deactivation message if no traffic is detected on the CC for a given set of times. By evading that Configured SCells are deactivated, they are activated before being schedulable. PCell needs to be always activated for the user, and there is no substance to any deactivation techniques. The lively Packet Scheduler (PS) at stage layer 2 is accountable for scheduling qualified users on configured and activated CCs. In the LTE Release-8 PS framework [285], the lowest frequency domain scheduling resolution inside every CC is a Physical Resource Block (PRB) which contains 12 sub-carriers per PRB, establishing a corresponding bandwidth of 180 kHz. The main objective of PS from multi-user frequency domain scheduling is to obtained diversity through assigning the PRB to diverse users which practice best channel services, with CA the LTE-Advanced PS functionality is quite the same as PS for LTE Release-8. Nevertheless, LTE-Advanced PS is permissible to manage users through multiple CCs. LTE-Advanced relies on a self-governing link adaptation, transport blocks, and HARQ for every CC that open multiple implementations ways of the scheduler, e.g., techniques of scheduling can be complete in parallel for dissimilar CCs, counting certain management that certifies sprite and combined control for users scheduled on multiple CCs [272].

Sending commands on the control channel is used in LTE Release-8 for user dynamic scheduling facilitation that called the PDCCH, which being time multiplexed. Before the data channel in every Transmission Time Interval (TTI) [277]. Every PDCCH is restricted just to one CC. The per-user similar address does not depend on the CC where it is arranged, in 3GPP LTE terminology, it is entitled as Cell Radio Network Temporary Identifier (C-RNTI). Though the eNB in LTE-Advanced is allowed to forward a scheduling grant on each CC to schedule the user on alternative CC, the cross-CC scheduling functionality is unified using attaching a so-called CIF to the DL Control Information (DCI). For user allocation UL and DL traffic, the DCI to indicate it while CIF to find on which required CC, the user's data are transmitted. Payload size increasing marginally when the CIF is attached to the DCI, the transmission data are constant, due to weaker coding, the link functioning is somewhat more lacking. On a per UE basis, the configuration of every user and interpretation of the CIF is semi-statical. Therefore, complete backward companionable with legacy Release-8 manipulators do not have CIF in the DCI transmitted on the PDCCH. For extra optimizing control and data channel, is functioning through multiple CCs the cross-CC scheduling functionality deals with additional system flexibility. Furthermore, to enhance the dynamic Layer-2 packet method of scheduling, the LTE Release-8 similarly supports the Semi-Persistent-Scheduling (SPS) for the deterministic traffic flows like VoIP that maintains control channel resources [277]. SPS also supporting for LTE-Advanced with CA, while its limitation is, it can be configured through users PCell only through RRC signalling.

**c) Primary Cell and Secondary Cell Management**

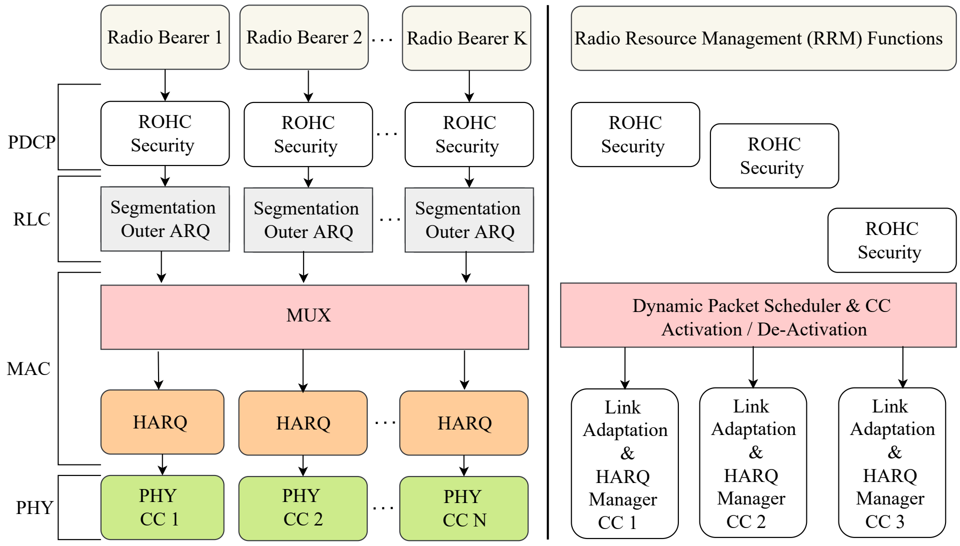


Figure 4.8: From left to right the overview of DL user plane architecture and RRM algorithms, adapted from [278].

PCell and SCell is the control technique that manages the network to add/remove SCell or switch the user equipment PCell. RRC idle user equipment unit establishes an RRC connection toward a serving cell that automatically considers as PCell. With the RRC connection on the PCell, for UE traffic demand the network can further configure SCell according to the UE capability of performing CA. The RRC connection is using to convey the necessary information of an SCell to the UE, also the functionality of reconfiguration, addition, and removal of SCell to UE is accomplished through RRC connection. To advance the quality of the link the PCell of UE can be further change to provide the balancing between different SCell. PCell variation does not essentially require UE to switch to single-carrier operation. Intra-LTE handover in LTE-Advanced permits the of focus PCell to configure one or more SCell for UE to utilize instantly when handover occurred.

**d) eNB Implementation**

For contiguous CA the DL transmitter chain block diagram is shown in Figure. 4.9.

It shows in Figure. 4.9 that it required a single transmitter chain with one IFFT because the carrier is considered contiguous. For efficiently supporting the wide bandwidth essential for LTE-Advanced, Linear Power Amplifier (LPA) mixing methods are necessary to be considered, it is capable of accompanying 20-30 MHz modulation bandwidth. For combining LPA resources, distinctive techniques are frequently considered: cavity, hybrid, coherent combining, and employing Fourier Transform matrix. Selection between these methods is dependent on the design criteria like the cost, LPA bandwidth, complexity, whole transmission bandwidth, also the main influential band whose combining is contiguous or non-contiguous. Considering non-contiguous aggregation, LPA must not be apprehensive as, like multiple transmitter chains, containing Inverse Fast Fourier Transforms (IFFTs) is necessary. For this type of CA, the transmitter should be prudently designed, which can be separate from blocking the mixing of signals that can lead to false emissions.

**e) UE Implementation**

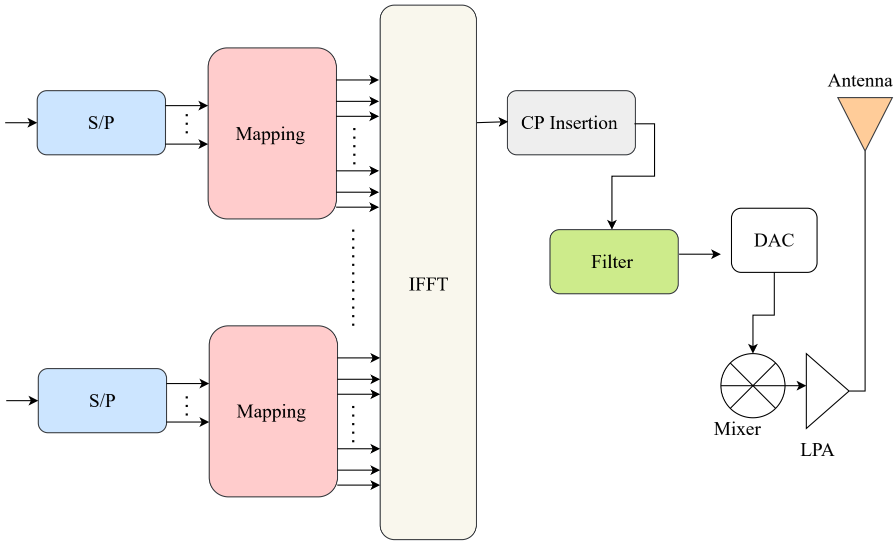


Figure 4.9: Block diagram for DL transmitter CA, adapted from [288].

Single-Carrier Frequency Division Multiple Access (SC-FDMA) using DFT-Spread OFDM in LTE uplink is a physical layer approach system. OFDM and SC-FDMA have several resemblances, among them, the main one is frequency domain orthogonality between users. SC-FDMA has lower power amplifier de-rating obligations that improve the battery life and prolong the range [289]. Using $N$ x SC-FDMA in UL the CA is supported, for the value of $N$ equal to two the block diagram for UL indicating is presented in Figure. 4.10.

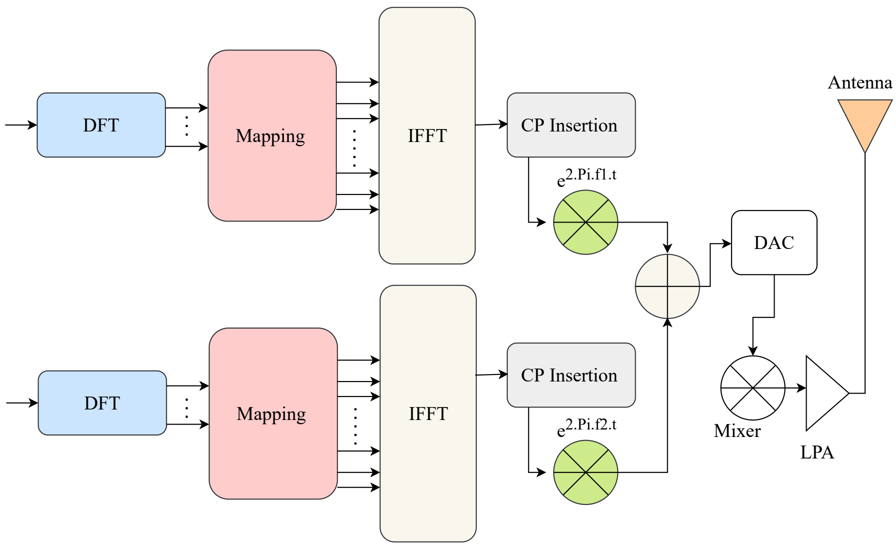


Figure 4.10: Transmitter block diagram for UL CA, adapted from [288].

DL a distinct transmitter chain can be cast-off. While for the implementation of CA in UL $N$ DFT-IFFT sets are essential [288]. When the transmitter is on multiple carriers, the single carrier stuff in the UL is no lengthier treating. Thus, the cubic metric rises that needs higher back-off in power amplifier, thus lessening extreme transmit power at the UE. A detailed evaluation of the cubic metric for the diverse figure of SC-FDMA carriers is shown in Figure. 4.11. As clearly shown, it has considerable expansion in cubic metric while they consider transmitting using multiple UL carriers. Though in suitable channel conditions, the multicarrier transmission drive is usually limited to UEs, it will have no harm of coverage for those users. Apart from this, the advanced transmission power drive is mandatory and can influence battery life.

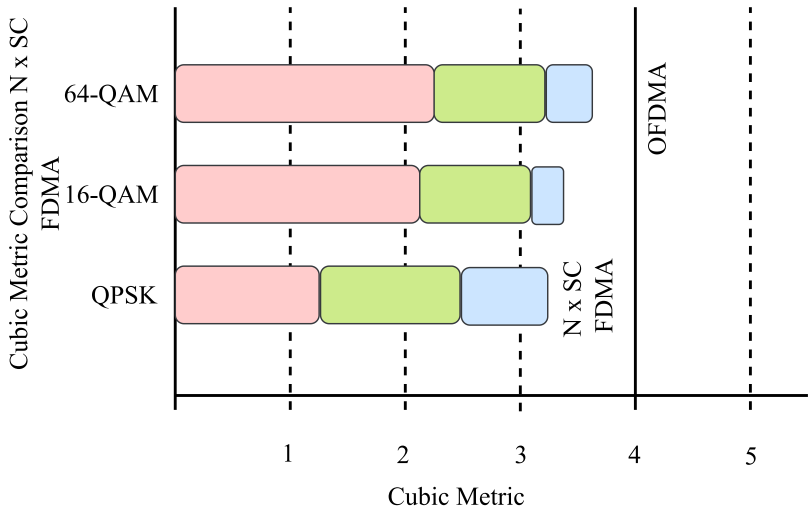


Figure 4.11: Cubic metric comparison for $N$ x SC-FDMA.

On the other side, at the cell edge, the users would be scheduled just on a single carrier. As a consequence, coverage might be enhanced, since the eNB can be dynamically allocating the users to the best UL carrier.

## 4.3 Performance Evaluation of Pico-Cellular Scenarios

LTE-Sim is an open-source framework proposed to perform the verification of LTE-based systems and to simulate LTE networks [275]. It includes several aspects of LTE technical specifications, such as Evolved Packet System (EPS) and Evolved Universal Terrestrial Radio Access (E-UTRA), allowing for the use of single-cell and multi-cell environments and handover procedures alongside traffic generators and scheduling procedures.

### 4.3.1 LTE-Sim Packet Level Simulator

The ecosystem of LTE-Sim was built using the $C{+}{+}$ programming language and the objected-oriented paradigm to ensure modularity, being composed of 90 classes. The protocol stack of LTE-Sim is shown in Figure. 4.12.

The four main components of the project are:

- The simulator;
- Network Manager;
- Flows Manager;
- Frame Manager.

Radio resource allocation is made in the time-frequency domain with the time domain resources being allocated according to each TTI with a duration of 1 ms. The frequency do-

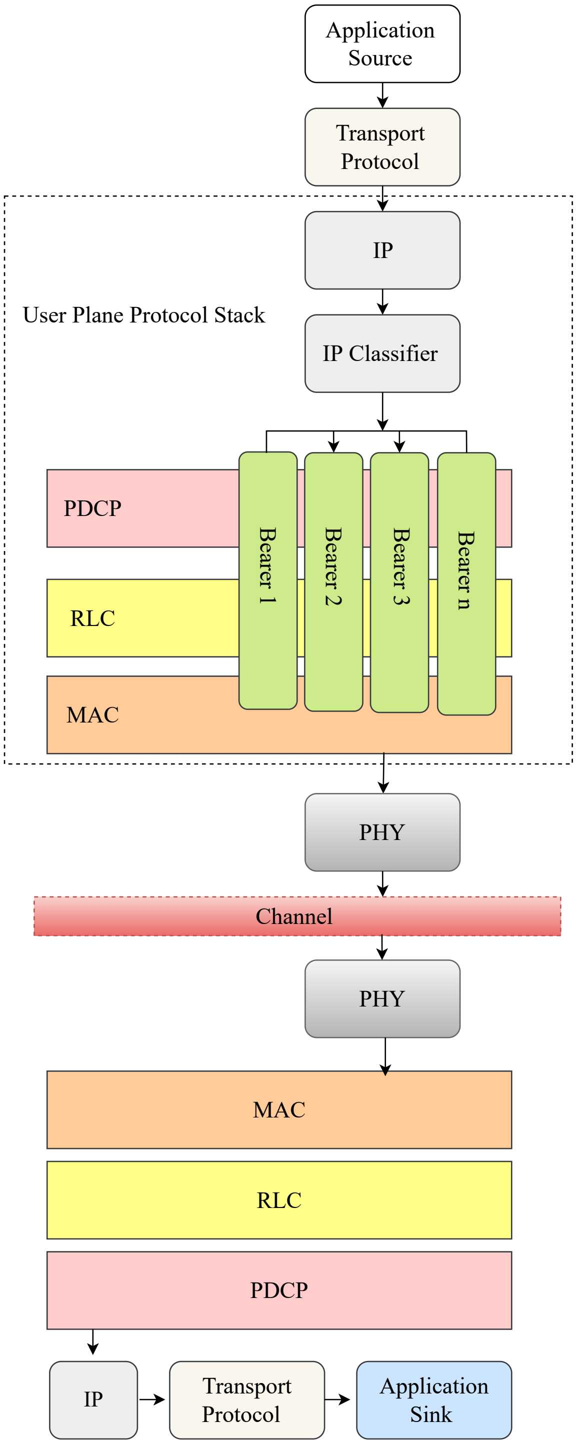


Figure 4.12: Protocol stack of LTE-Sim, adapted from [275].

main, on the other hand, considers the division of the bandwidth into sub-channels of 18 kHz. For every TTI, there are 14 OFDM symbols divided into 0.5 ms, with each consecutive TTI forming an LTE frame.

Regarding the application layer, the simulator offers four different traffic generators:

- Trace-based;
- Voice over IP (VoIP);

• Constant Bit Rate (CBR);

• Infinite Buffer.

The trace-based application uses trace files extracted from [290], that provides video traces created by the encoding of uncompressed video files [291] that allow the simulation of realistic video files transmissions.

VoIP applications operate by coding voice messages and sending them as data packets over IP-based networks and are common on telephony systems [292]. In LTE-Sim, these applications use flows based on G.729 which is a coder consisting of nano-rate that uses fixed-point arithmetic operations and works at 8 kbits/s [293]. The simulator uses a Markov chain with the VoIP applications being divided into ON/OFF periods where the source sends packets of 20 bytes during the ON period and within intervals of 20 ms and keeps a zero transmission rate during the OFF period.

CBR refers to an encoding technique which allows for the use of applications that keep the bit rate the same throughout the transmission [294]. One of the disadvantage of these types of applications is the lack of optimization in the relation quality versus storage. The simulator allows the configuration of packet size and packet time interval for this kind of applications.

The infinite buffer generator works by creating applications that always have packets to be sent by the source.

At the level of channel structure, the simulator works with all the bandwidths for LTE-based systems i.e., 1.4, 3, 5, 10, 15, and 20 MHz, offering a bandwidth manager that allows for each device under a simulated scenario to know the bandwidth being used, using a PHY object defined to each device. Furthermore, two types of frame structures are available i.e., FDD and TDD following the specifications for E-UTRA.

The FDD frame structure, referred to as frame structure type 1, is composed of 10 subframes available for DL and also 10 subframes for UL with transmissions at each 10 ms interval in the latter case [295], being applicable to full-duplex and half-duplex. Each radio frame is composed of 20 slots and each subframe comprises two consecutive slots, as shown in Figure. 4.13.

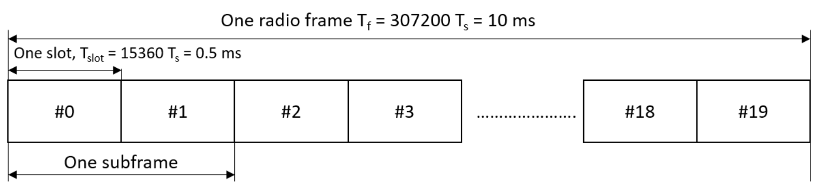


Figure 4.13: FDD frame structure, adapted from [295].

The TDD frame structure is represented in Figure. 4.14, where each radio frame is divided in two halves that in turn are composed of subframes corresponding to every TTI.

The simulator computes the SINR for each sub-channel as follows:

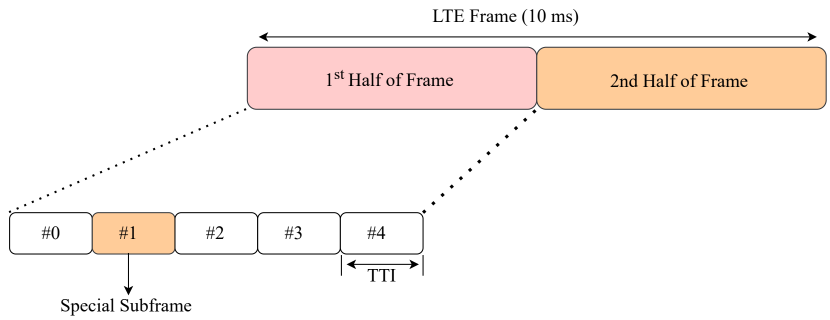


Figure 4.14: TDD frame structure, adapted from [295].

$$\text{SINR}_{i,j} = \frac{P_{RX,i,j}}{(F \cdot N_0 B) + I} \quad (4.2)$$

where $F$ is the noise figure, $N_0$ is the noise spectral density, $B$ is the bandwidth for a resource block, and $I$ is the interference computed for the eNBs sharing the same frequency resources.

For the transmit power $P_{RX,i,j}$, in this study one considers a normalized transmit power computed to ensure the delivery of SINR for all cell radius, for the 2.6 GHz and 3.5 GHz frequency bands. Exponential Effective SNIR Mapping (EESM) computations are then extracted from these formulations for Signal to Interference & Noise Ratio (SINR).

Regarding mobility, LTE-Sim offers two implementations, i.e., random direction and random walk. In the random direction mobility model, an entity chooses a random direction in which to travel and moves towards the pre-defined border following that direction. When the entity achieves the border, it pauses its movement and chooses a new direction to follow [296]. For the random walk model, an entity chooses randomly a direction and a speed and moves from its current location to a new location using the variables assigned. For the results presented in the following sections, the random direction mobility model is used to perform the movements of the UEs.

#### 4.3.1.1 General Multi-band Scheduler

General Multi-band Scheduler (GMBS) scheduler described and proposed in [15], [297], [274] and [273] as a way to offer CA as resource to improving network capacity adding an extra dimension of scheduling at the TTI level. The authors proposed the scheduling solution by using Integer Programing (IGP) establishing a Profit Function (PF) which considers the ratio between the requested application rate and the available rate on the DL channel, as described in equation 4.3:

$$(PF) = \sum_{b=1}^{m} \sum_{u=1}^{n} W_{\text{b,u}} \cdot X_{\text{b,u}} \quad (4.3)$$

where $X_{\text{b,u}}$ indicates whether the UE is allocated in band $u$ or not. Also, in equation 4.3, $W_{\text{b,u}}$ is a normalized metric whose values is given by:

$$W_{\text{b,u}} = \frac{[1 - BER(CQI_{\text{b,u}})] \cdot R(CQI_{\text{b,u}})}{S_{\text{rate}}} \quad (4.4)$$

where $BER(CQI_{\text{b,u}})$ is the Bit Error Rate (BER), in taken from the previous DL transmission, $R(CQI_{\text{b,u}})$ is the throughput as function of the MCS and $S_{\text{rate}}$ is the bit rate of the video encoding service.

One considers that each UE in the network can only transmit and receive over a single frequency band at a time. This constraint is specified by equation 4.5:

$$(ACt) \sum_{b=1}^{m} X_{\text{b,u}} \leq 1, X_{\text{b,u}} \in \{0,1\} \, \forall u \in \{0, ..., n\} \quad (4.5)$$

Furthermore, a constraint is established to control the number of UEs allocated at each band at each given time. The constraint considers the maximum normalized load that a band can handle, as shown in equation 4.6:

$$(BC) \sum_{b=1}^{n} \frac{S_{rate} \cdot (1 + R_{Tx} \cdot BER(CQI_{b,u}))}{RCQI_{b,u}} \cdot \\ X_{\text{b,u}} \leq L_b^{MAX} \forall u \in \{0, ..., n\} \quad (4.6)$$

where $S_{rate}$ is the throughput of the requested service, which is normalized by the maximum throughput that the network can offer, $RCQI_{b,u}$. After the process of maximization is performed, an allocation matrix, $X = [x_{b,u}]$ is created to help to allocate RBs to the UEs.

#### 4.3.1.2 Enhanced Multi-band Scheduler

The Enhanced Multi-band Scheduler (EMBS) uses a scheduling metric to perform decisions about the allocation of each RB in each CC, according to equation 4.7:

$$W_{i,j,b} = D_{HOL,i} \cdot \frac{R(CQI_{i,j,b})^2}{\bar{R} \cdot S_{rate}} \quad (4.7)$$

where $R(CQI_{i,j,b})$ is the throughput for in the $i - th$ flow for band $b$ and $j - th$ sub channel as a function of MCS, $D_{HOL,i}$, $\bar{R}$, and $S_{rate}$ stands for the same parameters as in the GMBS.

#### 4.3.1.3 Basic Multi-band Scheduler

The BMBS - also simply referred as CRRM algorithm is also studied in the context of this work. This algorithm works by allocating UEs to a preselected frequency band, until a threshold, $L_b^{MAX}$, is reached. Once the threshold is reached, the remaining UEs are allocated to the next frequency band. Equation 4.8 describes the allocation process for this scheduler:

$$x_{bu} = \begin{Bmatrix} 1, & \text{if } L_b \leq L_b^{MAX} \\ 0, & \text{if } L_b > L_b^{MAX} \end{Bmatrix} \quad (4.8)$$

The GMBS is more complex when compared to EMBS and BMBS (i.e., CRRM) but it only allows for UEs to be allocated at one CC at the time, while EMBS uses a metric that allows for the allocation of a user in more than one CC. Also, the use of IGP makes the computation process in GMBS more demanding, which reduces its performance when the number of UEs is higher.

Further details on the extension of LTE-Sim to support CA and multi-band scheduling are given in [273] and [27], where previous research with non-uniform distribution of users within the cells is addressed.

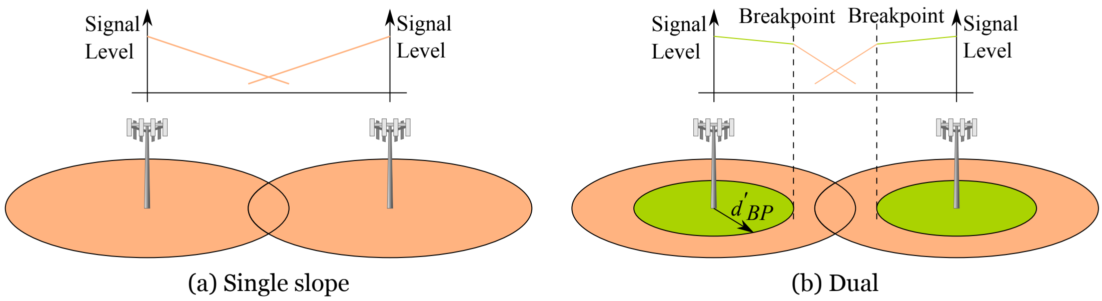


Figure 4.15: Different slope behaviors in the path loss models of cellular system.

### 4.3.2 Urban Pico-cell Dual Slope Path loss Modeling

Serval propagation path loss models are developed for cellular communication in a different environments, for example indoor, outdoor, urban, rural and suburban. These propagation models for the upcoming system need further enhancement because the previous generation was planned for lower frequencies. The propagation models can be deterministic, stochastic or empirical [298]. The deterministic model takes the location of the transmitter, the location of the receiver and importantly the properties of the environment. It uses electromagnetic wave propagation and also requires a 3-D map of the propagation environment. The stochastic takes the information about the environment and utilizes less power for processing. Empirical model is based on measurements. It is further divided into two dispersive, non-time dispersive and time dispersive. The first one considers various parameters for example antenna heights, distance, transmitter power, and frequency to predict average path loss. While the non-time dispersive offers information on approximately time dispersive characteristics of the channel. The ITU-R suggested the urban micro model with two slope, which can be applied in small cell environments [299].

This work considers dual slope path loss model with 2D urban micro from [299].The dual slope and signal slope model are shown in Figure 4.15. The definitions of distances in 2D are

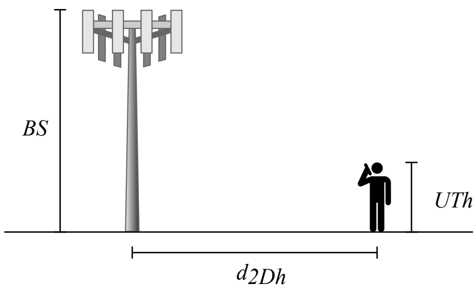


Figure 4.16: The Definition of $d_{2D}$ for outdoor Picocell users is adapted from [300].

shown in Fig. 4.16. The antenna height at the base station (BS) is defined by $h_{BS}$, while for the height of the user terminal (UT) is defined by $h_{UT}$. $d_{2D}$ is the distance between the UT and the BS, on the horizontal plane, in meters.Eq. 4.9 presents the path loss, $PL$, between the eNb, and UEs which is located up to the breakpoint distance.

$$PL_a(x) = 22.0\log_{10}(d) + 28.0 + 20\log_{10}(f_c), \quad (4.9)$$

where $d$ is expressed in meters while $f_c$ is the frequency given in GHz which is 2.6 and 3.5 GHz. For distances the longer above breakpoint distance, $PL$ is calculated by Eq. 4.10 as follows:

$$\begin{aligned} PL_b(x) = {} & 40.0\log_{10}(d) + 7.8 - 18\log_{10}(h_{BS} - 1.0) \\ & - 18\log_{10}(h_{UE} - 1.0) + 2\log_{10}(f_c), \end{aligned} \quad (4.10)$$

where $h_{BS}$ gives the eNb height while the $h_{UE}$ is the height of the user. The breakpoint distance, $d'_{BP}$, is calculated as:

$$d'_{BP} = \frac{4(h_{BS} - 1.0)(h_{UE} - 1.0)f_c}{c}, \quad (4.11)$$

where $c$ is the velocity of the RF signal in free space (equal to the speed of light), which is approximately $3 \times 10^8$ m/s. $d'_{BP}$ is either determined when the first Fresnel zone just touches the ground or by the turning point between the line of sight and none line of sight zones [301, 302].

The considered 2.6 GHz and 3.5 GHz frequency bands are given in Table 1 from [27]. The inter-band CA deployment scenario from Figure. 4.17 considers the existence of two collocated CCs hexagonal coverage zones operating at the frequency band 2.6 GHz and frequency band 3.5 GHz, while also considering the existence of the first tier of interferes, as illustrated in Figure. 4.17. The allocation of UEs at each CC is decided in every TTI, following the metrics of packet scheduler considered, the EMBS.

In the implementation of each multi-band scheduler, while optimizing the allocation of resources, an allocation matrix, $X = [x_{b,u}]$ is considered to help to allocating RBs to the UEs. After this allocation matrix is created, the Modified Largest Weighted Delay First (M-LWDF) DL packet scheduler is used to compute metrics to the assigned CC. This algorithm is de-

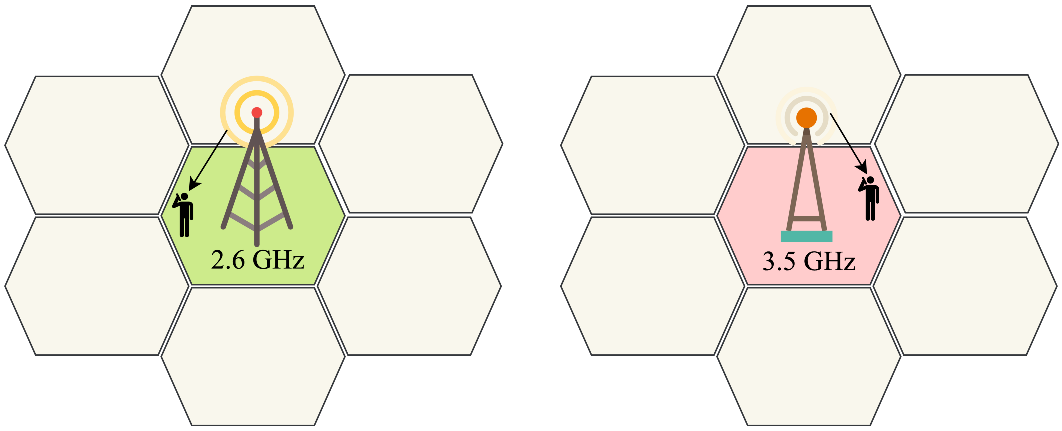


(a) Scenario for without CA at 2.6 GHz and 3.5 GHz

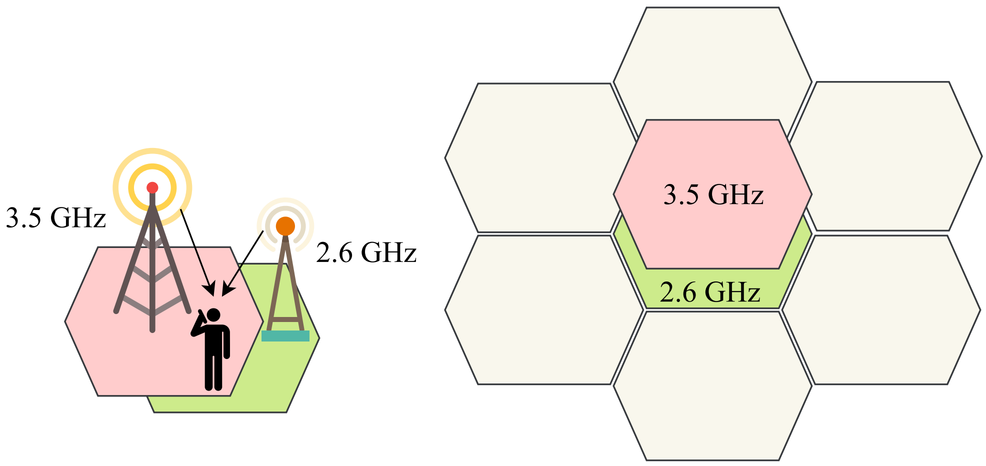


(b) Inter-band CA deployment scenario, adapted from [274]

Figure 4.17: Deployment scenarios for CA and with CA for cell radius 500 m.

signed to support multiple data users while considering different QoS parameters [303], by computing a metric $W_{i,j,b}$ as follows:

$$W_{i,j,b} = \alpha_i D_{HOL,i} \times \frac{r_{i,j}}{R_{i,j}} \quad (4.12)$$

where $D_{HOL,i}$ is the $i-th$ flow head of line packet delay, $\bar{R}_i$ is the flow average transmission rate, given by equation 4.13 and $r_{i,j}$ is the instantaneous available rate for each sub channel in each flow:

$$\bar{R}_i(k) = 0.8\bar{R}_i(k-1) + 0.2\bar{R}_i(k) \quad (4.13)$$

In equation 4.13, $R_i(k)$ is the throughput achieved in each flow and $R_i(k-1)$ is the throughput for the previous TTI. Furthermore, in equation 4.12, the parameter $\alpha_i$ is used to ensure precedence to users with strongest requirements in terms of acceptable loss rate in cases of flows with equal $HOL$. The variable $\alpha_i$ is computed as follows:

$$\alpha_i = \frac{log(\delta_i)}{\tau_i} \quad (4.14)$$

where $\delta_i$ is the probability that the delay will exceed the established threshold of $\tau_i$.

The description of the applied multi-band schedulers is as follows, adapted from [27]:

### 4.3.3 Scenario

Inter-band CA with uniform user distribution in the Pico-cell is considered. For CA, considered the two frequency bands, 2.6 GHz and 3.5 GHz (inter band CA with EMBS), as shown in Figure 4.5b. Deployed two scenarios, first is with out CA as shown in Figure 4.17a and second is with CA which is shown in Figure 4.17b. For without CA the same set of parameter are considered, and evaluated separately for each frequency band (with frame level scheduling). The cell radius for the aggregation is 500 meters (Pico-cell) [304]. For scheduling through two bands, EMBS is considered. The simulations are obtained with the LTE-sim simulator [275], where the distribution of the users is updated with path loss models to the simulator. Considered the 20 MHz bandwidth. The motivation behind this work is to consider inter band CA to allocate resources with multiple frequency bands to obtain a high data rate with low interference.

The cell radius is in range of 500 meters to evaluate CA (EMBS) scheduling and without CA (Frame level scheduling) in a small cell radius (Pico-cell) range. The improvement and reuse of bandwidth can be achieve by splitting more longer radius cells (Macro-cell) into small cells radius and then scheduling by multiple bands, which is the main aim of the work. In this work, the Macro-cell is parted to Pico-cell radius, further changing the radius to shorter

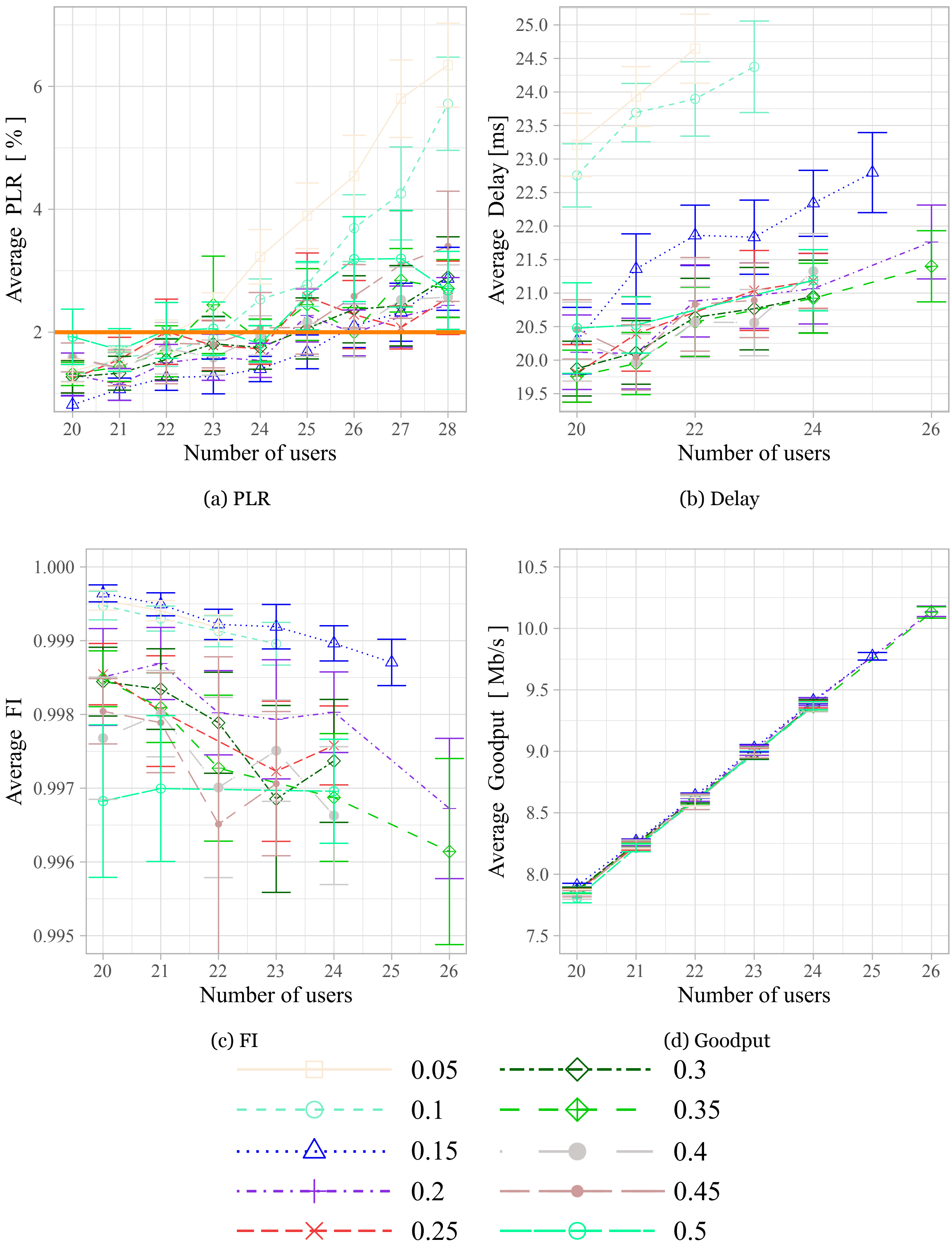


Figure 4.18: Average cell PLR as a function of UEs for $R = 500$ m, without CA considering 2.6 GHz.

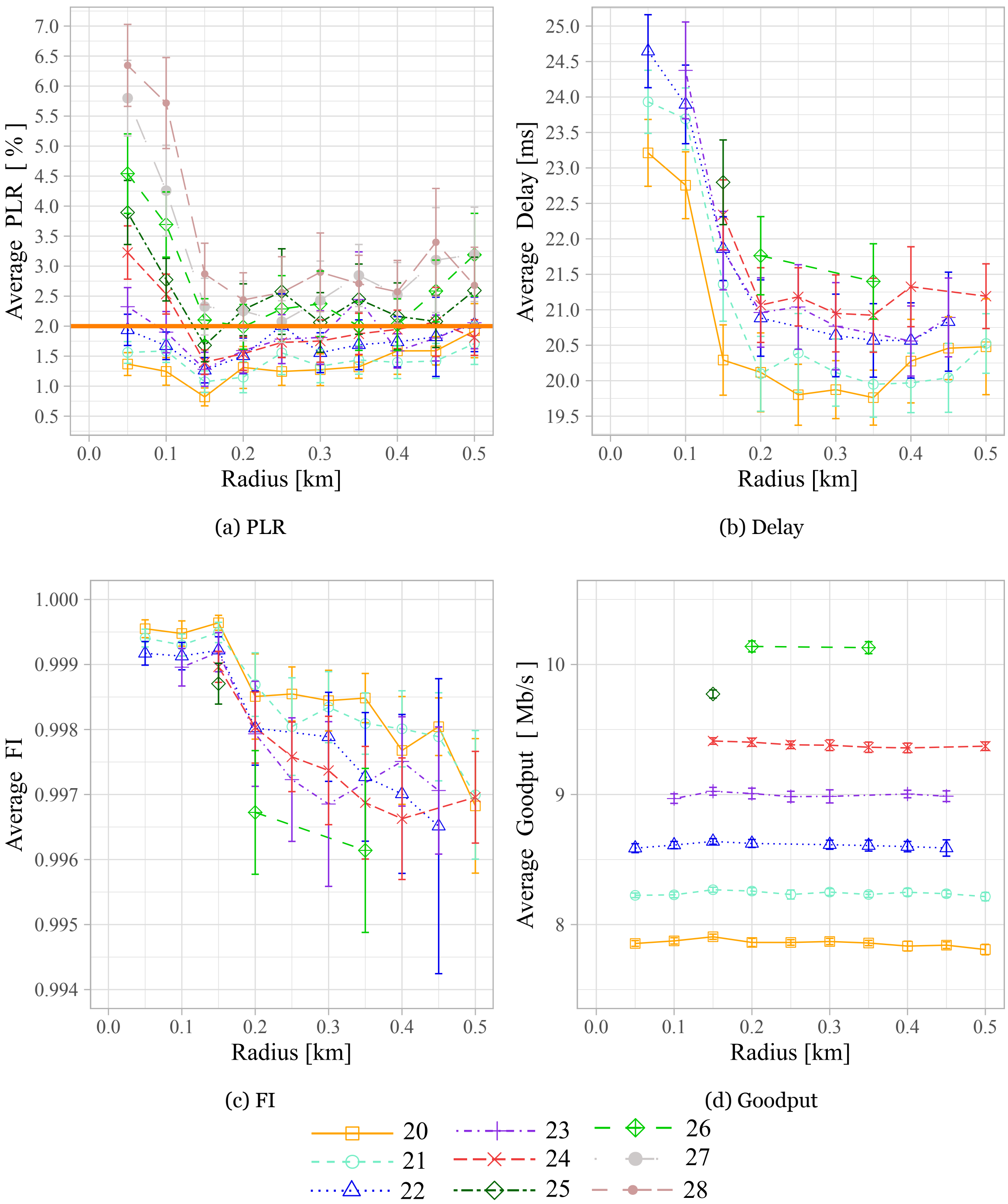


Figure 4.19: Average cell PLR, delay, FI and goodput as a function of $R = 500$ m for UEs, without CA considering 2.6 GHz.

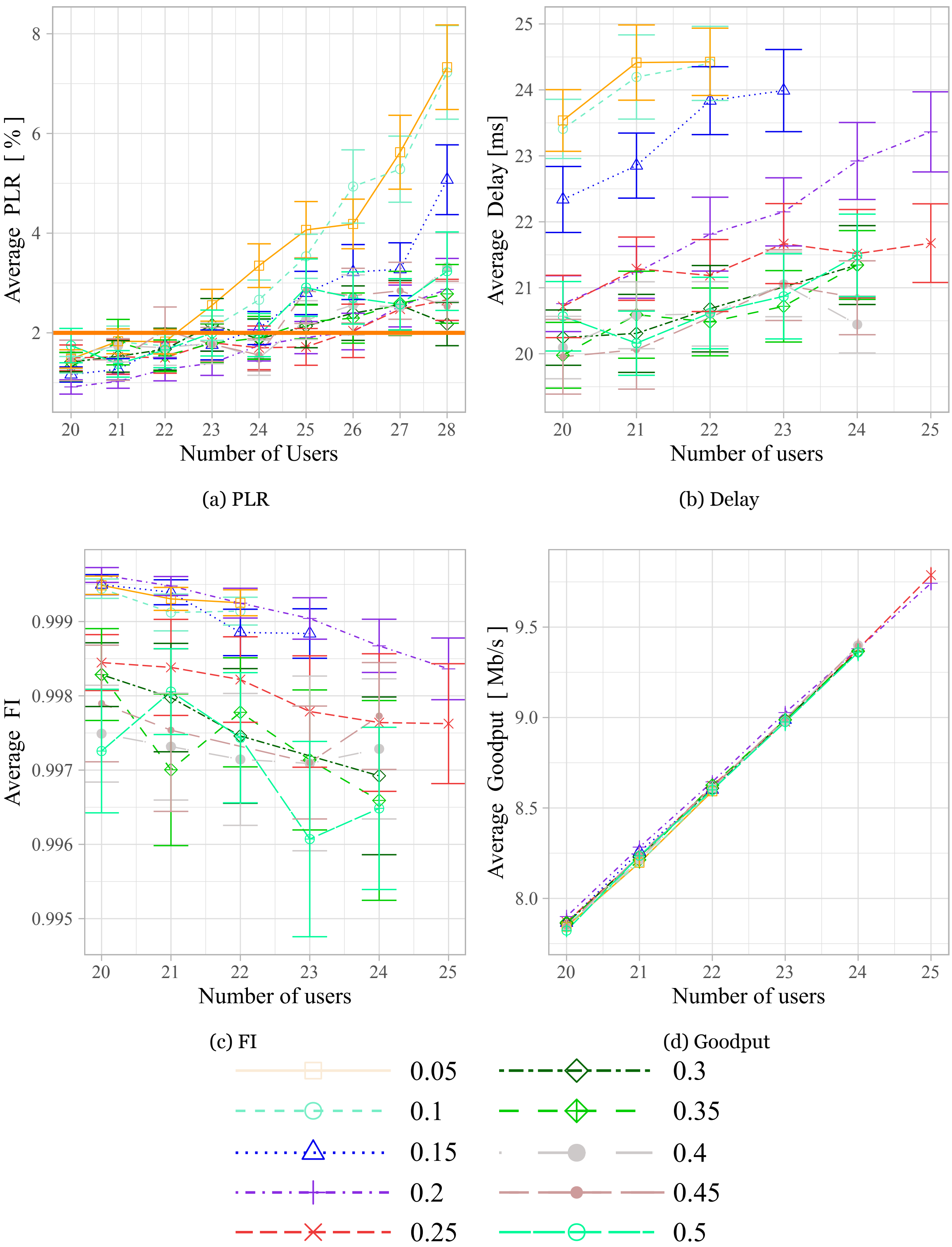


(a) PLR

(b) Delay

(c) FI

(d) Goodput

Figure 4.20: Average cell PLR as a function of UEs for $R = 500$ m, without CA considering 3.5 GHz.

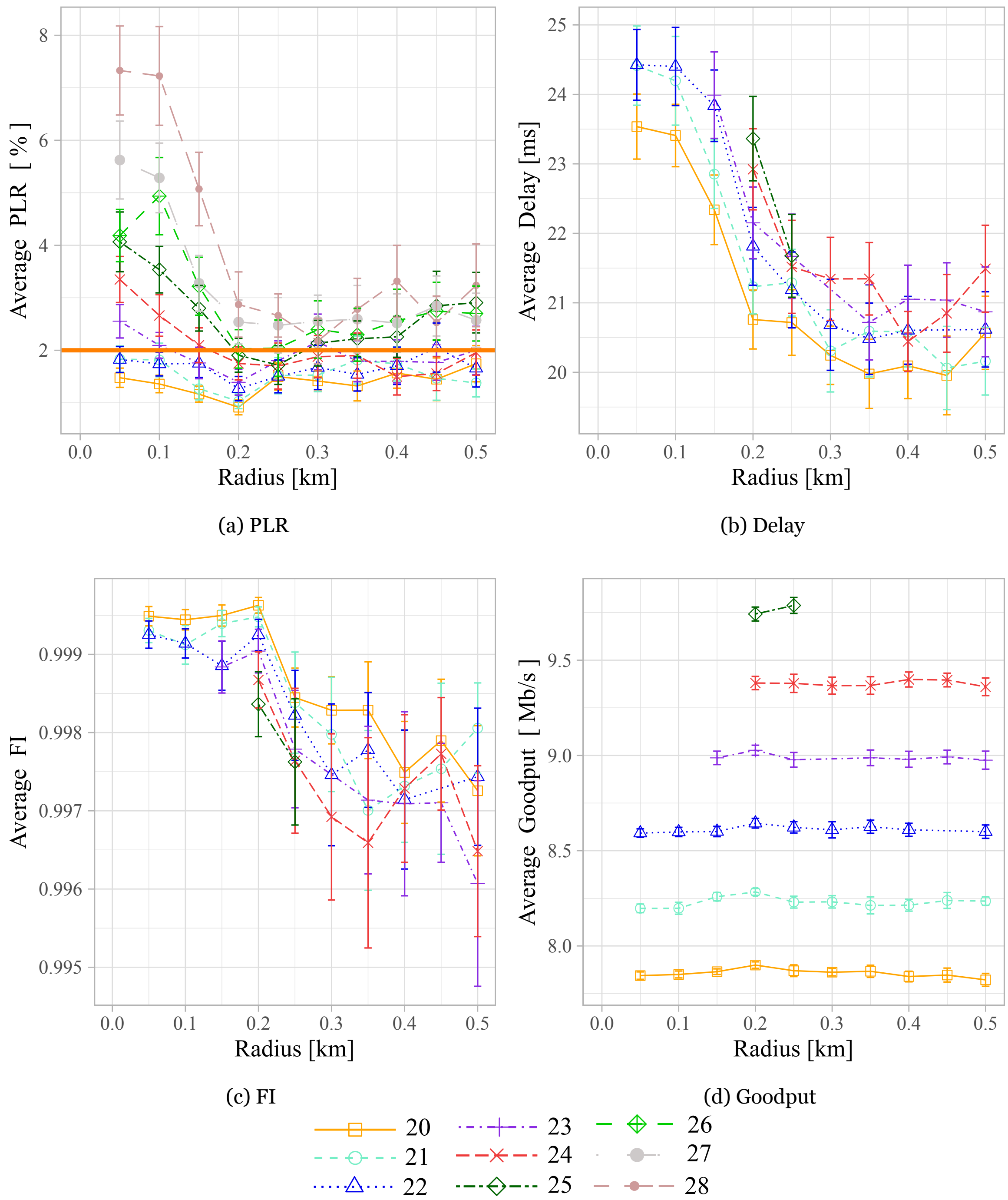


(a) PLR

(b) Delay

(c) FI

(d) Goodput

Figure 4.21: Average cell PLR, delay, FI and goodput as a function of $R = 500$ m for UEs, with without CA at 3.5 GHz.

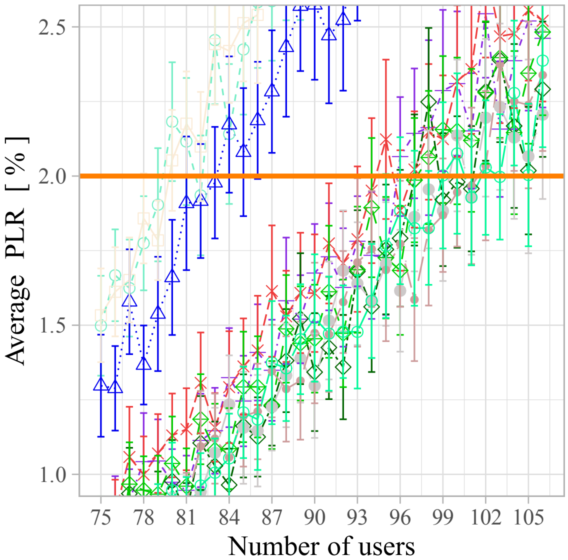


(a) PLR

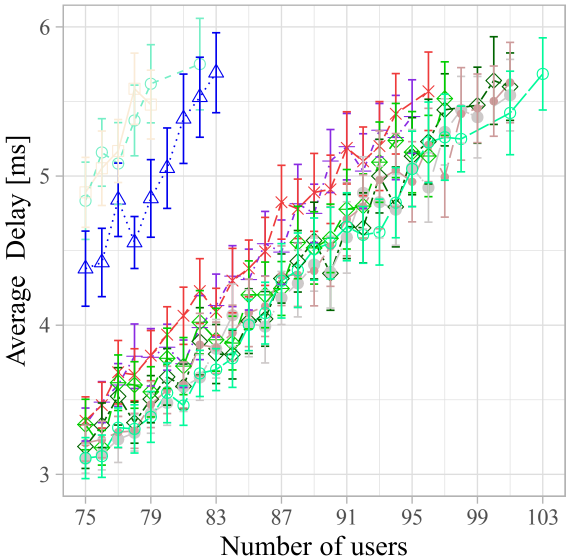


(b) Delay

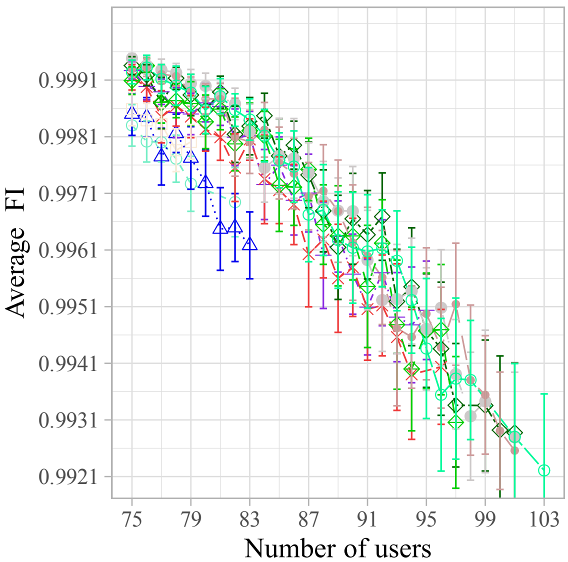


(c) FI

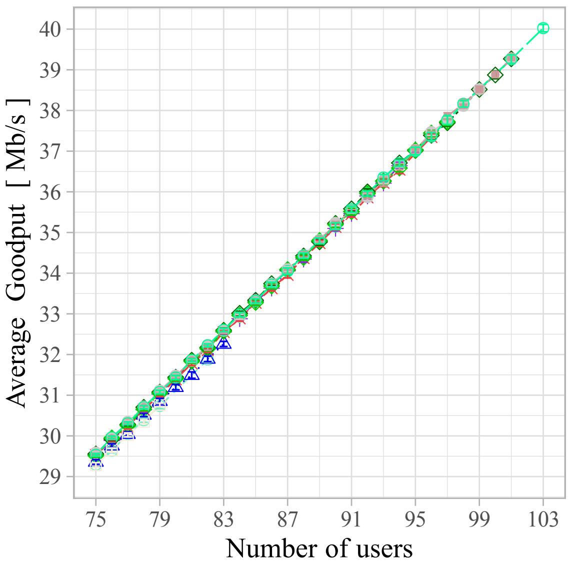


(d) Goodput

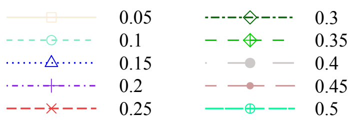


Figure 4.22: Average cell PLR, delay, FI and goodput as a function of UEs for $R = 500$ m, with CA considering 2.6 GHz and 3.5 GHz.

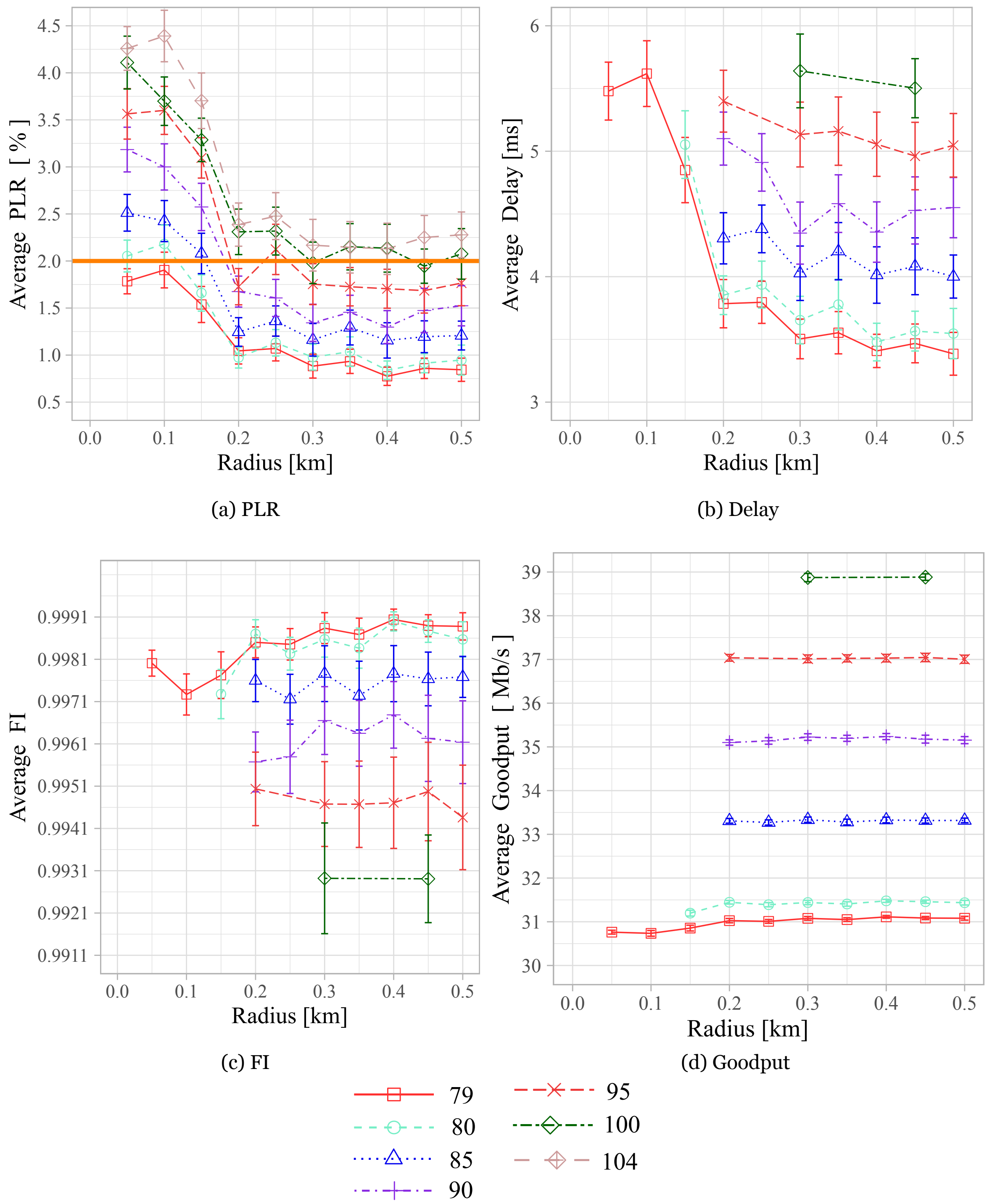


Figure 4.23: Average cell PLR, delay, FI and goodput as a function of $R = 500$ m for UEs, with CA considering 2.6 GHz and 3.5 GHz.

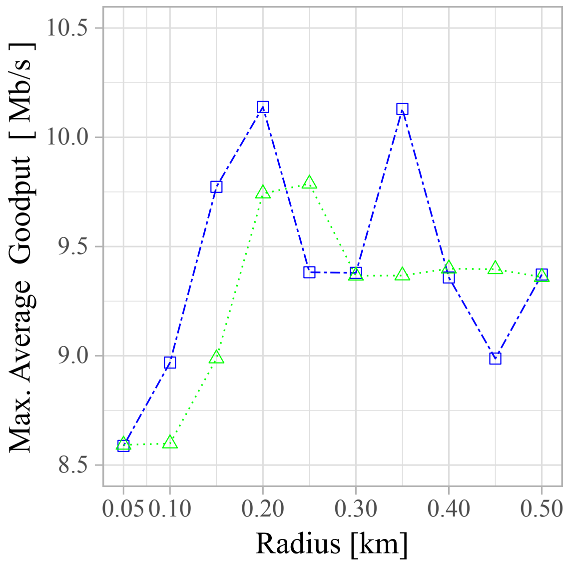


(a) Simulated maximum average good put, for with out CA at 2.6 GHz and 3.5 GHz

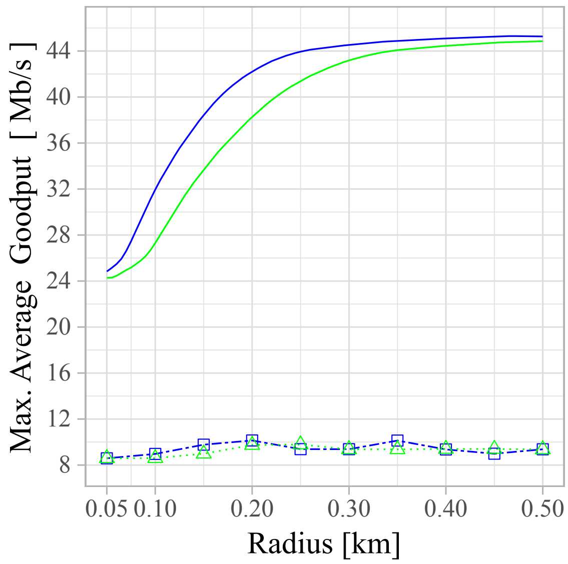


(b) Simulated maximum average good put, for with out CA at 2.6 GHz and 3.5 GHz and comparative analytical supported good put

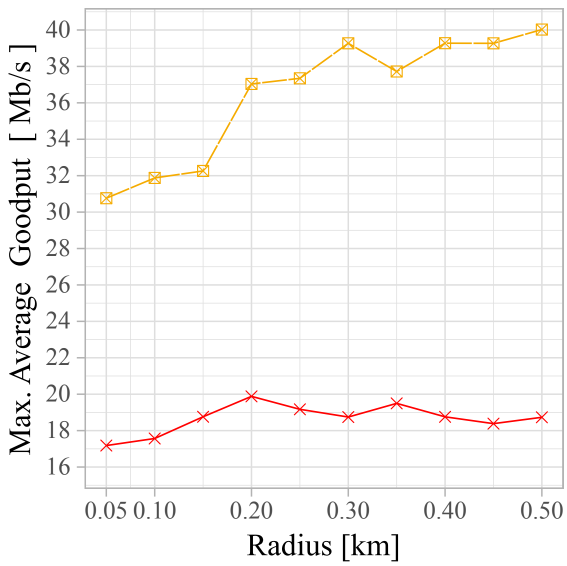


(c) Goodput


Figure 4.24: Simulated maximum average good put, its comparison with analytical supported goodput, and the 2.6 GHz and 3.5 GHz summation of simulated results presented in (a).

Table 4.1: Parameters used while simulating the CA and without CA scenario.

| Parameters | Values/Name |
|---|---|
| Number of cells | 7 |
| Application | Video |
| Frame structure | FDD |
| Speed of UE [km/h] | 3 |
| Delay [s] | 0.1 |
| Video bit rate [kb/s] | 440 |
| Transmit Power for 2.6 GHz[dBm] | 40 |
| Transmit Power for 3.5 GHz [dBm] | 42.2478 |
| Number of users for Without CA | 20 to 26 |
| Number of users for CA | 90 to 106 |
| Radius [m] | 500 |
| Bandwidth [MHz] | 20 |
| Cluster ($K$) | 3 |
| Path loss model | Dual slope (urban micro) |
| Schedulers for CA | EMBS |
| Schedulers for without CA | FLS |
| Number of simulations for each combination | 50 |
| Height of BS [m] | 10 |
| Height of UE [m] | 1.5 |
| Break point distance for 2.6 GHz [m] | 156 |
| Break point distance for 3.5 GHz [m] | 210 |
| Simulations duration [s] | 46 |
| Flow duration [s] | 40 |

ranges. The work considers the 4G protocols to obtain comparable CA results. The users are randomly moving at a speed of 3 km/h. The simulation parameter for the scenario is presented In Table 4.1.

### 4.3.4 Simulation Results

CA with scheduler is implemented upon the LTE-Sim stack, it was possible to evaluate the performance by computing the average Packet Loss Ratio (PLR), goodput, and delay. Compared the scenario of two separated LTE-A networks operating at the 2.6 GHz and 3.5 GHz frequency bands (without CA) and the scenarios with CA between the two bands that are managed by EMBS.

To perform the underlying simulations, one first considers a cell radius of 500 meters , with the number of UEs from 79 to 106. The simulations are executed a total of 50 times and the results for the measured parameters are the average of the total number of simulations. The simulations were performed with transmissions based on video traces of 440 kb/s video bit rate, considering a maximum delay of 0.1 s, with flow durations of 40 s assuming that the UE distributed are moving with a speed of 3 kmph.

The acquired results for the case without CA 2.6 GHz, 3.5 GHz and combine with CA, as a function of users, are shown respectively in Figures 4.18,4.20 and 4.22. While as function of radius is shown in Figure 4.19, 4.21, and 4.23.

The variation of the average cell PLR with the number of UEs are presented in Figure 4.18a 4.20a, and 4.22a, where the orange line highlights the points corresponding to a PLR 2%.

As GMBS and EMBS work presented in [15] with CA, considering the single slope path loss model. The proposed work comparing the results with [15] while considering dual slope path loss model. The EMBS schedulers of the presented work perform better than [15]. With EMBS (with CA) presenting a lower value of average PLR than the case of without CA of 2.6 GHz and 3.5 GHz. The presented approaches (with CA) comparative to the work presented in [15], provides higher support (50 % more users). The break point distance for 2.6 GHz is 156 m, while for 3.5 GHz its 210 m. This break point distance is calculated by equation 4.11. One can see that in Figure 4.19a, 4.21a, and 4.23a average PLR decreasing until the break point distance for both bands (with CA and without CA), after the break point distance the average PLR increase and then lower than before or equal until 400 meters, for different number of users. Overall the proposed approach support more users with lower PLR than single slope model [15].

Comparing CA scenario results shown in Figure 4.22a with a scenario without CA at 2.6 GHz shown in Figure 4.18a, and with result scenario without CA at 3.5 GHz shown in Figure 4.20a. The CA scenario support 100 UE with below 2% of PLR, while without CA scenario supports 24 UE in case of 2.6 GHz and 23 UE in case of 3.5 GHz. It concludes that with CA scenario, can support more than 3 times higher UE than without CA scenario.

The average delay is evaluated considering the defined parameters (less than 150 ms). Figures 4.18b, 4.20b, and 4.22b shows the variation of the delay in ms, for the given number of users. It is possible to see that with CA, it support UE with lower delay in rage of 3 ms to 6 ms, shown in Figure 4.22b for even higher number of users. While in case of without CA scenario the delay is between 19.5 ms to 25 ms shown in Figures 4.18b and in Figure 4.20b, which is higher in both cases for without CA scenario (2.6 GHz and 3.5 GHz), compared to CA scenario for cell of radius (50 m to 500 m).

The average fairness index is presented in Figure 4.18c, 4.20c, and 4.22c. The values is in range of zero and one. For both scenario the fairness is decreasing as the number of user increase, comparatively the CA scenario proved better fairness for higher users. But overall the resources are equally distributing among the users.

Figures 4.18d, 4.20d, and 4.22d presents the variation of the supported goodput with the number of users (for radii up to 500 m). It obtained that as the number of UEs increases, the schedulers tends to perform better [15]. In comparison CA scenario support maximum goodput 40 Mb/s, while without CA scenario it can support maximum goodput 10 Mb/s. The CA scenario provider almost three time higher good put compare to without CA scenario for different radius. By considering CA, mobile operators and service providers can deliver services to mobile subscribers with ensuring satisfactory levels of quality of services. It reducing the levels of packet loss ratio, and thus increasing the throughput.

### 4.3.5 Comparison of Maximum Supported Goodput Obtained Through Computations and Simulations

To understating the achieved results through simulations. It is important to first analyze the results through computations. For this purpose, the system capacity is first calculated. The calculated results for maximum supported goodput are obtained through equation 4.9, and 4.10, the breakpoint distance through 4.11.

The simulated goodput, without CA scenario for both 2.6 GHz and 3.5 GHz are shown in Figure 4.24a. In Figure 4.24b computed results combined with simulated results for maximum supported goodput are shown. The computed maximum supported goodput is almost 45 Mb/s for both bands, while through simulations the maximum supported goodput for without CA scenario at 2.6 GHz and 3.5 GHz is almost 10 Mb/s. Which is almost 4 times less goodput than calculated goodput. The obtained results through simulations considering the CA scenario and the sum (of 2.6 GHz and 3.5 GHz goodput without the CA scenario, simulated) are shown in Figure 4.24c. One can see with the CA scenario the goodput of calculated results is very close to simulated results of CA. According to this comparison, its concluded that our obtained result through CA approximately near to the calculated results, which mean one can achieve the system capacity by CA.

From system capacity study, it is possible to obtained the **cost/revenue trade-off**, where multi-band Scheduling and CA (EMBS) is compared with the case without CA. The cost/revenue trade-off for CA and with out CA scenario are presented in section 6.6. The results for the cost/revenue trade-off are presented in Figure 6.7.

## 4.4 Summary and Conclusion

The chapter provides a detailed overview of LTE-advanced CA. According to the literature review, when the spectrum's resource becomes scarcer, the CA will become an essential scheme in the upcoming communications system. Have explained the necessary CA and system capacity optimization concepts for LTE-Advanced. Using wide bandwidth, CA provides higher data rates and enables flexible and optimal utilization of frequency resources. The CA between non-contiguous frequency bands offers novel opportunities to get more benefit from frequency assets for LTE-Advanced in different bands.

Real-world application of CA has been explored within the context of LTE-Advanced, via the use of an integrated Common Radio Resource Management (CRRM) entity that performs inter-band CA via the scheduling of two Carrier Components (i.e., band 2.6 GHz and band 3.5 GHz). The primary motivation behind this work is to have a framework that can deliver services to mobile subscribers, ensuring satisfactory quality of service levels, reducing the levels of packet loss ratio, provide support to more UEs, and thus increasing the throughput. Simulations presented in this chapter the LTE-Sim packet-level simulator was considered, where the proposed multi-band scheduler (EMBS) were tested for applications based on traces of videos of 440 Kb/s.

To evaluate system capacity, scenarios have been considered where different cell radius and number of uniformly distributed user equipment were used in simulations obtained data to assess the system's performance. First, a scenario has been considered where the cell radius was 500 m, and the number of UEs changed from 75 to 106. In this first case, the proposed scheduler have been tested, and their performance has been analysed, for CA with the small cell radius and number of UEs. The analysis of proposed scenario demonstrates that CA's use considerably reduces the levels of PLR.

Due to statistical multiplexing gain, CA is capable of surpassing the increase in the number of resources for given cell radius and number of UEs. Values obtained in this study have also been used to estimate system capacity by considering a threshold of 2% for PLR. Under these assumptions, one has been able to obtain values for the goodput of 40 Mb/s for a cell radius of 500 m and of 29 Mb/s for a cell radius of 50 m, which is 3 times higher than without CA case. The benefits will be confirmed by the analysis of the cost/revenue trade-off in Chapter 6.

# Chapter 5

# Modelling and Optimization of Femto-cells in Heterogeneous Network for 5G and Beyond

## 5.1 Introduction

During the last four decades, the world has perceived four generations (1G, 2G, 3G and 4G) of mobile communications. Around 1980, the first mobile generation emerged based on analog transmission. This technology was limited to voice services. In the 1990s, the second generation introduced the concept of digital transmission on the radio link. Its targeted service was also the voice services. In the initial stage, there were several second-generation technologies, like global mobile systems, digital advanced mobile phone systems, personal digital cellular and CDMA-based IS-95 technology. Later in the 2000s, the third generation got entry. This generation was the decisive step to high-quality mobile broadband and wireless internet access. This technology was enabled by high-speed packet access. For several years, we have been in the era of 4G mobile technology [305]. International Telecommunication Union introduced the fourth generation, and they specified the critical characteristics of standards for it. The discussion of 5G technology began approximately in 2012. NR is the set of standards that trade the 4G standards. 5G NR supports a high data rate equivalent to fiber. That supports applications which require higher data, like video streaming and gaming. Also, it has low latency, which can fulfil the requirement of low latency applications. One of the essential supports of 5G New Radio (NR) is, it can connect the massive device by densification (small cells). The 5G NR standard is proposed by the 3GPP. 3GPP first release about 5G NR is Release 15 [306], and they have further updates in Release 16 [307], and release 17 [308].

According to [309], the 5G can cover different aspects of user services requirements. But due to a massive number of connected devices demands and high data rate requirements, the current network needs evaluation in network structure. HetNet has been under investigation for many years. Comparing the HetNet with a homogeneous network, the HetNet can improve users service quality and resource utilization. This quality of service can be enhanced by putting the small cells inside the Micro cells and Micro cells converge area. Due to massification, it can suffer from interference. Improved reuse algorithms are required to avoid it. The service of Femto-cells can be obtained indoors to address the insignificant coverage problem of buildings. Deploying Femto-cells inside the network can reduce the network cost [310]. Some service providers have started their solutions for indoor users, but there are still many challenges to address.

In the scope of Femto-cell in Hetnet, in this Chapter, the Femto-cells simulation are analyzed by putting the Femto-cells within a Macro-cell while considering the indoor scenario for Femto-cells. The simulation results are performed with 5G NR features viewing the 5G-air-simulator [311]. The work studies the performance of Femto-cells, with indoor coverage. The theoretical SINR is studied, and after that, the simulation approach is expended to obtain the indoor Femto-cells results. Based on the enhanced version of the 5G-air-simulator the M-LWDF and FLS schedulers are tested. The M-LWDF performs better than the FLS. The works present that with considered applications, it's possible to achieve the reduction in transmitter power and increase the number of connected devices with quality of service, without compromising network performance. The results are obtained for number of connected users with goodput and packet loss ratio. Further, the fairness results are obtained to analyze the resource allocation fairness.

### 5.1.1 Motivations and Challenges

The cellular system began with BS deployment through wide area coverage. Currently the 5G and beyond trend toward the small cell deployment [312]. The deployment of small cells improves the quality of services and system capacity. The short-range cells enable improvement in the carrier to interference ratio and also enhance the service quality and system capacity. The reduction of cell size and improvement in system perforce can be described by considering Shannon's law [312].

Currently, 80% of traffic is indoor, which assisting by eNBs/gNb. The increased demand for indoor traffic is a challenge for the operators. The data hungry application required higher throughput. When the high data rate indoor traffic is served by outdoor BS, with higher modulation coding schemes for example 64/128/256 QAM. The walls (impassable) of the depth building, or congested, faces obstacles that make the signal weak for indoor convergence. To increase the system capacity the 5G network uses higher frequency but that creates the same issue for indoor traffic, when using the higher modulation order then it serves the indoor user with either week signal or no coverage at all.

One solution to solve the scarcity of indoor convergence is to resort to smaller eNB coverage [312] [313]. Yet these solutions has not overcome the identified issues. It cannot eliminate the indoor walls and other obstacles among the eNB and UE. To achieve higher indoor capacity, Femto-cells are developed in a heterogeneous network, which can provide indoor coverage, where there is resorting to the traditional eNB [312]. Femto-cells are small easy to install and less expensive with low operating costs. Deployed Femto-cells are not only for a house but also to deploy in the industrial environment and shopping centres.

The uncoordinated and disordered deployment of small cells tends to have high interface problems for both UL and DL. To address this issue, power control and scheduling algorithms have been proposed, which relieve the interference while enhancing the small cell operations. To overcome the uncoordinated deployment of the Femto-cells, the positioning algorithms for interference control are being developed.

The reaming Chapter is organized as in Section 5.2, it overview 5G NR features,deployment modes, its spectrum requirements, resource grid with frame structure and data rate calculation are presented. The 5G NR data rate is shown with a diagram with details of mathematical understanding elaborated. The overview of 5G waveform candidate is given in Section 5.3.

Femtocell deployment scenario is presented in Section 5.4, followed by the Frame level Scheduling (FLS) and Modified largest Weight Delay First (M-LWDF) algorithms. The considered path loss model is given. Performance evaluation of Femto-cells in heterogeneous network are presented in Section 5.5, with SINR study and simulations analysis, while results are presented at the end of the section, Mathematical understanding of average SINR results for proposed 25 Femto-cells with reuse pattern two are given in detail. The conclusion is given at the end of the chapter.

## 5.2 5G New Radio

5G New Radio is the set of standards which replace the 4G wireless standards. Its main goal is to enhance the spectrum efficiency of mobile broadband. 5G NR important understandings are presented below.

### 5.2.1 5G NR Features and its Benefits

Features and benefits of 5G NR [314]:

- Operating in sub 6 GHz and mm-wave spectrum that gives benefits of 10X to 100X capacity;
- Its scalable numerology makes it possible to support multiple bandwidths and spectrum's;
- Scalable OFDM based air-interface to support a comprehensive range of services;
- Lean carrier design, less interference with low power consumption;
- Due to the support of advanced channel coding, it is benefited with considerable data block support with low complexity;
- Backhaul and integrated access support higher coverage and low cost;
- The connectivity, sessions and mobility are quite flexible, which gives benefits of better optimization for many services;
- Access channels and beam formed control support provide more excellent coverage;
- Higher spectral usage that enhanced efficiency.

### 5.2.2 5G NR Deployment Modes

It has two types, Figure 5.1 a) Non stand alone b) Standalone. Standalone 5G does not depend on an LTE evolved packet core for operation. It has a dedicated network function and equipment. The radio unit is connected with cloud-native, service-based core network functions. In this case, the network function is cloud-native and virtualized. Benefits of 5G standalone [315]:

- Can support eMBB , URLLC , and mMTC;
- It can take the benefit of network slicing;

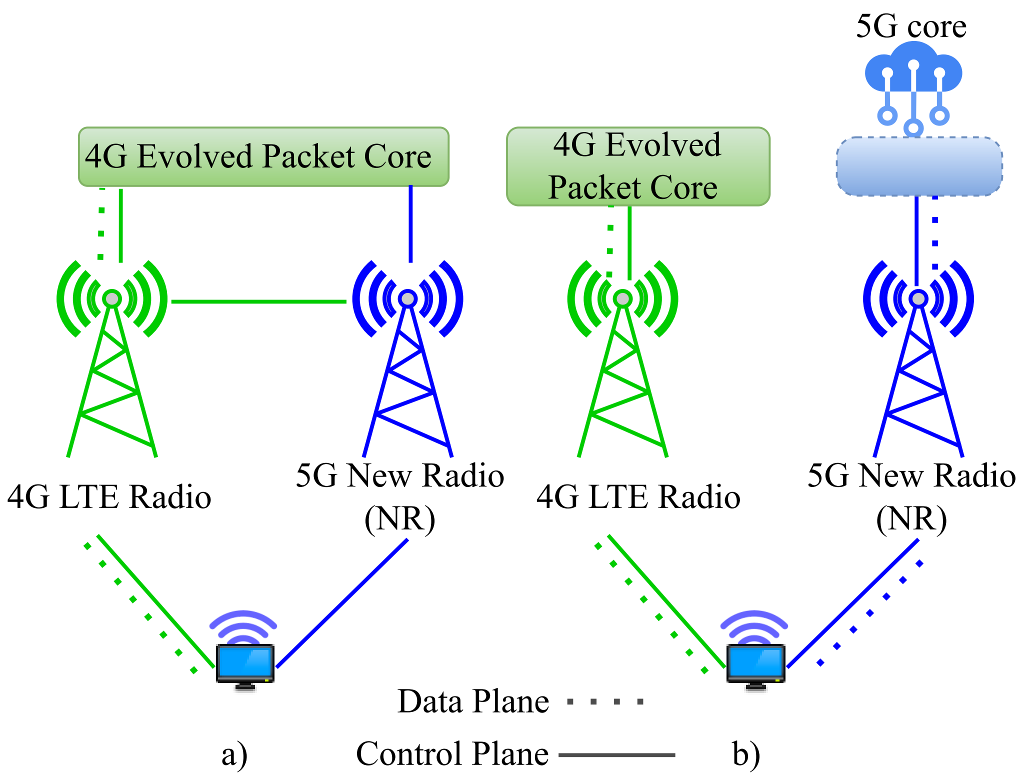


Figure 5.1: a) Non stand alone 5G uses a 4G LTE control plane to manage connectivity and authorization and b) Standalone uses a 5G core to manage connectivity and user authentication [316].

- More flexible and dynamic.

While in non-stand-alone 5G network, it depends on LTE core infrastructure. The radio unit is attached with an LTE core. In this case, the network functions are dedicated. Benefits of 5G non-standalone:

- Faster roll-out;
- Improve and can maximize the network assets;
- Low investment.

### 5.2.3 5G NR Spectrum

5G NR support mid-band high band and low band frequency band. The 5G standard defined the ranges for carrier frequencies < 6GHz with TDD & FDD (FR1) and FR2 (23-53 GHz with TDD). The two frequency band ranges are available for 5G technology. The FR1 is presented in Table 5.1 and FR2 in Table 5.2. 5G NR supporting band contains unlicensed spectrum also that can be accessed by anyone.

### 5.2.4 NR Resource Grid

The NR 5G resource grid is defined in Figure 5.2. If we compared the LTE resource grid [319] with 5G NR it looks over all identical as to 5G NR [320], but in 5G NR, there is a difference that the NR resource grid's physical dimension is changeable and depending on numerology

Table 5.1: operating frequencies for 5G NR (FR1) [317, 318].

| Band | UL [GHz] | DL [GHz] | Duplex Mode |
|---|---|---|---|
| n1 | 1.92-1.989 | 2.11-2.17 | FDD |
| n2 | 1.85-1.91 | 1.93-1.99 | FDD |
| n3 | 1.171-1.785 | 1.93-1.99 | FDD |
| n5 | 0.824-0.849 | 0.869-0.894 | FDD |
| n7 | 2.5-2.67 | 2.62-2.69 | FDD |
| n8 | 0.88-0.915 | 0.925-0.96 | FDD |
| n20 | 0.832-0.862 | 0.791-0.821 | FDD |
| n28 | 0.703-0.748 | 0.758-0.803 | FDD |
| n66 | 1.71-1.78 | 2.11-2.2 | FDD |
| n70 | 1.695-1.71 | 1.995-2.02 | FDD |
| n71 | 0.663-0.698 | 0.617-0.652 | FDD |
| n74 | 1.427-1.47 | 1.475-1.518 | FDD |
| n38 | 2.57-2.62 | 2.57-2.62 | TDD |
| n41 | 0.663-0.698 | 0.617-0.651 | TDD |
| n50 | 1.431-1.517 | 1.431-1.517 | TDD |
| n51 | 1.427-1.432 | 1.427-1.432 | TDD |
| n77 | 3.3-4.2 | 3.3-4.2 | TDD |
| n78 | 3.3-3.8 | 3.3-3.8 | TDD |
| n79 | 4.4-5 | 4.4-5 | TDD |

Table 5.2: Operating frequencies for 5G NR (FR2) [317, 318].

| Band | UL [GHz] | DL [GHz] | Duplex Mode |
|---|---|---|---|
| n257 | 26.5-29.5 | 26.5-29.5 | TDD |
| n258 | 24.25-27.5 | 24.25-27.5 | TDD |
| n259 | 39.5-43.5 | 39.5-43.5 | TDD |
| n260 | 37.0-40.0 | 37.0-40.0 | TDD |
| n261 | 27.5-28.35 | 27.5-28.35 | TDD |

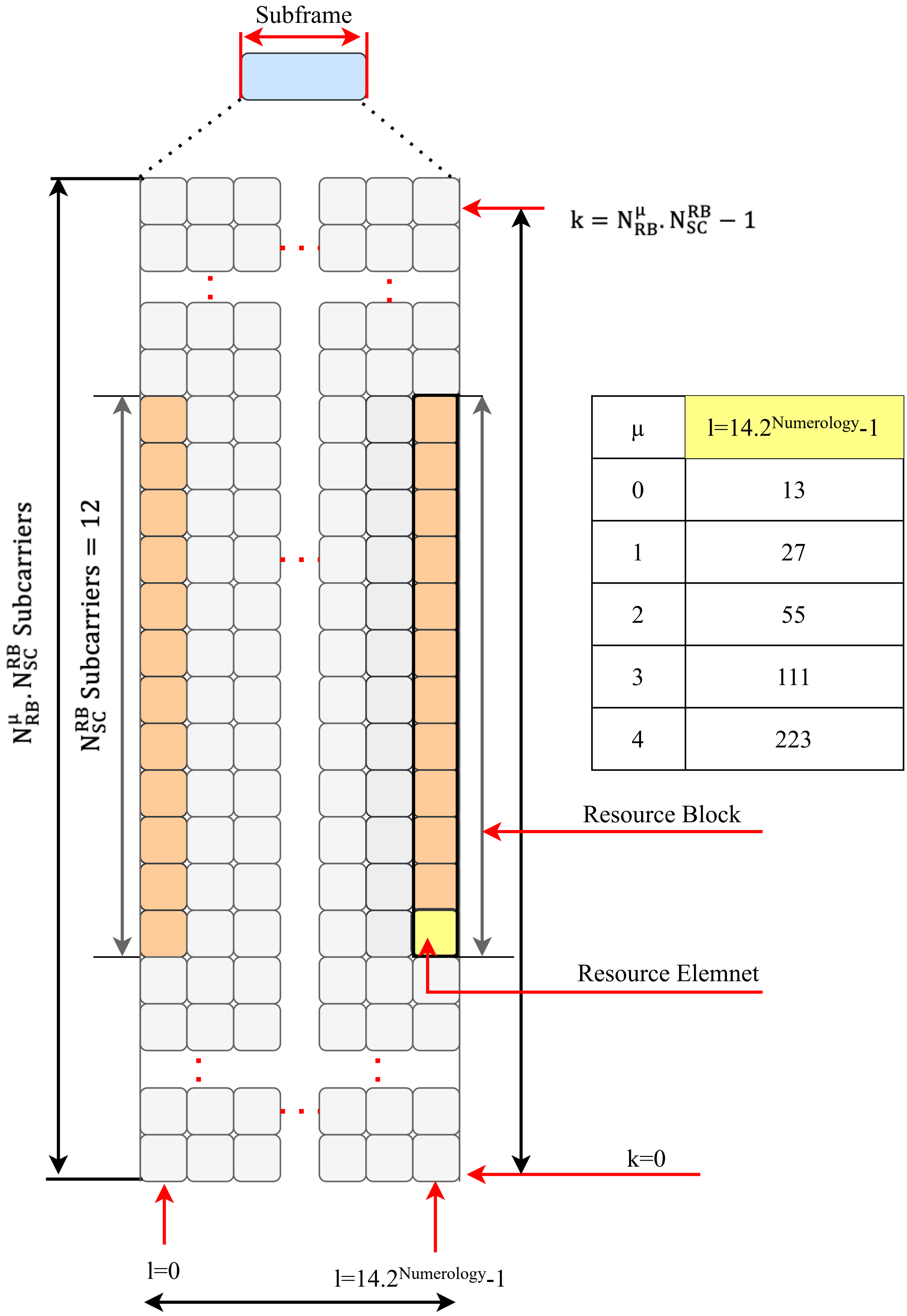


| μ | $l=14.2^{Numerology}-1$ |
|---|---|
| 0 | 13 |
| 1 | 27 |
| 2 | 55 |
| 3 | 111 |
| 4 | 223 |

Figure 5.2: 5G NR resource grid, details of resource element and resource block with define numerology.

(it is possible to change of the number of OFDM symbols within a radio frame and sub carrier spacing).

The resource element of NR is the same as LTE. One resource element is one OFDM symbol in the time domain while one sub carrier in the frequency domain. It is defined as $(k, l)p,$. In frequency domain $k$ is the sub carrier index, and time-domain l is the OFDM symbol position. $p$ represents the antenna port and  the sub carrier spacing. NR resource Block is defined in [320]. It is the 12 consecutive sub carriers in the frequency domain. One resource grid is created for one antenna port and numerology. $N_{SC}^{RB}$ is equal to 12 sub carriers per resource block. Resource grid is made of $N_{grid,x}{}^{size,\mu} * N_{SC}^{RB}$ sub carriers and $N_{symb}{}^{subframe,\mu}$ OFDM symbols.

### 5.2.5 Sub-Carrier Spacing and Numerology

Compared to LTE symbol length and sub carrier spacing (numerology), the 5G NR numerology is a notable difference. The main difference is that 5G NR supports multiple different types of sub carrier spacing, while in LTE, only one 15 kHz sub carrier spacing is acceptable. The 5G NR sub carrier spacing with the corresponding numerology is illustrated in Figure 5.3. Figure 5.3 shows numerology zero representing 15 kHz, the same as LTE, but 5G NR also supports sub carrier spacing 30 kHz, 60 kHz, 120 kHz, and 240 kHz.

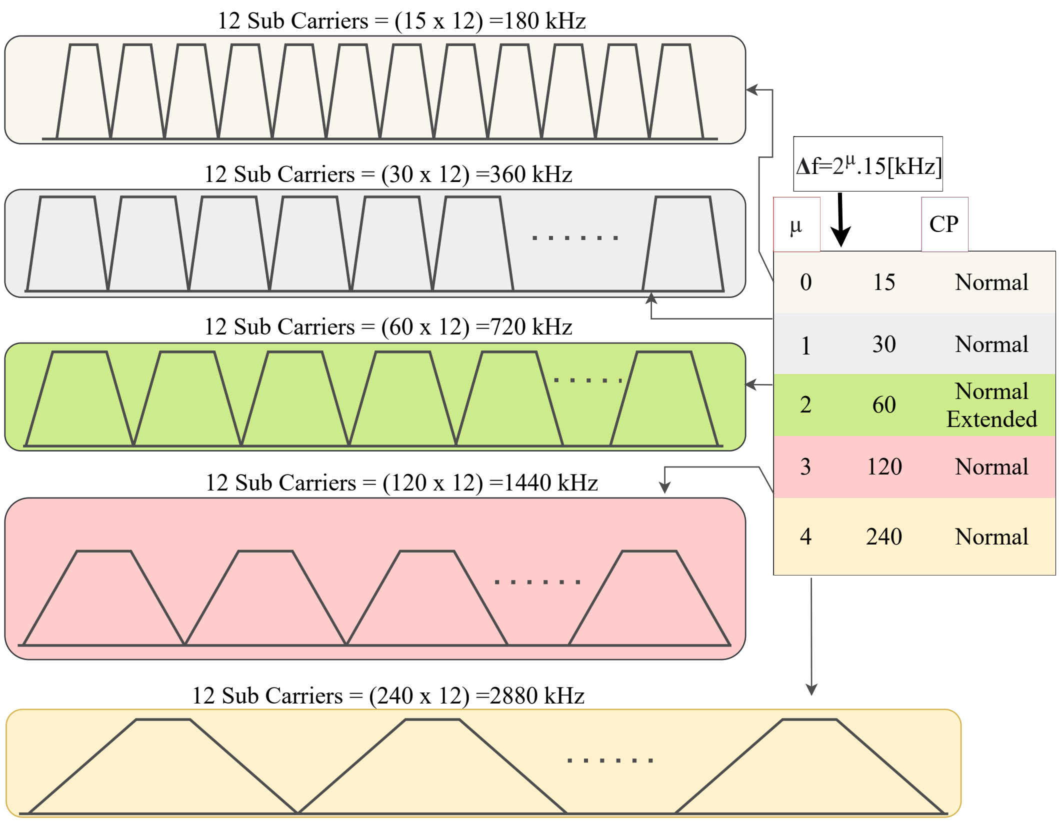


Figure 5.3: Supported transmission numerology and sub-carrier spacing.

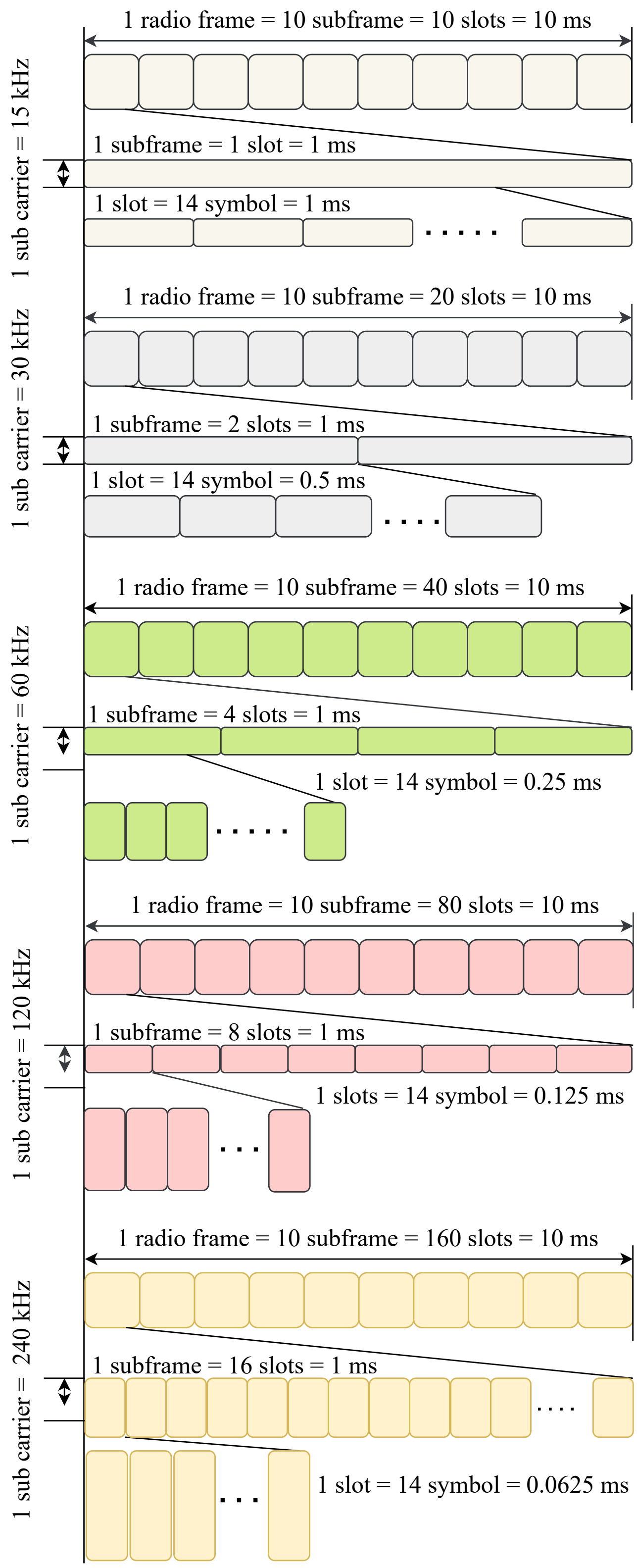


Figure 5.4: 5G NR Radio frame structure for each numerology and slot configuration [321].

### 5.2.6 Frame Structure

As explained earlier that the 5G NR supports different sub-carrier spacing. Because of variable sub-carrier spacing, the radio frame structures differ slightly for different numerology. The length of sub frame and size of one radio frame is identical regardless of numerology. As it can illustrate in Figure 5.4 that the total length of one radio frame is always the same 10 ms, and also the length of the sub frame is 1 ms. The difference among different numerology is the number of symbols per slot. The number of symbols within the same slot does not change with numerology. It changes if slot configuration types are changed. If the configuration is zero, the number of symbols for a slot is 14, and if it is one, then the symbol per slot slot is seven. The details for radio frame structure with define numerology and slot configuration are define bellow:

- Numerology 0: with this numerology, the sub frame has one slot, the total slots are then ten, and the symbols are 14 within a slot;
- Numerology 1: with this numerology, the sub frame has two slots, the total slots are then 20, and the symbols are 14 within a slot;
- Numerology 2: with this numerology, the sub frame has four slots, the total slots are then 40, and the symbols are 14 within a slot;
- Numerology 3: with this numerology, the sub frame has eight slots, the total slots are then 80, and the symbols are 14 within a slot;
- Numerology 4: with this numerology, the sub-frame has 16 slots, the total slots are then 160, and the symbols are 14 within a slot.

### 5.2.7 Slot Length

The slot length is dependent on numerology. Different numerology has different subcarriers. The wider the sub carrier spacing, the shorter the slot length. Per slot length is shown in the Figure 5.5 for defined numerology's.

### 5.2.8 Sampling Time

Sampling time depends on sub carrier spacing mainly. 5G NR sampling time as:

$$T_c = \frac{1}{\Delta f_{\max} \cdot N_f} \quad (5.1)$$

$$\Delta f_{\max} = 450 \times 10^3 \quad (5.2)$$

$$N_f = 4096 \quad (5.3)$$

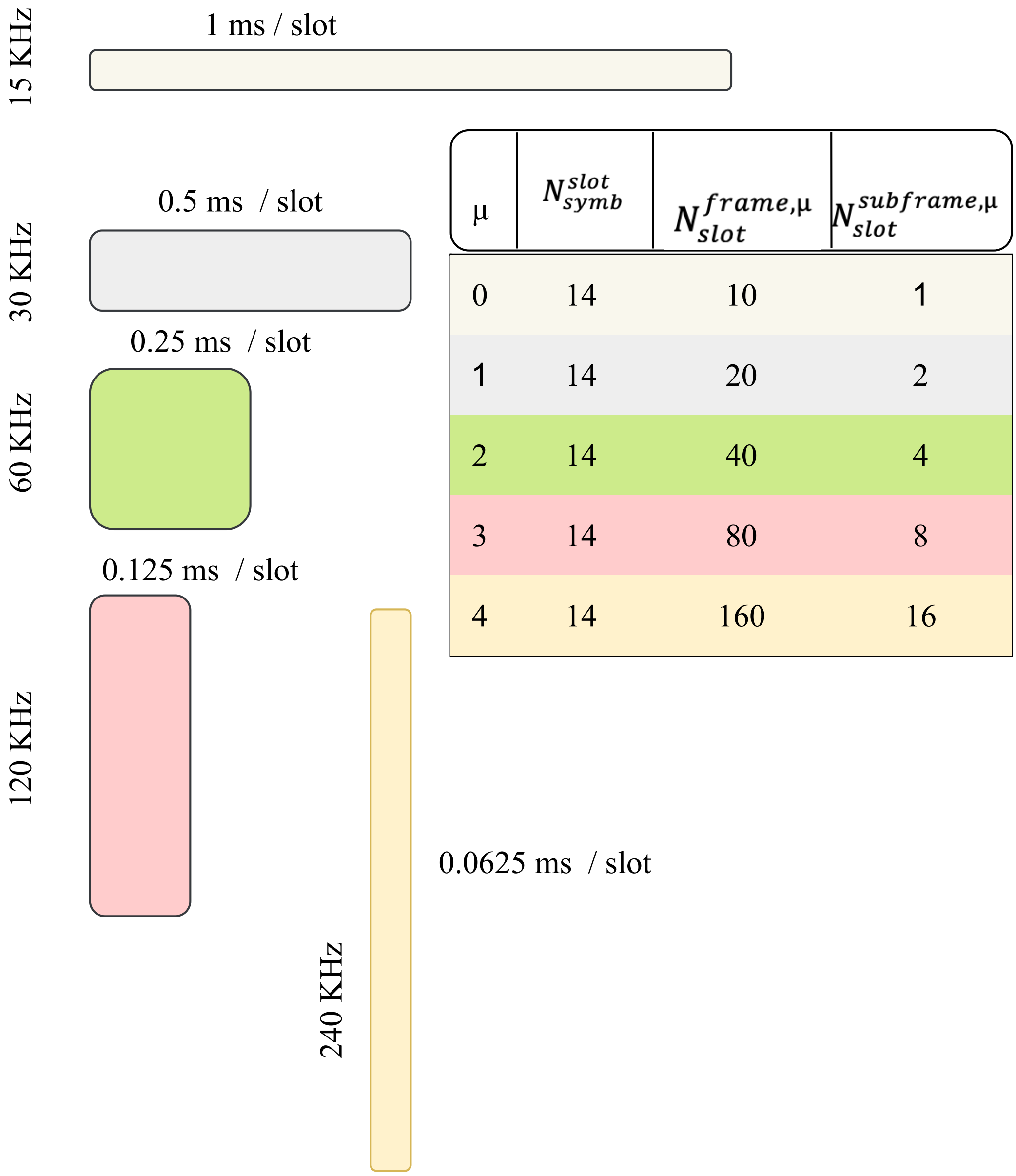


| μ | $N_{symb}^{slot}$ | $N_{slot}^{frame,\mu}$ | $N_{slot}^{subframe,\mu}$ |
|---|---|---|---|
| 0 | 14 | 10 | 1 |
| 1 | 14 | 20 | 2 |
| 2 | 14 | 40 | 4 |
| 3 | 14 | 80 | 8 |
| 4 | 14 | 160 | 16 |

Figure 5.5: 5G NR slot length for different numerology.

$$T_c = 0.509\,ns \quad (5.4)$$

$T_c$ sampling time in time domain,$N_f$ is FFT size and $\Delta f_{max}$ sub carrier spacing. Sampling time for sub-carrier spacing 15 kHz, it is the same as LTE 20 MHz sampling rate, can be calculated as:

$$T_s = \frac{1}{\Delta f_{\text{max}} \cdot N_f} \quad (5.5)$$

$$\Delta f_{\text{max}} = 15 \times 10^3 \quad (5.6)$$

$$N_f = 2048 \quad (5.7)$$

$$T_s = 32.552\,ns \quad (5.8)$$

Where $T_s$ is sampling time. The relationship between 5G NR and LTE sampling time is $K$ = LTE sampling time/5G NR sampling time = $T_s$ /$T_c$ =64. Radio frame time can be calculated as:

$$\Delta f_{\text{max}} = 450 \times 10^3 \quad (5.9)$$

$$N_f = 4096 \quad (5.10)$$

$$T_f = \left(\frac{\Delta f_{max} \cdot N_f}{100}\right) T_c = 10\text{ ms} \quad (5.11)$$

Frame and sub-frame detail are given in detail in Figure 5.4, sub-frame time can be calculated as [321, 322]:

$$T_f = \left(\frac{\Delta f_{max} \cdot N_f}{1000}\right) T_c = 1 \text{ ms} \quad (5.12)$$

### 5.2.9 5G NR Data Rate Calculations

The NR approximation of data rate with a defined number of aggregated carriers in a band or band combinations are expressed with mathematical formula presented in Figure 5.6. Where $j$ defines the maximum number of supported aggregated carriers, and $R_{max}$ represents the maximum code rate proposed by 3GPP 948/1024 [317]. $v$ is the supporting layer, and its higher value is 8. $Q_m^{(j)}$ is the number of bits per symbol, which depend on modulation schemes. $f$ is the scaling factor which is varying. , represent numerology. $T_s^\mu = 10^{-3}/2^\mu$ is the $T_s^\mu = 10^{-3}/2^\mu$ duration $T_s^\mu = 10^{-3}/2^\mu$ of the OFDM symbol in a sub frame for given numerology. $N_{\text{PRB}}^{BW(j),\mu}$ It is RB allocation in a given bandwidth with numerology. $BW^{(j)}$ is the bandwidth of UE in the given band or band combination. $OH^{(j)}$ the overhead, which get the following values [308]:

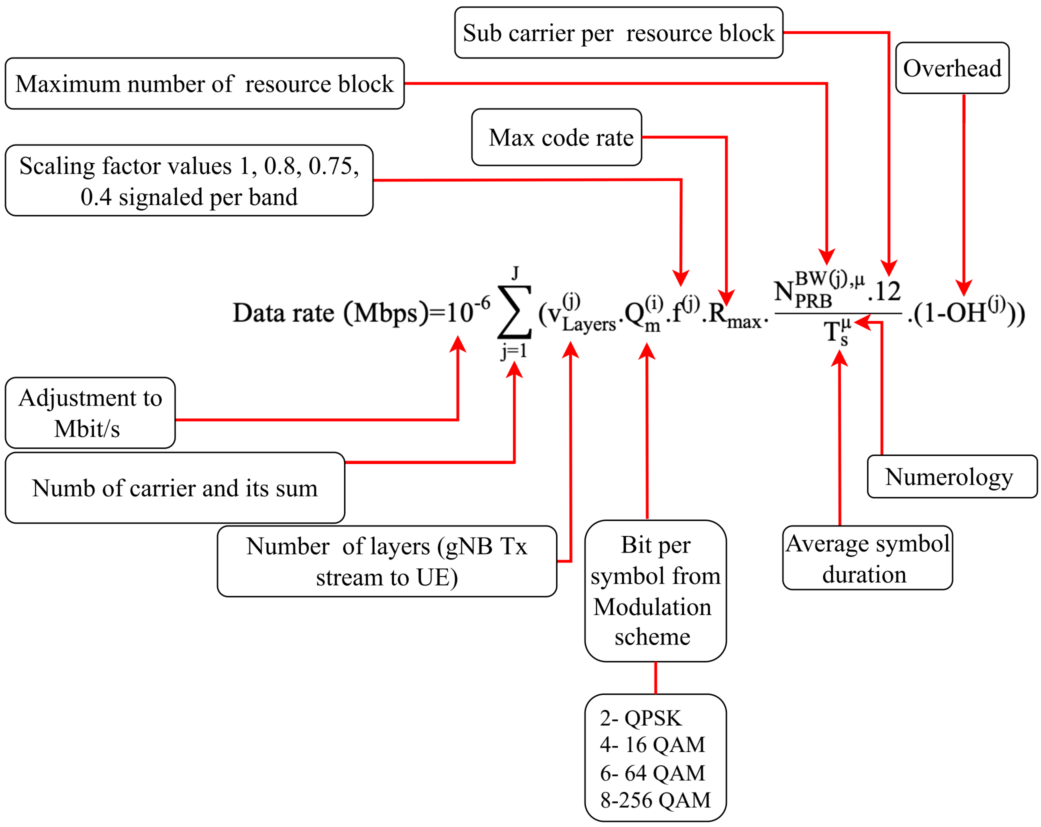


Figure 5.6: Maximum Supported data rate for DL/UL [308].

- 0.14, for frequency range FR1 for DL;
- 0.18, for frequency range FR2 for DL;
- 0.08, for frequency range FR1 for UL;
- 0.10, for frequency range FR2 for UL.

To calculate the data rate one need to calculate the PRB first, and define the sub carrier spacing, and other required parameters. In Subsection 5.2.9.1 the frequency domain and time domain details of resource block are discussed and calculated, for given numerology, in Subsection 5.2.9.2 the examples with formulas of finding number of resource blocks are explained. Further guard band are discussed and its mathematical expression are defined. Modulation and code rate and layer mapping are required which are are explained in Section 5.2.10, 5.2.11 and 5.2.12.

To calculate the data rate the following formula can be use and its details explanations are presented in Figure 5.6.

$$\text{Data rate (Mbps)} = 10^{-6} \sum_{i=1}^{J} \left( v_{Layers}^{(j)} \cdot Q_m^{(i)} \cdot f^{j)} \cdot R_{\max} \cdot \frac{N_{PRB}^{BW(j),\mu} \cdot 12}{T_s^{\mu}} \cdot \left(1 - OH^{(j)}\right) \right) \tag{5.13}$$

$$\text{Data rate (Mbps)} = 10^{-6} \times 1 \times 1 \times 8 \times 1 \times \frac{948}{1024} \times (270 \times 12) \times \frac{(14 \times 2^0)}{10^{-3}} \times (1 - 0.14) = 288.9 \, \text{Mbits / s} \tag{5.14}$$

#### 5.2.9.1 Resource Block

As 5G NR, one RB contains 12 sub carriers in the frequency domain. Compared to LTE, the resource block bandwidth of LTE is 180 kHz fixed, while in NR, it's not specified, which is dependent on sub carrier spacing. How to calculate resource block bandwidth for each numerology is given below.

- If Numerology = 0 and $\Delta f$ =15 kHz, then one resource block is (15 x 12) kHz = 180 kHz in frequency domain. In this case the 1 radio frame is = 10 sub frames = 10 slots = 10 ms. Where the 1 sub frame = 1 slots = 1 ms, 1 slot = 14 symbols = 1 ms. Then one resource block is equal to 1 ms in time domain, more detail of slots and time domain are explained in Figure 5.5 and in Figure 5.4.
- If Numerology = 1 and $\Delta f = 30kHz$, then one resource block is (30 x 12) kHz = 360 kHz in frequency domain, normal cyclic prefix. In this case the 1 radio frame is = 10 sub frames = 20 slots = 10 ms. Where the 1 sub frame = 2 slots = 1 ms, 1 slot = 14 symbols = 0.5 ms. Then one resource block is equal to 0.5 ms in time domain.
- If Numerology = 2 and $\Delta f = 60kHz$, then one resource block is (60 x 12) kHz = 720 kHz in frequency domain, normal cyclic prefix. In this case the 1 radio frame is = 10 sub frames = 40 slots = 10 ms. Where the 1 sub frame = 4 slots =1 ms, 1 slot = 14 symbols = 0.25 ms. Then one resource block is equal to 0.25 ms in time domain.
- If Numerology = 3 and $\Delta f = 120kHz$, then one resource block is (120 x 12) kHz = 1440 kHz in frequency domain, normal cyclic prefix. In this case the 1 radio frame is = 10 sub frames = 80 slots = 10 ms. Where the 1 sub frame = 8 slots =1 ms, 1 slot = 14 symbols = 0.125 ms. Then one resource block is equal to 0.125 ms in time domain.
- If Numerology = 4 and $\Delta f = 240kHz$, then one resource block is (240 x 12) kHz = 2880

kHz in frequency domain, normal cyclic prefix. In this case the 1 radio frame is = 10 sub frames = 160 slots = 10 ms. Where the 1 sub frame = 16 slots =1 ms, 1 slot = 14 symbols = 0.0625 ms. Then one resource block is equal to 0.0625 ms in time domain.

#### 5.2.9.2 Total Possible Resource Block After Guard Band

The maximum transmission bandwidth and guard band for a single UE channel are given in Table 5.3 with sub-carrier spacing. Transmission bandwidth and channel bandwidth configuration for one NR channel are shown in Figure 5.7. The guard band can be calculated as:

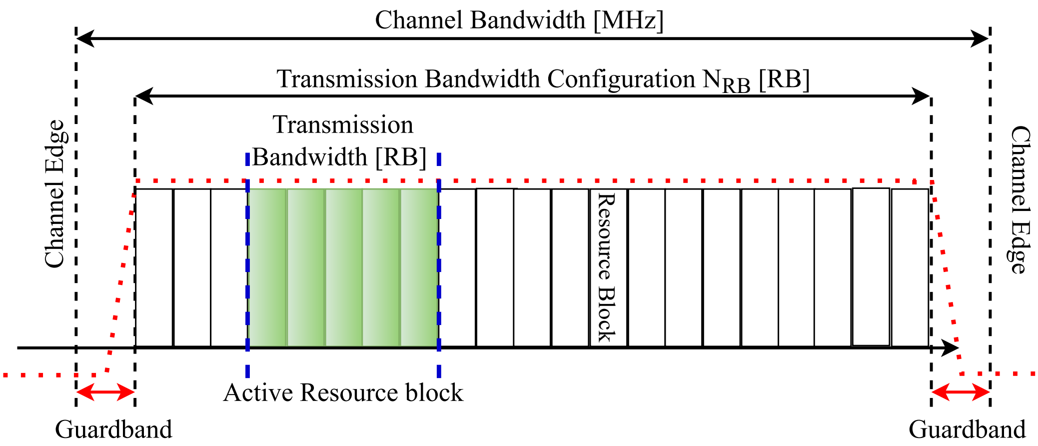


Figure 5.7: Transmission bandwidth and channel bandwidth configuration for one NR channel [306].

$$\text{Guard band } = (\text{ Channel BW } \times \text{ 1000 kHz}) - \text{RB value } \times \text{SCS} \times 12)/2 - \text{SCS}/2 \quad (5.15)$$

To find the number of resource blocks, then channel bandwidth, guard band and one resource block bandwidth, numerology, and $\Delta f$ values are required. These values are mentioned in Table 5.3. For different values differed number of resource block can be calculated as:

- If the Numerology=0, $\Delta f$ = 15 kHz and one resource block BW is 180 kHz, channel bandwidth = 50 MHz with guard BW = 692.5 kHz then number of resource blocks are:

$$\begin{aligned} \text{Number of Resource blocks } &= \frac{(\text{Channel BW } - 2 \times \text{ Guard band})}{\text{1 Resource block BW}} \\ &= \left(50 \times 10^3 - 2 \times 692.5\right) / 180 \end{aligned} \quad (5.16)$$

$$\text{Number of Resource blocks } = 270\, PRB \quad (5.17)$$

- If the Numerology=1, $\Delta f$ = 30 kHz and one resource block BW is 360 kHz, channel bandwidth = 100 MHz with guard BW = 845 kHz then number of resource blocks are:

Table 5.3: Maximum transmission bandwidth (number of resource blocks) and guard band for each UE channel bandwidth [306].

Maximum transmission bandwidth configuration NRB

| SCS KHz | 5 MHz | 10 MHz | 15 MHz | 20 MHz | 25 MHz | 30 MHz | 40 MHz | 50 MHz | 100 MHz |
|---|---|---|---|---|---|---|---|---|---|
| | Number of resource blocks | | | | | | | | |
| 15 | 25 | 52 | 79 | 106 | 133 | 160 | 216 | 270 | N/A |
| 30 | 11 | 24 | 38 | 51 | 65 | 78 | 106 | 133 | 273 |
| 60 | N/A | 11 | 18 | 24 | 31 | 38 | 51 | 65 | 135 |

Minimum guard band for each UE channel bandwidth

| SCS KHz | 5 MHz | 10 MHz | 15 MHz | 20 MHz | 25 MHz | 30 MHz | 40 MHz | 50 MHz | 100 MHz |
|---|---|---|---|---|---|---|---|---|---|
| 15 | 242.5 | 312.5 | 3882.5 | 452.5 | 522.5 | 592.5 | 552.5 | 692.5 | N/A |
| 30 | 505 | 665 | 645 | 805 | 785 | 945 | 905 | 1045 | 845 |
| 60 | N/A | 1010 | 990 | 1330 | 1310 | 1290 | 1610 | 1570 | 1370 |

$$\text{Number of RBs} = (\text{Channel BW} - 2\times \text{ Guard band})/1 \text{ Resource block BW} \quad (5.18)$$

$$= \left(100 \times 10^3 - 2 \times 845\right)/360 \quad (5.19)$$

$$\text{Number of Resource blocks} = 273\,\text{PRB} \quad (5.20)$$

- If the Numerology=2, $\Delta f$ = 60 kHz and one resource block BW is 720 kHz, channel bandwidth = 100 MHz with guard BW = 1370 kHz then number of resource blocks are:

$$\text{Number of Resource blocks} = \frac{(\text{Channel BW} - 2\times \text{ Guard band})}{1 \text{ Resource block BW}} \quad (5.21)$$

$$= \left(100 \times 10^3 - 2 \times 1320\right)/720 \quad (5.22)$$

$$\text{Number of Resource blocks } = 135\,\text{PRB} \quad (5.23)$$

### 5.2.10 Modulation

The Modulation Coding Scheme (MCS) gives useful bits that can be transported by one symbol. In 5G and 4G, the resource element contains the symbol. Through the MCS, it defines useful bits per resource element. In wireless transmission, MCS depends on the quality of the radio signal. With better quality of channel conditions, the higher the MCS results, the higher the bit transfer within a symbol. In the case of 5G NR, it supports the Quadrature Phase Shift Keying (QPSK), 16 Quadrature Amplitude Modulation (QAM), 64 QAM and 256 QAM modulation. If one selects QPSK, then 2 bits can be transmitted per resource element, while in the case of 256, it will be 8 bits per resource element. 16, 64 and 256 are modulation orders for QAM Modulation. To get the number of bits, one can use the formula as given:

$$2^n = \text{ Modulation \quad order} \quad (5.24)$$

In 3GPP release 17 [321], the formula for QPSK, 16 QAM, 64 QAM and 256 QAM modulation formulations are explained by:

#### 5.2.10.1 QPSK

In this case, the pairs of bits can be mapped to a symbol $d(i)$ through a given formula. To get the values of $b(i)$, a Table 5.2.3.2-2 in 3GPP release 17 are presented [321].

$$d(i) = \frac{1}{\sqrt{2}}[(1 - 2b(2i) + j(1 - 2b(2i+1)] \quad (5.25)$$

#### 5.2.10.2 16 QAM

In this case, the quadruplets of bits can be mapped to a symbol d(i), through a given formula.

$$\begin{aligned} d(i) = \frac{1}{\sqrt{42}}\{(1 - 2\,b(6i)[4 - (1 - 2\,b(6i+2))[2 - (1 - 2\,b(6i+4))]] + j(1 - 2\,b(6i \\ +1))[4 - (1 - 2\,b(6i+3))[2 - (1 - 2\,b(6i+5))]]\} \end{aligned} \quad (5.26)$$

### 5.2.11 Code Rate

The code rate is the ratio between total transmitted bit (Redundant Bits + Useful) and a number of useful bits. The code rate with modulation order and modulation are given in Table 5.4.

$$\text{Coderate } (R) = \frac{n}{n+k} \quad (5.27)$$

### 5.2.12 Layer Mapping

It is proposed by 3GGP in Chapter 7 of [321] that complex-valued modulation symbols for the codeword to be transmitted and to be mapped between one to four layers. Complex-valued modulation symbols $d^{(q)}(0), \ldots, d^{(q)}\left(M_{symb}^{(q)} - 1\right)$ for codeword q to be mapped onto the layers.

$$\mathbf{x}(i) = \left[\begin{array}{ccc} x^{(0)}(i) & \ldots & x^{(v-1)}(i) \end{array}\right]^T \quad (5.28)$$

$i = 0, 1, \ldots, M_{symb}^{layer} - 1$. v is the layers, $M_{symb}^{layer}$ per layer the number of modulations.

## 5.3 Multi Carrier Waveform Candidates for Beyond 5G

As discussed in Chapter 1 in details that 5G and beyond support diverse scenarios. Which is xMBB, mMTC and uMTC are shown in Figure 1.1. First one (xMBB) provides service like increased data rates, but also improved QoE through reliable provisioning of moderate rates. It degrades the performance gracefully in terms of data rate and latency as the number of users increases. Whereas mMTC provides connectivity for a large number of devices. To design new waveform the desires of the above scenario must be consider, where each scenario has its own requirements [21].

There are several challenges that need to be well-thought-out while designing the 5G, as system would be complex, costly and inefficient by designing a distinct radio system for respectively above-mentioned service to meet heterogeneous desires. A new waveform must have following qualities to realize the demands of 5G; OoBE, relaxed synchronization and flexibility. Low OoBE reduces the guard band to a smaller value to acquire spectrum efficient transmission [3]. It also offers a basis for supporting many types of services with special frame structure existing in one base band with almost ignorable interference [4].

### 5.3.1 Wave Forms Comparison and Beyond 5G Perspectives

Detailed comparison among 5G wave forms is given in Table.A.1. F-OFDM has smaller filter length as compared to UFMC, GFDM and FBMC that lead to consume less resources. Inter sub carrier interference in GFDM is very high, because of non-orthogonal sub carriers, hence high order filtering, tail biting and pre/post processing is required to minimize it, whereas no pre or post processing is required in F-OFDM. FBMC have best OoBE but it has limited application, when combining it in multiple antenna transmission. Whereas F-OFDM provides better transmission with multiple antenna system without any extra processing, FOFDM is more flexible to others as it provides flexible frequency multiplexing and diverse solutions

Table 5.4: Modulation coding scheme index with modulation order and code rate [323].

| MSC Index | Modulation Order $Q_m$ | Code Rate $R_{max}$ | Spectral Efficiency |
|---|---|---|---|
| 0 | 2 | 120 | 0.2344 |
| 1 | 2 | 193 | 0.377 |
| 2 | 2 | 308 | 0.6016 |
| 3 | 2 | 449 | 0.877 |
| 4 | 2 | 602 | 1.1758 |
| 5 | 4 | 378 | 1.4766 |
| 6 | 4 | 434 | 1.6953 |
| 7 | 4 | 490 | 1.9141 |
| 8 | 4 | 553 | 2.1602 |
| 9 | 4 | 616 | 2.4063 |
| 10 | 4 | 658 | 2.5703 |
| 11 | 6 | 466 | 2.7305 |
| 12 | 6 | 517 | 3.0293 |
| 13 | 6 | 567 | 3.3223 |
| 14 | 6 | 616 | 3.6094 |
| 15 | 6 | 666 | 3.9023 |
| 16 | 6 | 719 | 4.2129 |
| 17 | 6 | 772 | 4.5234 |
| 18 | 6 | 822 | 4.8164 |
| 19 | 6 | 873 | 5.1152 |
| 26 | 8 | 916.5 | 7.1602 |
| 27 | 8 | 948 | 7.4063 |
| 28 | 2 | Reser-ved | Reser-ved |

depending on each user specifications.

When bursts are very short, OFDM-inspired waveform generated the lowest latency's competed to the other wave forms that are affected by the ramp-up and the ramp down generated by the filtering operation. In paper [324], it is analyzed that F-OFDM equipped systems can perform better than OFDM, when power amplification is not an issue, it gives better SNR than all other wave forms. Our future plan to work and study PAPR considering for better spectral localization using the above 5G waveform candidates. More details of wave forms comparison are presented in details in appendix A.

## 5.4 Deployment of Femto-cells in Heterogeneous Network

### 5.4.1 Femto-Cell Deployment Scenario

In the simulation environment, the heterogeneous network is considered. Firstly deployed the Macro-cell. Inside the Macro-cell, build an N number of buildings. The N number buildings are randomly distributing every seed of simulations. The definition of scenario shadows the assumptions from 3GPP technical specification [325]. The apartments have square geometry and are kept next to others with 5 x 5 grid. The scenario contains 25 Femto-cells, with reuse pattern two and bandwidth 10 MHz + 10 MHz. Where the Macro-cell with bandwidth equal to 20 MHz.

They Femto-cell in the building (inside the apartments) are deployed by deployment ratio, either deployed in all the apartments or not in all. It is varying from zero to one. If the mode is one all the apartments have Femto-cell for serving the users. This assumption puts high pressure on the system since usually, as in [312], the deployment ratio is 0.2. In this analysis, the considered deployment mode is that all the apartments have their own Femto-cell. The Femto-cell is always in the middle of the apartment. However, optimal placings are not deliberate. The optimal placing is determined in [326].

In paper [327], the hypothesis has illicit small cell deployment, which could harm the Femto-cells communication is studied. Illicit small cells can increase the interfaces. For dealing with the co-channel interfaces in many studies frequency reuse is assumed. In the proposed scenario frequency reuse pattern two is used. While the Macro-cell is considered the frequency reuse one. In this work, the Femto-cell with the same frequency act and interfere with the neighbour Femto-cells.

Within a reasonable range, this analysis considers the variation in Femto-cell (transmitters power), with a side length of apartments. The reduction of transmitter power can affect the coverage, stated in [328]. While presented in [325] that with decreasing transmitter power one can reduce the interference's. Our analysis studies the variation of transmitter power of Femto-cell layers without compromising system performance.

The wall lengths and Femto-cell transmit power vary. First considered the wall length 10 meters and varied the transmit power (10 dBm and 20 dBm) , and then 20 meters, respectively. The users are uniformly distributed while each user receives the interference from nearby

Table 5.5: Parameters used while simulating the Femto-cells scenario in Hetnet environment.

| Parameters | Values/Name |
|---|---|
| Number of Macro-cell | 1 |
| Macro-cell cluster | 1 |
| Bandwidth Macro-cell [MHz] | 20 MHz |
| Radius Macro-cell [km] | 1 |
| Transmit power of Macro [dBm] | 43 |
| Bandwidth Femto-cells [MHz] | 10+10 |
| Femto-cells cluster | 2 |
| Number of Femto-cells | 25 |
| Transmit Power of Femto-cells [dBm] | 0, 10, and 20 |
| Number of users per Femto-cell | 30 to 37 |
| Geometry of apartments (Femto-cells) | 5 x 5 |
| Users positions | Random |
| Application | Video |
| Number of building | 1 |
| Number of floors | 1 |
| Access policy | Open |
| Deployment density | Dense |
| Frame structure | FDD |
| Speed of UE [km/h] | 3 |
| Maximum delay [s] | 0.1 |
| Video bit rate [Kbps] | 440 |
| Transmit Power of Femto-cells [dBm] | 0, 10, and 20 |
| Walls side length [m] | 10, 20 |
| Schedulers | M-LWDF, FLS |
| Frequency [GHz] | 2 |
| Number of simulations for each combination | 50 |
| Simulations duration [s] | 30 |
| Path loss model for Femto-cells | WINNER II |

Femto and Macro-cell, also the interface form near by users. The Femto-cell only serves the users. The Femto-cell deployment in side the building is shown in diagram 5.8.

The traffic for the user is supported by Femto-cells and they exchange the data continuously with them. The video application is considered. In Femto-cells, the available packet schedulers allocate the radio resources among the users. The packet schedulers make the decision for sharing the resource based on the channel quality indicator. The channel quality indicator determines the channel strength through feedback, which helps to improve the data rate. With channel quality indicator information, the Femto-cells manage the data requirement of the user. Which ensures the required system quality.

In 5G there is a trade-of among the delay, PLR and goodput for the performance evaluation of scheduling packets. For the proposed video application frame level scheduler and M-LWDF are considered in simulations although looking for system saturation. Different schedulers comparison eases the identification of different schedulers with its limitation and advantages in indoor scenarios [329]. With the increase in the number of UE in each Femto-cell, the saturation of the system is achieved. Compare to simulated work from [330] [331] [312]. Our proposed scenario supports higher users per Femto-cells.

Due to the beneficial properties of NR, the proposed work considers the variable subcarrier spacing and numerology zero while the frame structure is consider with 10 subframe of 10 ms with different number of slots. The details of considered parameters are presented in table 5.5.

The proposed work is complementary to the work presented in [312], [14], [332] in an altered manner. The proposed work considered the path loss model which keeps the count of walls among the users and Femto-cells. The working depth gives the variation of supported UE with system saturation as a function of transmitter power and apartments side length, which is conceded with a narrow confidence interval.

### 5.4.2 Path Loss Models

For the path loss model, firstly parted the network into two tiers. For the first tier, considered the Macro-cell with path loss model Macro urban of 3GPP, E-UTRA, and E-UTRAN [333] [311]. While the second tier is the Femto-cells tier, which is indoor, the WINNER II downlink model is considered [334].

$$\begin{aligned}\text{First tier path loss } &= 80 + 40 \times (1 - 4 \times 0.001 \times (H_M - H_b)) \times \log_{10}(d \times 0.001) \\ &\quad -18 \times \log_{10}(H_M - H_b) + 21 \times \log_{10}(f)\end{aligned} \tag{5.29}$$

Where the $H_b$ is the average budling height and $H_M$ Macro-cell height, $d$ is the distance between the user and base station, and $f$ is the frequency.

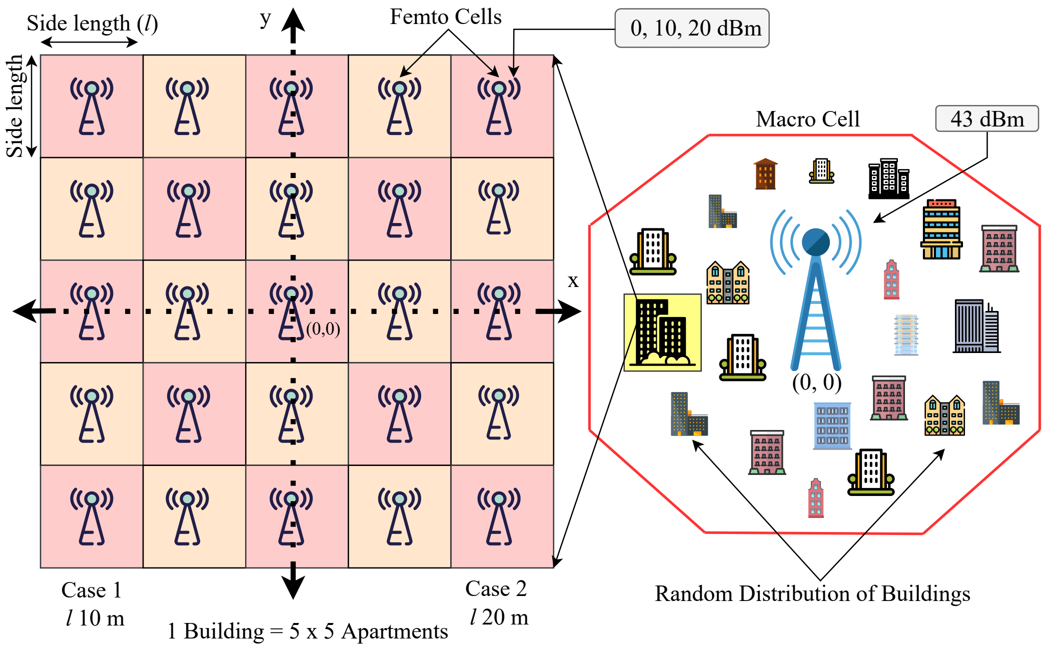


Figure 5.8: Simulation scenario considering Femto-cells inside Macro-cell with variable side length and transmitter power.

$$\text{Second tier path loss } = A \times \log_{10}(d) + B + C \times \log_{10}(2.0/5.0) + 10.0 \times nbWalls[n] + 20.0 \times nbWalls[0] \quad (5.30)$$

For the line of sight, the value of $A$=18.7, $B$= 46.8, and $C$= 20.0 where for non-line of sight these values are $A$=20.0, $B$= 46.4, and $C$= 20.0. $nbWalls$ defines the number of walls, where $nbWalls\ [externalwalls] = 0$ and $nbWalls\ [internal] = n$.

### 5.4.3 Packet Schedulers

For the overall system performance analysis in DL, Frame level Scheduling (FLS) and M-LWDF are considered [312]. These schedules are available on the 5G-air simulator [335]. According to [312], these schedulers are channel sensitive. For example, the UE immediately sent the CQI report to Femto-cells. The CQI report presents the quality experienced by the user and is predictable by a scheduler. Following the schedulers are discussed in detail.

#### 5.4.3.1 Frame Level Scheduling

In first case its is considered that the scheduling resource allocation to the user is based on frame. Frame level Scheduling (FLS) scheduling strategies adopted are two-level, based on upper level and lower level it is dynamically inter-reacted to allocate the RBs to the corresponding users. It is specified that the data packets are transmitted frame by frame in real time source to satisfy the delay constraints. In case of upper level its separated to both real time and non-real time traffic [336]. While In the case of the lower level it is considered, the

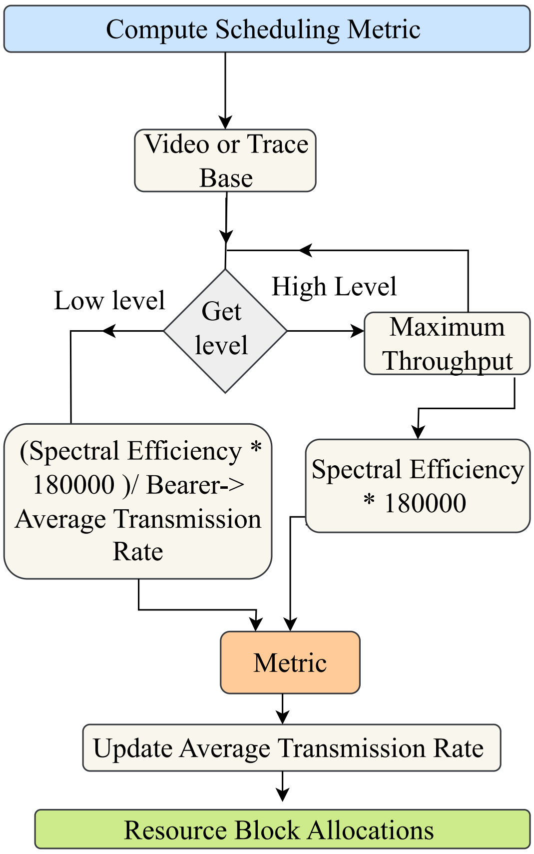


Figure 5.9: Frame level scheduling scheduling algorithm [335].

metric is divided by the average transmission rate (deliberating Proportional Fair). It means that for every TTI in the lower level, the RBs are allocated to the UEs using Proportional Fair [275, 337] concept while seeing the bandwidth requirement of FLS. The computed algorithm presented in 5.9 are considered for simulations prospective. The following equation can give the amount of transmitted data.

$$v_i(k) = h_i(k) * q_i(k) \quad (5.31)$$

In $k^{\text{th}}$ frame and $i^{\text{th}}$ flow, the $v_i\ (k)$ amount of data can be transmitted. It means that the $v_i\ (k)$ is obtained by filtering the signal $q_i\ (k)$ time-invariant linear filter with pulse response $h_i(k)$.

#### 5.4.3.2 Modified Largest Weighted Delay First

Another scheduler algorithm shown in Figure 5.10, second case considers M-LWDF. This scheduler considered both QoS and delay constrains while scheduling to a user [48]. It's given support to different data user according to QoS requirements [275].

For each real time flow a packet delay with the threshold $\tau_i$ is considered. Probability $\delta_i$ is give the maximum probability that the delay $D_{\text{HOL},i}$ of the head-of-line [275]. For this implementing of M-LWDF Scheduler, those packets which belong to real time flow from the

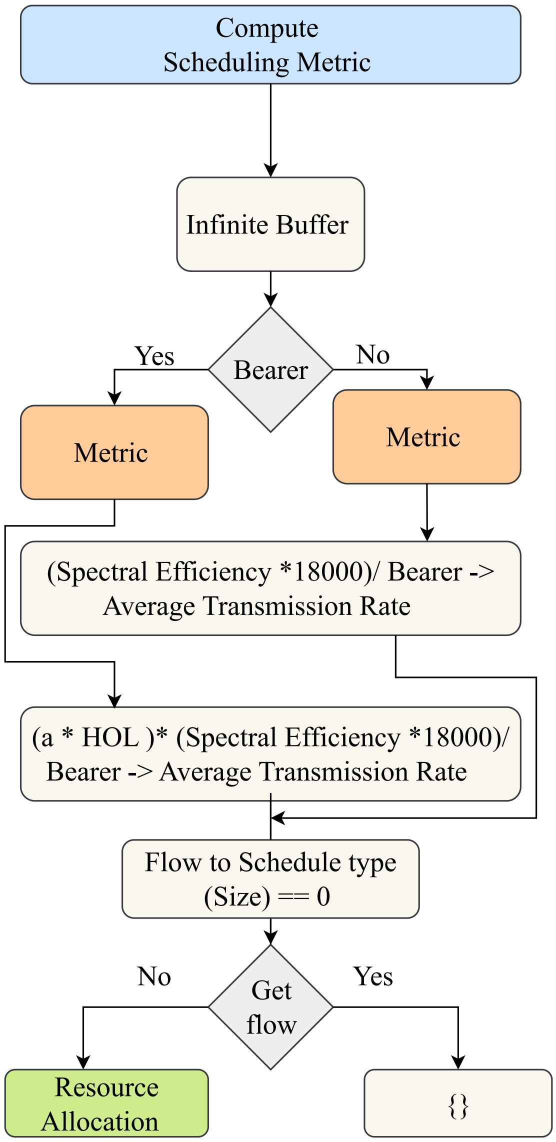


Figure 5.10: Modified largest weighted delay first scheduler algorithm [335].

MAC are erasing if they did not transmit before the deadline.

For highest delay to prioritize real time flows for their head of line packets with finest channel situations, the metric can be defined as:

$$w_{i,j} = \alpha_i D_{\mathrm{HOL},i} \cdot \frac{r_{i,j}}{\overline{R_i}} \quad (5.32)$$

$$\alpha_i = -\frac{\log \delta_i}{\tau_i} \quad (5.33)$$

where $D_{\mathrm{HOL}}$ is the head on the line delay for user $i$ packet; $\delta_i$ is the acceptable loss rate for user $i$ packet; $\tau_i$ is the delay threshold for user $i$ packet.

## 5.5 Performance Evaluation of Femto-cells in Heterogeneous Network

In this section, the system performances are evaluated for DL with considering parameters. For overall system performance evaluation, the updated 5G-air simulator [311] is considered for simulations.

### 5.5.1 Study of Average SINR

The theoretical study of the average signal-to-interference-plus-noise ratio (SINR) is presented in this section with the variation of transmitter power and the side length of the apartment. The goal is to evaluate the performance through simulations with theoretical illustrations.

#### 5.5.1.1 Signal to Noise Ratio for Femto-cells Indoor with Resue Pattern two

SINR is the measurement of the signal-to-noise ratio. Its unit is dB. To understand the SINR well, let's express it by an example. Let's suppose we have a 20 dB SINR measurement. It means that the required signal power is 20 dB better than noise power. If we convert the 20 dB to linear, its results are 100 times better than noise power [338].

To examine the average SINR in the indoor Femto-cell scenario. A 25 Femto-cell is considered inside the building for the specified apartment. While placing the apartment inside the building, a 3GPP grid 5x5 grid geometry is studied, as shown in Figure 5.8. Reusing patterns two and one are used in this research to improve coverage and reduce interference. For opportunistic low interference for Femto-cells, reuse pattern two is used, while reuse pattern one is considered for the middle interference scenario.

The total bandwidth considered in the research is 20 MHz. According to reuse pattern 2, the bandwidth is divided into two 10 MHz parts. For the Femto-cells shown in Figure 5.11, the pink apartments use the 10 MHz first part, while the rest of the remaining orange colour Femto-cells use the other 10 MHz part to maximize the supported throughput.

The users are deployed uniformly inside the apartment while the Femto-cell serves the user. In this case, the users and Femto-cell have no walls between them. When the own Femto-cell serves the user with a given frequency band, it faces interference from co-channel Femto-cells, as shown in Figure 5.11.

Due to the consideration of pattern reuse two, we have three rings of interference:

- First ring is when the users are inside apartments 0, and user face neighbouring node interfaces from apartments 1, 2, 3 and 4. As shown in Figure 5.11 a). The red walls of apartments represent the Femto-cell apartment interfering with cells to co channels neighbouring.
- Second ring is when the users are inside apartments 0, and user face neighbouring node interfaces from 5, 6, 7 and 8 . As shown in Figure 5.11 b). The red walls of of apartments represent the interfering adjacent apartments Femto-cell.
- Third ring is when the users are inside apartments 0, and user face neighbouring node interfaces from 9, 10, 11 and 12. As shown in Figure 5.11 c). The red walls of apartment represents the interfering adjacent apartments Femto-cell.

#### 5.5.1.2 SINR from Considered UE at Coordinates

Let consider the scenario shown in Figure5.12, where the user is consider in this case in Femto-cell 0, which is serves by Femto-cell 0 and receiving interference from Femto-cell 2.

Conventionally, the SINR from UE, at a define place with the coordinates ($x$, $y$), served by a cell with a transmitter power $P_{Tx}$ can calculate as:

$$\text{SINR}(P_{Tx}, x, y) = \frac{P_{ownFemto}(P_{Tx}, x, y)}{(1-\alpha)\cdot P_{ownFemto}(P_{Tx}, x, y) + P_{nhFemto}(P_{Tx}, x, y) + P_{noise}}, \quad (5.34)$$

$P_{ownFemto}$ is the average value of power received by user from own Femto-cell. Where the $P_{nhFemto}$ is the average interference power from neighboring Femto-cells. $\alpha$ is codes orthogonality factor. $P_{noise}$ thermal noise power can be calculate as:

$$P_{noise} = -174 + 10 * \log_{10} BW - 30 + NF, \quad (5.35)$$

Where NF is noise figure The received power from own Femto-cell can be calculate as:

$$P_{ownFemto}(P_{Tx}, x, y) = P_{Tx} G_{Tx} G_{Rx} 10^{-\frac{PL}{10}} \quad (5.36)$$

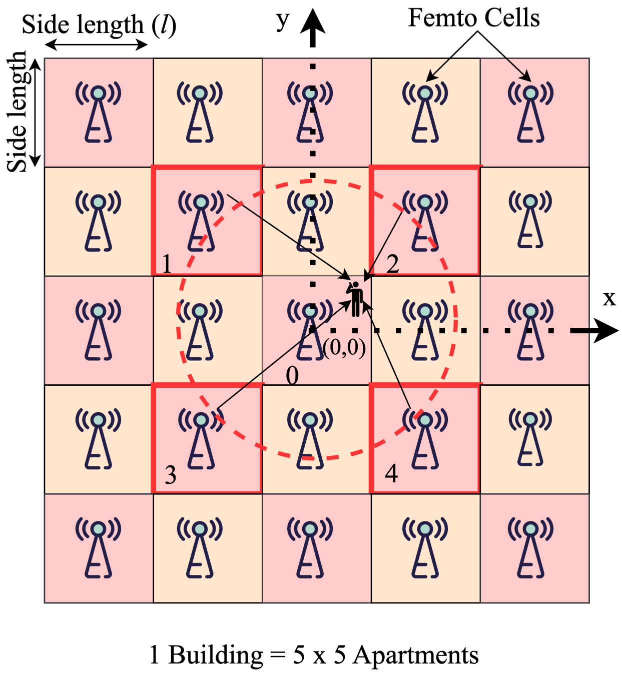


(a) Deployment ring one

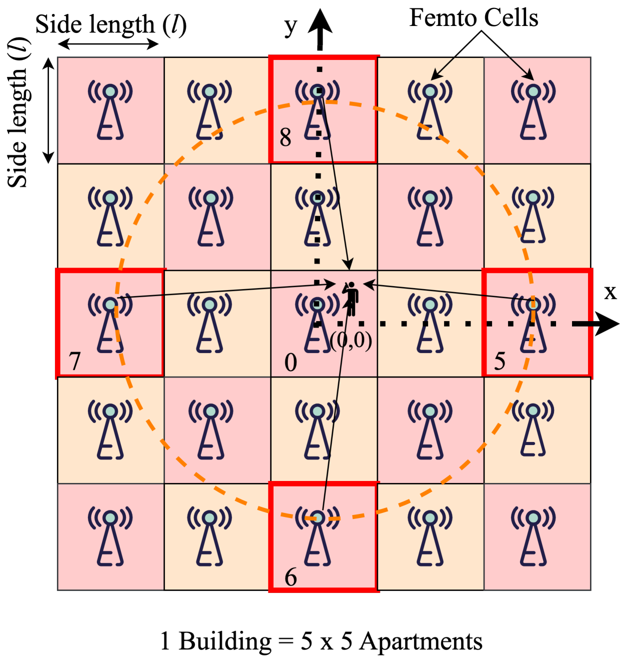


(b) Deployment ring two

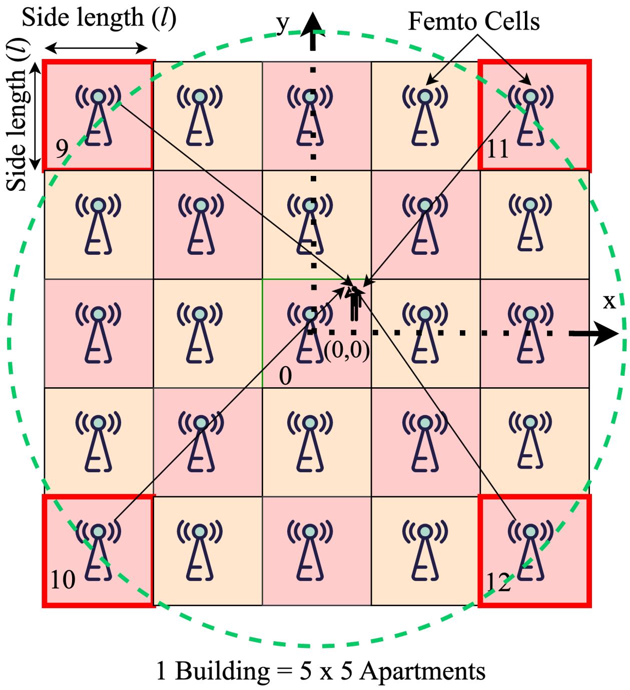


(c) Deployment ring three

Figure 5.11: Three different interference rings with the reuse pattern two, for Femto-cells indoor deployment.

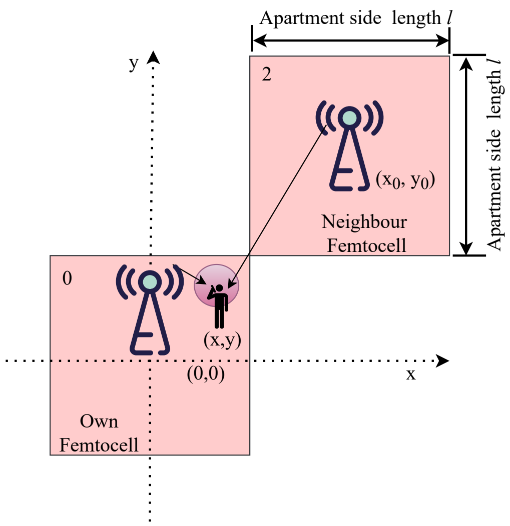


Figure 5.12: Receiving signal from own Femto-cell and interference from neighboring Femto-cell.

$G_{Rx}$ and $G_{Tx}$ receiver and transmitter gains where $PL$ is the path loss.$N$ define the total number of neighbor cells which interfering.

Where the received interfering power from neighbor Femto-cells can be calculate:

$$P_{nhFemto}(P_{Tx}, x, y) = \sum_{i=1}^{N} I_i(P_{Tx}, x, y) \quad (5.37)$$

$i^{th}$ cell interference is $I_i$ can be define as:

$$I_i(P_{Tx}, x, y) = P_{Tx}G_{Tx}G_{Rx}10^{-\frac{PL(x,y)_i}{10}} \quad (5.38)$$

where the value of $i$ give the idea from where (which Femto-cell) the interference is received.

For getting the average interference generated by all neighbors Femto-cells can be get by integrating all the interference power in the effected area of cell. By integrating over the cell area, the average level of power received from neighboring Femto-cells $\bar{I}$ can be calculated as:

$$\bar{I} = \int_x \int_y f_I(P_{Tx}, x, y)dxdy = \int_x \int_y \frac{P_{Tx}G_{Tx}G_{Rx}}{A_{Apt}} PL(x, y)dxdy, \quad (5.39)$$

$A_{Apt}$ is the overall effected area of Femtocell

#### 5.5.1.3 Average SINR for Proposed 25 Femto-cells

In this research, the user is distributed uniformly in each apartment with a Femto-cell each. The average SINR received by a user depends on the side wall length $l$ (mean the area) and the Femto-cell transmitter power [312]. The average SINR can be define as:

$$\overline{\mathrm{SINR}}(l, P_{Tx}) = \frac{\overline{P}_{ownFemto}(l, P_{Tx})}{(1-\alpha)\overline{P}_{ownFemto}(l, P_{Tx}) + \overline{P}_{nhFemto}(l, P_{Tx}) + P_{noise}} \quad (5.40)$$

where $\alpha$ is assumed equal to 1. The average interference power is $\overline{P_{nh}}(l, P_{Tx})$ which is from neighbor Femto-cells.

To get the average interference received from neighbor Femto-cells one can calculate the average interference power because by integration of it one can get the average interference level. $\overline{P}_{nhFemto}$ is the average interference power can be calculated as:

$$\overline{P}_{nh}(l, P_{Tx}) = \sum^{n_T} \bar{I}(l, P_{Tx}), \quad (5.41)$$

where $n_T$ is the total number of interfering neighbors Femto-cells. By integrating the average interference received level from neighbor Femto-cells one can define the average level of interference as:

$$\bar{I}_i(l, P_{Tx}) = \sum_{i=1}^{n_T} \int_{\Gamma_x^i} \int_{\Gamma_y^i} f_{I_i}(P_{Tx}, x, y) dy dx = \sum_{i=1}^{n_T} \int_{\Gamma_x^i} \int_{\Gamma_y^i} \frac{P_{Tx} G_{Tx} G_{Rx}}{A_{Apt}} PL(x, y) dx dy. \quad (5.42)$$

For different distance among the UE and Femto-cells one can calculate the average interference as:

$$\bar{I}_i(l, P_{Tx}) = \sum_{i=1}^{n_T} \int_{\Gamma_x^i} \int_{\Gamma_y^i} f_{I_i}(P_{Tx}, x, y) dy dx. \quad (5.43)$$

The integration regions for an interference Femto-cells can be defined as:

$$\Gamma_x^i = \{[-l/2, l/2]\} \quad (5.44)$$

and

$$\Gamma_y^i = \{[-l/2, l/2]\}. \quad (5.45)$$

The assumed parameters $G_{Tx}$=5 dBi and $G_{Rx}$=0 dBi values are defined according to [14]. In the Femtocell first tier, $f_I(P_{Tx}, x, y)$ is defined as:

$$\begin{aligned}
f_{I_1}(P_{Tx}, x, y) &= \tfrac{P_{Tx}G_{Tx}G_{Rx}}{l^2}10^{-\frac{20*\log_{10}\left(\sqrt{(x-l)^2+(y-l)^2}\right)+46.4+20*\log_{10}\left(\frac{2}{5}\right)+2*10}{10}} \\
f_{I_2}(P_{Tx}, x, y) &= \tfrac{P_{Tx}G_{Tx}G_{Rx}}{l^2}10^{-\frac{20*\log_{10}\left(\sqrt{(x-l)^2+(y+l)^2}\right)+46.4+20*\log_{10}\left(\frac{2}{5}\right)+2*10}{10}} \\
f_{I_3}(P_{Tx}, x, y) &= \tfrac{P_{Tx}G_{Tx}G_{Rx}}{l^2}10^{-\frac{20*\log_{10}\left(\sqrt{(x+l)^2+(y+l)^2}\right)+46.4+20*\log_{10}\left(\frac{2}{5}\right)+2*10}{10}} \\
f_{I_4}(P_{Tx}, x, y) &= \tfrac{P_{Tx}G_{Tx}G_{Rx}}{l^2}10^{-\frac{20*\log_{10}\left(\sqrt{(x+l)^2+(y-l)^2}\right)+46.4+20*\log_{10}\left(\frac{2}{5}\right)+2*10}{10}}
\end{aligned} . \quad (5.46)$$

Where $l$ is positive (5.43). Accounting only the Femto-cells from the first tier :

$$\int_{\Gamma^i_{x,y}} (P_{Tx}, x, y)dydx = P_{Tx}G_{Tx}G_{Rx}10^{-\frac{\sum_{i=1}^{4}\int_{\Gamma^i_{x,y}}(20*\log\left(\sqrt{x^2+y^2}\right)+46.4+20*\log_{10}\left(\frac{2}{5}\right)+2*10)dydx}{10*A_{cell}}} . \quad (5.47)$$

First interfering Femtocell in the first tier, the exponent in (5.47), [339] can be defined as:

$$\iint_{-l/2}^{l/2} 20 * \log_{10}\left(\sqrt{(x-l)^2 + (y-l)^2}\right) + 46.4 + 20 * \log_{10}\left(\frac{2}{5}\right) + 2 * 10 \, \mathrm{d}y \, \mathrm{d}x. \quad (5.48)$$

The user receiving the average power from its own Femtocell is constant its not depend on reuse pattering. it can be obtain similar ($\overline{P}_{ownFemto}(P_{Tx,x,y})$) but with different integrate function.

$$\overline{P}_{ow}(l, P_{Tx}) = \int_y \int_x \frac{P_{Tx}G_{Tx}G_{Rx}}{A_{ow}} 10^{-\frac{18.7*\log_{10}\left(\sqrt{(x^2+y^2}\right)+46.8+20*\log_{10}\left(\frac{2}{5}\right)}{10}} dxdy. \quad (5.49)$$

#### 5.5.1.4 Average SINR Results For Proposed 25 Femto-cells With Resue Pattern Two

The results presented in Figure 5.13 is the result for three rings shown in Figure 5.11. As a function of transmitter power, $P_Tx$ and side length $l$ of the apartment's walls are presented for the average SINR. In our scenario, the $P_Tx$ is variable from 0 dBm to 20 dBm while the side wall length is 10 meters and 20 meters. As in the first ring, there are four nearly interfering Femto-cells (and two walls between the receiver and the interferer node), shown in Figure 5.11 a). Because of it, the transmitter power variation does not affect the SINR values, Figure 5.13 a). While in the 2nd ring Figure 5.11 b), there are interfering Femto-cells with not much different distance than 1st ring (and two walls between the receiver and the interferer node), which have almost the same behaviour as first ring, the behavior of second ring shown in Figure 5.13 b). But if we see the 3rd ring Figure 5.11 c), due to longer distance from central cell of interfering Femtocell (and four walls between the receiver and the interferer node), it has an apparent variation with changing the apartment side walls,

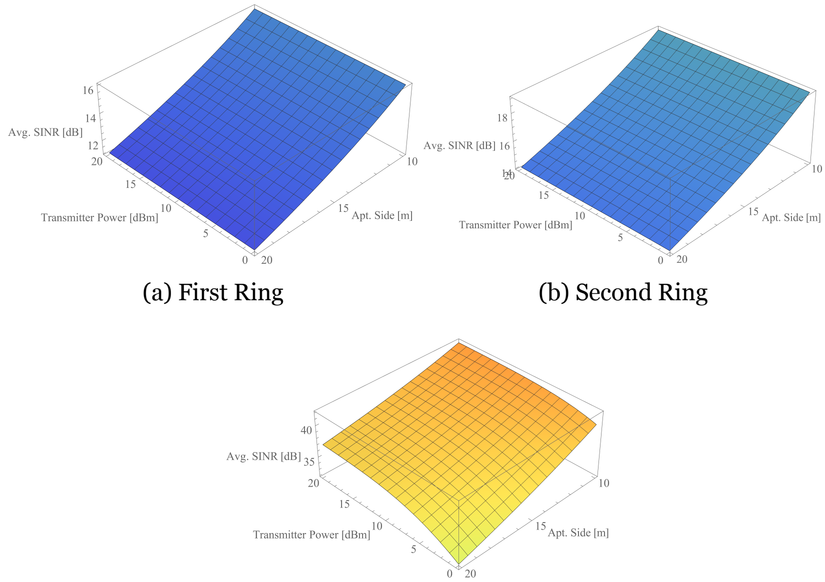


(a) First Ring (b) Second Ring

(c) Third Ring

Figure 5.13: Average SINR for an apartment side length from 10 to 20 m and a transmitter power from 10dBm to 20 dBm, three different interference rings with the reuse pattern two, for Femto cells indoor deployment.

Figure 5.13 c). Comparatively, for these three rings, it is analysed that with the decrease (increase distance and increase number of walls) in interfering Femto-cells, the average SINR increases by our proposed pattern.

### 5.5.2 Simulations Results

Simulations are performed with the updated version of the 5G air-simulator to analyze the variation in PLR, goodput and delay with video application, the updated code is given in appendix C.

The obtained result compares the results of two schedulers, M-LWDF and FLS with variation of transmitter power and side length of the apartment. The research published in [312] proposed a different scheduler where they consider 4G terminology, while in our case, we used 5G variable numerology and frame structure. Compared to [312], 5G new radio over the 4G with our proposed approach gives more than two time better results.

#### 5.5.2.1 Packet Loss Ratio

The PLR is the ratio between the total sent packet and the entire last packet. Each packet would have its deadline if the desired delay didn't reach its destination. Then the scheduler tries to reduce the number of lost packets due to deadline expiry. The objective of scheduling algorithms is to guarantee the packet's arrival and minimize packet loss [340]. The fraction of last packets due to the expiration deadline is considered for evaluating the scheduler's performance. If this fraction is a lower value, it's regarded as the best condition to schedule real-time traffic.

The average PLR as a function of the number of users is shown in Figure 5.14. The orange

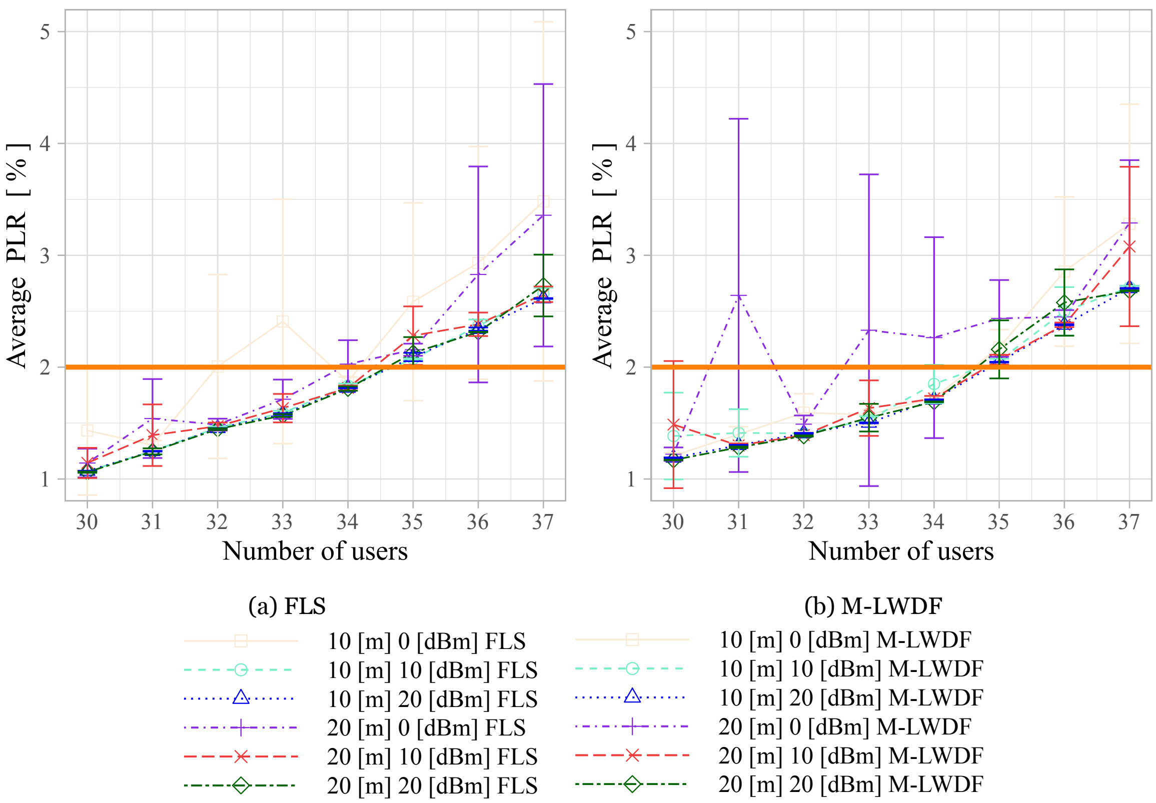


(a) FLS

(b) M-LWDF

Figure 5.14: Average PLR for FLS and M-LWDF for an apartment side length 10 and 20 m and a transmitter power 0 dBm, 10dBm and 20 dBm for 5G.

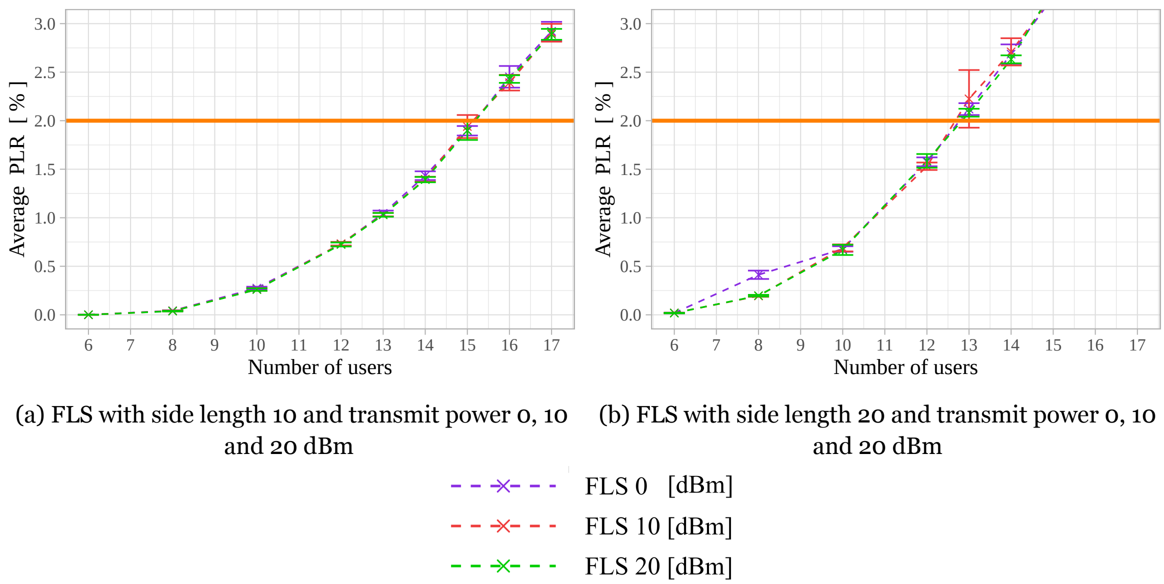


(a) FLS with side length 10 and transmit power 0, 10 and 20 dBm

(b) FLS with side length 20 and transmit power 0, 10 and 20 dBm

Figure 5.15: Average PLR for FLS as reference for our results adopted from [312] for 4G.

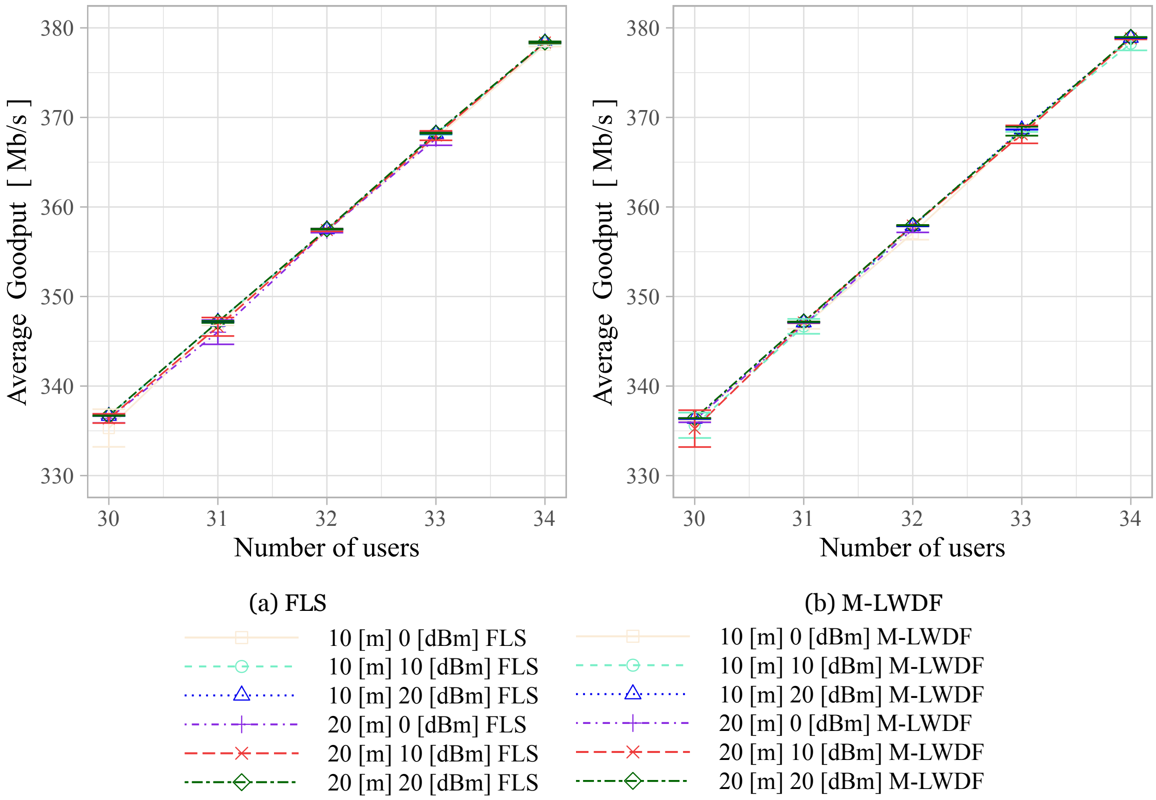


Figure 5.16: Average goodput for FLS and M-LWDF for an apartment side length 10 and 20 m and a transmitter power 0 dBm, 10dBm and 20 dBm.

line considers the threshold of less than two percent. The PLR higher than 2 percent are discarded values.

According to [341], the PLR less than 2% is precise. The literature expressed that PLR with less than 2%, with video application transmit accurately for the requirements. For PLR the comparison of two cases are shown in Figure 5.14a and 5.14b, the first one FLS with side length 10 m, 20 m and transmit power is 0 dBm, 10 dBm and 20 dBm. The second one is M-LWDF with side length 10 m, 20 m and transmit power is 0 dBm, 10 dBm and 20 dBm.

Comparing both cases M-LWDF give higher confidence interval. One can see that both schedulers are supporting the same number of users within less than a two percent of threshold limit, but the M-LWDF gives higher confidence interval values than FLS, specially in longer side length. For the given set of power and side length our proposed work support maximum number of users 37.

Comparing our simulation results with the work presented in [312], as a reference the Figure 5.15 adopted from [312] for FLS are given, our proposed work support more than two times user with lower PLR for same set of parameters for the defined scheduler.

#### 5.5.2.2 Goodput

Goodput is the rate at which the valuable data arrives at its destination. The proposed work considers the scenario between the gNb (source) and uniform users (destination) in a simulator. The results obtained for goodput are shown in Figure 5.16. As shown in Figure 5.16, both schedulers goodput performs better for different side lengths and power, while the M-LWDF performs better over FLS. One can see that the maximum average goodput value achieved the proposed work is around 380 Mb/s with M-LWDF, while in [312] the maximum supported goodput is 119 Mb/s for FLS for 4G. The obtain (goodput) results with proposed approach are almost more than two times of work presented in [312]. So for FLS the average goodput for 34 users with transmitter power 20 dBm and 20 meters of side wall length is 378.397 Mb/s while for M-LWDF is almost 380 Mb/s for 5G. The simulated resulted are in line with the theoretical study from Section 5.5.1. With the video application it is clear that the schedulers performs identical. The variation come only with the apartment side length.

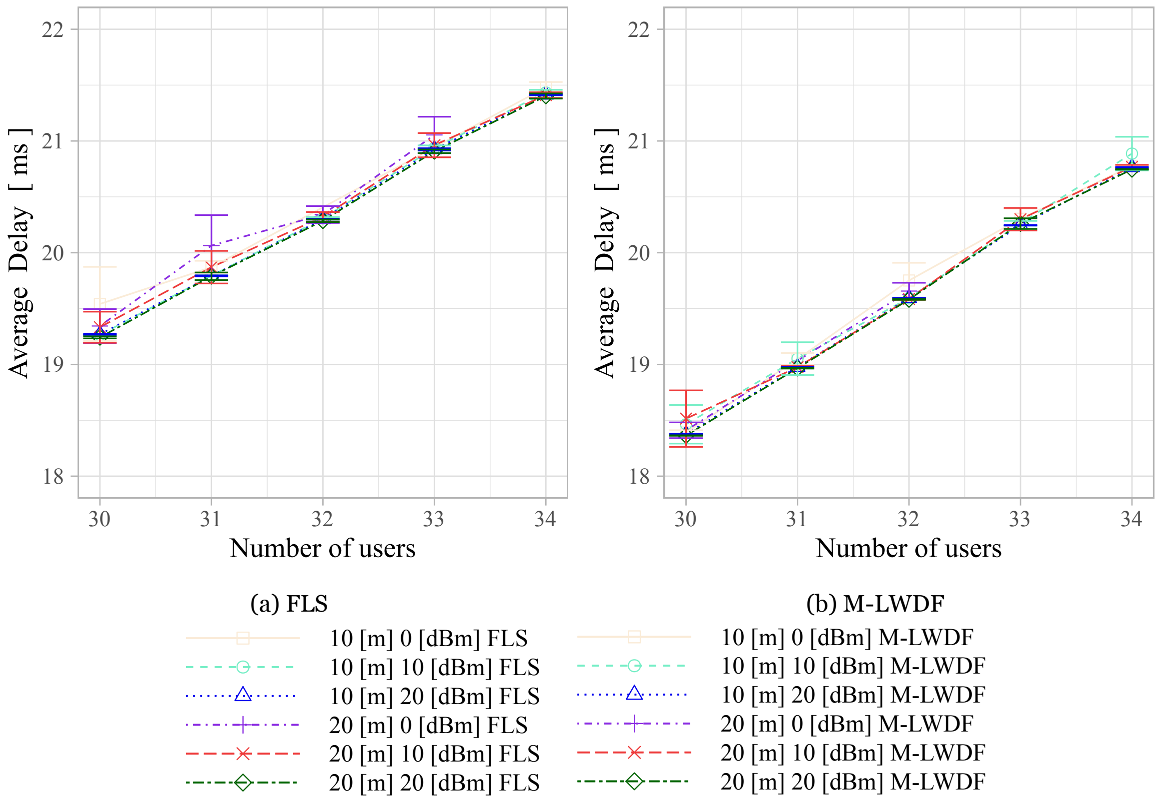


Figure 5.17: Average delay for FLS and M-LWDF for an apartment side length 10 and 20 m and a transmitter power 0 dBm, 10dBm and 20 dBm.

#### 5.5.2.3 Delay

The curves for delay for both schedulers are shown in Figure 5.17. One can see that the delay increases with the number of users. The maximum average delay for FLS is 21.5 ms, while for M-LWDF is 20.6 ms. The delay of FLS is higher than M-LWDF. At the saturation level, for PLR<2%, none of the schedulers surpass the preferred maximum delay of 150 ms for video.

#### 5.5.2.4 Fairness

It is essential to serve the users with possible fairly resource allocation through Femto-cell. In the case of non-fair allocation, it will result in imbalanced throughput distribution. To achieve the highest network throughput and fair resource distribution, all the flow essentially needs equivalent channel states. Though, the channel conditions in practice are almost different. That's why equitable throughput distribution does lead to the highest available throughput. For this situation, finding a better best trade-off between these two objectives is necessary. Jain's FI is well-known metric considering fairness, and fair allocation of resources between the traffic flows. It is defined as follows:

$$FI = \frac{\left(\sum_{c \in C} R_c\right)^2}{|C| \sum_{c \in C} \left(R_c\right)^2} \quad (5.50)$$

In Jain's FI, $C$ defines the set of data flow. For example $C = 1, 2, ..., |C|$. The limit of Jain's FI lies in a range of (0, 1). Where one is maximum fairness and zero the lower, in this work, a Jain's FI is considered. Wireless networks have different kinds of traffic flow, and these different kind of traffic flows have different transmission priorities. For example, VoIP and VID have higher transmission importance than BE flows.

In simulation video application are considered. The FI is the values between 0 and 1, which mean the 0 the worst and 1 the best. In this work the considered scheduler are enough fair and provide better resource allocation to the user, one can see the result shown in Figure 5.18 are enough fair for all the user for both schedulers. The limit of FI is equal to 1. For all the supported users the values is near to one, however the variation seen in longer side length of the apartment.

## 5.6 Summary and Conclusions

The Chapter overviews the 5G NR basic concepts at the beginning, and then discuss the NR features and benefits, followed by its mathematical aspect. It is found that 5G is operating in the FR1 and FR2 spectrum, which gives benefits of 10X to 100X capacity. With densification of the network, it can support massive devices, and due to its variable numerology, it can support multiple bandwidths. In 5G NR, there is a difference that the NR resource grid's physical dimension is changeable. Depending on numerology, it is possible to change the number of OFDM symbols within a radio frame and sub-carrier spacing.

Due to enormous demands in indoor communication, this work studies indoor Femto-cell deployment. The analysis offers the study of indoor Femto-cell coverage. The work considers the 3GPP small cell deployment assumption and the apartments 5 x 5 grid topology. The work studied the variation in transmit power with geometrical dimension for Femto-cells in the 5G scenario.

The theoretical study presented with simulations. Three rings are given for the theoretical

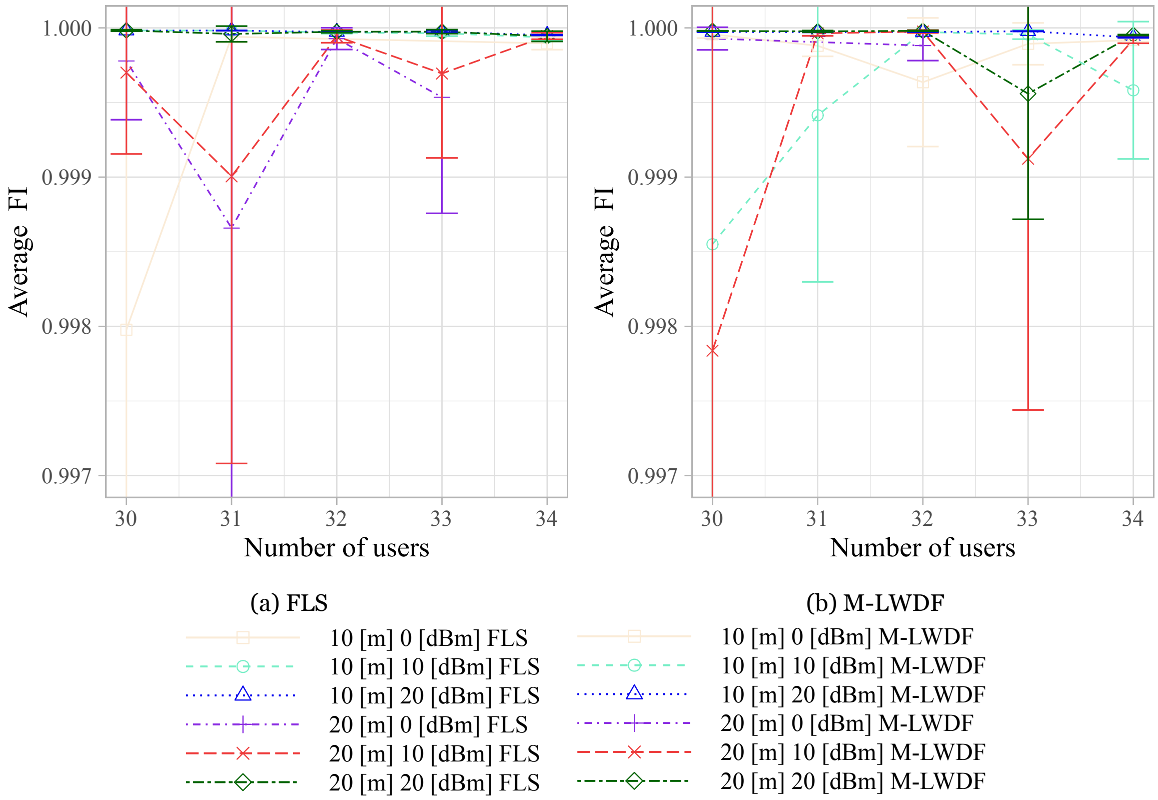


Figure 5.18: Average FI for FLS and M-LWDF for an apartment side length 10 and 20 m and a transmitter power 0 dBm, 10 dBm and 20 dBm.

research of average SNR. In the first one, when the apartments side length is fixed with the variation in transmit power, then no impact on SINR. In the 2nd and 3rd ring, when the sum of interferes decreases, the average SINR rises. Conversely, with the increase in side length and the decrease in the transmitter power, signal strength is insufficient to attain a rise in the average SINR.

The 5G air-simulator is updated to deploy indoor Femto-cell with proposed assumptions with uniform distribution. For all the possible combinations of apartments side length and transmitter power, the maximum number of supported users surpassed by more than two time and also provide more than two time gooput result with better result for delay compared to papers mentioned in the literature. The M-LWDF scheduler shows better results in terms of PLR, delay and goodput over the FLS. Comparatively, for these three rings, it is analysed that with the decrease in interference, the average SINR increases for the considered pattern.

# Chapter 6

# Cost Revenue Trade-off for HetNets with Small Cell in the Sub-6 GHz Operating Band

## 6.1 Introduction

In the era of digitization and industrial expansion, Industry 4.0 is thriving on the foundation of the connected society and emerging technologies. The evolving industrial age will significantly advance the value-chain automation, security, and business models [342]. World wide mobile operators are in the deployment phase of the Fifth Generation (5G) networks, which have become critical for the smart industries. 5G New Radio (NR) offers higher bandwidth, lower latency, and a higher device density than the existing mobile network.

5G Radio Access Network (RAN) dis-aggregation has opened up new opportunities. 3GPP and Telecom industries have defined transport interfaces (backhaul, fronthaul, and mid-haul) and functional splits to incorporate network flexibility and openness. Network Functions Virtualization (NFV) enabled the Mobile Network Operators (MNOs) to implement fully–centralized C–RAN and dis-aggregated RAN architectures. 3GPP's Release 15 [343] defines a flexible 5G RAN architecture with the gNodeB split into the Central Unit (CU), Distributed Unit (DU), and Radio Unit (RU), as shown in Figure 3.5. CU and DU are used to implement different split options. The high-level functions are distributed over the mid-haul (CU and DU). By 2026, it is expected to have around 2.5 billion 5G voice users [344], experiencing high-end interactive calling features. Endless opportunities have opened up new business and investment models for providers and users. The transforming technologies will evolve and develop hand-in-hand with significant revenue opportunities. Companies are significantly making investments in 5G and beyond technologies. The critical attributes for the telecommunication sector are the cost revenue trade-off and underlying profit.There is disruptive cross-sector competition among the MNOs and vendors. The MNOs expected to implement business models to support 5G services to serve the goal of ubiquitous connectivity.

Different services, such as emerging applications, factory automation, and autonomous driving, has stringent latency, throughput and reliability requirements. These requirements open new challenges to network management and architecture design. It makes it tough for the operators to trade and select the proper set of splitting. Functional splitting is the critical enabler of a future wireless network. It allows the coordination of performance features such as latency, throughput and cost. To analyze the optimal split option for higher throughput with low latency and minimum cost, this study analyzed split 6 and 7 with Video (VI) and VI+Best Effort (BE) applications. Suggested the best option for minimum cost without affecting system performance. A similar study on functional splits is presented in [155], [345].

This chapter aims is to understand the cost/revenue trade-off of a 5G pico/micro cellular scenario by using the 5G-air-simulator [311]. The output of the simulations enables to analyze the Packet Loss Ratio (PLR), average delay, goodput and number of supported users for the 2.6 GHz, 3.5 GHz and 5.62 GHz frequency bands. Supported goodput curves for video (VI) and VI+best effort(BE) are used as an input to the cost/benefit analysis whilst comparing functional split 6 and 7 with cases where functional splitting is not considered at all.

The remaining of the Chapter is organized as follows. Section 6.2 shortly discusses the 3GPP functional splitting, where the details discussion of functional splitting is presented in Chapter 3. Section 6.3 scenario and approach description. Section 6.4 discusses the achieved results, followed by the cost/revenue, and profit analysis in Section 6.5. Finally, in Section 6.7, the main conclusions of this work are drawn.

## 6.2 3GPP Functional Splitting Techniques on 5G NR

3GPP has defined functional splitting while suggesting eight split options and extending them to further sub-splitting possibilities [346]. DUs' functions reside near the user and will be placed at the antenna side. The functions in the CU will benefit from centralization processes and the high processing power within data centers. The functional splits proposed by 3GPP and enhanced Common Public Radio Interface (eCPRI), Small cell forum, and Next Generation Mobile Networks (NGMN) [20], are presented in Figure 3.5.

Authors in [129] have proposed different functional splitting in higher-layer to enhance the CPRI requirements, while the authors in [128] proposed to shift the radio processing functions from the BBU to the Remote Radio Head (RRH) to decrease the load on the fronthaul.

Split 7 has further sub-splits, sub-divided into 7.1, 7.2, and 7.3. That include RRH functionalities like Inverse Fast Fourier Transform (IFFT), resource mapping, precoding, and cyclic prefix addition that reduces the load on the fronthaul. The lower physical layer (in some cases higher physical layer) is processed at the RRH, while the other functions are processed at the edge of the cloud. 3GPP suggests that the MAC-PHY split (6) between the Media Access Control (MAC) and Physical Layer (PHY) shifts the RF, PHY and other functionalities to the RRH.

Split one is the split between the Radio Resource Control (RRC) and the Packet Data Convergence Protocol (PDCP), while split two is the split between the PDCP and Radio Link Control (RLC). In split 2, the RRC and PDCP are kept in the BBU, and all the other processing functionalities (RLC, MAC, PHY, and RF) are processed at the RRH.

Split option 1 to option 6 are well-thought-out with higher layer splitting suggestion [131]. The eCPRI specification defines the split options with different nomenclatures like A, B, C, D, ID, IID and E [130, 131] eCPRI considered the splits ID, IID, within the PHY layer corresponding to the option 7. It also considers the split E, corresponding to option eight, in line with the usual functional split used by CPRI, where the D splits are taken as split 6.

## 6.3 5G NR Scenario and Approach

In the scope of this chapter, the cost/revenue trade-off of splits 6 and 7 (two options that encourage the centralization concept) are analyzed in the small cell environment. Based on our assumptions for a micro cellular scenario, we explored whether split 6 is the best solution for small cell deployments [347], as it can improve not only the data rate but also reduce the cost of the network and power consumption.

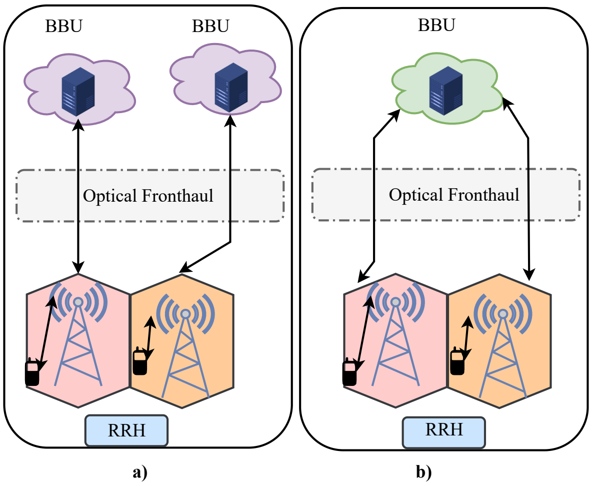


Figure 6.1: BBU with RRH (a) one to one and multiple RRH (b) one to many.

The one-to-many configuration between the BBU and RRH exhibits efficient resource management while, in the one-to-one configurations, as illustrated in Figure 6.1 (a), each RRH is connected to one single BBU. The users in each RRH are scheduled in different frames. All the bandwidth is allocated to one RRH, and the spectrum is reused for each cell. In Figure 6.1 (b), the BBU connects to multiple RRHs, and the users in different RRHs share the same resource units of only one BBU whilst scheduling it within the same frame. If the user is unavailable or the traffic is low, the nearby cell zooms out while the quiet traffic cells go to sleep This procedure reduces the power consumption and the complexity of the shared BBU.

We have simulated a scenario with nineteen cells in the 5G-air-simulator [311] and considered the Proportional-Fair (PF) packet scheduler. The central cell is the cell of interest and only communicates with User Equipment (UE). The UEs are deployed inside the central cell, and the remaining 18 cells are only interfering cells. The procedure for deploying users with a uniform distribution in the 5G-air simulator [311]. The deployed users are limited to the central cell and can not leave the central cell to nearby cells, as shown in Figure 6.2. Reuse pattern three ($k = 3$) is considered. From this analysis, can determine the number of supported users and goodput.

We have considered functional split 6 and split 7 (7.2) [346]. The split 6 is ideal for small cell deployment, while split 7 (mainly sub split 7.2) requires high fibre capacity, which increases the fronthaul price.

For this simulations, have compared the 5G radio performance of the NR operating bands (2.6 GHz, 3.5 GHz and 5.62 GHz) for Video (VI) and Video plus Best-Effort (VI+BE) by con-

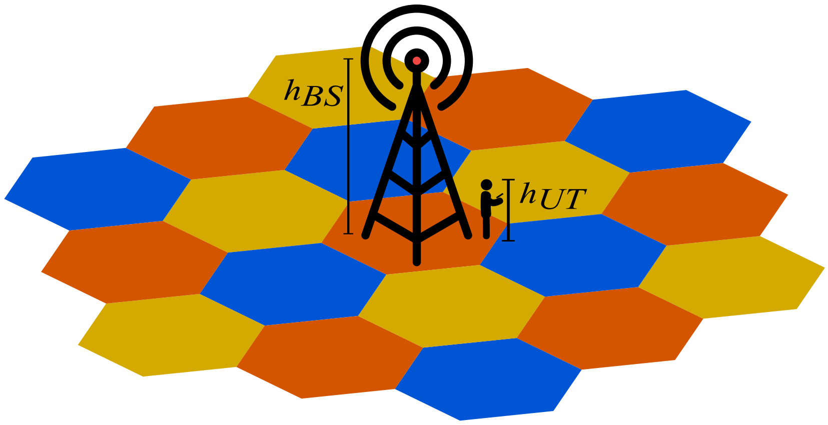


Figure 6.2: Micro cell with interfaces with one cell having users while others are interfering.

sidering the Proportional Fair (PF) packet scheduler. Assumptions are as follows:

- For video only, have considered a video trace of the simulator [348].
- For the best effort flows, have considered infinite buffer sources [348].
- PF schedules the traffic of a user when its instantaneous channel quality is relatively high compared to its own average channel condition over time. The PF scheduler is used as a typical way to find a trade-off between requirements of fairness and spectral efficiency. It is effective in reducing variations in user bit rates with little average bit rate degradation, as long as user average values of SINR are fairly uniform [312].

The simulation parameters are presented in Table 6.1. Numerology zero with a sub-carrier spacing of 15 kHz is considered, with ten subframes in a single frame. Each single frame duration is 10 ms, while each sub-frame is 1 ms. Every sub frame further contains one slot which carries 14 symbols. The height of the base station is settled to $h_{Bs}$ = 10 m in the simulated scenario. The cell radius varies from 15 m to 1000 m. The transmission time interval (TTI) is 1 ms. The actual time for the simulations is 46 s, and the period of each one of the video streams is 40 s. The results are obtained by getting an average of 50 simulations.

## 6.4 5G NR Simulation Results

The scenario from Figure 6.2 has been simulated to obtain the packet loss ratio. As shown in Figure 6.3, for the longest values of the cell radius, the minimum value for PLR occurs at 5.62 GHz fro long cell radius, but PLR = 2% occurs at the same number of users as for the shortest cell radius at lower frequency bands. The PLR at 2.6 GHz is less than 3.5 GHz and 5.62 GHz. For example, if consider the case of $R$ = 0.04 km then, in Figure 6.3 a), the 2.6 GHz band supports almost five users with minimum PLR compared to others. With the same cell radius, in Figure 6.3 b), the PLR of the 3.5 GHz band goes above 2% with five users. At the 5.62 GHz band, the PLR crosses the 2% target PLR for the same cell radius, and six users are supported. At 2.6 GHz, almost 9 users are supported (with PLR less than 2%) for the same cell radius. For cell radius of 1 km, the 5.62 GHz frequency band performs better than the 2.6 GHz and 3.5 GHz bands.

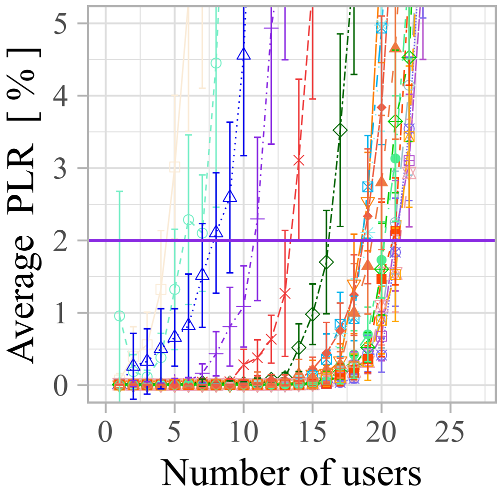


(a) Average PLR for 2.6 GHz.

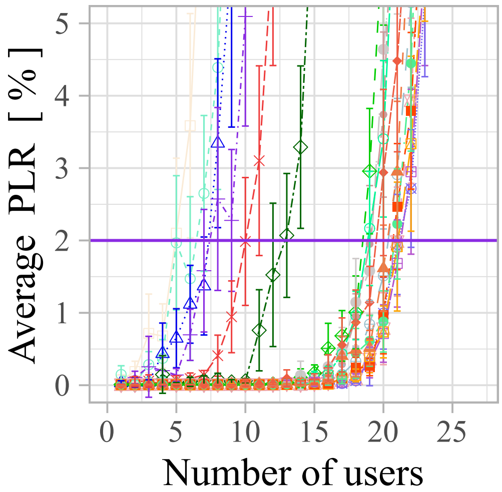


(b) Average PLR for 3.5 GHz.

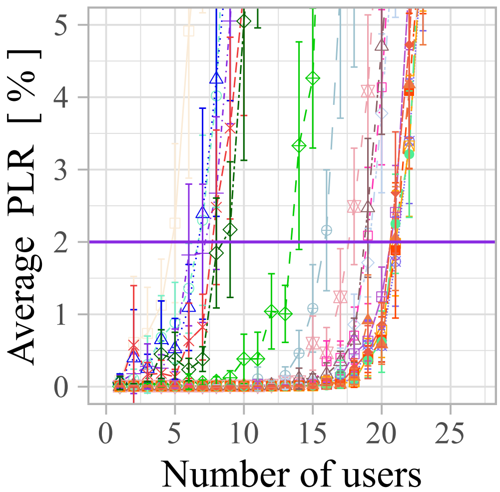


(c) Average PLR for 5.62 GHz.

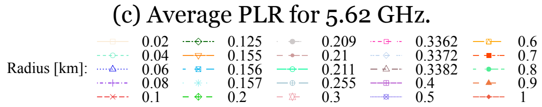


Figure 6.3: Average PLR for 2.6 GHz, 3.5 GHz,and 5.62 GHz with number of supported users.

Table 6.1: Simulations parameters

| | | | |
|---|---|---|---|
| Frequency Band | 2.6 GHz | 3.5 GHz | 5.62 GHz |
| NR operating band | n7 | n78 | n46 |
| Numerology $\mu$ | 0 | | |
| Frame duration [ms] | 10 | | |
| Subcarrier spacing | 15 kHz | | |
| Number of subframes per radio frame | 10 | | |
| Number of slots per subframe | 1 | | |
| Number of symbols per slot | 14 | | |
| Number of slots | 10 | | |
| Transmitter power small cells [dBm] | 40 | 42.2478 | 46.6953 |
| Transmitter power UT [dBm] | 23 | | |
| Number of BS | 19 | | |
| Reutilization | 3 | | |
| Bandwidth per tier [MHz] | 20 | | |
| Cell radius [m] | 1 km | | |
| Effective UT height [m] | 1.5 | | |
| Effective BS height [m] | 10 | | |
| Scheduler | PF | | |
| Applications | VI and VI+BE | | |
| Video bit rate [Mb/s] | 3.1 | | |
| Number of simulations | 50 | | |
| Simulation duration [s] | 46 | | |
| Flows duration [s] | 40 | | |

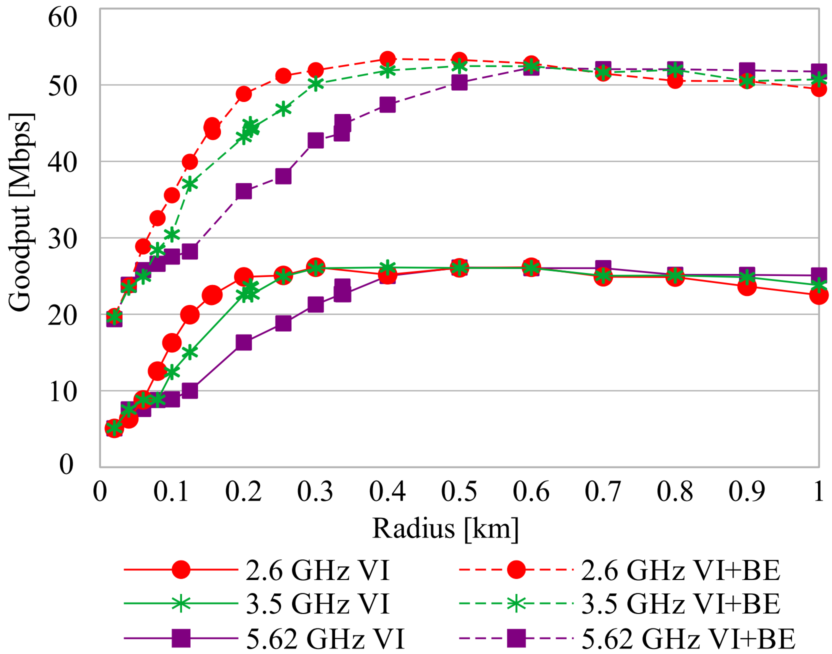


Figure 6.4: Goodput as a function of $R$, for the 2.6 GHz, 3.5 GHz, and 5.62 GHz bands, with VI and VI+BE traffic.

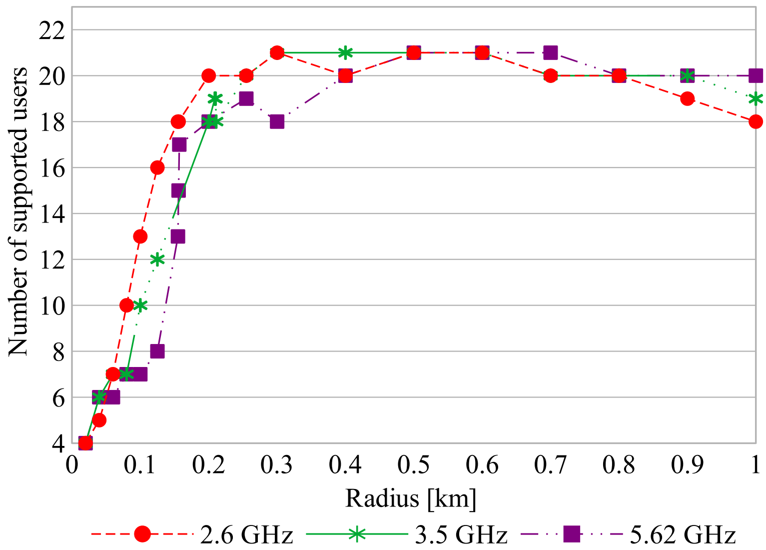


Figure 6.5: Number of supported users as a function of $R$.

Figure 6.4 shows the average goodput as a function of $R$, varying from from 0.015 to 1 km. To obtain these results with a given set of parameters, we have first performed the simulation for Video (VI) and then for Video Plus Best Effort (VI+BE). It is demonstrated that, for the shortest cell radii, at 2.6 GHz, VI+BE provides a higher supported goodput than in the 2.6 GHz VI case. Besides, with VI+BE, in comparison to the 5.62 GHz and 3.5 GHz frequency bands, the 2.6 GHz frequency band performance is better. Furthermore, the 3.5 GHz VI+BE and VI case serve better than the 5.62 GHz VI+BE and VI cases, respectively, for a shorter cell radius range (up to circa 400 m). For the shortest cell radii, the 5.62 GHz band achieves higher PLRs (above 2%). On the other hand, for values of cell radius beyond 0.6 km, the 5.62 GHz band provides higher goodput than the 2.6 and 3.5 GHz bands.

Figure 6.5 shows the number of supported users as a function of $R$. It clearly shows that the 2.6 GHz band supports a higher number of users for the shortest cell radius. As shown in Figure 6.5, for cell radii up to 400 m, the 2.6 GHz band supports 21 users (its maximum value among the bands). For $R$s beyond 700 m, the 5.62 GHz supports a higher number of users.

## 6.5 Revenue, Cost and Profit analysis

The economics of mobile radio networks includes the perspectives of subscribers, network operators, service providers, regulators, and equipment suppliers. The main concern of the subscribers, regulators and vendors are discussed in [349]. The main goal of network operators and services providers is to increase his company profits. As a result, their objective is to determine the best configuration that would maximize his anticipated net profits [349]. Availability of affordable prices of services (i.e., television and streaming) is the concern of the service providers. In the cellular planning process, the operator goals are to identify the best operating point that will maximize projected revenues. The technology to be employed, the size of the cell, and the number of channels to use in each cell are a few examples of the

Table 6.2: Values for costs without splitting & with splits 6/7.

| Parameters | Without splitting | Split 6 | Split 7 |
|---|---|---|---|
| $BS_{cost}$ | 100% | 25% | 20% |
| $C_{BS}$ [€] (RRH+BBU) | 5700 | – | – |
| $C_{BBUplusFH}$ [€] | 2000 (FH) | 2000+1067 | 2000+1333 |
| $C_{RRH}$ [€] | 5700 (BS) | 1425 | 1140 |
| $C_{BH}$[€] | 2000 (3000 € for fiber instead of FSO) | | |
| $C_{inst}$ [€] | 200 | | |
| $R_{b-ch}$ [kb/s] | 144 | | |
| $C_{M\&O}$ [€] | 200 | | |
| $C_{Bh}$[€/km$^2$] | 3000 | | |
| $C_{fi}$ [€/km$^2$] | 13.01 (2.6 GHz) | | |
| $C_{fi}$ [€/km$^2$] | 10.58 (3.5 GHz) | | |
| $C_{fi}$ [€/km$^2$] | 0 (5.62 GHz) | | |
| Auction [€] | 6000000 (2.6 GHz) | | |
| Auction [€] | 4880000 (3.5 GHz) | | |
| $T_{bh}$ | 86400 | | |
| $C_b$ without splitting [€] | 2380 | | |
| $C_b$ for Split 6 [€] | 1281.4 | | |
| $C_b$ for Split 7 [€] | 1338.4 | | |
| $R_{Rb}$ [€/MB] | 0.0004 | | |
| Total area of Portugal [km$^2$] | 92212 | | |
| Project duration [years] | 5 | | |

key aspects that need to be addressed [350], [351], [352].

The authors from [350], [351], and [352] propose to divide the cost of the system into two categories: capital costs (planning and setting up of a cell site) and operational costs (operation, management, and maintenance). On the one hand, capital costs include both fixed costs (such as licensing, fees, and spectrum auctions) and costs based on the quantity of BSs and transceivers, both of which are costs per unit of area. On the other hand, the operational expenses of the system, are partially determined by the quantity of transceivers and BSs per unit of area.

To analyse the cost/revenue trade-off with functional splits 6 and 7, the models from [353] and [352] have been considered. The revenues per cell, $R_v/cell$[€], can be achieved as a function of the throughput per Base Station (BS), $R_{(b-sup)}$ BS [kb/s], and the revenue of a channel with a data rate $R_{b[\text{kb/s}]}$, $R_{R_b[€}$ [€/min], and $T_{bh}$ corresponding the equivalent duration of busy hours per day [351], $R_v$/cell[€] can be obtained by following equation. The revenue per coverage zone can be calculated as follows:

$$(Rv)_{\text{cov-zone}} = \frac{N_{\text{hex.}}\, R_{(b-sup)equiv} \cdot T_{bh} \cdot R_{R_b[€/\min]}}{R_{b-ch[kb/s]}} \quad (6.1)$$

where $R_{R_b[e/\min]}$ is the revenue of a channel with data rate $R_{b[\text{kb/s}]}$, $N_{hex/\text{km}^2}$ is the number of hexagonal areas,$R_{b-ch[\text{kb/s}]}$ is the channel's data rate and $T_{bh}$ represents busy hours per day and the number of busy days per year. With the above equation, one can obtain the revenue per unit area by considering the revenue per cell and the number of cells per unit of area.

The analysis proposed in this work considers that the costs will be evaluated on an annual basis. Parameters are presented in Table 6.2. First, defined the price per unit of area as follows:

$$C_{\left[€/km^2\right]} = C_{fi\left[€/km^2\right]} + C_b \cdot N_{hex/km^2} \quad (6.2)$$

$C_{fi[€/km2]}$ Represents the fixed terms of the costs, $C_b$ is the cost per BS given by equation 6.3 and $N_{hex/km^2}$ is the number of hexagonal coverage zones per unit of area and is given by equation (6.4):

$$C_b = \frac{C_{RRH} + C_{Bh} + C_{BBUplusFH} + C_{\text{inst}}}{N_{year}} + C_{M\&O} \quad (6.3)$$

$$N_{hex/km^2} = \frac{2}{3 \cdot \sqrt{3} \cdot R^2} \quad (6.4)$$

where $C_{RRH}$ is the cost of the RRH (in the case 'without splitting' RRH+BBU are together), $C_{Bh}$ is the cost of the Backhaul, $C_{BBU+FH}$ is the cost of the BBU plus fronthaul, $C_{inst}$ is the installation cost of the BS and $C_{M\&O}$ is the maintenance and operation cost, as presented in Tab. 6.2. One-to-many BBU/RRH mapping is assumed (6 RRHs per BBU).

The analysis based in the main land of Portugal, and assumed the licence value from the auction of ANACOM for the 3.5 GHz band, which is 36.90 million €, while for the 2.6 GHz band it is 6 million €, and zero € for the 5.62 GHz unlicensed band, for 20 MHz bandwidth, for $k$ = 3 (in the auction 30 lots of 10 MHz, were considered). By dividing this cost per square kilometre, by the number of years for the project, one obtains an annual fixed cost of 79.38 €/km$^2$ for the 3.5 GHz bands [10], as follows:

$$C_{fi\left[€/km^2\right]} = \frac{\frac{\text{licence price}}{\text{country area}}}{N_{\text{year}}} \quad (6.5)$$

$N_{\text{year}}$ represents the project's lifetime.

The profit is presented in percentage terms in Figure 6.6 for split 7 and for split 6 , one can get these results by considering equations 6.1 and 6.5 to get profit equation 6.6. The profit is given by equation (6.6):

$$P_{ft\left[€/km^2\right]=} R_v - C \quad (6.6)$$

while the net revenue gives the profit in percentage, i.e., the difference between the revenue and cost, normalized by the cost, as follows, equation (6.7):

$$P_{ft[\%]} = \frac{R_{v\left[€/km^2\right]} - C_{\left[€/km^2\right]}}{C_{\left[€/km^2\right]}} \quad (6.7)$$

Revenue of VI and VI+BE per km can be calculated according to equation (6.8):

$$R_{V\left[€/km^2\right]} = N_{hex\left[km^2\right]*} \frac{R_{b-\sup[kb/s]\cdot 60\cdot 6\cdot 240} \cdot R_{R_{b[€/min]}}}{R_{b-ch[kb/s]}} \quad (6.8)$$

Revenues are considered on an annual basis, where thought 6 busy hours per day, 240 busy days per year [350], and the price of a 3.1 Mbps channel per minute (corresponding to the price of $\approx$ 1MB), [€/min] = 0.0004, which is very low as compared to the value considered in [354].

Although the curves with the cost and revenue per square kilometer as a function of the cell radius, are not represented, it can mention that the VI+BE traffic gives the best revenue per square kilometre compared to VI. The 2.6 GHz revenue is higher than the 3.5 GHz and 5.62 GHz bands in for both VI and VI+BE cases. Moreover, the cost for 2.6 GHz, 3.5 GHz and 5.62 GHz are compared with the values of the revenue. The cost for the 2.6 GHz band is lower than at 3.5 GHz (and higher than at the 5.62 GHz unlicensed band, as the price for this band is zero).

For all of the frequencies bands, the cost when functional splits are considered is lower than in the case where there is no functional splitting (”without” scenario).

With split option 6, results for the cost and revenue indicate that the cost for the 2.6 GHz frequency band is lower than for the 3.5 GHz band. Besides, the 5.62 GHz band has the lowest cost of all considered bands. For VI and VI+BE traffic, split option 6 and 7 revenues at 2.6 GHz are higher than in the 3.5 GHz and 5.62 GHz bands.

Fig. 6.6 shows the profit in percentage terms. It is observed that the profit of the split 7 (sub-split option 7.2 has been adopted), case with VI+BE, is higher than the one for split 7, case with VI, shown in Fig. 6.6a. For example, if we look at the 2.6 GHz frequency band, in the scenario of split 7 shown in Fig. 6.6a, in the case of VI+BE traffic, one gets the most elevated peak of the supported goodput (corresponding to PLR of 2%). Profit reaches above 800% for $R = 400$ m. The 2.6 GHz frequency band performs better than all other bands.

Fig. 6.6b shows the split 6 profit in percentage terms for the three frequency bands. Again, it is found that VI+BE traffic performs better than supporting VI alone. Besides, the 2.6 GHz frequency band performance is also the best one. For a cell radius of 400 m, the peak profit achieves above 800% with slight advantage to split the sub-split option 7.2. The decision between the advantage of split 6 versus split 7 is very sensitive to the cost parameters, namely the costs for the BBU, FH and RRH.

The best profit occurs for the VI+BE traffic at all frequency bands. For the shorter radius (400 m) 5.62 GHz frequency band profit is lower than 2.6 and 5.62 GHz band for both split options.

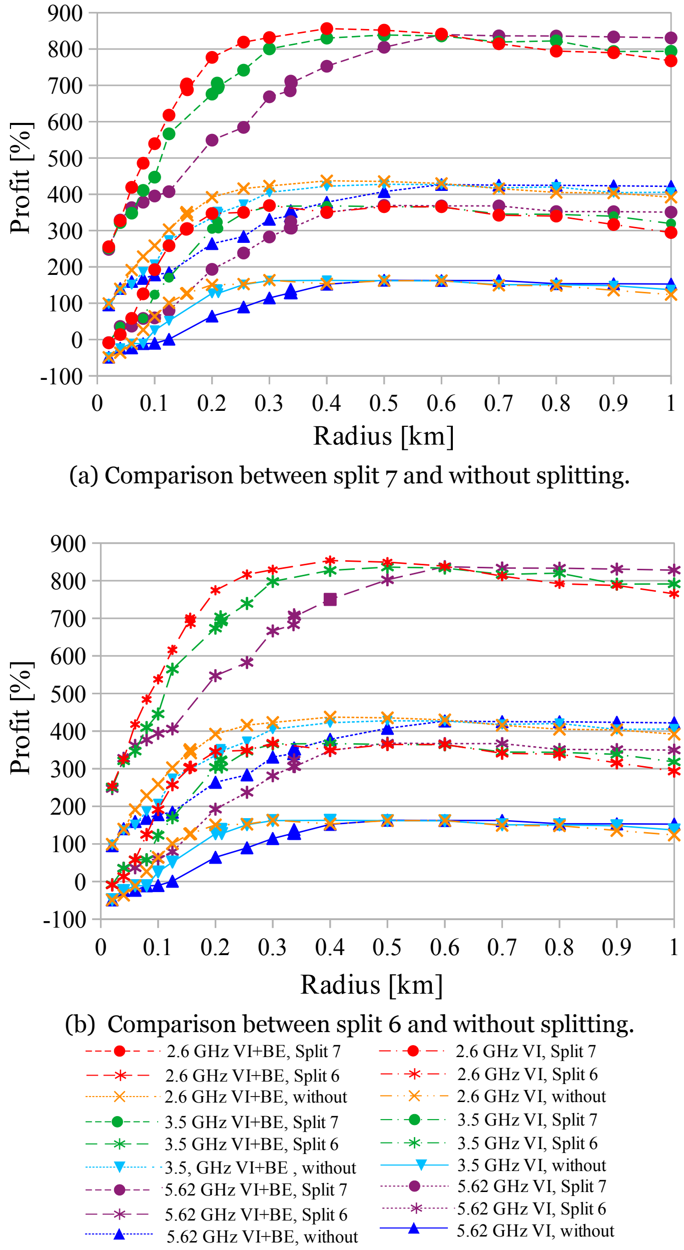


(a) Comparison between split 7 and without splitting.

(b) Comparison between split 6 and without splitting.

Figure 6.6: Profit in percentage terms "without" splitting and functional splits 6, 7, considering VI or VI+BE traffic.

## 6.6 Cost Revenue Trade-off for CA in 4G

For 4G, in this section of the Chapter, the studied held based on the service/operator point of view, with the goal to obtain the maximum profit from the business for example reducing the cost and increasing the revenue. The study presented 5 years project duration, for 4G. This work does not completely aim to obtain the economic study, but the objective is to provide

Table 6.3: Values for cost revenue analysis for scenario with CA and without CA .

| Parameters | Without CA | With CA |
|---|---|---|
| $BS_{cost}$ | 500 | 2 x 500 |
| $C_b$ [€] | 330 | 550 |
| $C_{BH}$[€] | 150 | |
| $C_{inst}$ [€] | 100 | |
| $R_{b-ch}$ [kb/s] | 144 | |
| $C_{M\&O}$ [€] | 150 | |
| $C_{fi}$ [€/km$^2$] | 13.01 (2.6 GHz) | |
| $C_{fi}$ [€/km$^2$] | 10.58 (3.5 GHz) | |
| $C_{fi}$ [€/km$^2$] | 0 (5.62 GHz) | |
| Auction [€] | 6000000 (2.6 GHz) | |
| Auction [€] | 4880000 (3.5 GHz) | |
| $T_{bh}$ | 86400 | |
| $R_{Rb}$ [€/MB] | 0.09 | |
| Total area of Portugal km$^2$ | 92212 | |
| Years | 5 | |

a preliminary contribution with a basic understanding considering CA to offer assistance for cellular planning optimization.

From the perspective of radio resources management and cellular planning, the key aim of the operators is to determine the optimal operating point which can rise revenue. The main things which effecting the revenue, contains the type of technology used, the size of the cell and the number of radio resources used per cell. Therefore, it is essential to identify the cost of the main components of the cellular system. Which principally has a direct relation with maximum cell coverage or the reuse pattern. In proposed work scenario it is considered for without CA scenario each station contain single eNB transmitter, while two for the case of CA. The major part of the system cost contains: (a) capital costs of BS, backhaul, site of the cell and its planning also installation, and (b) operation expenses which include the maintenance, administration and operation cost [27]. The capital cost further includes the licensing of the spectrum (auction), the number of eNBs and transceivers per kilometre and its installation, hardware core equipment cost.

The analysis is obtained, based on our assumptions and analysis [27] BS cost, backhaul cost, installation cost of the BS, operation and maintenance cost, which are presented in Table 6.3.

The analysis is based in the main land of Portugal, and have assume the licence value from the auction of ANACOM for the 3.5GHz band, which is 4880000 €, while for the 2.6 GHz band it is 6000000 €, and for 20 MHz bandwidth (for $k$ = 3, with 30 lots of 10 MHz). Dividing cost per square kilometre, by total years of project, its will give the annual fixed cost.

The mathematical formulation for the presented work are given in section 6.5 of Chapter in details. Annual basis revenue are acquired, where thought 6 busy hours each day, 240 busy days each year [350], with the price for Mbps channel per minute (with almost price of $\approx$ 1MB), [€/min] = 0.09.

Based on the presented values for the cost, and with simulated goodput for CA and with CA scenario, we considered the mathematical formulation (cost revenue analysis) from section 6.5 of Chapter to perform the analysis.

The cost and revenue without the CA and with the CA are presented in Figure 6.7a. If we compare the 2.6 GHz and 3.5 GHz without the CA scenario, the 2.6 GHz compared to 3.5 GHz almost gives similar costs and generates nearly the same revenues. While if compare the CA scenario with the without CA scenario, the cost of CA is slightly higher than Without CA. The cost of CA is higher because it is using two-fold of the resources because of two different transmitters (other resources include backhaul, RRH and auction of two bands). The maximum possible profit comparison in percentage terms is shown in Figure 6.7b. It is clearly shown that the profit of CA is more than 4 times of without of CA scenario. This means that the slight increase in the cost of CA gives back more than 4-time profit of without CA scenario.

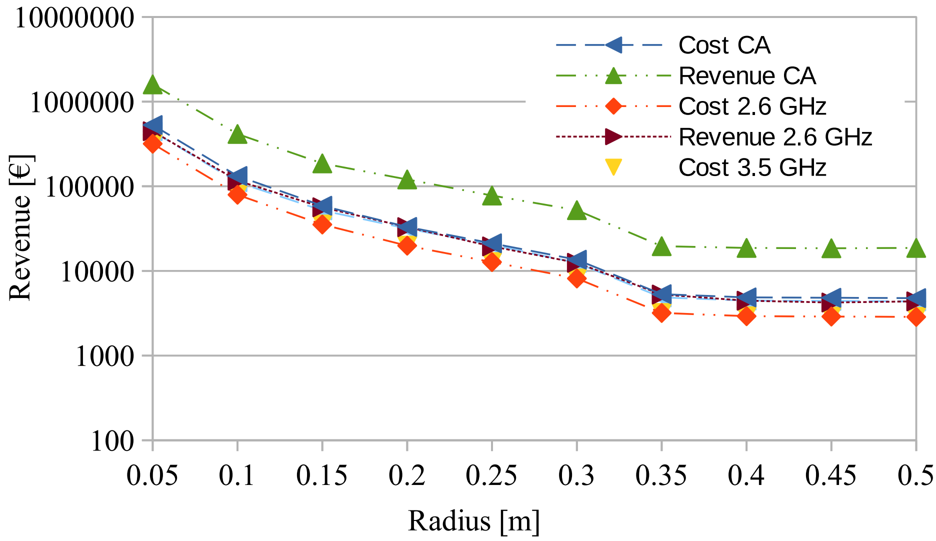


(a) Cost and revenue for CA, and without CA scenario at 2.6 GHz and 3.5 GHz

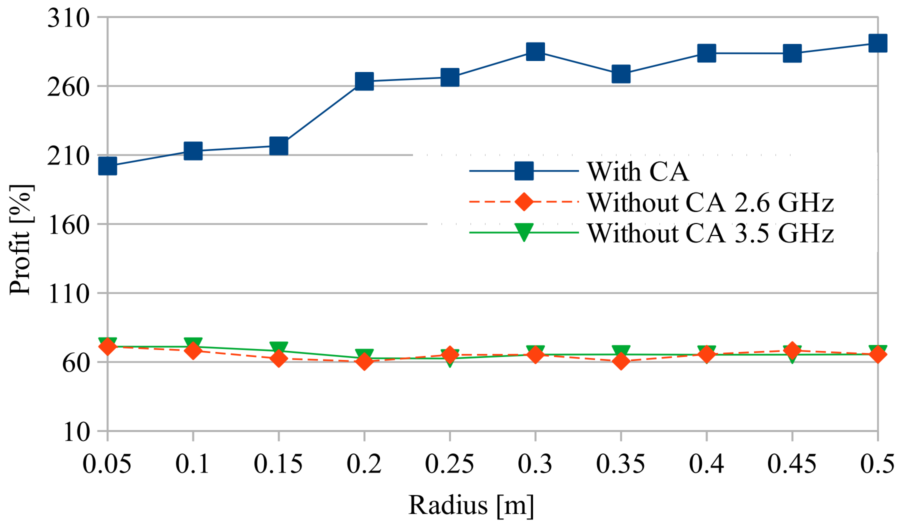


(b) Profit in percentage for both with CA and without CA scenario at 2.6 GHz and 3.5 GHz

Figure 6.7: Cost and revenue for CA, and without CA scenario.

## 6.7 Summary and Conclusions

The chapter provided the analysis of the cost/revenue trade-off by considering 5G NR (numerology) deployments without and with functional splitting (split 6 and 7). The 2.6, 3.5 and 5.62 GHz frequency bands were considered and simulations were performed for users either using VI or VI+BE traffic. Based on those results, the goodput, the number of supported users and PLR are evaluated for three frequency bands. Revenues depends on the supported average goodput, obtained for the PLR target of 2% (average delay was never the limiting factor). With VI+BE the 2.6 GHz frequency band supports higher goodput in the range of shorter cell radius (pico cells). For longer cell radii, the 5.62 GHz GHz provide higher goodput. The 3.5 GHz band provide higher average supported goodput than the 5.62 GHz band for shorter cell radii (small cells).

For the shortest cell radius, the best is to select the 2.6 GHz frequency band to support a higher number of users and higher average goodput. Overall, the best revenues are achievable with split 6 and 7 for the 2.6 GHz band with VI+BE traffic, with lower cost and higher profitability. It is shown that, for cell radii up to 300-600 m, the split 6 and 7 provide higher profit compared to the case without splits for all frequency bands (slight advantage for split 7), with maximum achievable profit for cell radius of circa 400 m (at 2.6 GHz).

For 4G with Picocells, from the analysis of the economic trade-off, the EMBS multi-band scheduler can provide higher revenue, compared to those without CA. The CA apart from massive connectivity with higher goodput is also paramount from a business perspective.

# Chapter 7

# Conclusion and Topics for Further Work

## 7.1 Conclusion

This thesis has covered aspects of 4G and 5G and has given a road map toward the 6G with possible use cases. The first chapter is about the initial introduction, which introduces the work as state-of-the-art and adds the contribution to the work at the end of the Chapter. A deep survey of the research literature (uses cases, challenges, and requirements) is provided. The result first focused on CA in the 4G scenario. A comprehensive study is offered to evaluate the 5G waveforms candidates from theory to hardware complexity. The functional splitting of the network is familiarised very well within the current essentials of the network. To accomplish 5G requirements, the work has contributed toward the Hetnet concerning Femto-cell to analyse the massification of the network. The need for standardization and its group discussion and literature are discussed with state of art. The cost revenue, which is essential for today's prevailing splitting techniques, are analyzed, and proposed the best one among the functional split option for different cell radius. The 5G NR with intense graphical discussion and mathematical understanding are elaborated. The work has the further outstanding implementation of 5 NR in real-time scenarios explained in the appendixes.

The literature review presents an overview of the standardization process and emphasizes 5G and beyond standardization while considering the challenges of spectrum usage in upper-frequency bands. From a technology perspective, 5G and beyond will provide a vast opportunity to the users and MNOs to explore different services and use cases. It is learned that the scope of standards and technology development needs to be broadened to support future ecosystems. Products must comply with the standards to keep the full capabilities of upcoming networks. Higher layers are available for research, bringing new challenges and enormous opportunities.

In 5G phase-2 and future communication generations, network slicing is expected to be one of the most influential technologies and provide solutions tailored to specific end-users, varying from residential to industrial or corporate. It can evolve and shift the telecommunication industry to the next level by allowing more flexible and reliable design. It is required to enhance network infrastructure and incorporates virtualization and softwarization to make the best use of services provided by network slices. It will allow operators to offer premium services to their customers. Moreover, NS will enhance the business opportunities in many sectors, which will gain attraction by increasing revenues. It is worth noting that network slicing supports the economic model and service differentiation that meets the end-user service level agreements.

As a result of RAN splitting and virtualization, network deployments are more flexible and facilitate the creation of a multi-vendor marketplace for different radio and network components that are different from the traditional business models. By creating various interfaces between layers through splitting, new hardware and software products can be designed and fabricated while guaranteeing interoperability between elements produced by different manufacturers. Expected 5G and beyond reliability and resilience are commonly cited to enable remote surgeries with physicians commanding high precision robots from remote hospitals in real-time and to support high-speed nano-robot communications for in-body healthcare applications. More realistically, 5G and beyond will serve the needs of the industry 4.0 and beyond. Moving the processing functionalities from the RRHs to the DUs and CUs may be advantageous as the RAN architecture evolve and leads to an economy of scale. Many functional splits, serving various use cases, have been devised but have limitations. For example, the 3GPP split option 8 requires a data rate much higher than the total user data rate and a distance between CU and DU lower than 20 km. The split option 7.2 has been preferred by the O-RAN ALLIANCE. Different splitting implies different data rate and latency requirements. For example, to implement split option 6, the PHY and RF are in the DU while the MAC is in the CU. The MAC layer performs functionalities like the computation/calculations and operations in CU considering software, whereas the RF (DU) takes care of the rest of the functionalities, resulting in high hardware costs. Various standardization bodies are actively working to provide energy-efficient, reliable, and economic solutions by allowing BBUs to support multi-RF units. The O-RAN ALLIANCE intends to support diversified 4G to 5G and beyond use cases by developing the specifications and architectures with new open interfaces to control the DU and CU with the so-called RAN Intelligent Controller. Academia, industries, and research organizations are working toward an open RAN infrastructure to support RAN dis-aggregation. The O-RAN ALLIANCE implements different intelligent processing algorithms to deploy flexible and economic networks. Integrated Access Backhauling (IAB), edge processing with cloud, and virtualized (also Fog) RAN are open research areas that have the potential to incorporate intelligence into the network to support 5G second phase and 6G deployments.

On the side of CA, the overview for LTE-advanced CA is presented. According to the literature review, CA will become a significant scheme in an upcoming communications system when the spectrum's resource becomes scarcer. By using wide bandwidth, CA provides higher data rates and enables flexible and optimal utilization of frequency resources. Mainly, the CA between non-contiguous frequency bands offers novel opportunities to benefit from LTE-Advanced frequency assets in different bands. Due to statistical multiplexing gain, CA is capable of surpassing the increase in the number of resources for given cell radius and number of UEs. Based on the results obtained in this study, it can be concluded that CA (EMBS) significantly improves the performance of the 2.6 GHz and 3.6 GHz bands in terms of average delay, maximum supported UEs, and goodput. Without carrier aggregation, the average delay for the 2.6 GHz band is measured at 25.5 ms, accommodating a maximum of 26 supporting UEs. Similarly, the 3.6 GHz band exhibits an average delay of 25 ms, with a maximum of 25 supporting UEs. However, when CA is enabled for both bands, the system demonstrates remarkable enhancements. It supports a total of 103 UEs within an average delay of just 6 ms for both 2.6 GHz and 3.5 GHz band. One has been able to obtain values for the goodput of 40 Mbps for a cell radius of 500 m and of 29 Mbps for a cell radius of 50 m, which is 3 times higher than without CA case. Furthermore, allocating multiple carrier components resource and modification of transmission parameters like coding schemes, transmission power, and modulation for various carrier components are still open research topics.

The thesis, further provided an overview of the 5G NR with Femto-cells analysis in Hetnet scenario. 5G is operating in the FR1 and FR2 spectrum, which gives benefits of 10X to 100X capacity. With densification of the network, it can support massive devices, and due to its variable numerology, it can support multiple bandwidths. In 5G NR, there is a difference that the NR resource grid's physical dimension is changeable. Depending on numerology, it is possible to change the number of OFDM symbols within a radio frame and sub-carrier spacing. 5G with 4G results are compared, considering 5G NR feature we got more than two time greater number of supported users, while almost more than more than two higher supported goodput with proper fair resource allocation.

Due to enormous demands in indoor communication, this work studies indoor Femto-cell deployment. The analysis offers the study of indoor Femto-cell coverage. The work considers the 3GPP small cell deployment assumption and the apartments 5 x 5 grid topology. The work studied the variation in transmit power with geometrical dimension for Femto-cells in the 5G scenario. The theoretical study presented with simulations. Conversely, with the increase inside length and the decrease in the transmitter power, signal strength is insufficient to attain a rise in the average SINR. The 5G air-simulator is updated to deploy indoor Femto-cell with proposed assumptions with uniform distribution. The analysis of the Femto-cells indoor scenario reveals interesting findings regarding the performance of the FLS and M-LWDF scheduler. Both schedulers demonstrate their capability to support a significantly higher number of UEs compared to previous literature.The results indicate that both FLS and M-LWDF schedulers can accommodate up to 34 UEs while maintaining a minimal PLR of only 2%. This is a notable improvement compared to prior studies, which reported a maximum of 13 UEs for FLS with higher delay. Therefore, the proposed FLS and M-LWDF schedulers prove to be more efficient in terms of capacity and performance. The achieved goodput and delays also contribute to the positive assessment of the schedulers. The FLS scheduler supports goodput of 378 Mbps with maximum delay of 21.5 ms, while the M-LWDF scheduler achieves a slightly higher goodput of 380 Mbps with maximum delay of nearly 21 ms. For all the possible combinations of apartments side length and transmitter power, the maximum number of supported numbers surpassed the number of users by more than two times compared to papers mentioned in the literature.

A comprehensive set of cost/trade-off analyses of 5G NR for functional split six and split seven, for three frequency bands (2.6 GHz, 3.5GHz and 5.62 GHz) are presented. Based on our analysis for lower radius values, the best is to select the 2.6 GHz to achieve lower PLR (less than two %) and to support a higher number of users (21 UEs) and better goodput (maximum 55 Mbps). Overall, we acquired that the best revenues are achievable with split 6 and 7 for 2.6 GHz, low cost, and higher profitability (maximum 800 %). It is obtained that for the lower value of radius until the 400 m in the range of small cell radius, split option 6 and 7 provides higher profit for all frequency bands compared to without splitting case. In 4G, with CA, from the analysis of the economic trade-off with Picocell, the EMBS multi-band scheduler can provide higher revenue, compared to those without CA. It is clearly shown that the profit (maximum 280%) of CA is more than 4 times of without of CA (maximum 60%) scenario. This means that the slight increase in the cost of CA gives back more than 4-time profit of without CA scenario.

The basic functionality and characteristics of emerging 5G waveforms are presented. In addition, a comparative analysis has been given of different wave forms. Filter-based wave forms have much better OoBE as compared to OFDM, which results in better wave forms to cope with 5G challenges. FMBC has the best OoBE as compared to others but has higher computational complexity. UFMC and GFDM have better OoBE characteristics, but they have higher complexity as well as asynchronous transmission capabilities issues, whereas F-OFDM has better OoBE with moderate complexity, which is suitable for flexibility and asynchronous transmission scenarios.

## 7.2 Future Work

The future network will make it possible to totally digitalis, programmable and automate the world of connected, machines, things and humans. The sensation and all supreme experiences will be transparent across the restrictions of physical and virtual realities. Due to the full inclusion of AI and automated machines the network traffic will not only be created by humans but also by connected machines. Due to an increase in the number of devices, a enhanced densified network is required.

In this thesis, different perspectives are covered. However, some open problems needed to be solved. As we analyzed the small cells. To shift small cell technology to the next level, standardization needs to update the concepts of small cells in the correspondences of network densification. It needs stronger improving security, and proper resource allocation in situations of functional splitting with flexibility. A centralized mechanism is required to address the resource allocation and fulfil the requirements of specific services with handovers. Future research will consider CA and HetNets with small cells (overlaid with Macro-cells) deployment with NS and centralized BBU in heterogeneous networks.

# References

[1] H. Tullberg, P. Popovski, Z. Li, M. A. Uusitalo, A. Hoglund, O. Bulakci, M. Fallgren, and J. F. Monserrat, “The METIS 5G system concept: Meeting the 5G requirements,” *IEEE Communications magazine*, vol. 54, no. 12, pp. 132–139, 2016. 1, 2, 206

[2] L. Zhang, A. Ijaz, P. Xiao, and R. Tafazolli, “Multi-service system: An enabler of flexible 5G air interface,” *IEEE Communications Magazine*, vol. 55, no. 10, pp. 152–159, 2017. 1

[3] R. Gerzaguet, D. Kténas, N. Cassiau, and J. Doré, “Comparative study of 5G waveform candidates for below 6 GHz air interface,” in *Proceedings of the ETSI Workshop on Future Radio Technologies-Air Interface, Sophia Antipolis, France*, 2016, pp. 27–28. 1, 133

[4] X. Zhang, M. Jia, L. Chen, J. Ma, and J. Qiu, “Filtered-OFDM-enabler for flexible waveform in the 5th generation cellular networks,” in *2015 IEEE Global Communications Conference (GLOBECOM)*. IEEE, 2015, pp. 1–6. 1, 133

[5] F. Schaich and T. Wild, “Relaxed synchronization support of universal filtered multicarrier including autonomous timing advance,” in *2014 11th International Symposium on Wireless Communications Systems (ISWCS)*. IEEE, 2014, pp. 203–208. 1

[6] M. Simsek, D. Zhang, D. Öhmann, M. Matthé, and G. Fettweis, “On the flexibility and autonomy of 5G wireless networks,” *IEEE Access*, vol. 5, pp. 22 823–22 835, 2017. 1

[7] W. Zhao, Y. Shen, P. Xu, Y. Wei, Z. Yuan, and W. Jian, “Statistic division multiplexing for wireless communication systems,” in *2015 5th International Conference on Information Science and Technology (ICIST)*. IEEE, 2015, pp. 392–397. 3

[8] M. J. Lopez-Morales, D. A. Urquiza-Villalonga, D. Gonzalez-Morin, N. Nidhi, B. Khan, F. Kooshki, A. Al-Sakkaf, L. Leyva, H. Farkhari, D. Medda *et al.*, “MOOC on” Ultradense Networks for 5G and its Evolution”: Challenges and Lessons Learned,” in *2022 31st Annual Conference of the European Association for Education in Electrical and Information Engineering (EAEEIE)*. IEEE, 2022, pp. 1–6. 3, 9

[9] N. Alliance, “5G White Paper (Final Deliverable),” 2015. 4, 35, 38, 42

[10] H. Zhang, N. Liu, X. Chu, K. Long, A.-H. Aghvami, and V. C. Leung, “Network slicing based 5G and future mobile networks: mobility, resource management, and challenges,” *IEEE communications magazine*, vol. 55, no. 8, pp. 138–145, 2017. 4, 35, 42

[11] K. Flynn. (2019) A global partnership. [Online]. Available: https://www.3gpp.org/release-15 4, 35, 39

[12] B. Khan, Nidhi, H. Odetalla, A. Flizikowski, A. Mihovska, J.-F. Wagen, and F. J. Velez, “Survey on 5G Second Phase RAN Architectures and Functional Splits,” *submitted for possible publication to IEEE Surveys and Tutorials*, Sep. 2022. 8, 81

[13] B. Khan, A. Mihovska, R. Prasad, F. J. Velez *et al.*, "Trends in Standardization Towards 6G," *Journal of ICT Standardization*, pp. 327–348, 2021. 8, 15, 17, 36, 44

[14] R. R. Paulo, F. J. Velez, and B. Khan, "Study of Indoor Small Cell Deployments," *Journal of Mobile Multimedia*, pp. 329–344, 2021. 8, 137, 145

[15] B. Khan, R. Anderson, P. Rui, and F. J. Velez, "Deployment of Beyond 4G Wireless Communication Networks with Carrier Aggregation," 2020. 8, 16, 64, 83, 99, 113

[16] B. Khan, Nidhi, M. Albena, P. Rui, and F. J. Velez., "Cost Revenue Trade-off for the 5G NR Small Cell Network in the Sub-6 GHz Operating Band," in *WPMC 2022: Wireless Personal Multimedia Communications,.AARHUS University Denmark, 20 September 2022*, 2022, pp. 1–6. 9

[17] B. Khan, A. Mihovska, R. Prasad, V. K. Poulkov, F. J. Velez *et al.*, "Dynamic Resource Block Allocation and Isolation in Network Slicing," in *12th Symposium on COmmunications, NAvigation, SENsing and SErvices (CONASENSE) 2022 CONASENSE 2022*. River Publishers. 9

[18] M. J. Lopez-Morales, D. A. Urquiza-Villalonga, D. Gonzalez-Morin, N. Nidhi, B. Khan, F. Kooshki, A. Al-Sakkaf, L. Leyva, H. Farkhari, D. Medda *et al.*, "Inovação no Desenvolvimento do Curso Online Acessível a Todos (MOOC) sobre "Redes Ultra-densas 5G e sua Evolução"," in *Congresso Nacional de Práticas Pedagógicas no Ensino Superior-CNaPPES. 22*. Escola Superior de Enfermagem de Coimbra. 9

[19] B. Khan, A. Mihovska, R. Prasad, F. J. Velez *et al.*, "A Study on Cross-Carrier Scheduler for Carrier Aggregation in Beyond 5G Networks," in *2022 3rd URSI Atlantic and Asia Pacific Radio Science Meeting (AT-AP-RASC)*. IEEE, 2022, pp. 1–4. 9

[20] ——, "Overview of Network Slicing: Business and Standards Perspective for Beyond 5G Networks," in *2021 IEEE Conference on Standards for Communications and Networking (CSCN)*. IEEE, 2021, pp. 142–147. 9, 15, 154

[21] B. Khan and F. J. Velez, "Multicarrier waveform candidates for beyond 5G," in *2020 12th International Symposium on Communication Systems, Networks and Digital Signal Processing (CSNDSP)*. IEEE, 2020, pp. 1–6. 9, 133, 209

[22] G. Koutitas and P. Demestichas, "Challenges for energy efficiency in local and regional data centers," *Journal of Green Engineering*, vol. 1, no. 1, pp. 1–32, 2010. 16

[23] S. Dekleva, J. P. Shim, U. Varshney, and G. Knoerzer, "Evolution and emerging issues in mobile wireless networks," *Communications of the ACM*, vol. 50, no. 6, pp. 38–43, 2007. 16

[24] I. Cerutti, L. Valcarenghi, and P. Castoldi, "Designing power-efficient WDM ring networks," in *International Conference on Networks for Grid Applications*. Springer, 2009, pp. 101–108. 16

[25] W. Vereecken, L. Deboosere, P. Simoens, B. Vermeulen, D. Colle, C. Develder, M. Pickavet, B. Dhoedt, and P. Demeester, "Energy efficiency in thin client solutions," in *International Conference on Networks for Grid Applications*. Springer, 2009, pp.

109–116. 16, 17

[26] P. S. R. Henrique and R. Prasad, *6G The Road to the Future Wireless Technologies 2030*. River Publishers, 2021. 17, 19

[27] D. Robalo and F. J. Velez, “Economic trade-off in the optimization of carrier aggregation with enhanced multi-band scheduling in LTE-Advanced scenarios,” *EURASIP Journal on Wireless Communications and Networking*, vol. 2015, no. 1, pp. 1–19, 2015. 18, 85, 101, 102, 104, 164

[28] K. Flynn, “A global partnership,” *Release 15*, 2018. 18, 26

[29] A. A. Esswie and K. I. Pedersen, “Opportunistic spatial preemptive scheduling for URLLC and eMBB coexistence in multi-user 5G networks,” *Ieee Access*, vol. 6, pp. 38 451–38 463, 2018. 19

[30] W. Saad, M. Bennis, and M. Chen, “A vision of 6G wireless systems: Applications, trends, technologies, and open research problems,” *IEEE network*, vol. 34, no. 3, pp. 134–142, 2019. 19

[31] Y. Luo, L. Pu, G. Wang, and Y. Zhao, “RF energy harvesting wireless communications: RF environment, device hardware and practical issues,” *Sensors*, vol. 19, no. 13, p. 3010, 2019. 19

[32] S. Elmeadawy and R. M. Shubair, “Enabling technologies for 6G future wireless communications: Opportunities and challenges,” *arXiv preprint arXiv:2002.06068*, 2020. 19, 33

[33] P. K. Agyapong, M. Iwamura, D. Staehle, W. Kiess, and A. Benjebbour, “Design considerations for a 5G network architecture,” *IEEE Communications Magazine*, vol. 52, no. 11, pp. 65–75, 2014. 20

[34] J. Hoydis, M. Kobayashi, and M. Debbah, “Green small-cell networks,” *IEEE Vehicular Technology Magazine*, vol. 6, no. 1, pp. 37–43, 2011. 21

[35] J. M. Peha, “Spectrum management policy options,” *IEEE Communications Surveys*, vol. 1, no. 1, pp. 2–8, 1998. 22

[36] B. Hassan, S. Baig, and M. Asif, “Key Technologies for Ultra-Reliable and Low-Latency Communication in 6G,” *IEEE Communications Standards Magazine*, vol. 5, no. 2, pp. 106–113, 2021. 22

[37] M. Matinmikko-Blue, S. Yrjölä, and P. Ahokangas, “Spectrum management in the 6G era: The role of regulation and spectrum sharing,” in *2020 2nd 6G Wireless Summit (6G SUMMIT)*. IEEE, 2020, pp. 1–5. 22

[38] P. U. Adamu and M. López-Benítez, “Performance Evaluation of Carrier Aggregation as a Diversity Technique in mmWave Bands,” in *2021 IEEE 93rd Vehicular Technology Conference (VTC2021-Spring)*. IEEE, 2021, pp. 1–5. 23

[39] J. M. Romero-Jerez, F. J. Lopez-Martinez, J. F. Paris, and A. Goldsmith, “The fluctuating two-ray fading model for mmWave communications,” in *2016 IEEE Globecom Workshops (GC Wkshps)*. IEEE, 2016, pp. 1–6. 23

[40] J. Zhang, W. Zeng, X. Li, Q. Sun, and K. P. Peppas, "New results on the fluctuating two-ray model with arbitrary fading parameters and its applications," *IEEE transactions on vehicular technology*, vol. 67, no. 3, pp. 2766–2770, 2017. 23

[41] Qualcomm. (2020) Global update on spectrum for 4G 5G. [Online]. Available: https://www.qualcomm.com/content/dam/qcomm-martech/dm-assets/documents/spectrum-for-4g-and-5g.pdf 25

[42] Y.-N. R. Li, M. Chen, J. Xu, L. Tian, and K. Huang, "Power saving techniques for 5G and beyond," *IEEE Access*, vol. 8, pp. 108 675–108 690, 2020. 25

[43] F. Zheng, W. Li, P. Yu, and L. Meng, "User Association Based Cooperative Energy-Saving Mechanism in Heterogeneous 5G Access Networks," in *2016 IEEE International Conference on Internet of Things (iThings) and IEEE Green Computing and Communications (GreenCom) and IEEE Cyber, Physical and Social Computing (CPSCom) and IEEE Smart Data (SmartData)*. IEEE, 2016, pp. 765–768. 25

[44] S. Cass, "Taking AI to the edge: Google's TPU now comes in a maker-friendly package," *IEEE Spectrum*, vol. 56, no. 5, pp. 16–17, 2019. 25

[45] P. Marshall, *Three-Tier Shared Spectrum, Shared Infrastructure, and a Path to 5G*. Cambridge University Press, 2017. 25

[46] T. Takiguchi, K. Kiyoshima, Y. Sagae, K. Yagyu, H. Atarashi, and S. Abeta, "Performance Evaluation of LTE-Advanced Heterogeneous Network Deployment Using Carrier Aggregation between Macro and Small Cells," *IEICE transactions on communications*, vol. 96, no. 6, pp. 1297–1305, 2013. 25

[47] U. Challita, L. Dong, and W. Saad, "Proactive resource management for LTE in unlicensed spectrum: A deep learning perspective," *IEEE transactions on wireless communications*, vol. 17, no. 7, pp. 4674–4689, 2018. 26

[48] W. Rouwet, "Open Radio Access Network (O-RAN) Systems Architecture and Design," in *Open Radio Access Network (O-RAN) Systems Architecture and Design*, W. Rouwet, Ed. Academic Press, 2022, pp. 237–263. [Online]. Available: https://www.sciencedirect.com/science/article/pii/B9780323919234000045 26, 27, 139

[49] Chung, Yao-Liang and Jang, Lih-Jong and Tsai, Zsehong, "An efficient downlink packet scheduling algorithm in LTE-advanced systems with carrier aggregation," in *2011 IEEE Consumer Communications and Networking Conference (CCNC)*. IEEE, 2011, pp. 632–636. 26

[50] L. Chen, W. Chen, X. Zhang, and D. Yang, "Analysis and simulation for spectrum aggregation in LTE-advanced system," in *2009 IEEE 70th Vehicular Technology Conference Fall*. IEEE, 2009, pp. 1–6. 27

[51] D. P. Sharma and S. K. Gautam, "Distributed and prioritised scheduling to implement carrier aggregation in LTE advanced systems," in *2014 Fourth International Conference on Advanced Computing & Communication Technologies*. IEEE, 2014, pp. 390–393. 27

[52] J. An, K. Yang, J. Wu, N. Ye, S. Guo, and Z. Liao, "Achieving sustainable ultra-dense heterogeneous networks for 5G," *IEEE Communications Magazine*, vol. 55, no. 12, pp. 84–90, 2017. 28

[53] K. Sharma, "Comparison of energy efficiency between macro and micro cells using energy saving schemes." *Journal of the Institute of Engineering*, 2017. 29

[54] O. University. (2021) 6G Flagship. [Online]. Available: www.oulu.fi/6gflagship/ 35, 44

[55] "Network slicing explained," Nov 2020. [Online]. Available: https://www.nokia.com/about-us/newsroom/articles/network-slicing-explained/ 36

[56] N. Alliance, "Description of network slicing concept," *NGMN 5G P*, vol. 1, no. 1, 2016. 36, 42

[57] N. ETSI, "Network functions virtualisation (NFV); terminology for main concepts in NFV," *Group Specification, Dec*, 2014. 36, 38, 40

[58] C. Lanting and A. Rodriguez-Ascaso. (2021) ETSI: Understanding ICTStandardization: Principles and Practice. [Online]. Available: https://www.etsi.org/images/files/Education/UnderstandingICTStandardizationLoResWeb20190524.pdf 37

[59] X. Foukas, G. Patounas, A. Elmokashfi, and M. K. Marina, "Network Slicing in 5G: Survey and Challenges," *IEEE Communications Magazine*, vol. 55, no. 5, pp. 94–100, 2017. 38

[60] S. Redana, Ö. Bulakci, A. Zafeiropoulos, A. Gavras, A. Tzanakaki, A. Albanese, A. Kousaridas, A. Weit, B. Sayadi, B. T. Jou *et al.*, "5G PPP architecture working group: View on 5G architecture," 2019. 38

[61] A. Devlic, A. Hamidian, D. Liang, M. Eriksson, A. Consoli, and J. Lundstedt, "NESMO: Network slicing management and orchestration framework," in *2017 IEEE International Conference on Communications Workshops (ICC Workshops)*. IEEE, 2017, pp. 1202–1208. 38

[62] P. Subedi, A. Alsadoon, P. Prasad, S. Rehman, N. Giweli, M. Imran, and S. Arif, "Network slicing: a next generation 5G perspective," *EURASIP Journal on Wireless Communications and Networking*, vol. 2021, no. 1, pp. 1–26, 2021. 38

[63] N. Abdelkafi, R. Bolla, C. J. Lanting, A. Rodriguez-Ascaso, M. Thuns, and M. Wetterwald, "UNDERSTANDING ICT STANDARDIZATION: PRINCIPLES AND PRACTICE," 2019. 39

[64] GSMA. (2021) E2E Network Slicing Architecture Version 1.0. [Online]. Available: https://www.gsma.com/newsroom/wp-content/uploads//NG.127-v1.0-2.pdf 39

[65] P. Rost, C. Mannweiler, D. S. Michalopoulos, C. Sartori, V. Sciancalepore, N. Sastry, O. Holland, S. Tayade, B. Han, D. Bega *et al.*, "Network slicing to enable scalability and flexibility in 5G mobile networks," *IEEE Communications Magazine*, vol. 55, no. 5, pp. 72–79, 2017. 39

[66] X. De Foy and A. Rahman, "Network slicing-3GPP use case," *Working Draft, IETF*

*Secretariat, Internet-Draft draft-defoy-netslices-3gpp-network-slicing-02*, 2017. 39

[67] K. Flynn, "A global partnership," Mar 2020. [Online]. Available: https://www.3gpp.org/release-16 39, 47

[68] 3GPP, "A global partnership," Dec 2020. [Online]. Available: https://www.3gpp.org/release-17 39

[69] C.-Y. Chang and N. Nikaein, "Closing in on 5G control apps: enabling multiservice programmability in a disaggregated radio access network," *IEEE vehicular technology magazine*, vol. 13, no. 4, pp. 80–93, 2018. 40

[70] GSMA. (2018) Use Case Requirements. [Online]. Available: https://www.gsma.com/futurenetworks/resources/network-slicing-use-cases-requirements-2/. 40

[71] S. Wijethilaka and M. Liyanage, "Survey on network slicing for Internet of Things realization in 5G networks," *IEEE Communications Surveys & Tutorials*, vol. 23, no. 2, pp. 957–994, 2021. 40, 41

[72] ITU-T. (2019) Progress of 5G studies in ITU-T: overview of SG13 standardization activities . [Online]. Available: https://www.itu.int/en/ITU-T/Workshops-and-Seminars/20180604/Documents/Session1.pdf 40, 54

[73] "Focus Group on Machine Learning for Future Networks including 5G." [Online]. Available: https://www.itu.int/en/ITU-T/focusgroups/ml5g/Pages/default.aspx 41

[74] ITU-T, "Architectural framework for machine learning in future networks including IMT-2020 ," Jun 2019. [Online]. Available: https://www.itu.int/rec/T-REC-Y.3172/en 41

[75] ITU, "Machine learning marketplace integration in future networks including IMT-2020," Oct 2020. [Online]. Available: https://www.itu.int/rec/T-REC-Y.3176-202009-P 41

[76] ONF. (2019) Transport API (TAPI) 2.0 Overview Version 0.0 August. [Online]. Available: https://opennetworking.org/wp-content/uploads/2017/08/TAPI-2-WP_DRAFT.pdf 41

[77] L. Deng, H. Deng, and A. Mayer. (2021) Harmonizing Open Source and Standards: A Case for 5G Slicing. [Online]. Available: https://www.onap.org/wp-content/uploads/sites/20/2020/03/\ONAP_HarmonizingOpenSourceStandards_031520.pdf 41, 45

[78] L. Xiao, X. Wan, X. Lu, Y. Zhang, and D. Wu, "IoT security techniques based on machine learning: How do IoT devices use AI to enhance security?" *IEEE Signal Processing Magazine*, vol. 35, no. 5, pp. 41–49, 2018. 41

[79] F. Hussain, S. A. Hassan, R. Hussain, and E. Hossain, "Machine learning for resource management in cellular and IoT networks: Potentials, current solutions, and open challenges," *IEEE Communications Surveys & Tutorials*, vol. 22, no. 2, pp. 1251–1275, 2020. 43

[80] A. Thantharate, R. Paropkari, V. Walunj, and C. Beard, "DeepSlice: A deep learning approach towards an efficient and reliable network slicing in 5G networks," in

*2019 IEEE 10th Annual Ubiquitous Computing, Electronics & Mobile Communication Conference (UEMCON)*. IEEE, 2019, pp. 0762–0767. 43

[81] J. Mei, X. Wang, and K. Zheng, "Intelligent network slicing for V2X services toward 5G," *IEEE Network*, vol. 33, no. 6, pp. 196–204, 2019. 43

[82] L. Zhao and L. Li, "Reinforcement learning for resource mapping in 5G network slicing," in *2020 5th International Conference on Computer and Communication Systems (ICCCS)*. IEEE, 2020, pp. 869–873. 43

[83] S. De Bast, R. Torrea-Duran, A. Chiumento, and H. Pollin, Sofie and Gacanin, "Deep reinforcement learning for dynamic network slicing in IEEE 802.11 networks," in *IEEE INFOCOM 2019-IEEE Conference on Computer Communications Workshops (INFOCOM WORKSHOPS)*. IEEE, 2019, pp. 264–269. 43

[84] M. Jiang, M. Condoluci, and T. Mahmoodi, "Network slicing management & prioritization in 5G mobile systems," in *European Wireless 2016; 22th European Wireless Conference*. VDE, 2016, pp. 1–6. 43

[85] J. Haas, T. Pierce, and E. Schutter, "Data center design guide," *Program overview, Report by The Green Grid*, 2009. 44

[86] T. . I. Association. (2021) 5GPPP: European Vision for the 6G NetworkEcosystem. [Online]. Available: 5g-ppp.eu/european-vision-for-the-6g-network-ecosystem/.DOI:10.5281/zenodo.5007671 44

[87] T. Spanjaard. (2020) Who Will Standardize 6G? Smartinsights. [Online]. Available: Smartinsightswww.smartinsights.net/single-post/who-will-standardize-6g 44

[88] E. R. S. P. Group. (2021) RSPG Additional spectrum needs and guidance onthe fast rollout of future wireless broadband networks. [Online]. Available: //rspg-spectrum.eu/wp-content/uploads/2021/02/RSPG21-008finalDraftRSPGOpin 44

[89] M. Lennighan. (2021) Vodafone Germany Launches a Network Offensive. [Online]. Available: //Telecoms.com/,26May2021,telecoms.com/509917/vodafone-germany-launches-a-network-offensive/ 44

[90] A. Hernandez. (2021) Techaeris: "South Korea Eyes 2028 to LAUNCH 6G,Samsung Leads the Charge. [Online]. Available: techaeris.com/2021/06/23/south-korea-eyes-2028-to-launch-6g-samsung-leads-the-charge/ 44

[91] G. Kalfas, M. Agus, A. Pagano, L. A. Neto, A. Mesodiakaki, C. Vagionas, J. Vardakas, E. Datsika, C. Verikoukis, and N. Pleros, "Converged analog fiber-wireless point-to-multipoint architecture for eCPRI 5G fronthaul networks," in *2019 IEEE Global Communications Conference (GLOBECOM)*. IEEE, 2019, pp. 1–6. 47, 55

[92] J. Mocerino, "Paper - 5G backhaul/fronthaul opportunities and challenges - NCTA technical papers, url=https://www.nctatechnicalpapers.com/Paper/2019/2019-5g-backhaul-fronthaul-opportunities-and-challenges," Oct 2019. 47

[93] J. Liu, M. Sheng, L. Liu, and J. Li, "Network densification in 5G: From the short-range

communications perspective," *IEEE Communications Magazine*, vol. 55, no. 12, pp. 96–102, 2017. 47

[94] M. A. Habibi, M. Nasimi, B. Han, and H. D. Schotten, "A comprehensive survey of RAN architectures toward 5G mobile communication system," *IEEE Access*, vol. 7, pp. 70 371–70 421, 2019. 47

[95] L. M. P. Larsen, A. Checko, and H. L. Christiansen, "A Survey of the Functional Splits Proposed for 5G Mobile Crosshaul Networks," *IEEE Communications Surveys Tutorials*, vol. 21, no. 1, pp. 146–172, Firstquarter 2019. 47, 54, 66, 68, 81

[96] O-RAN Alliance. (2021) O-RAN FH Lib Introduction. [Online]. Available: https://docs.o-ran-sc.org/projects/o-ran-sc-o-du-phy/en/latest/Introduction_fh.html 49, 50, 51

[97] O-RAN Working Group 4. (2022) O-RAN Fronthaul Control, User and Synchronization Plane Specification 8.01. [Online]. Available: https://orandownloadsweb.azurewebsites.net/specifications 49, 50, 51

[98] M. Polese, L. Bonati, S. D'Oro, S. Basagni, and T. Melodia, "Understanding o-ran: Architecture, interfaces, algorithms, security, and research challenges," *arXiv preprint arXiv:2202.01032*, 2022. 50, 51, 66

[99] O.-R. F. W. Group *et al.*, "Control, user and synchronization plane specification," *O-RAN, Specification*, 2019. 50

[100] D. H. Morais, *5G and Beyond Wireless Transport Technologies*. Springer, 2021. 51, 52

[101] N. Verma and P. K. Mishra, "Traffic Scheduler for BBU Resource Allocation in 5G CRAN," in *2022 8th International Conference on Advanced Computing and Communication Systems (ICACCS)*, vol. 1. IEEE, 2022, pp. 719–724. 51

[102] R. S. Shetty, *5G Mobile Core Network*. Springer, 2021. 51

[103] E. Dahlman, G. Mildh, S. Parkvall, P. Persson, G. Wikström, and H. Murai, "5G evolution and beyond," *IEICE Transactions on Communications*, vol. 104, no. 9, pp. 984–991, 2021. 51

[104] A. De la Oliva, J. A. Hernandez, D. Larrabeiti, and A. Azcorra, "An overview of the CPRI specification and its application to C-RAN-based LTE scenarios," *IEEE Communications Magazine*, vol. 54, no. 2, pp. 152–159, 2016. 51

[105] G. Kún, P. J. Varga, T. Wührl, D. Wührl, S. Gyányi, L. Nádai, and R. Kovács, "" Opened" or" Closed" RAN in 5G," in *2022 IEEE 20th Jubilee World Symposium on Applied Machine Intelligence and Informatics (SAMI)*. IEEE, 2022, pp. 000 347–000 352. 51

[106] E. Sarikaya and E. Onur, "Placement of 5G RAN Slices in Multi-tier O-RAN 5G Networks with Flexible Functional Splits," in *2021 17th International Conference on Network and Service Management (CNSM)*. IEEE, 2021, pp. 274–282. 51

[107] N. Agarwal, N. Kundap, P. Joglekar, and B. S. Chaudhari, "Photonic-Based Front-Mid-

Backhaul Access for 5G," in *Sustainable Communication Networks and Application*. Springer, 2022, pp. 347–358. 52

[108] H. U. Adoga and D. P. Pezaros, "Network Function Virtualization and Service Function Chaining Frameworks: A Comprehensive Review of Requirements, Objectives, Implementations, and Open Research Challenges," *Future Internet*, vol. 14, no. 2, p. 59, 2022. 52

[109] I. Da Silva, S. E. El Ayoubi, O. M. Boldi, Ö. Bulakci, P. Spapis, M. Schellmann, J. F. Monserrat, T. Rosowski, G. Zimmermann, D. Telekom *et al.*, "5g ran architecture and functional design," *METIS II white paper*, 2016. 52

[110] A. Garcia-Saavedra, X. Costa-Perez, D. J. Leith, and G. Iosifidis, "Fluidran: Optimized vran/mec orchestration," in *IEEE INFOCOM 2018-IEEE Conference on Computer Communications*. IEEE, 2018, pp. 2366–2374. 52

[111] C. F. Lanzani, G. Kardaras, and D. Boppana, "Remote Radio Heads and the evolution towards 4G networks," *ALTERA radiocomp white paper*, pp. 1–5, 2009. 52

[112] S. H. Haji, S. Zeebaree, R. H. Saeed, S. Y. Ameen, H. M. Shukur, N. Omar, M. A. Sadeeq, Z. S. Ageed, I. M. Ibrahim, and H. M. Yasin, "Comparison of software defined networking with traditional networking," *Asian Journal of Research in Computer Science*, pp. 1–18, 2021. 52

[113] B. M. Moura, G. B. Schneider, A. C. Yamin, H. Santos, R. H. Reiser, and B. Bedregal, "Interval-valued fuzzy logic approach for overloaded hosts in consolidation of virtual machines in cloud computing," *Fuzzy Sets and Systems*, 2021. 52

[114] L. Gavrilovska, V. Rakovic, and D. Denkovski, "From Cloud RAN to open RAN," *Wireless Personal Communications*, vol. 113, no. 3, pp. 1523–1539, 2020. 52

[115] D. Wypiór, M. Klinkowski, and I. Michalski, "Open RAN—Radio Access Network Evolution, Benefits and Market Trends," *Applied Sciences*, vol. 12, no. 1, p. 408, 2022. 53

[116] R. T. Rodoshi, T. Kim, and W. Choi, "Resource Management in Cloud Radio Access Network: Conventional and New Approaches," *Sensors*, vol. 20, no. 9, 2020. [Online]. Available: https://www.mdpi.com/1424-8220/20/9/2708 53

[117] Y. Yuan, "From C-RAN to O-RAN," *China Mobile Research Institute*, 2018. 53

[118] A. L. Ericsson AB, Huawei Technologies Co Ltd NEC Corporation and Nokia. (2015) Common Public Radio Interface (CPRI); Interface Specification. [Online]. Available: http://www.cpri.info/downloads/CPRI_v_7_0_2015-10-09.pdf 54

[119] C. P. R. Interface, "Interface specification," *CPRI Specification*, vol. 7, p. 0, 2015. 54

[120] P. Iovanna, F. Cavaliere, S. Stracca, L. Giorgi, and F. Ubaldi, "5G Xhaul and Service Convergence: Transmission, Switching and Automation Enabling Technologies, volume = 38," *JOURNAL OF LIGHTWAVE TECHNOLOGY*, 2020. [Online]. Available: https://www.ieee.org/publications/rights/index.html 54

[121] N. C. Ericsson AB, Huawei Technologies Co. Ltd and Nokia. (2019) Common Public

Radio Interface: eCPRI Interface Specification, eCPRI Specification V2.0 . [Online]. Available: http://www.cpri.info/downloads/eCPRI 54, 68, 69

[122] 3GPP. (2016) Study on New Radio Access Technology. [Online]. Available: https://www.3gpp.org/ftp/Specs/archive/38_series/38.801/ 54, 55, 56

[123] M. Waqar and A. Kim, "Performance Improvement of Ethernet-Based Fronthaul Bridged Networks in 5G Cloud Radio Access Networks," *Applied Sciences*, vol. 9, no. 14, 2019. [Online]. Available: https://www.mdpi.com/2076-3417/9/14/2823 54

[124] S. T. Le, S. Wesemann, R. Dischler, and S. Venkatesan, "A Joint Wireless-Optical Front-haul Solution for Multi-user Massive MIMO 5G RAN," in *2020 European Conference on Optical Communications (ECOC)*, 2020, pp. 1–4. 54

[125] X. Costa-Perez, J. Swetina, T. Guo, R. Mahindra, and S. Rangarajan, "Radio access network virtualization for future mobile carrier networks," *IEEE Communications Magazine*, vol. 51, no. 7, pp. 27–35, July 2013. 55

[126] M. Peng, Y. Li, J. Jiang, J. Li, and C. Wang, "Heterogeneous Cloud Radio Access Networks: A New Perspective for Enhancing Spectral and Energy Efficiencies," *IEEE Wireless Communications*, vol. 21, 10 2014. 55, 74

[127] S.-Y. Lien, S.-C. Hung, K.-C. Chen, and Y.-C. Liang, "Ultra-low-latency ubiquitous connections in heterogeneous cloud radio access networks," *IEEE Wireless Communications*, vol. 22, no. 3, pp. 22–31, June 2015. 55, 74

[128] I. NTT DOCOMO, "3GPP TSG RAN3,"Study on New Radio Access Technology: Radio Access Architecture and Interfaces," R3-161687," Draft TR 38.801, Aug, Tech. Rep., 2016. 55, 154

[129] S. C. Virtualization, "Functional splits and use cases," in *Small Cell Forum release*, vol. 6, 2016. 55, 61, 66, 67, 68, 154

[130] Moniem-Tech. (2021) Functional Split Options for 5G Networks. [Online]. Available: https://moniem-tech.com/2021/04/05/functional-split-options-for-5g-networks/ 55, 56, 154

[131] S. T. Le, T. Drenski, A. Hills, M. King, K. Kim, Y. Matsui, and T. Sizer, "400Gb/s real-time transmission supporting CPRI and eCPRI traffic for hybrid LTE-5G networks," in *Optical Fiber Communication Conference*. Optical Society of America, 2020, pp. Th4C–4. 55, 154

[132] Huber+Suhner. 5G Fundamentals Functional Split Overview. [Online]. Available: https://www.hubersuhner.com/en/documents-repository/technologies/pdf/fiberoptics-documents/5g-fundamentals-functional-split-overview 55

[133] S. Sirotkin, *5G Radio Access Network Architecture: The Dark Side of 5G*. Wiley Online Library, 2021. 57, 80

[134] telecominfraproject.com. Telecom Infra Project 2016 Summit. [Online]. Available: https://telecominfraproject.com/events/tip-summit-2016/ 57

[135] rcrwireless.com. Open RAN 101–A timeline of Open RAN journey

in the industry: Why, what, when, how? [Online]. Available: https://rcrwireless.com/20200715/open_ran/open-ran-101-a-timeline-of-open-ran-journey-in-the-industry-reader-forum 57

[136] O.-R. S. Community. (2019) O-RAN Software Community. [Online]. Available: https://o-ran-sc.org/ 57, 74, 75, 76, 78

[137] J. Wang, H. Roy, and C. Kelly, "OpenRAN: the next generation of radio access networks," *Telecom Infra Project*, 2019. 57

[138] A. Sharma. (2021) Exploring functional splits in 5G RAN. [Online]. Available: https://www.rcrwireless.com/20210317/opinion/readerforum/exploring-functional-splits-in-5g-ran-tradeoffs-and-use-cases-reader-forum 58

[139] L. Hansen, "Design and deployment considerations for Cloud-RAN based mobile networks," *Technical University of Denmark*, vol. 49, pp. 203–230, 2017. 58, 60

[140] D. Chitimalla, K. Kondepu, L. Valcarenghi, M. Tornatore, and B. Mukherjee, "5G fronthaul–latency and jitter studies of CPRI over Ethernet," *Journal of Optical Communications and Networking*, vol. 9, no. 2, pp. 172–182, 2017. 59, 60, 82

[141] J. Duan, X. Lagrange, and F. Guilloud, "Performance analysis of several functional splits in C-RAN," in *2016 IEEE 83rd Vehicular Technology Conference (VTC Spring)*. IEEE, 2016, pp. 1–5. 59, 60, 82

[142] "gNodeB - IS-wireless, url=https://www.is-wireless.com/networks/software/gn-odeb/," Dec 2021. 59, 60, 63, 66

[143] "IS-Wireless 5G-MadetTogether," Jan 2022. [Online]. Available: https://www.is-wireless.com/ 59, 82

[144] N. P. Anthapadmanabhan, A. Walid, and T. Pfeiffer, "Mobile fronthaul over latency-optimized time division multiplexed passive optical networks," in *2015 IEEE International Conference on Communication Workshop (ICCW)*. IEEE, 2015, pp. 62–67. 60

[145] D. Harutyunyan and R. Riggio, "Flex5G: Flexible functional split in 5G networks," *IEEE Transactions on Network and Service Management*, vol. 15, no. 3, pp. 961–975, 2018. 60, 61, 63

[146] N. Kazemifard and V. Shah-Mansouri, "Minimum delay function placement and resource allocation for Open RAN (O-RAN) 5G networks," *Computer Networks*, vol. 188, p. 107809, 2021. 60

[147] M. Makhanbet, X. Zhang, H. Gao, and H. A. Suraweera, "An overview of cloud RAN: Architecture, issues and future directions," in *International Conference on Emerging Trends in Electrical, Electronic and Communications Engineering*. Springer, 2016, pp. 44–60. 60

[148] C. Ranaweera, E. Wong, A. Nirmalathas, C. Jayasundara, and C. Lim, "5G C-RAN architecture: A comparison of multiple optical fronthaul networks," in *2017 International conference on optical network design and modeling (ONDM)*. IEEE, 2017,

pp. 1–6. 60

[149] I. A. Alimi, A. L. Teixeira, and P. P. Monteiro, "Toward an efficient C-RAN optical fronthaul for the future networks: A tutorial on technologies, requirements, challenges, and solutions," *IEEE Communications Surveys and Tutorials*, vol. 20, no. 1, pp. 708–769, 2017. 60

[150] P. Arnold, N. Bayer, J. Belschner, and G. Zimmermann, "5G radio access network architecture based on flexible functional control/user plane splits," in *2017 European Conference on Networks and Communications (EuCNC)*. IEEE, 2017, pp. 1–5. 60, 66

[151] M. A. Imran, S. A. R. Zaidi, and M. Z. Shakir, *Fronthaul and Backhaul Networks for 5G and Beyond*. IET, 2017. 60, 64, 65

[152] A. Garcia-Saavedra, J. X. Salvat, X. Li, and X. Costa-Perez, "WizHaul: On the centralization degree of cloud RAN next generation fronthaul," *IEEE Transactions on Mobile Computing*, vol. 17, no. 10, pp. 2452–2466, 2018. 60

[153] P. J. Urban, G. C. Amaral, G. Żegliński, E. Weinert-Raczka, and J. P. von der Weid, "A tutorial on fiber monitoring for applications in analogue mobile fronthaul," *IEEE Communications Surveys & Tutorials*, vol. 20, no. 4, pp. 2742–2757, 2018. 60

[154] Y. Tsukamoto, H. Hirayama, S. I. Moon, S. Nanba, and H. Shinbo, "Feedback Control for Adaptive Function Placement in Uncertain Traffic Changes on an Advanced 5G System," in *2021 IEEE 18th Annual Consumer Communications & Networking Conference (CCNC)*. IEEE, 2021, pp. 1–6. 60

[155] H. Mei and L. Peng, "Flexible functional split for cost-efficient C-RAN," *Computer Communications*, vol. 161, pp. 368–374, 2020. 60

[156] E. Datsika, J. Vardakas, K. Ramantas, P.-V. Mekikis, I. T. Monroy, L. A. Neto, and C. Verikoukis, "SDN-enabled resource management for converged Fi-Wi 5G Fronthaul," *IEEE Journal on Selected Areas in Communications*, 2021. 60

[157] F. Z. Morais, C. A. da Costa, A. M. Alberti, C. B. Both, and R. da Rosa Righi, "When SDN meets C-RAN: A survey exploring multi-point coordination, interference, and performance," *Journal of Network and Computer Applications*, vol. 162, p. 102655, 2020. 59, 67, 68

[158] 3GPP. (2017) Evolved Universal Terrestrial Radio Access (E-UTRA); Physical channels and modulation (3GPP TS 36.211 version 14.4.0 Release 14) . [Online]. Available: https://www.etsi.org/deliver/etsi_ts/136200_136299/136211/14.04.00_60/ts_136211v140400p.pdf 60

[159] B. khan, A. Wakeel, J. Majid, and M. M. Shahbaz, "Flexible Hardware Implementation of Universal Filtered Multi-Carrier Systems," in *2019 2nd International Conference on Communication, Computing and Digital systems (C-CODE)*, 2019, pp. 1–6. 60

[160] M. A. A. d. G. A. P. N. B. M. Anna Tzanakaki. (2018) System architecture and preliminary evaluations . [Online]. Available: https://www.5g-picture-project.eu/

download/5g-picture_D2.2.pdf 60

[161] C.-Y. Chang, N. Nikaein, R. Knopp, T. Spyropoulos, and S. S. Kumar, “FlexCRAN: A flexible functional split framework over ethernet fronthaul in Cloud-RAN,” in *2017 IEEE International Conference on Communications (ICC)*, 2017, pp. 1–7. 60, 63

[162] M. Sauter and G. From, “From GSM to LTE,” 2011. 60

[163] R. Al-obaidi, A. Checko, H. Holm, and H. Christiansen, “Optimizing Cloud-RAN deployments in real-life scenarios using Microwave Radio,” in *2015 European Conference on Networks and Communications (EuCNC)*. IEEE, 2015, pp. 159–163. 61

[164] A. Pizzinat, P. Chanclou, F. Saliou, and T. Diallo, “Things you should know about fronthaul,” *Journal of Lightwave Technology*, vol. 33, no. 5, pp. 1077–1083, 2015. 61

[165] A. Maeder, M. Lalam, A. De Domenico, E. Pateromichelakis, D. Wübben, J. Bartelt, R. Fritzsche, and P. Rost, “Towards a flexible functional split for cloud-RAN networks,” in *2014 European Conference on Networks and Communications (EuCNC)*. IEEE, 2014, pp. 1–5. 61, 65

[166] R. I. Rony, E. Lopez-Aguilera, and E. Garcia-Villegas, “Cost Analysis of 5G Fronthaul Networks Through Functional Splits at the PHY Layer in a Capacity and Cost Limited Scenario,” *IEEE Access*, vol. 9, pp. 8733–8750, 2021. 63

[167] ——, “Optimization of 5G fronthaul based on functional splitting at PHY layer,” in *2018 IEEE Global Communications Conference (GLOBECOM)*. IEEE, 2018, pp. 1–7. 63

[168] F. Kaltenberger, A. P. Silva, A. Gosain, L. Wang, and T.-T. Nguyen, “OpenAirInterface: Democratizing innovation in the 5G Era,” *Computer Networks*, vol. 176, p. 107284, 2020. 63

[169] J. Domingues, F. D. L. Coutinho, P. M. C. Marques, S. S. Pereira, H. S. Silva, and A. S. R. Oliveira, “MPSoC Fast Prototyping of a Reconfigurable DU Downlink Transmission Chain for 5G New Radio,” in *2020 International Workshop on Rapid System Prototyping (RSP)*, 2020, pp. 1–7. 63

[170] A. M. Alba, J. H. G. Velásquez, and W. Kellerer, “An adaptive functional split in 5G networks,” in *IEEE INFOCOM 2019 - IEEE Conference on Computer Communications Workshops (INFOCOM WKSHPS)*, 2019, pp. 410–416. 63

[171] A. Martinez Alba, J. H. Gomez Velasquez, and W. Kellerer, “Traffic Characterization of the MAC-PHY Split in 5G Networks,” in *2019 IEEE Global Communications Conference (GLOBECOM)*, 2019, pp. 1–6. 63

[172] F. D. L. Coutinho, J. D. Domingues, P. M. C. Marques, S. S. Pereira, H. S. Silva, and A. S. R. Oliveira, “Towards the Flexible and Efficient Implementation of the 5G-NR RAN Physical Layer,” in *2021 IEEE Radio and Wireless Symposium (RWS)*, 2021, pp. 130–132. 63

[173] J. K. Chaudhary, A. Kumar, J. Bartelt, and G. Fettweis, “C-RAN Employing xRAN Functional Split: Complexity Analysis for 5G NR Remote Radio Unit,” in *2019 European Conference on Networks and Communications (EuCNC)*, 2019, pp. 580–585.

63, 65

[174] A. M. Alba, S. Janardhanan, and W. Kellerer, "Enabling dynamically centralized RAN architectures in 5G and beyond," *IEEE Transactions on Network and Service Management*, 2021. 63

[175] F. Debbabi, R. Jmal, and L. Chaari Fourati, "5G network slicing: Fundamental concepts, architectures, algorithmics, projects practices, and open issues," *Concurrency and Computation: Practice and Experience*, p. e6352, 2021. 63

[176] S. S. Jaffer, A. Hussain, M. A. Qureshi, J. Mirza, and K. K. Qureshi, "A low cost PON-FSO based fronthaul solution for 5G CRAN architecture," *Optical Fiber Technology*, vol. 63, p. 102500, 2021. 63

[177] Y. Alfadhli, Y.-W. Chen, S. Liu, S. Shen, S. Yao, D. Guidotti, S. Mitani, and G.-K. Chang, "Latency performance analysis of low layers function split for URLLC applications in 5G networks," *Computer Networks*, vol. 162, p. 106865, 2019. 63

[178] O. Dizdar, Y. Mao, W. Han, and B. Clerckx, "Rate-splitting multiple access: A new frontier for the PHY layer of 6G," in *2020 IEEE 92nd Vehicular Technology Conference (VTC2020-Fall)*. IEEE, 2020, pp. 1–7. 63

[179] G. Cisek and T. P. Zieliński, "Validation of cloud-radio access network control unit with intra-PHY architecture: Hardware-in-the-loop framework based on frequency-domain channel models," *Transactions on Emerging Telecommunications Technologies*, vol. 32, no. 1, p. e4134, 2021. 63

[180] G. S. 38.321. (2017) NR; Medium Access Control (MAC) protocol specification. [Online]. Available: https://portal.3gpp.org/desktopmodules/Specifications/SpecificationDetails.aspx?specificationId=3194 61, 64

[181] E. Mataj, "Network slicing and QoS in 5G systems and their impact on the MAC layer," Ph.D. dissertation, Politecnico di Torino, 2020. 61

[182] N. Alliance, "5G End-to-End Architecture Framework v2. 0," NGMN Alliance, Tech. Rep., 2018.[Online]. Available: https://www. ngmn. org ..., Tech. Rep., 2018. 64

[183] Devopedia. (2021) 5G NR MAC." Version 3 . [Online]. Available: https://devopedia.org/5g-nr-mac 64

[184] B. Khan and F. J. Velez, "Multicarrier Waveform Candidates for Beyond 5G," in *2020 12th International Symposium on Communication Systems, Networks and Digital Signal Processing (CSNDSP)*, 2020, pp. 1–6. 64, 203

[185] A. Nanjundappa, S. Singh, and G. Jain, "Enhanced multi-RAT support for 5G," in *2018 15th IEEE Annual Consumer Communications Networking Conference (CCNC)*, 2018, pp. 1–2. 64

[186] R. Agrawal, A. Bedekar, T. Kolding, and V. Ram, "Cloud RAN challenges and solutions," *Annals of Telecommunications*, vol. 72, no. 7, pp. 387–400, 2017. 64

[187] N. Alliance, "Further study on critical C-RAN technologies," *Next Generation Mobile Networks*, 2015. 64

[188] P. wireless. (2020) 5G FUNCTIONAL SPLITS . [Online]. Available: https://www.parallelwireless.com/wp-content/uploads/5G-Functional-Splits-V3.pdf 64

[189] E. Datsika, J. Vardakas, G. Kalfas, C. Vagionas, A. Mesodiakaki, and C. Verikoukis, "End-to-End Delay Performance of Analog Fiber Wireless Architecture for 5G NR Fronthaul," in *2020 22nd International Conference on Transparent Optical Networks (ICTON)*, 2020, pp. 1–4. 64, 65

[190] G. Mountaser, M. L. Rosas, T. Mahmoodi, and M. Dohler, "On the Feasibility of MAC and PHY Split in Cloud RAN," in *2017 IEEE Wireless Communications and Networking Conference (WCNC)*, 2017, pp. 1–6. 64, 65

[191] G. T. R. WG3. (2016) Transport requirement for CU and DU functional splits options . 64

[192] S. cell Forum. (2021) S-RU and S-DU Test Support . [Online]. Available: https://www.smallcellforum.org/reports/s-ru-and-s-du-test-support/ 65

[193] D. Harutyunyan and R. Riggio, "Flex5G: Flexible Functional Split in 5G Networks," *IEEE Transactions on Network and Service Management*, vol. 15, no. 3, pp. 961–975, 2018. 65

[194] S. Matoussi, I. Fajjari, S. Costanzo, N. Aitsaadi, and R. Langar, "5G RAN: Functional Split Orchestration Optimization," *IEEE Journal on Selected Areas in Communications*, vol. 38, no. 7, pp. 1448–1463, 2020. 65

[195] "On the feasibility of MAC and PHY split in cloud RAN, author=Mountaser, Ghizlane and Rosas, Maria Lema and Mahmoodi, Toktam and Dohler, Mischa," in *2017 IEEE Wireless Communications and Networking Conference (WCNC)*. IEEE, 2017, pp. 1–6. 65

[196] L. Larsen, F. Slyne, G. Mountaser, M. Ruffini, and T. Mahmoodi, "Experimental Demonstration of RAN Functional Split over virtual PON Transport Network," *arXiv preprint arXiv:2104.04645*, 2021. 65

[197] S. Potharaju, F. Anderson, C. Carty, and I. Gandhi, "APPLICATION SPECIFIC 5G RAN SPLIT OPTIONS IN A SINGLE RADIO UNIT," 2021. 65

[198] Y. Ren, W. Yang, X. Zhou, H. Chen, and B. Liu, "A survey on TCP over mmWave," *Computer Communications*, 2021. 65

[199] G. Garcia-Aviles, M. Gramaglia, P. Serrano, F. Gringoli, S. Fuente-Pascual, and I. L. Pavon, "Experimenting with open source tools to deploy a multi-service and multi-slice mobile network," *Computer Communications*, vol. 150, pp. 1–12, 2020. 65

[200] A. M. Alba, J. H. G. Velásquez, and W. Kellerer, "Traffic characterization of the MAC-PHY split in 5G networks," in *2019 IEEE Global Communications Conference (GLOBECOM)*. IEEE, 2019, pp. 1–6. 65

[201] D. Harutyunyan, R. Riggio, S. Kuklinski, and T. Ahmed, "CU placement over a reconfigurable wireless fronthaul in 5G networks with functional splits," *International Journal of Network Management*, vol. 30, no. 1, p. 2086, 2020. 65

[202] P. C. Philip and M. Abdel-Hafez, “A Review on Ultra Reliable and Low Latency Communications (PHY and MAC Layer Perspectives),” 2020. 65

[203] Y. Xiao, J. Zhang, and Y. Ji, “Can Fine-Grained Functional Split Benefit to the Converged Optical-Wireless Access Networks in 5G and Beyond,” *IEEE Transactions on Network and Service Management*, vol. 17, no. 3, pp. 1774–1787, 2020. 65

[204] I. Koutsopoulos, “The Impact of Baseband Functional Splits on Resource Allocation in 5G Radio Access Networks.” 65

[205] G. S. Birring, P. Assimakopoulos, and N. J. Gomes, “An Ethernet-Based Fronthaul Implementation with MAC/PHY Split LTE Processing,” in *GLOBECOM 2017 - 2017 IEEE Global Communications Conference*, 2017, pp. 1–6. 65

[206] Techplayon. (2017) 5G NR gNB Logical Architecture and Its Functional Split Options. [Online]. Available: https://www.techplayon.com/5g-nr-gnb-logical-architecture-functional-split-options/ 65

[207] G. Mountaser, M. Condoluci, T. Mahmoodi, M. Dohler, and I. Mings, “Cloud-RAN in Support of URLLC,” in *2017 IEEE Globecom Workshops (GC Wkshps)*, 2017, pp. 1–6. 66

[208] B. Guo, C. Ye, H. Yu, Y. Sun, Y. Wang, Y. Yuan, X. Zhang, and H. Yang, “Implementation of C-RAN Architecture with CU/DU Split on a Flexible SDR Testbed,” in *2019 IEEE Wireless Communications and Networking Conference (WCNC)*, 2019, pp. 1–6. 66

[209] R. Kumar, A. Francini, S. Panwar, and S. Sharma, “Dynamic control of RLC buffer size for latency minimization in mobile RAN,” in *2018 IEEE Wireless Communications and Networking Conference (WCNC)*, 2018, pp. 1–6. 66

[210] N. Makris, C. Zarafetas, P. Basaras, T. Korakis, N. Nikaein, and L. Tassiulas, “Cloud-Based Convergence of Heterogeneous RANs in 5G Disaggregated Architectures,” in *2018 IEEE International Conference on Communications (ICC)*, 2018, pp. 1–6. 66

[211] F. Z. Morais, G. M. de Almeida, L. Pinto, K. V. Cardoso, L. M. Contreras, R. d. R. Righi, and C. B. Both, “PlaceRAN: Optimal Placement of Virtualized Network Functions in the Next-generation Radio Access Networks,” *arXiv preprint arXiv:2102.13192*, 2021. 66

[212] I. A. Alimi and P. P. Monteiro, “Functional Split Perspectives: A Disruptive Approach to RAN Performance Improvement,” *Wireless Personal Communications*, vol. 106, no. 1, pp. 205–218, 2019. 66

[213] J. Rao and S. Vrzic, “Packet Duplication for URLLC in 5G: Architectural Enhancements and Performance Analysis,” *IEEE Network*, vol. 32, no. 2, pp. 32–40, 2018. 66

[214] R. K. Saha, Y. Tsukamoto, S. Nanba, K. Nishimura, and K. Yamazaki, “Novel M-CORD Based Multi-Functional Split Enabled Virtualized Cloud RAN Testbed with Ideal Fronthaul,” in *2018 IEEE Globecom Workshops (GC Wkshps)*, 2018, pp. 1–7.

66

[215] P. Arnold, N. Bayer, J. Belschner, and G. Zimmermann, "5G radio access network architecture based on flexible functional control / user plane splits," in *2017 European Conference on Networks and Communications (EuCNC)*, 2017, pp. 1–5. 66

[216] P.-H. Kuo and A. Mourad, "Millimeter wave for 5G mobile fronthaul and backhaul," in *2017 European Conference on Networks and Communications (EuCNC)*, 2017, pp. 1–5. 66

[217] A. Martinez Alba and W. Kellerer, "A Dynamic Functional Split in 5G Radio Access Networks," in *2019 IEEE Global Communications Conference (GLOBECOM)*, 2019, pp. 1–6. 66

[218] B. H. Kim and D. Calin, "On the Split-TCP Performance over Real 4G LTE and 3G Wireless Networks," *IEEE Communications Magazine*, vol. 55, no. 4, pp. 124–131, 2017. 66

[219] H. Sato, H. Yukio, K. Nakura, and S. Kozaki, "Reducing Uplink Transmission Latency for Applying TDM-PON to Mobile Fronthaul," in *2018 European Conference on Optical Communication (ECOC)*, 2018, pp. 1–3. 66

[220] L. Wang and S. Zhou, "Flexible Functional Split and Power Control for Energy Harvesting Cloud Radio Access Networks," *IEEE Transactions on Wireless Communications*, vol. 19, no. 3, pp. 1535–1548, 2020. 66

[221] N. Mharsi, M. Hadji, D. Niyato, W. Diego, and R. Krishnaswamy, "Scalable and cost-efficient algorithms for baseband unit (BBU) function split placement," in *2018 IEEE Wireless Communications and Networking Conference (WCNC)*, 2018, pp. 1–6. 66

[222] L. M. Moreira Zorello, S. Troia, M. Quagliotti, and G. Maier, "Power-aware optimization of baseband-function placement in cloud radio access networks," in *2020 International Conference on Optical Network Design and Modeling (ONDM)*, 2020, pp. 1–6. 66

[223] Y. Yoshida, "Mobile Xhaul Evolution: Enabling Tools for a Flexible 5G Xhaul Network," in *2018 Optical Fiber Communications Conference and Exposition (OFC)*, 2018, pp. 1–85. 66

[224] P. Nuggehalli, "LTE-WLAN aggregation [Industry Perspectives]," *IEEE Wireless Communications*, vol. 23, no. 4, pp. 4–6, 2016. 66

[225] N. C. Ericsson AB, Huawei Technologies Co. Ltd and Nokia. (2018) Interface Specification, Common Public Radio Interface, eCPRI Specification V1.1 . [Online]. Available: http://www.cpri.info/downloads/eCPRI_v_1_1_2018_01_10.pdf 66

[226] L. Valcarenghi, K. Kondepu, F. Giannone, and P. Castoldi, "Requirements for 5G fronthaul," in *2016 18th International Conference on Transparent Optical Networks (ICTON)*. IEEE, 2016, pp. 1–5. 66

[227] M. Huang and X. Zhang, "Distributed MAC Scheduling Scheme for C-RAN with Non-Ideal Fronthaul in 5G Networks," in *2017 IEEE Wireless Communications and Net-*

*working Conference (WCNC)*, 2017, pp. 1–6. 67

[228] G. T. R. WG3. (2016) Transport requirement for CU and DU functional splits options. [Online]. Available: https://www.3gpp.org/DynaReport/TDocExMtg--R3-93--31675.htm 67, 68

[229] M. 3GPP, "3GPP TR 38.801 V14. 0.0 (2017-03): Study on new radio access technology: Radio access architecture and interfaces," 2017. [Online]. Available: https://www.3gpp.org/ftp/Specs/archive/38_series/38.801/ 67

[230] 3GPP. (2017) 3GPP TR 38.801 V14.0.0 (2017-03): Radio access architecture and interfaces. [Online]. Available: https://www.3gpp.org/ftp//Specs/archive/38_series/38.801/38801-e00.zip 68

[231] Bartelt, J and Vucic, N and Camps-Mur, D and Garcia-Villegas, E and Demirkol, I and Fehske, A and Grieger, M and Tzanakaki, A and Gutiérrez, J and Grass, E and Lyberopoulos, G and Fettweis, G, "5G transport network requirements for the next generation fronthaul interface," *EURASIP J. Wirel. Commun. Netw.*, vol. 2017, no. 1, p. 89, 2017. [Online]. Available: https://doi.org/10.1186/s13638-017-0874-7 68

[232] P. Perry, C. Browning, B. Scotney, A. Delmade, S. McClean, L. Barry, A. Peters, and P. Morrow, "Comparison of Analogue and Digital Fronthaul for 5G MIMO Signals," in *ICC 2020 - 2020 IEEE International Conference on Communications (ICC)*, 2020, pp. 1–6. 68

[233] A. D. La Oliva, X. C. Perez, A. Azcorra, A. D. Giglio, F. Cavaliere, D. Tiegelbekkers, J. Lessmann, T. Haustein, A. Mourad, and P. Iovanna, "Xhaul: toward an integrated fronthaul/backhaul architecture in 5G networks," *IEEE Wireless Communications*, vol. 22, no. 5, pp. 32–40, 2015. 68

[234] W. Li, A. Chen, T. Li, R. V. Penty, I. H. White, and X. Wang, "Novel Digital Radio Over Fiber (DRoF) System With Data Compression for Neutral-Host Fronthaul Applications," *IEEE Access*, vol. 8, pp. 40 680–40 691, 2020. 68

[235] G. Otero Pérez, D. Larrabeiti López, and J. A. Hernández, "5G New Radio Fronthaul Network Design for eCPRI-IEEE 802.1CM and Extreme Latency Percentiles," *IEEE Access*, vol. 7, pp. 82 218–82 230, 2019. 68

[236] J. Kim, M. Sung, S.-H. Cho, Y.-J. Won, B.-C. Lim, S.-Y. Pyun, J. K. Lee, and J. H. Lee, "OTA Enabled 147.4 Gb/s eCPRI-Equivalent-Rate Radio-Over-Fiber Link Cooperating with mmWave-Based Korea Telecom 5G Mobile Network for Distributed Antenna System," in *2019 Optical Fiber Communications Conference and Exhibition (OFC)*, 2019, pp. 1–3. 68

[237] G. Brown. (2020) 5G NETWORK & SERVICE STRATEGIES - 2020 OPERATOR SURVEY . [Online]. Available: https://www.readkong.com/page/5g-network-service-strategies-2020-operator-survey-2219563 69

[238] A. Osseiran, J. F. Monserrat, and P. Marsch, *5G mobile and wireless communications technology*. Cambridge University Press, 2016. 69

[239] S. Bjmstad, D. Chen, and R. Veisllari, "Handling Delay in 5G Ethernet Mobile Fronthaul Networks," in *2018 European Conference on Networks and Communications (EuCNC)*, 2018, pp. 1–9. 69

[240] H. J. Son and S. Shin, "Fronthaul Size: Calculation of maximum distance between RRH and BBU," in *NETMANIAS*, 2014. 69

[241] N. C. Ericsson AB, Huawei Technologies Co. Ltd and Nokia. (2018) Interface Specification, Common Public Radio Interface, eCPRI Specification V1.1 . [Online]. Available: http://www.cpri.info/downloads/eCPRI_v_1_1_2018_01_10.pdf 69

[242] L. M. Larsen, M. S. Berger, and H. L. Christiansen, "Fronthaul for Cloud-RAN enabling network slicing in 5G mobile networks," *Wireless Communications and Mobile Computing*, vol. 2018, 2018. 69

[243] D. T. Kiet, T. M. Hieu, N. Q. Hung, N. Van Cuong, V. T. Van, and P. N. Cuong, "Research and Implementation of eCPRI Processing Module for Fronthaul Network on FPGA in 5G – NR gNodeB Base Station," in *2020 4th International Conference on Recent Advances in Signal Processing, Telecommunications Computing (SigTelCom)*, 2020, pp. 1–5. 70

[244] Y. K. S. Whitehead. (2020) 1914.3 (RoE) eCPRI Transport. [Online]. Available: https://frame.co.uk/wp-content/uploads/2020/04/mt1000a-ecpri-er1100.pdf 70

[245] P. Semov, H. Al-Shatri, K. Tonchev, V. Poulkov, and A. Klein, "Implementation of machine learning for autonomic capabilities in self-organizing heterogeneous networks," *Wireless Personal Communications*, vol. 92, no. 1, pp. 149–168, 2017. 72

[246] Y. Lin, L. Shao, Z. Zhu, Q. Wang, and R. K. Sabhikhi, "Wireless network cloud: Architecture and system requirements," *IBM Journal of Research and Development*, vol. 54, no. 1, pp. 4–1, 2010. 72

[247] X. Wang, C. Cavdar, L. Wang, M. Tornatore, H. S. Chung, H. H. Lee, S. M. Park, and B. Mukherjee, "Virtualized cloud radio access network for 5G transport," *IEEE Communications Magazine*, vol. 55, no. 9, pp. 202–209, 2017. 73

[248] M. Mukherjee, L. Shu, and D. Wang, "Survey of fog computing: Fundamental, network applications, and research challenges," *IEEE Communications Surveys & Tutorials*, vol. 20, no. 3, pp. 1826–1857, 2018. 74

[249] R. K. Naha, S. Garg, D. Georgakopoulos, P. P. Jayaraman, L. Gao, Y. Xiang, and R. Ranjan, "Fog computing: Survey of trends, architectures, requirements, and research directions," *IEEE access*, vol. 6, pp. 47 980–48 009, 2018. 74

[250] V. S. Pana, O. P. Babalola, and V. Balyan, "5G radio access networks: A survey," *Array*, vol. 14, p. 100170, 2022. [Online]. Available: https://www.sciencedirect.com/science/article/pii/S2590005622000315 74

[251] K. Liang, L. Zhao, X. Zhao, Y. Wang, and S. Ou, "Joint resource allocation and coordinated computation offloading for fog radio access networks," *China communications*, vol. 13, no. Supplement2, pp. 131–139, 2016. 74

[252] H. Zhang, Y. Qiu, X. Chu, K. Long, and V. C. Leung, “Fog Radio Access Networks: Mobility Management, Interference Mitigation, and Resource Optimization,” *IEEE Wireless Communications*, vol. 24, no. 6, pp. 120–127, Dec 2017. 74

[253] T. I. Project. (2022) Open RAN. [Online]. Available: https://telecominfraproject.com/ 74

[254] E. Jordan. (2021) Open RAN functional splits, explained. [Online]. Available: https://www.5gtechnologyworld.com/open-ran-functional-splits-explained/ 75

[255] i. C. Technologies. (2020) XRAN technology. [Online]. Available: https://itechinfo.ru/content/ 75

[256] O. Sunay, T. Vachuska, and S. Das. (2020) O-RAN ARCHITECTURE CONSISTENT µONOS-BASED CLOUD-NATIVE nRT-RIC AND xAPPS PLATFORM. [Online]. Available: https://opennetworking.org/sd-ran/ 75

[257] x. F. Rod Stuhlmuller. (2018) xRAN Forum Merges With C-RAN Alliance to Form ORAN Alliance. [Online]. Available: https://www.businesswire.com/news/home/20180227005673/en/xRAN-Forum-Merges-C-RAN-Alliance-Form-ORAN/ 75

[258] T. I. Project. (2016) OpenRAN. [Online]. Available: https://telecominfraproject.com/openran/ 75

[259] S. Marek. (2018) xRAN, Open vRAN, and OpenRAN: What’s the Difference? [Online]. Available: https://www.sdxcentral.com/articles/news/xran-open-vran-and-openran-whats-the-difference/2018/04/ 75

[260] J. L. Hardcastle. (2018) Cisco Launches Open vRAN Initiative. [Online]. Available: https://www.sdxcentral.com/articles/news/cisco-launches-open-vran-initiative/2018/02/ 75

[261] P. wireless. (2020) Everything You Need to Know about Open RAN. [Online]. Available: https://www.parallelwireless.com/wp-content/uploads/Parallel-Wireless-e-Book-Everything-You-Need-\to-Know-about-Open-RAN.pdf 75

[262] M. Polese, R. Jana, V. Kounev, K. Zhang, S. Deb, and M. Zorzi, “Machine learning at the edge: A data-driven architecture with applications to 5G cellular networks,” *IEEE Transactions on Mobile Computing*, 2020. 76

[263] C. P. R. Interface, “eCPRI Interface Specification,” *Interface specification, ecpri specification v1*, vol. 1, 2019. 76

[264] Altiostar. (2020) New Business Models. [Online]. Available: https://www.altiostar.com/new-network-model/new-business-models/ 76, 78

[265] F. Mode. (2019) Open RAN: Catalyzing 5G Use Case Innovations. [Online]. Available: https://www.thefastmode.com/expert-opinion/15608-open-ran-catalyzing-5g-use-case-innovations 78

[266] O. Alliance, “O-RAN use cases and deployment scenarios,” *White Paper*, 2020. 78, 79, 80

[267] ORAN. (2022) Virtual Exhibition. [Online]. Available: www.virtualexhibition.o-

ran.org 79

[268] ETSI. (2020) Network Functions Virtualisation (NFV). [Online]. Available: https://www.etsi.org/technologies/nfv 80

[269] M. Klinkowski, "Latency-aware DU/CU placement in convergent packet-based 5G fronthaul transport networks," *Applied Sciences*, vol. 10, no. 21, p. 7429, 2020. 81

[270] Z. Shen, A. Papasakellariou, J. Montojo, D. Gerstenberger, and F. Xu, "Overview of 3GPP LTE-advanced carrier aggregation for 4G wireless communications," *IEEE Communications Magazine*, vol. 50, no. 2, pp. 122–130, February 2012. 83

[271] Y. Yang, H. Hu, J. Xu, and G. Mao, "Relay technologies for WiMax and LTE-advanced mobile systems," *IEEE Communications Magazine*, vol. 47, no. 10, pp. 100–105, October 2009. 83

[272] M. Iwamura, K. Etemad, M. Fong, R. Nory, and R. Love, "Carrier aggregation framework in 3GPP LTE-Advanced [WiMAX/LTE Update]," *IEEE Communications Magazine*, vol. 48, no. 8, pp. 60–67, August 2010. 83, 87, 88, 90, 92, 93

[273] D. Robalo, F. J. Velez, R. R. Paulo, and G. Piro, "Extending the lte-sim simulator with multi-band scheduling algorithms for carrier aggregation in lte-advanced scenarios," in *2015 IEEE 81st Vehicular Technology Conference (VTC Spring)*. IEEE, 2015, pp. 1–6. 85, 99, 101

[274] D. L. S. Robalo, *Planning and dynamic spectrum management in heterogeneous mobile networks with QoE optimization*, P. Universidade da Beira Interior, Covilhã, Ed., 2014. 85, 99, 103

[275] G. Piro, L. A. Grieco, G. Boggia, F. Capozzi, and P. Camarda, "Simulating LTE Cellular Systems: An Open-Source Framework," *IEEE Transactions on Vehicular Technology*, vol. 60, no. 2, pp. 498–513, Feb 2011. 85, 96, 97, 104, 139

[276] R. R. Paulo, F. J. Velez, and G. Piro, "Performance Evaluation and Packet Scheduling in HeNB Deployments," in *2018 IEEE 88th Vehicular Technology Conference (VTC-Fall)*, 2018, pp. 1–6. 85

[277] L. Liu, M. Li, J. Zhou, X. She, L. Chen, Y. Sagae, and M. Iwamura, "Component Carrier Management for Carrier Aggregation in LTE-Advanced System," in *2011 IEEE 73rd Vehicular Technology Conference (VTC Spring)*, May 2011, pp. 1–6. 87, 90, 93

[278] G. Yuan, X. Zhang, W. Wang, and Y. Yang, "Carrier aggregation for LTE-Advanced mobile communication systems," *IEEE Communications Magazine*, vol. 48, no. 2, pp. 88–93, February 2010. 88, 91, 94

[279] H. Lee, S. Vahid, and K. Moessner, "A Survey of Radio Resource Management for Spectrum Aggregation in LTE-Advanced," *IEEE Communications Surveys Tutorials*, vol. 16, no. 2, pp. 745–760, Second 2014. 88, 92

[280] M. A. M. Al-Shibly, M. H. Habaebi, and J. Chebil, "Carrier aggregation in Long Term Evolution-Advanced," in *2012 IEEE Control and System Graduate Research Colloquium*, July 2012, pp. 154–159. 90

[281] S. Parkvall, A. Furuskär, and E. Dahlman, "Evolution of LTE toward IMT-advanced," *IEEE Communications Magazine*, vol. 49, no. 2, pp. 84–91, February 2011. 90

[282] I. F. Akyildiz, D. M. Gutierrez-Estevez, and E. C. Reyes, ""The evolution to 4G cellular systems: LTE-Advanced"," *Physical Communication*, vol. 3, no. 4, pp. 217 – 244, 2010. [Online]. Available: http://www.sciencedirect.com/science/article/pii/S1874490710000303 90

[283] K. Meik, "LTE-Advanced technology introduction white paper," *Rohde & Schwarz*, pp. 3–22, 2010. 90

[284] *TS 36.300, Evolved Universal Terrestrial Radio Access (E-UTRA) and Evolved Universal Terrestrial Radio Access Network (E-UTRAN)*, 3rd Generation Partnership Project, Jan. 2014, tSG RAN, V11.8.0. 91

[285] K. I. Pedersen, T. E. Kolding, F. Frederiksen, I. Z. Kovacs, D. Laselva, and P. E. Mogensen, "An overview of downlink radio resource management for UTRAN long-term evolution," *IEEE Communications Magazine*, vol. 47, no. 7, pp. 86–93, July 2009. 91, 93

[286] A. Holma, Harri e Toskala, *LTE para UMTS: acesso via rádio baseado em OFDMA e SC-FDMA*, J. W. . . Sons, Ed., 2009. 92

[287] Y. Wang, K. I. Pedersen, T. B. Sørensen, and P. E. Mogensen, "Carrier load balancing and packet scheduling for multi-carrier systems," *IEEE Transactions on Wireless Communications*, vol. 9, no. 5, pp. 1780–1789, May 2010. 92

[288] R. Ratasuk, D. Tolli, and A. Ghosh, "Carrier Aggregation in LTE-Advanced," in *2010 IEEE 71st Vehicular Technology Conference*, May 2010, pp. 1–5. 95

[289] B. Classon, K. Baum, V. Nangia, R. Love, Y. Sun, R. Nory, K. Stewart, A. Ghosh, R. Ratasuk, W. Xiao, and J. Tan, "Overview of UMTS Air-Interface Evolution," in *IEEE Vehicular Technology Conference*, Sep. 2006, pp. 1–5. 95

[290] V. T. Library, "Mirrors," http://trace.eas.asu.edu, accessed: 2019-10-03. 98

[291] P. Seeling and M. Reisslein, "Video Transport Evaluation With H.264 Video Traces," *IEEE Communications Surveys Tutorials*, vol. 14, no. 4, pp. 1142–1165, Fourth 2012. 98

[292] P. C. K. Hung and M. V. Martin, "Security Issues in VOIP Applications," in *2006 Canadian Conference on Electrical and Computer Engineering*, May 2006, pp. 2361–2364. 98

[293] ITU-T, "G.729 : Coding of speech at 8 kbit/s using conjugate-structure algebraic-code-excited linear prediction (CS-ACELP)," https://www.itu.int/rec/T-REC-G.729-201206-I/en, accessed: 2019-10-03. 98

[294] Y. Ghiassi-Farrokhfal and J. Liebeherr, "Output characterization of constant bit rate traffic in FIFO networks," *IEEE Communications Letters*, vol. 13, no. 8, pp. 618–620, August 2009. 98

[295] *3GPP TS 36.211 version 13.0.0 Release 13, Evolved Universal Terrestrial Radio*

*Access (E-UTRA), Physical channels and modulation*, 3rd Generation Partnership Project, Jun. 2016, technical Specification Group Radio Access Network. 98, 99

[296] T. Camp, J. Boleng, and V. Davies, "A survey of mobility models for ad hoc network research," *Wireless Communications and Mobile Computing*, vol. 2, 08 2002. 99

[297] O. Cabral, F. Meucci, A. Mihovska, F. J. Velez, N. R. Prasad, and R. Prasad, ""Integrated Common Radio Resource Management with Spectrum Aggregation Over Non-Contiguous Frequency Bands"," *Wireless Personal Communications*, vol. 59, no. 3, pp. 499–523, Aug 2011. [Online]. Available: https://doi.org/10.1007/s11277-011-0242-6 99

[298] E. Teixeira, S. Sousa, F. J. Velez, and J. M. Peha, "Impact of the propagation model on the capacity in small-cell networks: Comparison between the UHF/SHF and the millimeter wavebands," *Radio Science*, vol. 56, no. 5, pp. 1–13, 2021. 101

[299] ITU, "Guidelines for evaluation of radio interface technologies for IMT-Advanced," ITU, Tech. Rep. Rep. ITU-R M.2135-1, 12 2009. [Online]. Available: https://www.itu.int/pub/R-REP-M.2135-1-2009 101

[300] ——, "Guidelines for evaluation of radio interface technologies for IMT-2020," ITU, Tech. Rep. Report ITU-R M.2412-0, 11 2017. [Online]. Available: https://www.itu.int/dms_pub/itu-r/opb/rep/R-REP-M.2412-2017-PDF-E.pdf 102

[301] H. Munir, S. A. Hassan, H. Pervaiz, Q. Ni, and L. Musavian, "Resource Optimization in Multi-Tier HetNets Exploiting Multi-Slope Path Loss Model," *IEEE Access*, vol. 5, pp. 8714–8726, 2017. 102

[302] A. Turkmani and A. Arowojolu, "Estimation of signal strength characteristics in typical microcell environments for PCN networks," in *Proceedings of 2nd IEEE International Conference on Universal Personal Communications*, vol. 1, Oct 1993, pp. 69–73 vol.1. 102

[303] R. Basukala, H. A. M. Ramli, and K. Sandrasegaran, "Performance analysis of EXP/PF and M-LWDF in downlink 3GPP LTE system," in *2009 First Asian Himalayas International Conference on Internet*, Nov 2009, pp. 1–5. 104

[304] P. Serra and A. Rodrigues, "Picocell positioning in an LTE network," in *7th Congress of the Portuguese Committee of URSI*, 2013. 104

[305] E. Dahlman, S. Parkvall, and J. Skold, *5G NR: The next generation wireless access technology*. Academic Press, 2020. 117

[306] ETSI, "User Equipment (UE) radio transmission and reception," 3rd Generation Partnership Project, Tech. Rep. V15.2.0, Sep. 2018. [Online]. Available: https://www.etsi.org/deliver/etsi_ts/138100_138199/13810101/15.02.00_60/ts_13810101v150200p.pdf 117, 130, 131

[307] 3GPP, "Technical Specification Group Services and System Aspects (Release 16) ," 3rd Generation Partnership Project, Tech. Rep. V16.2.0, June. 2022. [Online]. Available: https://www.3gpp.org/ftp/Specs/archive/21_series/21.916/ 117

[308] ——, "NR; User Equipment (UE) radio access capabilities (Release 17) ," 3rd Generation Partnership Project, Tech. Rep. V17.0.0, March. 2022. [Online]. Available: https://www.3gpp.org/ftp/Specs/archive/38_series/38.306/ 117, 128

[309] Y. Xu, G. Gui, H. Gacanin, and F. Adachi, "A survey on resource allocation for 5G heterogeneous networks: Current research, future trends, and challenges," *IEEE Communications Surveys & Tutorials*, vol. 23, no. 2, pp. 668–695, 2021. 117

[310] P. Lin, J. Zhang, Y. Chen, and Q. Zhang, "Macro-femto heterogeneous network deployment and management: from business models to technical solutions," *IEEE Wireless Communications*, vol. 18, no. 3, pp. 64–70, 2011. 117

[311] S. Martiradonna, A. Grassi, G. Piro, and G. Boggia, "Understanding the 5G-air-simulator: A tutorial on design criteria, technical components, and reference use cases," *Computer Networks*, vol. 177, p. 107314, 2020. 118, 137, 141, 154, 155, 221

[312] R. R. Paulo and F. J. Velez, "An Extensive Study on the Performance Evaluation and Scheduling of HeNBs," *IEEE Access*, vol. 9, pp. 40 098–40 110, 2021. 118, 135, 137, 145, 147, 148, 149, 150, 156

[313] R. R. Paulo, F. J. Velez, and G. Piro, "Design of coordinated HeNB deployments," in *2018 IEEE 87th Vehicular Technology Conference (VTC Spring)*. IEEE, 2018, pp. 1–6. 118

[314] A. Ghosh, "5G new radio (NR): Physical layer overview and performance," in *Proc. IEEE Commun. Theory Workshop*, 2018, pp. 1–38. 119

[315] STLpartners. (2022) 5G Standalone vs Non-standalone: Deployment models . [Online]. Available: https://stlpartners.com/articles/telco-cloud/5g-deployment-models-standalone-vs-non-standalone/ 119

[316] Techtarget. (2022) What's happening with standalone 5G? . [Online]. Available: https://www.techtarget.com/searchnetworking/tip/Whats-happening-with-standalone-5G 120

[317] 3GPP, "Technical Specification Group Radio Access Network; E-UTRA (Evolved Universal Terrestrial Radio Access) - NR Dual Connectivity (EN-DC) of LTE 1 Down Link (DL) / 1 Up Link (UL) and inter-/intra-band NR 2 Down Link (DL) / 2 Up Link (UL) bands (Frequency Range 1 (FR1) + Frequency Range 2 (FR2)) (Release 15) ," 3rd Generation Partnership Project, Tech. Rep. V15.0.0, June. 2018. [Online]. Available: https://www.3gpp.org/ftp/Specs/archive/37_series/37.864-11-22/ 121, 128

[318] R. Dilli, "Analysis of 5G wireless systems in FR1 and FR2 frequency bands," in *2020 2nd International Conference on Innovative Mechanisms for Industry Applications (ICIMIA)*. IEEE, 2020, pp. 767–772. 121

[319] M. Lee and S. K. Oh, "On resource block sharing in 3GPP-LTE system," in *The 17th Asia Pacific Conference on Communications*, 2011, pp. 38–42. 120

[320] 3GPP, "NR; Physical channels and modulation," *3rd Generation Partnership Project (3GPP), Technical Specification (TS) 38.211*, vol. 9, 2018. 120, 123

[321] ——, "NR;Physical channels and modulation (Release 17) ," 3rd Generation Partnership Project, Tech. Rep. V17.2.0, June. 2022. [Online]. Available: https://www.3gpp.org/ftp/Specs/archive/38_series/38.211/ 124, 127, 132, 133

[322] sharetechnote. (2021) 5G/NR - Frame Structure . [Online]. Available: https://www.sharetechnote.com/html/5G/5G_FrameStructure.html 127

[323] 3GPP, "NR; Physical layer procedures for data ," 3rd Generation Partnership Project, Tech. Rep. V15.3.0, Sep. 2018. [Online]. Available: https://www.3gpp.org/ftp/Specs/archive/38_series/38.214/ 134

[324] F. A. de Figueiredo, N. F. Aniceto, J. Seki, I. Moerman, and G. Fraidenraich, "Comparing f-OFDM and OFDM performance for MIMO systems considering a 5G scenario," in *2019 IEEE 2nd 5G World Forum (5GWF)*. IEEE, 2019, pp. 532–535. 135, 209

[325] 3GPP. (2009) Simulation Assumptions and Parameters for FDD HeNB RF Requirements, Standard 3GPP, R4-092042, 3rd Generation Partnership Project, Tech. Rep. Meeting 51, May 2009. [Online]. Available: https://www.3gpp.org/ftp7tsg_ran/WG4_Radio/TSGR4_51/Documents/R4_092042.zip 135

[326] S. Wang, W. Guo, and T. O'Farrell, "Optimising femtocell placement in an interference limited network: Theory and simulation," in *2012 IEEE Vehicular Technology Conference (VTC Fall)*. IEEE, 2012, pp. 1–6.

[327] K. Yan, H.-C. Wu, S.-H. Fang, C. Wang, S. Li, and L. Zhang, "Indoor femtocell interference localization," *IEEE Transactions on Wireless Communications*, vol. 19, no. 8, pp. 5176–5187, 2020. 135

[328] C.-J. Liu, P. Huang, L. Xiao, and A.-H. Esfahanian, "Inter-femtocell interference identification and resource management," *IEEE Transactions on Mobile Computing*, vol. 19, no. 1, pp. 116–129, 2019. 135

[329] G. Piro, L. A. Grieco, G. Boggia, R. Fortuna, and P. Camarda, "Two-level downlink scheduling for real-time multimedia services in LTE networks," *IEEE Transactions on Multimedia*, vol. 13, no. 5, pp. 1052–1065, 2011. 137

[330] J. Jalali, A. Khalili, and H. Steendam, "Antenna selection and resource allocation in downlink MISO OFDMA femtocell networks," in *2020 IEEE 91st Vehicular Technology Conference (VTC2020-Spring)*. IEEE, 2020, pp. 1–6. 137

[331] Z. Liu, W. Wang, K. Y. Chan, K. Ma, and X. Guan, "Rate maximization for hybrid access femtocell networks with outage constraints based on pricing incentive mechanism," *IEEE Transactions on Vehicular Technology*, vol. 69, no. 6, pp. 6699–6708, 2020. 137

[332] M. M. Nasralla, N. Khan, and M. G. Martini, "Content-aware downlink scheduling for LTE wireless systems: A survey and performance comparison of key approaches," *Computer Communications*, vol. 130, pp. 78–100, 2018. 137

[333] E.-U. 3GPP and E-UTRAN. (2017) LTE physical layer; Radio Frequency (RF) system scenarios (Release 14), Technical Report 36201, 3rd Generation Partnership Project.

[Online]. Available: https://portal.3gpp.org 137

[334] Y. d. J. Bultitude and T. Rautiainen, "IST-4-027756 WINNER II D1. 1.2 V1. 2 WINNER II Channel Models," 2007. 137

[335] S. Martiradonna, A. Grassi, G. Piro, and G. Boggia, "5G-air-simulator: An open-source tool modeling the 5G air interface," *Computer Networks*, vol. 173, p. 107151, 2020. 138, 139, 140

[336] E. M. Ang, K. K. Wee, Y. H. Pang, and S. H. Lau, "Two-Level Scheduling Framework with Frame Level Scheduling and Exponential Rule in Wireless Network," in *2014 International Conference on Information Science & Applications (ICISA)*, 2014, pp. 1–4. 138

[337] F. Afroz, S. Barua, and K. Sandrasegaran, "Performance analysis of FLS, EXP, LOG and M-LWDF packet scheduling algorithms in downlink 3GPP LTE system," *International Journal of Wireless & Mobile Networks*, 2014. 139

[338] Techplayon. (2021) Signal to Interference and Noise Ratio . [Online]. Available: https://www.techplayon.com/signal-to-interference-and-noise-ratio-snir/ 141

[339] O. M. B. Cabral, "Optimization of the interoperability and dynamic spectrum management in mobile communications systems beyond 3G," Ph.D. dissertation, Universidade da Beira Interior (Portugal), 2010. 146

[340] W. Mansouri, K. B. Ali, F. Zarai, and M. S. Obaidat, "Radio resource management for heterogeneous wireless networks: Schemes and simulation analysis," in *Modeling and Simulation of Computer Networks and Systems*. Elsevier, 2015, pp. 767–792. 147

[341] 3GPP, "Services and Service Capabilities (Release 15), Standard3GPP, TS 22.105, 3rd Generation Partnership Project, Tech. Rep. V15.0.0," 2018. [Online]. Available: https://www.3gpp.org/ftp/Specs/archive/25_series/25.892/25892-600.zip 149

[342] I. M. Álvaro. (2022) Telefonica: 5G era drives Smart and Connected Industry. [Online]. Available: https://www.telefonica.com/en/\communication-room/5g-era-drives-smart-and-connected-industry/ 153

[343] 3GPP. 3GPP TR 21.915 V15.0.0 (2019-09)-Release 15 Description. [Online]. Available: https://portal.3gpp.org/desktopmodules/\Specifications/SpecificationDetails.aspx?specificationId=3389 153

[344] Juniper. (2022) 5G voice users to reach 2.5 billion globally by 2026. [Online]. Available: https://www.juniperresearch.com/pressreleases/5g-voice-users-to-reach-2bn-globally-by-2026 153

[345] A. M. Alba, S. Pundt, and W. Kellerer, "Comparison of performance- and cost-optimal functional splits in 5G and beyond," in *2021 IEEE Global Communications Conference (GLOBECOM)*, 2021, pp. 01–06. 153

[346] 3GPP. (2016) Study on New Radio Access Technology. [Online]. Available: https://www.3gpp.org/ftp/Specs/archive/38_series/38.801/ 154, 155

[347] Huber and suhner. (2021) 5G Fundamentals: Functional splitting overview. [Online]. Available: https://www.hubersuhner.com/en/documents-repository/technologies/pdf/fiber-optics-documents/5g-fundamentals-functional-split-overview 155

[348] F. Capozzi, G. Piro, L. A. Grieco, G. Boggia, and P. Camarda, " On accurate simulations of LTE femtocells using an open source simulator," *EURASIP Journal on Wireless Communications and Networking*, vol. 2012, no. 1, pp. 1–13, 2012. 156

[349] B. Gavish and S. Sridhar, "Economic aspects of configuring cellular networks," *Wireless Networks*, vol. 1, pp. 115–128, 1995. 159

[350] F. J. Velez and L. M. Correia, "Cost/revenue optimisation in multi-service mobile broadband systems," in *The 13th IEEE International Symposium on Personal, Indoor and Mobile Radio Communications*, vol. 1. IEEE, 2002, pp. 177–181. 160, 162, 164

[351] F. J. Velez, O. Cabral, F. Merca, and V. Vassiliou, "Service characterization for cost/benefit optimization of enhanced UMTS," *Telecommunication Systems*, vol. 50, no. 1, pp. 31–45, 2012. 160

[352] K. Johansson, J. Zander, and A. Furuskar, "Modelling the cost of heterogeneous wireless access networks," *International journal of mobile network design and innovation*, vol. 2, no. 1, pp. 58–66, 2007. 160

[353] F. J. Velez and L. M. Correia, "Optimisation of mobile broadband multi-service systems based in economics aspects," *Wireless Networks*, vol. 9, no. 5, pp. 525–533, 2003. 160

[354] E. B. Teixeira, A. R. Ramos, M. S. Lourenço, F. J. Velez, and J. M. Peha, "Capacity/cost trade-off for 5G small cell networks in the UHF and SHF bands," in *2019 22nd International Symposium on Wireless Personal Multimedia Communications (WPMC)*. IEEE, 2019, pp. 1–6. 162

[355] J. Nadal, C. A. Nour, A. Baghdadi, and H. Lin, "Hardware prototyping of FBMC/O-QAM baseband for 5G mobile communication," in *Proceedings of the 2014 25th IEEE International Symposium on Rapid System Prototyping, New Delhi, India*, vol. 1617, 2014, p. 7277. 199, 206, 207

[356] Y. Liu, X. Chen, Z. Zhong, B. Ai, D. Miao, Z. Zhao, J. Sun, Y. Teng, and H. Guan, "Waveform design for 5G networks: Analysis and comparison," *IEEE access*, vol. 5, pp. 19 282–19 292, 2017. 200

[357] R. Datta, N. Michailow, M. Lentmaier, and G. Fettweis, "GFDM interference cancellation for flexible cognitive radio PHY design," in *2012 IEEE Vehicular Technology Conference (VTC Fall)*. IEEE, 2012, pp. 1–5. 200, 201

[358] G. Fettweis, M. Krondorf, and S. Bittner, "GFDM-generalized frequency division multiplexing," in *VTC Spring 2009-IEEE 69th Vehicular Technology Conference*. IEEE, 2009, pp. 1–4. 200, 201

[359] F. Schaich and T. Wild, "Waveform contenders for 5G—OFDM vs. FBMC vs. UFMC,"

in *2014 6th international symposium on communications, control and signal processing (ISCCSP)*. IEEE, 2014, pp. 457–460. 202, 203, 207, 209

[360] F. Kaltenberger, R. Knopp, C. Vitiello, M. Danneberg, and A. Festag, "Experimental analysis of 5G candidate waveforms and their coexistence with 4G systems," *JNCW, October*, 2015. 202, 203, 204

[361] L. Zhang, A. Ijaz, P. Xiao, M. M. Molu, and R. Tafazolli, "Filtered OFDM systems, algorithms, and performance analysis for 5G and beyond," *IEEE Transactions on Communications*, vol. 66, no. 3, pp. 1205–1218, 2017. 204, 205, 208

[362] S. Islam, M. Zeng, and O. A. Dobre, "NOMA in 5G systems: Exciting possibilities for enhancing spectral efficiency," *arXiv preprint arXiv:1706.08215*, 2017. 204, 205, 206

[363] X. Pei, Y. Chen, M. Wen, H. Yu, E. Panayirci, and H. V. Poor, "Next-Generation Multiple Access Based on NOMA With Power Level Modulation," *IEEE Journal on Selected Areas in Communications*, vol. 40, no. 4, pp. 1072–1083, 2022. 205

[364] H. Sadat, M. Abaza, A. Mansour, and A. Alfalou, "A Survey of NOMA for VLC Systems: Research Challenges and Future Trends," *Sensors*, vol. 22, no. 4, p. 1395, 2022. 206

[365] R. Knopp, F. Kaltenberger, C. Vitiello, and M. Luise, "Universal filtered multicarrier for machine type communications in 5G," in *Proc. Eur. Conf. Netw. Commun.(EUCNC)*, 2016, pp. 27–30. 206

[366] I. Gaspar, N. Michailow, A. Navarro, E. Ohlmer, S. Krone, and G. Fettweis, "Low complexity GFDM receiver based on sparse frequency domain processing," in *2013 IEEE 77th Vehicular Technology Conference (VTC Spring)*. IEEE, 2013, pp. 1–6. 207, 209

[367] V. Berg, J.-B. Doré, and D. Noguet, "A flexible radio transceiver for TVWS based on FBMC," *Microprocessors and Microsystems*, vol. 38, no. 8, pp. 743–753, 2014. 207

[368] J. Nadal, C. A. Nour, and A. Baghdadi, "Low-complexity pipelined architecture for FBMC/OQAM transmitter," *IEEE Transactions on Circuits and Systems II: Express Briefs*, vol. 63, no. 1, pp. 19–23, 2015. 207

[369] A. R. Jafri, J. Majid, M. A. Shami, M. A. Imran, and M. Najam-Ul-Islam, "Hardware complexity reduction in universal filtered multicarrier transmitter implementation," *IEEE Access*, vol. 5, pp. 13 401–13 408, 2017. 209

[370] N. Michailow, M. Matthé, I. S. Gaspar, A. N. Caldevilla, L. L. Mendes, A. Festag, and G. Fettweis, "Generalized frequency division multiplexing for 5th generation cellular networks," *IEEE Transactions on Communications*, vol. 62, no. 9, pp. 3045–3061, 2014. 209

[371] S. Min and H. L. Bertoni, "Effect of path loss model on CDMA system design for highway microcells," in *VTC'98. 48th IEEE Vehicular Technology Conference. Pathway to Global Wireless Revolution (Cat. No. 98CH36151)*, vol. 2. IEEE, 1998, pp. 1009–1013. 211

# Appendix A

# Multi carrier Waveform Candidates for Beyond 5G

## A.1 Introduction and Motivation

The leading objective of this appendix (A) is to present comparison and demonstrate a comprehensive overview of multi carrier wave forms with respective to base band complexity, data rate, OoBE, relax synchronization, latency and system flexibility. The proposed analysis shows the interest in designing and implementing alternatives waveform. Presented a comparative analysis of several waveform candidates FBMC,GFDM, UFMC,and f-OFDM basis on their complexity, hardware design and other valuable characteristics. Filter based wave forms have much better Out of OoBE as compared to OFDM. However, f-OFDM has smaller filter length compared to filter-based wave forms and provides better transmission with multiple antenna system without any extra processing, while providing flexible frequency multiplexing, shorter latency and relaxed synchronization as compared to other wave forms.

The remaining of this appendix is structured as follows. In Section A.2, a brief introduction of candidate wave forms is being discussed, while in Section A.3 the hardware complexity comparison of candidate wave forms is addressed, followed by a comprehensive summary of their characteristics comparison among the possible wave forms is given in detail. Finally, conclusions are drawn in Section A.4.

## A.2 Candidate Wave-Forms

A brief introduction of 5G waveform candidates is given in this section.

### A.2.1 FBMC

Figure A.1shows the structure of FBMC, where $K$ is the number of sub carriers and $T$ is the time interval of FBMC symbol. Compared to Orthogonal OFDM, it has three major differences from. First, it is using Offset Quadrature Amplitude Modulation (OQAM) mapping instead of QAM mapping. Each symbol is split into real and imaginary parts, and a time delay $(T/2)$ is applied on imaginary part. Then OQAM signals are combined and modulated by a specific sub carrier frequency and transmitted. Reverse process is applied on the receiver end. OQAM mapping reduces Inter Carrier Interference (ICI) when appropriate filtering is applied. Second it applied Poly Phase Network (PPN) filtering after IFFT process. This performs enhanced frequency and/or time localization depending on the shape and the length of the used prototype filter. This time and frequency localization reduce Inter Symbol Interference (ISI) and ICI respectively [355].

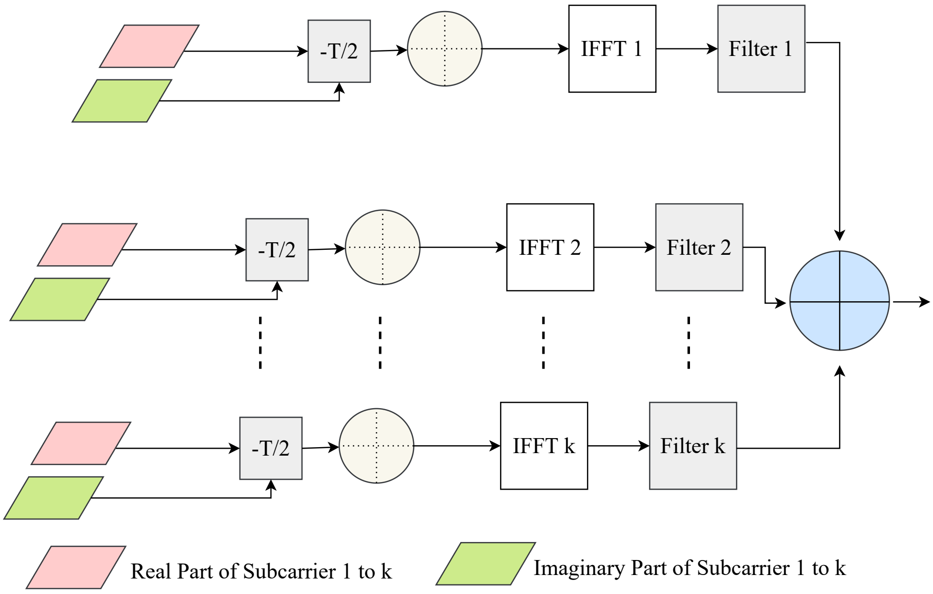


Figure A.1: System structure for FBMC, adapted from [356].

Third, no cyclic prefix is required because the best frequency and time localization through filtering and OQAM modulation process. Due to per sub carrier filtering and coordinating process of OQAM and filtering, better OoBE can be achieved, but Filter tail is much longer as compared to other filter-based wave forms which is not suitable for short packet transmission and low latency communication [356].

### A.2.2 GFDM

GFDM is generalized with a new concept and is composed of non orthogonal sub carrier which spread the data in time and frequency dimensional blocks as shown in Figure A.2. Total number of complex data symbols is equal to $KM$, where $K$ is number of sub carriers and $M$ is the number of sub symbols.

Figure A.3 shows the block diagram of the GFDM transceiver. Data coming from mapper is up sampled so that pulse-shaping circular filter $g[n]$ can be applied through a convolution process [357]. This filtering process is applied sub carrier wise that improves OoBE but generate ISI, which can be removed by adding the Cyclic Prefix (CP). To enhance the spectral efficiency, the tail biting technique can be applied to reduce the CP length [358].

GFDM provides a low latency signal because of circular filtering with prototype filters, instead of linear convolution that is used in FBMC. It used one CP for one block slightly than a CP for every multi carrier symbol, which results in enhanced spectral efficiency. ICI is not completely removed due to non-orthogonal neighbouring sub carriers.

### A.2.3 UFMC

UFMC is discussed in this part of the Chapter, which focuses the distinctions of upcoming modulations technique for 5G wireless communication technology. Fourth generation wireless communication system OFDM is an admirable choice, however 4G modulation tech-

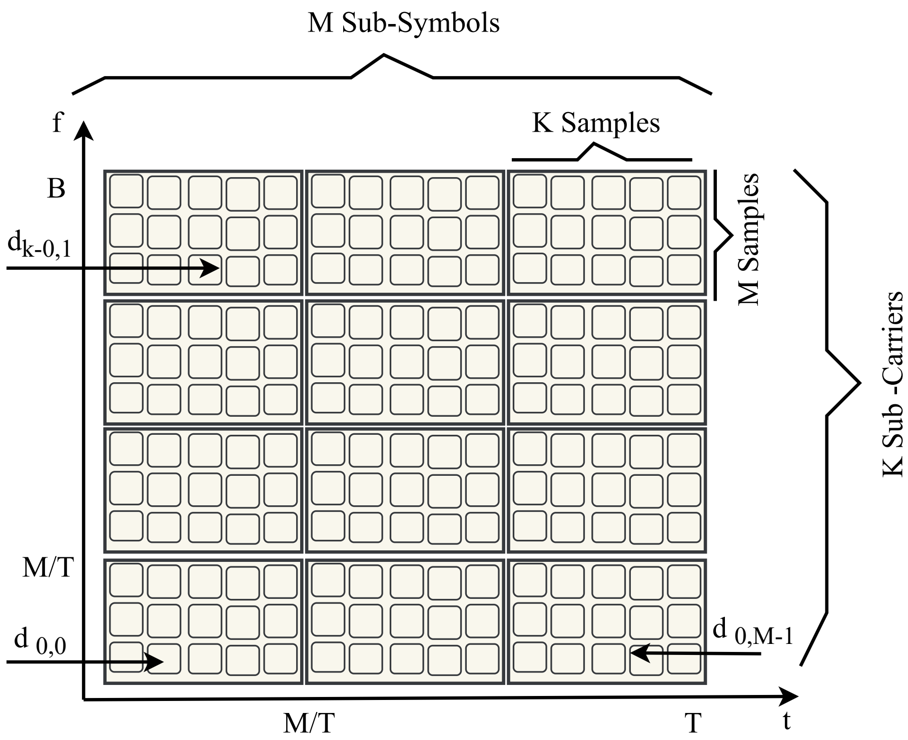


Figure A.2: Time and frequency blocks in GFDM, adapted from [357].

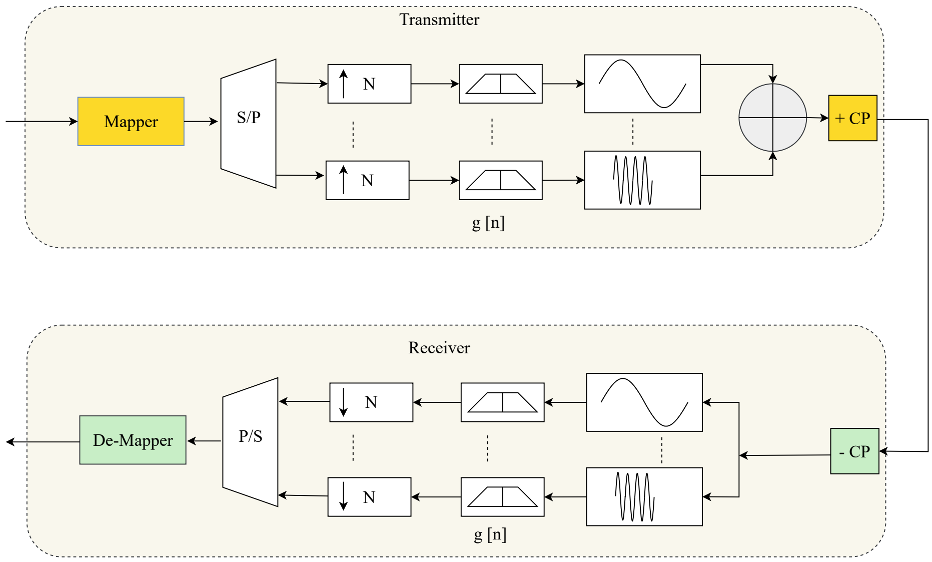


Figure A.3: GFDM modulation/demodulation function Block Diagram [358].

nique experience high Peak to Average Power Ratio (PAPR) hitch, also it has high side band leakage. The current 4G system depend on OFDM waveform, which is not suitable for supporting the 5G and beyond applications, that 5G and beyond will offer. 5G technology is expected to have different requirements higher data rates, lower latency and efficient spectrum usage when relate to the existing wireless technology.

Currently researchers working on multiple schemes and being investigated new wave forms. UFMC scheme, that can overcome the limitations of OFDM, the generalization of OFDM and FBMC scheme is UFMC. Thorsten Wild and Frank Schaich in paper [359] proposed the first model of UFMC.

Fig.A.4 shows the transmitter of this model, where 1024 points IDFT and filter Dolph-Chebyshev having length $L = 73$ in each branch are considered. The data from mapper is divided into number of RB (12 sub carrier) and before taking IDFT zero is padded to each branch. In each branch, data is shifted by 12 carriers and accordingly the zeros are padded.

Data is filtered using Dolph-Chebyshev after taking Inverse Discrete Fourier Transform (IDFT). Dolph-Chebyshev is a type of filter that minimizes side lobes and main lobe width in the spectrum. On each branch filter is a shifted version of Dolph-Chebyshev, which perform convolution operation. The output from each filter is then added to get final output. Efficient spectrum management is a clear advantage of the UFMC proposed in [360]. However, it has still high complexity than conventional OFDM, and further research is needed to investigate a scheme which can easily be implement on hardware.

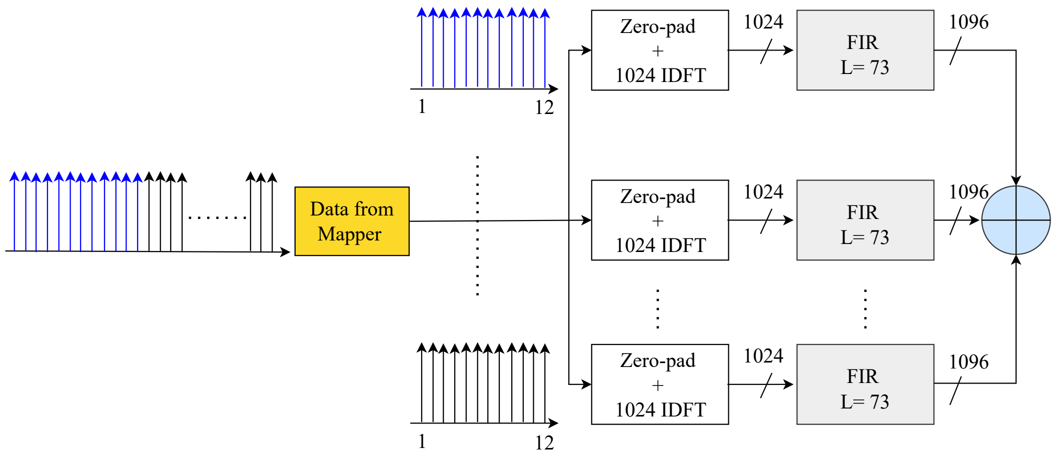


Figure A.4: UFMC transmitter previous scheme [360].

In [360] a new approach is presented for UFMC (basis on hardware) which is better than Thorsten Wild and Frank Schaich approach [359]. This modified method has two main differences from previous approach, the small size of IDFT and different shifting procedure of the signal. Changing the size of IDFT came from the knowledge of the identical shape spectrum. During experiments, first the IDFT size 64 is used, and then size 1024 is considered, presented by author in [360]. It has been observed that both of them have almost same spectrum shape. So, it is convenient to use the size of IDFT 64 instead of 1024 to save computational resources. IDFT size 64 is used in scheme of paper [360], while 1024 used in paper [359] which is complex architecture. The shapes for different IDFT sizes are presented by author in [184, 360]. Blue and red colour are used for UFMC and OFDM, respectively.

In the modified approach, the size of IDFT 1024 is replaced by $N$ point along with up-sampling and used multiplier at the end of each branch instead of shifted filter for shifting purpose. The use of shifting filter increasing the complexity due to the procedure of convolution is completed by means of complex filter taps that doubles the total of operations. By these two change the overall complexity is reduced. First step of both schemes modified, and previous method are same data from the mapper are divided into group of RBs before calculating IDFT each RB is zero-padded with $N$=12. The value of N is selected in such manner that spectral performance is not lost and improved computational complexity. By using the following equation, the dimension of IDFT is chosen according to the number of sub-bands:

$$N = \min\left(64, 2^{\lceil \log_2(12 \cdot B) \rceil}\right) \quad \text{(A.1)}$$

where $B$ represents the number of sub-bands. The minimum value between 64 and $2^{\lceil \log_2(12.B)}$ is calculated for IDFT. The filter is not shifted and has side lobe attenuation of 60 dB. Multiplier is used in last of each branch for shifting purposes. Figure A.5 shows the modified UFMC scheme in which the multiplier is used at the end for shifting proposes, the total number of sub band is B for RBs, the index used for $RB$ is $k$ starting from 0 or 1 and ends on $B-1$, n represents time index that starts from zero to $N+L-1$, $N = 1024$ and $L$ representing the filter length.

For long bursts, FBMC is very efficient for short burst transmissions, but UFMC is better than FBMC and OFDM. While FBMC suffers from high time domain overheads, UFMC support low latency and fast time division duplex switching.

### A.2.4 F-OFDM

System band width is divided among several sub bands to increased diversity of the system. In UFMC each Band is divided in sub bands called resource blocks. Each resource has the same sub carrier division, numerology and frame structure, whereas each user have their own characteristics on the basis of channel characteristics and data rates.

F-OFDM is same as UFMC with some differences: (1) Whole band is divided into multiple sub bands and each sub band have different bandwidth according to the requirement of user, as shown in Figure. A.6; (2) Sub carrier spacing in UFMC is the same for each sub band, whereas in F-OFDM sub carrier spacing is different in each sub band as the user required to use spectrum efficiently; (3) CP is added in each sub band to avoid ISI and length of CP is added flexibly as required to avoid extra spectrum usage; (4) IFFT is performed flexibly as requirement of each user.

F-OFDM transceiver block diagram is shown in Figure. A.7. Firstly, bit sequences are mapped into Binary Phase-Shift Keying (BPSK)/Amplitude Modulation (AM) symbols. Then using IFFT, symbols are mapped on orthogonal sub carriers and CP is added longer then channel

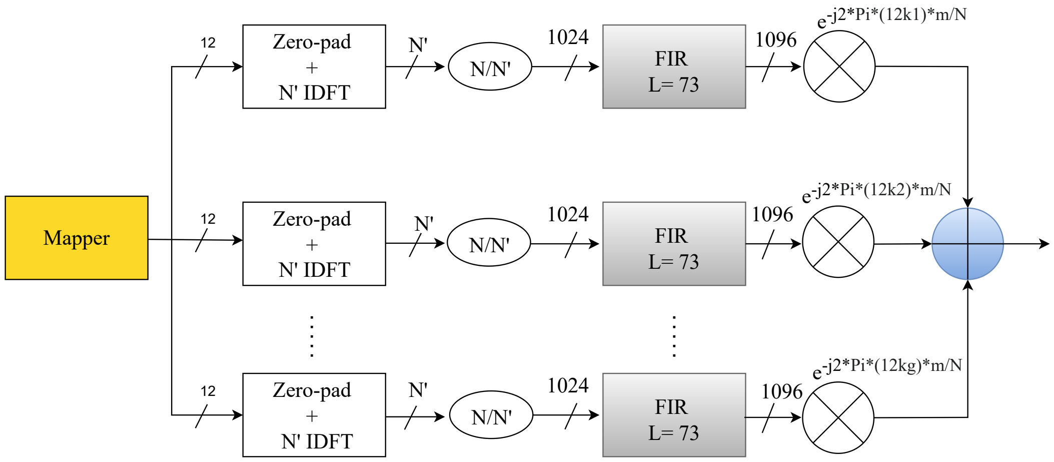


Figure A.5: UFMC modified scheme transmitter [360].

impulse response to avoid ICI and ISI. Then it passes through pulse shaping filter before transmitting on multi path fading channel. Length of the filter in F-OFDM is longer as of UFMC, Filter tails extends to nearby symbol, make it comparable to CP OFDM system [361]. By applying this flexible architecture desired advantages can be obtained. Firstly, OoBE can be reduced by designing a suitable structure for each sub band which reduces the guard band utilization.

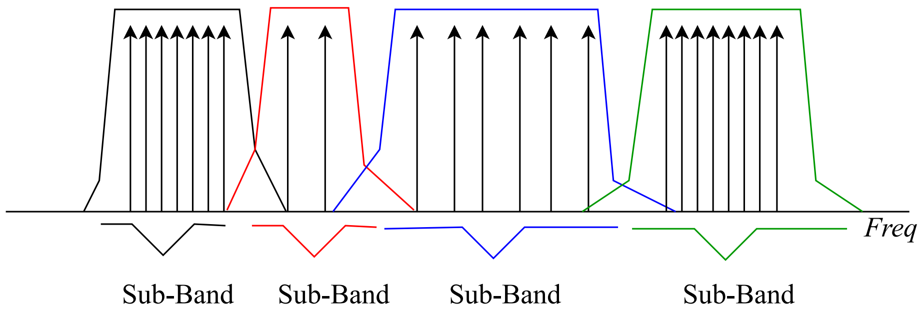


Figure A.6: Sub band division in F-OFDM [361].

Secondly, Asynchronous transmission is possible by applying flexible filter design for each sub band. Thirdly, each user needs based on their characteristic can be fulfilled by applying optimized numerology.

### A.2.5 NOMA

Non-orthogonal multiple access (NOMA) serves different users at the same time and frequency [362]. It has two main techniques, code domain and power domain serving. In the power domain, it attains multiplexing in the power domain while the code domain obtains the multiplexing by code domain. NOMA supports the superposition coding at the transmitter while the successive interference cancellation at the receiver. With the help of this, it supports multiplexing users in the power domain.

For example, a base station transmits the superposed signal to two users, as shown in Figure A.8. Let suppose the user one receives the higher gain, and user 2 receives the lower gain.

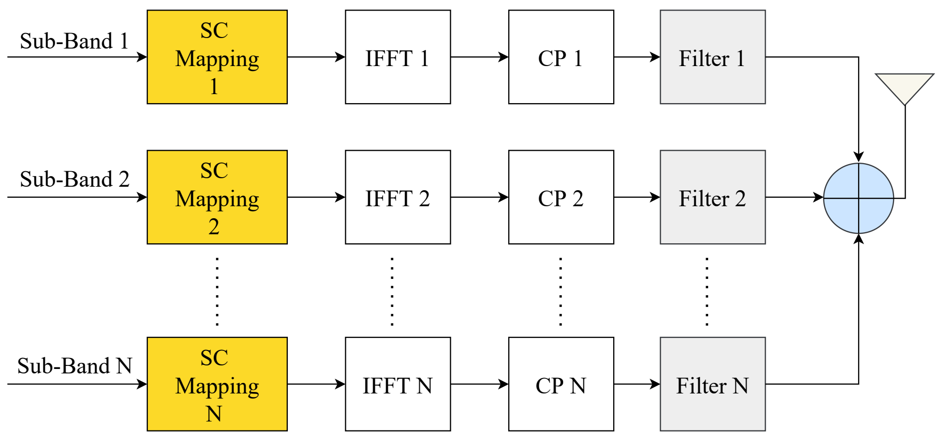


Figure A.7: Transmitter structure of F-OFDM [361].

In NOMA, user one is referred to as a strong user and user two the weak. In NOMA, user one subtracts its received signal from weak user (user two) through successive interference cancellation, after it possibly decodes its signal. While the second user considered the first user's signal (strong) as noise and distinguished signal quickly its own signal. The NOMA assigns more power to the weak user to ensure fairness during the higher interference [363].

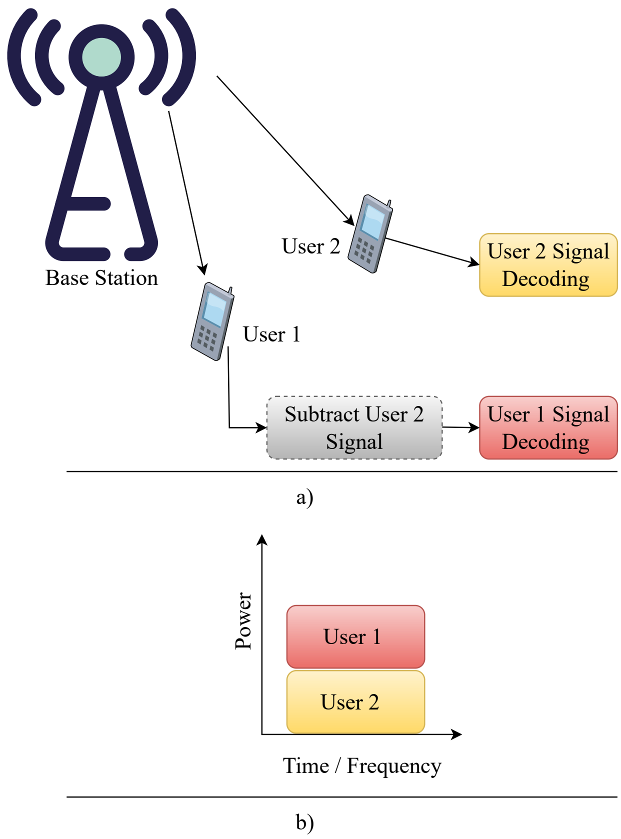


Figure A.8: NOMA serving users a) NOMA serving two user b) Allocation in power domain to two users [362].

#### A.2.5.1 Benefits of NOMA

- NOMA achieves high spectral efficiency by allocating multiple users at the same frequency and time;
- It has simultaneous transmission nature, it does not need to schedule in a time slot, and its benefit is supporting low latency applications;
- NOMA keeps the fairness and quality flexibility by power control among the users;
- Due to higher power allocation to a weak user, it offers a higher throughput at a cell edge.

#### A.2.5.2 Research Challenges of NOMA

- The inter carrier interference cancellation for NOMA is more complicated in dense networks with higher users [364];
- Its compatibility with carrier aggregation type is not yet defined;
- Physical layer security for NOMA is a changeling and open research problem [362];
- More effort is required to get the benefits of MIMO and mmWave.

## A.3 Hardware Complexity Comparison

### A.3.1 FBMC

A FBMC based implementation on Xilinx Kintex-7 XC7K325T FPGA is performed of a receiver, to achieve high flexibility and Low Adjacent Channel Leakage Ratio (ACLR) [1], to provide services for vacant channel in the spectrum and to avoid adjacent channel interference, also a comparison performed with OFDM. Where 512 is active sub carriers out of 1024 total sub carrier and overlapping ratio is 4. The detail of resource utilization in the hardware is given in Table [365]. Hence, it contains the extra complexity overhead of 10% in slice registers, 18% in Lookup Tables, 114% in DSP48E1 and 36% in RAM BLK's as compared to OFDM. At receiver side it increased the complexity overhead of 29% in Slice Registers, 27% in Lookup Tables, 60% in DSP48E1 and 249% in RAM BLK's. But ACLR and flexibility results were significantly greater as compared to OFDM.

FPGA based hardware implementation of FBMC is also performed in [355], as well as comparison with OFDM. In [355], Linear Phase Shift Registers (LFSR) are used to generate the random binary data instead of predefined samples, which occupy large memory. Comparative results consider IFFT (size of IFFT 512), 16 QAM constellation and 1 tap prototype filter(q=1). By considering these parameters OFDM required 3006 flip-flops, 3599 LUT's as logic, 912 LUT's as Random-Access Memory (RAM) and 16 real multipliers. Whereas, FBMC requires 5687 flip-flops, 7385 LUTs as logic, 1632 LUTs as RAM, and 40 real multiplier which are almost double as compared to OFDM. Clock cycles required in FBMC are 1076 as compared to 1064 in OFDM. By ignoring $M/2$ offset because real part is directly processed, which improves the latency in FBMC by considering reasonable hardware complexity.

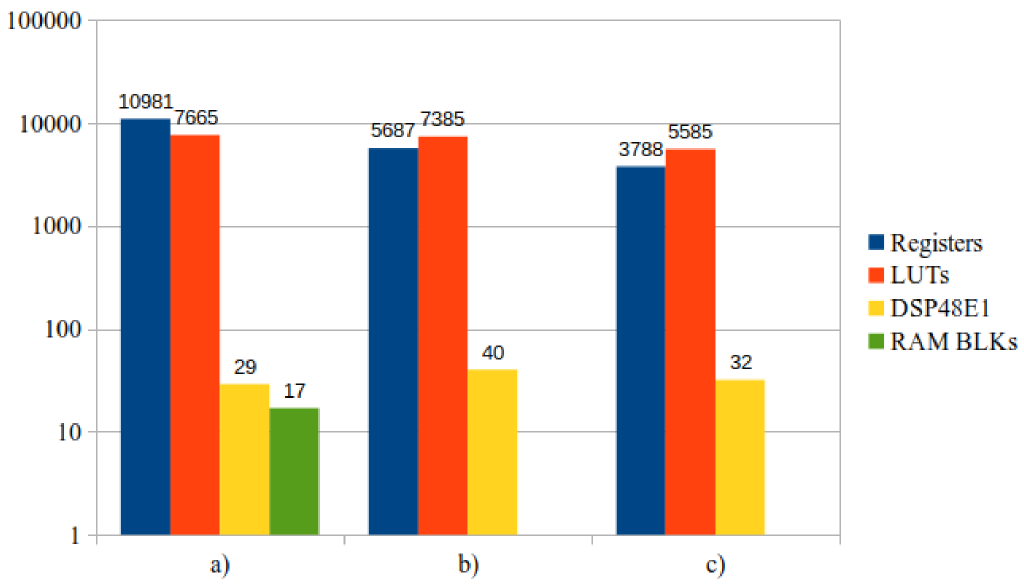


Figure A.9: Synthesis of the results for the used resource,a) [359], b) [355], and c) [366].

Table A.1: Comparison among 5G wave forms candidates.

| Waveform | Filter Length | Filter Granularity | Complexity | Latency | PAPR | OoBE |
|---|---|---|---|---|---|---|
| OFDM | ≤ CP Length | Whole Band | Low | Slightly Low | High | Bad |
| FBMC | = (3, 4, 5) × Symbol duration | Subcarrier | High | Very High | High | Best |
| GFDM | »Symbol duration | Subcarrier | High | High | Moderate | Good |
| UFMC | =ZP Length | Sub-band | Very High | Low | High | Good |
| F-OFDM | ≤ 1/2 × Symbol duration | Sub-band | Moderate | Low | High | Better |

Another FBMC based hardware implementation performed in [367]. The relation between even and odd samples at the output of IFFT, no twice calculation is required for IFFT, real and imaginary separately. IFFTs are divided into even and odd and only even part is used. Therefore, two real and imaginary terms are sent instead of one. This technique improves the complexity as compared to previous filter bank architectures. Filtering is performed by using IFFT block and PPN network. This proposed architecture complexity is half of the 2·N IFFT architecture. By using this technique half of the IFFTs are calculated and remaining samples values are achieved from the calculated ones. Synthesis results of these sources are shown in Figure. A.9.

### A.3.2 GFDM

A hardware architecture has been implemented by utilizing the pipe lining capabilities of FPGA [368], In this architecture data samples are in frequency domain passing through a filter delay process at transmitter. Data circulation is performed by activating a delay block, with last data sub carrier, then data is converted back into time domain by taking IFFT. More delay and filtering blocks are required at the receiver side, because of large filter bandwidth. First signal Converted to frequency domain from time domain and passes through delay blocks and then converted back into time domain by taking IFFT.

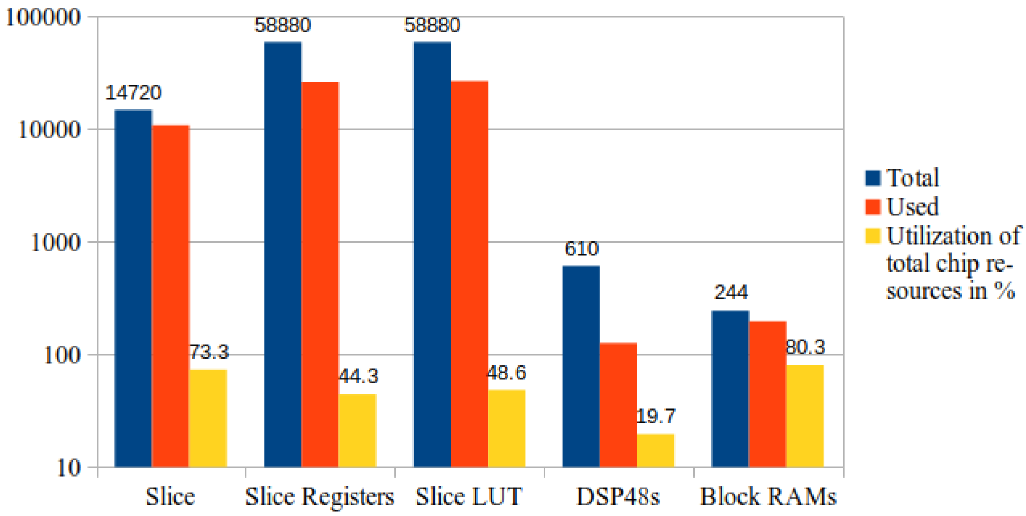


Figure A.10: Compilation of the results.

National Instruments Flex-RIO module is used for base band processing. GFDM transmitter utilizes 75% of total chip resources. Detailed results are shown in Figure.A.10. These results show that GFDM can be implemented with bearable complexity to achieve satisfactory results.

### A.3.3 F-OFDM

Overall complexity at transmitter and receiver is similar in Filtered OFDM . Complexity of the IFFT operations for single rate (SR) implementation in each sub band is given by [361]:

$$C_{IFFT-SR} = (N\log_2(N) - 3N + 4)/2 \quad \text{(A.2)}$$

K is the total number of sub bands. Filtering operations required LFN complex multiplications. Computational complexity for whole sub band in single rate implementation is as follows:

$$C_{SR}(Tx) = K(\,(N\log_2(N) - 3N + 4)\,/2 + L_F N) \quad \text{(A.3)}$$

For multi rate implementation, the complexity of the IFFT operations in each sub band is as follows:

$$C_{\text{IFFT-MR}} = (N\log_2(N) - 3N + 4)/2 \quad \text{(A.4)}$$

where $L_F M$ complex multiplications are required for filtering operation and K are the total number of sub bands. So total computational complexity of multi rate implementation for whole bandwidth is as follows:

$$C_{MR}(Tx) = K\left(\left(M\log_2(M) - 3M + 4\right)/2 + L_F M\right) \quad \text{(A.5)}$$

Computational complexity is significantly higher (up to 1000 times if number of sub bands are 100) as compared to OFDM while considering single rate implementation in Filtered OFDM. While multi rate implementation have comparable computational complexity as compared to OFDM by taking the advantage of up sampling operation.

### A.3.4 UFMC

The complexity in [369] work is one hundred and twenty times compared to CP-OFDM for 10 MHz channelization. While the complexity is 25 times as compared to OFDM on 60 dB side lobe work associated in [369] for the same channel requirements.

An efficient implementation solution, reduced IDFT block computations, filtering complexity solution and spectrum 112 out of 192 butterflies are executed, that is 42% reduction in computational complexity by using this proposed technique. In [366] the filter input multiplies with filter coefficients. when the filter output is essential the sample shifted to right by one location and then multiplies with filter coefficients for next output. In [370] multiplication of non- zeros sample with filter coefficients are useful.

For 73-tab FIR filter one possible scenario are shown [366] in which inputs are multiplies with coefficients, only non-zero samples are only useful the other multiplier use in this case is waste of hardware. The simplified architecture proposed in [359] which implement the idea of [366]. The sample once enter the filter and shift of memory element is competed, then for next 16 cycles for each one to generate 16 output of the filter coefficients are multiplexed. In this simplified solution just five multipliers, four adders, four shift registers and five 16-to-1 multiplexers will be castoff in comparison of shift registers, 73 multipliers and 72 adders [21]. By using this simplified architecture of IFFT and Filtering overall hardware complexity is reduced as compared to previous architectures [324].

## A.4 Conclusion

Filter based waveforms have gained much attention because of the requirement of asynchronous scenarios in 5G communications systems. In this work we have presented the basic functionality and characteristics of emerging 5G waveforms. In addition, a comparative analysis has been presented of different waveforms. Filter based waveforms have much better OoBE as compared to OFDM, which results in better waveform to cope with 5G challenges. FMBC has best OoBE as compared to others but it has higher computational complexity. UFMC and GFDM have better OoBE characteristics but they have higher complexity as well as asynchronous transmission capabilities issues, whereas F-OFDM has better OoBE with moderate complexity, which is suitable candidate for flexibility and asynchronous transmission scenarios.

# Appendix B

# Real Time Outdoor Analysis of Small Cell at 3.5 GHz

## B.1 Introduction

This work considers the outdoor scenario near the data centre in Covilha, Portugal. Have deployed our small cell towers for the purpose of our real-time deployment, as one can see our deployed tower graphically in Figure B.2 and real time in Figure B.3. Rohde and Schwarz SMM 100A vector signal generator for the transmit signal shown in FigureB.4 is used, which is connected to the antenna (RF) as shown in Figure B.5. This device generates the 5G NR signal for the range of FR1 And FR2. The device support below the 6 GHz band defined by 5G NR FR1. In our scenario, the considered transmit power 17 dBm, cell radius 400 meters, 3.5 GHz frequency band and the breaking point distance 269.25 meters. For the receiver side, Rohde and Schwarz FSH8 spectrum analyzer is used, which proved the services of spectrum analysis:

- It is considered to keep the transmitter at 0 meter and measured the receiving signal ;
- Did performed the analysis from 0 meters to transmitter and up to 400 meters ;
- The distance between different points of measurement was 10 meters. For example; started from 0 meters, then the next point of the measure was 20 m and 30 m;
- At each point of measurement, did 30 measurements;
- The analysis is performed in open space during the morning, afternoon, evening, and night.

The propagation behaviours of small cells are presented in [371]. Break point distance can be calculated as:

$$d_{BP} = h_{UE} \cdot h_{BS} \cdot \frac{f}{c} \quad \text{(B.1)}$$

Where $d_{BP}$ is break point distance, $h_{UE}$ is 0.5 m which is user equipment height, $h_{BS}$ is the hight of BS which is 11.25 m, $f$ is 3.5 GHz frequency, while c is $3 \times 10^8$.

## B.2 Motivation

The motivation behind this work was to analyze the spectrum in real time scenario and implement the 5G NR in an outdoor environment to characterize the small cell and transmit power.

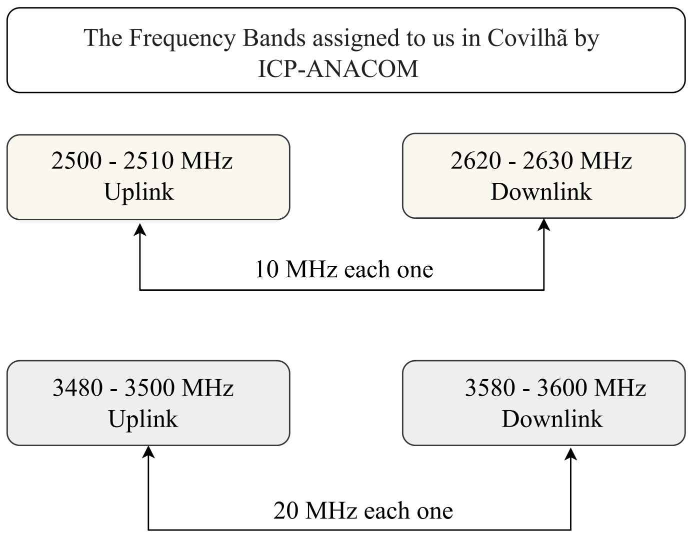


Figure B.1: The frequency bands assigned to us by ICP-ANACOM for research.

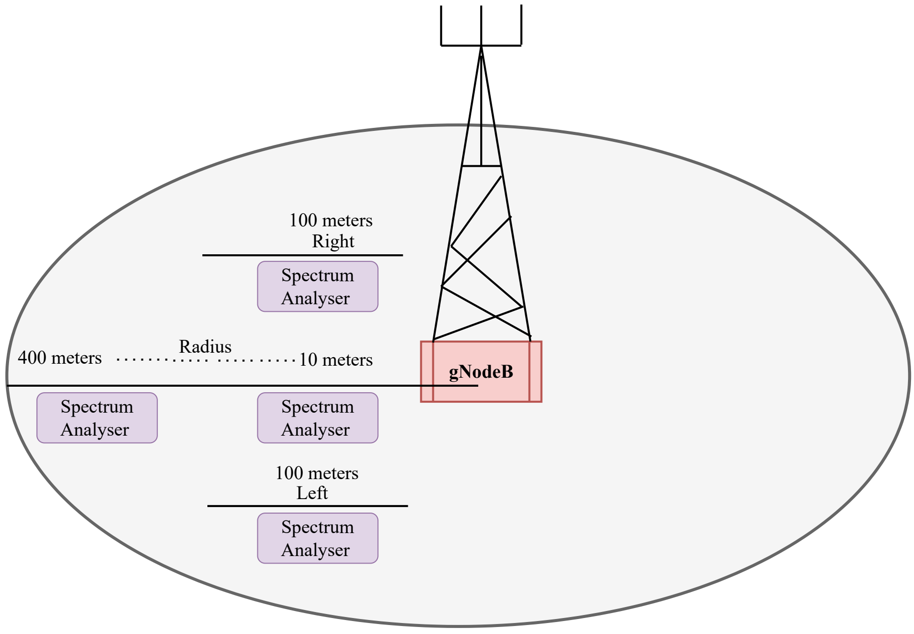


Figure B.2: Out door small cell scenario, having radius 400 m with gNB and spectrum analyser at different place.

Figure B.3: The broader view of implemented scenario contain all the setup together, which reflecting Figure B.2.


Figure B.4: Rohde and Schwarz SMM 100A vector signal generator for the transmitting signal.

Figure B.5: Transmitter at base station.

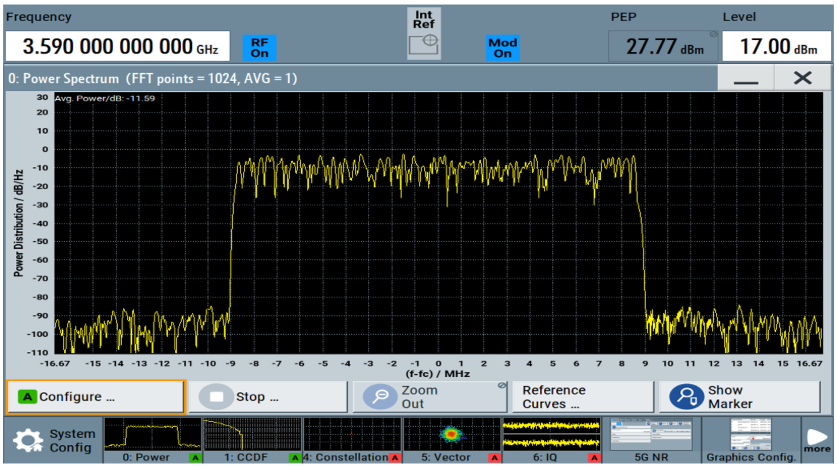

Figure B.6: Transmit power spectrum from gNB with 3.5 GHz band and 17 dBm power.

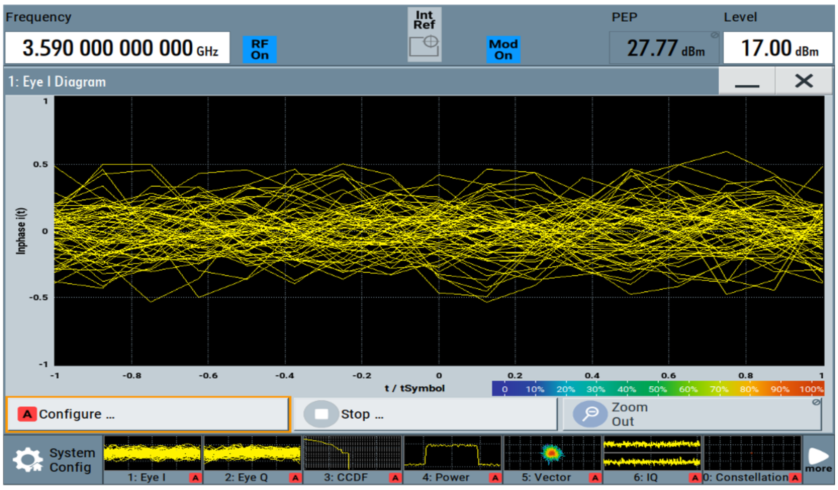

Figure B.7: Eye diagram while transmitting the signal.

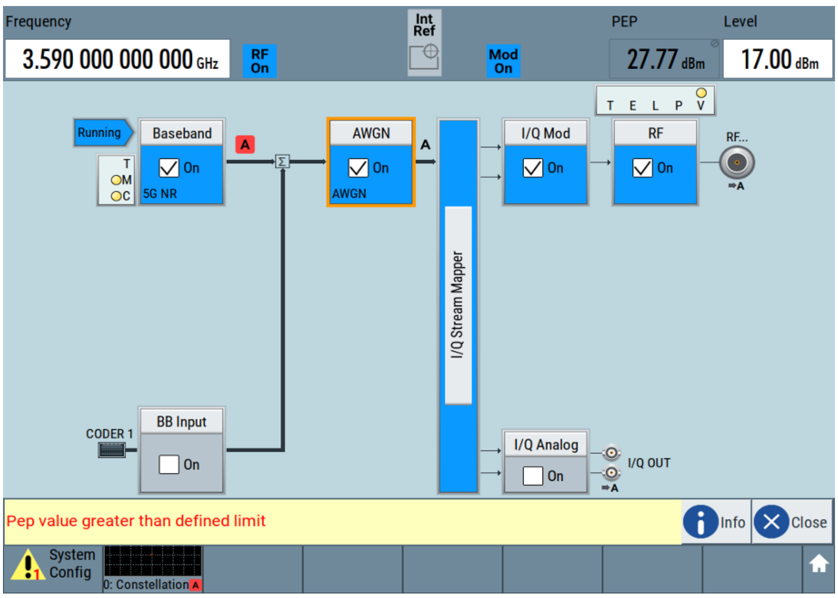

Figure B.8: Simulation approach to obtain the required output for analysis (base band signal processes selection).

Figure B.9: Receiving signal during the afternoon.

## B.3 Scenario

In this work, a small cell with a radius of 400 m are considered and analyzed the signal in three ways (to analysed the signal ) the centre, left side and right side, these sides of base station are shown in Figure B.2 :

- First,analyzed the signal directly from the centre of the transmitter (base station ), radius 400 m and the results are shown in Figure B.12 ;
- Then analyzed the signal from the right side of the transmitter with a distance of 0 m to 100 m. The results are shown in Figure B.13.
- Finlay, analyzed the signal from the left side of the transmitter with a distance of 0 m to 100 m. The results are shown in Figure B.14.

## B.4 Conclusion

It is found that when the receiver was near the base station, the received power was low mainly due to the antenna pattern (below the mast); when receiver moved above 10 meters, the received power was increasing, both in left and right side cases, and then tend to decrease near to 100 m. While in case of centre of the road received power behaviour was different, the received power was decreeing until the break point distance. When with the receiver it crossed the breaking point distance. The power at the middle again increased due to the surface reflection, but at the end, near to 400 meters, the power decreased sharply with the worst result (two slope behavior). With this behaviour of the received power, the study obtained the real-time behaviour for the dual-slope path loss model. The curve obtained in real time follows the dual-slope model, for received power before and after break point distance.


Figure B.10: The cart (with spectrum analyzer) at distance 400 meter from the transmitter with computer connected to obtain and save the results.

Figure B.11: The broader view of our implementation contain all the setup together, which reflecting Figure B.2.

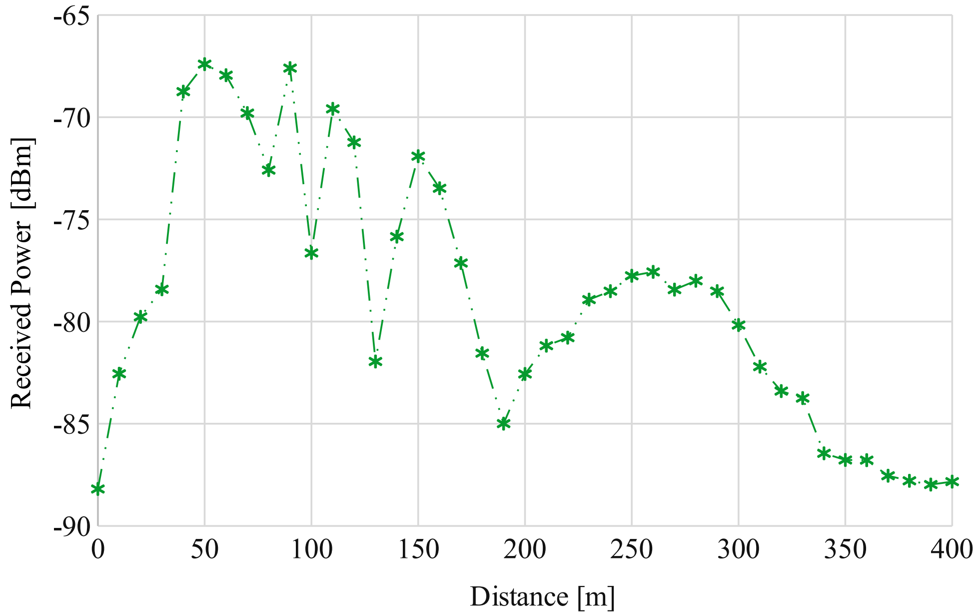


Figure B.12: Received power from gNB to spectrum analyzer (0 m to 400 m) at the center.

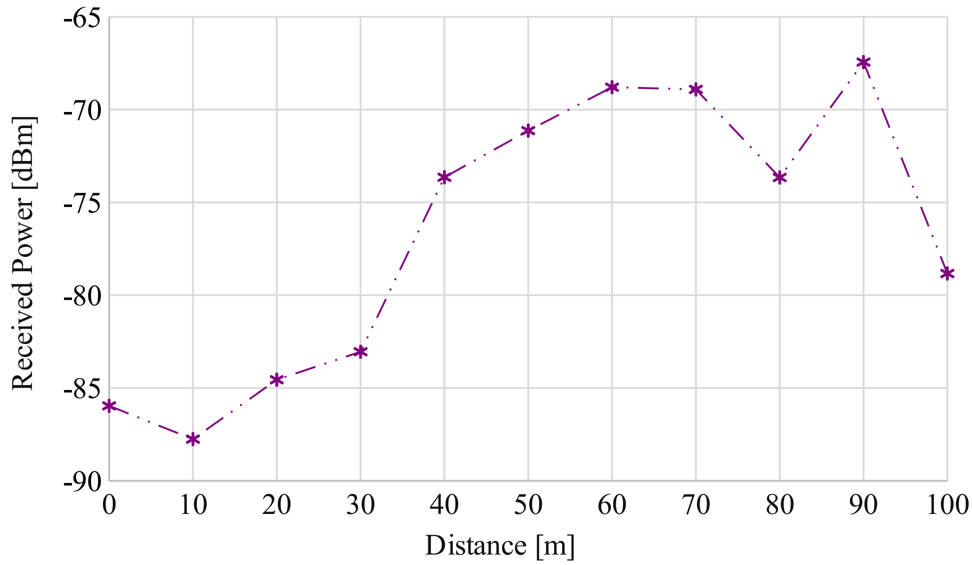


Figure B.13: Received power from gNB to spectrum analyzer at right side of gNB (0 m to 100 m).

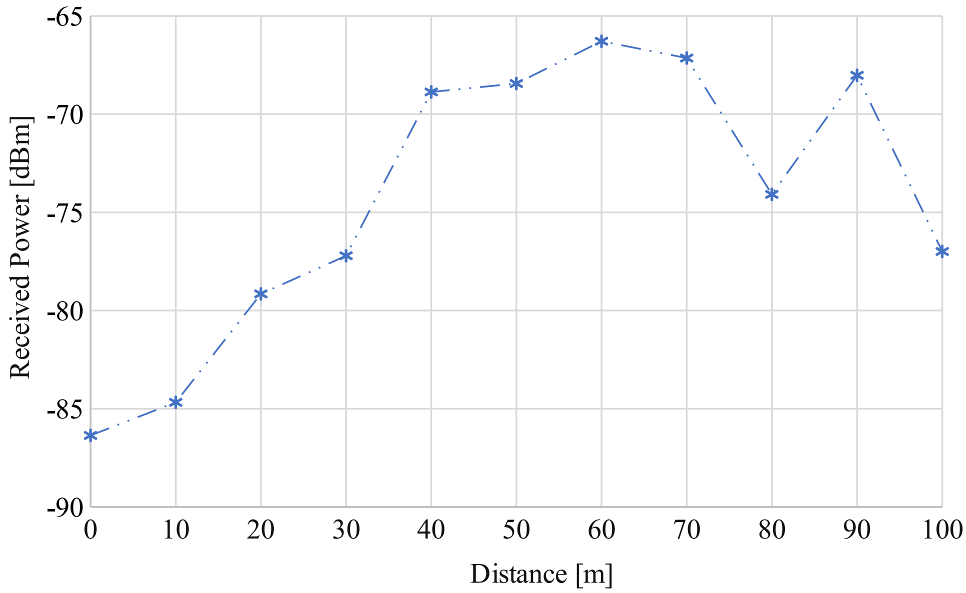


Figure B.14: Received power from gNB through spectrum analyzer at left side of gNB (0 m to 100 m).

# Appendix C

# Implementation of Femtocell into 5G Air Simulator

The 5G air-simulator is the open-source simulator [311], coded in C++, which has considered the 5G set of protocols. In our research for femtocells indoor deployment in the heterogenous network, we consider this open-source project. The code is father updated with parameters for our scenario and updated the code according to our desires.

```
/* -*- Mode:C++; c-file-style:"gnu"; indent-tabs-mode:nil; -*- */
/*
 * Copyright (c) 2020 TELEMATICS LAB, Politecnico di Bari
 *
 * This file is part of 5G-air-simulator
 *
 * 5G-air-simulator is free software; you can redistribute it and/or modify
 * it under the terms of the GNU General Public License version 3 as
 * published by the Free Software Foundation;
 *
 * 5G-air-simulator is distributed in the hope that it will be useful,
 * but WITHOUT ANY WARRANTY; without even the implied warranty of
 * MERCHANTABILITY or FITNESS FOR A PARTICULAR PURPOSE.  See the
 * GNU General Public License for more details.
 *
 * You should have received a copy of the GNU General Public License
 * along with 5G-air-simulator; if not, see <http://www.gnu.org/licenses/>.
 *
 * Author: Francesco Capozzi <f.capozzi@poliba.it>
 * Updated by: Bahram khan <bahram.khan@lx.it.pt>
 */

#include "../channel/RadioChannel.h"
#include "../phy/gnb-phy.h"
#include "../phy/ue-phy.h"
#include "../core/spectrum/bandwidth-manager.h"
#include "../networkTopology/Cell.h"
#include "../protocolStack/packet/packet-burst.h"
#include "../protocolStack/packet/Packet.h"
#include "../core/eventScheduler/simulator.h"
#include "../flows/application/InfiniteBuffer.h"
#include "../flows/application/VoIP.h"
#include "../flows/application/CBR.h"
#include "../flows/application/TraceBased.h"
#include "../device/IPClassifier/ClassifierParameters.h"
```

```
#include "../flows/QoS/QoSParameters.h"
#include "../flows/QoS/QoSForEXP.h"
#include "../flows/QoS/QoSForFLS.h"
#include "../flows/QoS/QoSForM_LWDF.h"
#include "../componentManagers/FrameManager.h"
#include "../utility/RandomVariable.h"
#include "../utility/UsersDistribution.h"
#include "../utility/IndoorScenarios.h"
#include "../load-parameters.h"
#include "../device/HeNodeB.h"
#include <iostream>
#include <queue>
#include <fstream>
#include <stdlib.h>
#include <cstring>

#include <vector>

static void SingleCellWithFemto (int argc, char *argv[])
{
  double radius = atof(argv[2]);
  int nbBuildings = atoi(argv[3]);
  int buildingType = atoi(argv[4]);
  double activityRatio = atof(argv[5]);
  int nbUE = atoi(argv[6]);
  int nbFemtoUE = atoi(argv[7]);
  int nbVoIP = atoi(argv[8]);
  int nbVideo = atoi(argv[9]);
  int nbBE = atoi(argv[10]);
  int nbCBR = atoi(argv[11]);
  int sched_type = atoi(argv[12]);
  int frame_struct = atoi(argv[13]);
  int speed = atoi(argv[14]);
  int accessPolicy = atoi(argv[15]);
  double maxDelay = atof(argv[16]);
  int videoBitRate = atoi(argv[17]);
  int seed;
  if (argc==19)
    {
      seed = atoi(argv[18]);
    }
  else
    {
```

```
      seed = -1;
    }

  int nbCell = 1;

  // define simulation times
  double duration = 30;
  double flow_duration = 20;

//  int cluster = 3; Updated by Bahram
//  double bandwidth = 20;
//


  int cluster_enb=1; //Updated by Bahram
  int bandwidth_enb=20; //Updated by Bahram

  int cluster_henb=2; //Updated by Bahram
  int bandwidth_henb=10; //Updated by Bahram






  // CREATE COMPONENT MANAGER
  Simulator *simulator = Simulator::Init();
  FrameManager *frameManager = FrameManager::Init();
  NetworkManager* nm = NetworkManager::Init();

  // CONFIGURE SEED
  if (seed >= 0)
    {
      srand (seed);
    }
  else
    {
      srand (time(nullptr));
    }
  cout << "Simulation with SEED = " << seed << endl;

  // SET SCHEDULING ALLOCATION SCHEME
   GNodeB::DLSchedulerType downlink_scheduler_type;
```

```
  switch (sched_type)
    {
    case 1:
      downlink_scheduler_type = GNodeB::DLScheduler_TYPE_PROPORTIONAL_FAIR;
      cout << "Scheduler PF "<< endl;
      break;
    case 2:
      downlink_scheduler_type = GNodeB::DLScheduler_TYPE_MLWDF;
      cout << "Scheduler MLWDF "<< endl;
      break;
    case 3:
      downlink_scheduler_type = GNodeB::DLScheduler_TYPE_EXP;
      cout << "Scheduler EXP "<< endl;
      break;
    case 4:
      downlink_scheduler_type = GNodeB::DLScheduler_TYPE_FLS;
      cout << "Scheduler FLS "<< endl;
      break;
    case 5:
      downlink_scheduler_type = GNodeB::DLScheduler_EXP_RULE;
      cout << "Scheduler EXP_RULE "<< endl;
      break;
    case 6:
      downlink_scheduler_type = GNodeB::DLScheduler_LOG_RULE;
      cout << "Scheduler LOG RULE "<< endl;
      break;
    case 7:
      downlink_scheduler_type = GNodeB::DLScheduler_TYPE_MAXIMUM_THROUGHPUT;
      cout << "Scheduler MT "<< endl;
      break;
    case 8:
      downlink_scheduler_type = GNodeB::DLScheduler_TYPE_ROUND_ROBIN;
      cout << "Scheduler RR "<< endl;
      break;
    default:
```

```
      downlink_scheduler_type = GNodeB::DLScheduler_TYPE_PROPORTIONAL_FAIR;
      break;
    }

  // SET FRAME STRUCTURE
  FrameManager::FrameStructure frame_structure;
  switch (frame_struct)
    {
    case 1:
      frame_structure = FrameManager::FRAME_STRUCTURE_FDD;
      break;
    case 2:
      frame_structure = FrameManager::FRAME_STRUCTURE_TDD;
      break;
    default:
      cout << "Error: invalid frame structure specified!" << endl;
      exit(1);
    }
  frameManager->SetFrameStructure(frame_structure);




  //create macro-cells
  vector <Cell*> *cells = new vector <Cell*>;
  for (int i = 0; i < nbCell; i++)
    {
      CartesianCoordinates center =
        GetCartesianCoordinatesForCell(i, radius * 1000.);

      Cell *c = new Cell (i, radius, 0.035, center.GetCoordinateX (), center.GetCoordinateY ());
      cells->push_back (c);
      nm->GetCellContainer ()->push_back (c);

      cout << "Created Cell, id " << c->GetIdCell ()
                <<", position: " << c->GetCellCenterPosition ()->GetCoordinateX ()
                << " " << c->GetCellCenterPosition ()->GetCoordinateY () << endl;
    }
```

```

  //////////////////////
  //create femto-cells
  //
  int femtoCellsInBuilding = 1;
  if ( buildingType == 0 )
    {
      femtoCellsInBuilding = 25;
    }
  else
    {
      femtoCellsInBuilding = 40;
    }
  int nbFemtoCells = nbBuildings * femtoCellsInBuilding;
  int firstFemtoinBuildingID = nbCell;
  int apartmentSide = 10; //[m]
  int nbFloors = 1;
  //users are distributed uniformly into a cell
  vector<CartesianCoordinates*> *building_positions = GetUniformBuildingDistribution (0, nbBuildings);

  for (int idBuilding = 0; idBuilding < nbBuildings; idBuilding++)
    {
      // Get Building Positions
      double buildingCenter_X = building_positions->at (idBuilding)->GetCoordinateX ();
      double buildingCenter_Y = building_positions->at (idBuilding)->GetCoordinateY ();

      nm->CreateBuildingForFemtocells( idBuilding, buildingType, apartmentSide, nbFloors,
                                      buildingCenter_X, buildingCenter_Y,
                                      firstFemtoinBuildingID, femtoCellsInBuilding);

      cout << "Created Building, id " << idBuilding
                << ", position: " << buildingCenter_X
                << " " << buildingCenter_Y
                << " and " << nbFloors << " floors"
                << " and " << femtoCellsInBuilding << " femtocells" << endl;
```

```

      firstFemtoinBuildingID += femtoCellsInBuilding;
    }
  //
  //
  ///////////////////////////
////Bahram code start
    ///////////////////////////
  /////
    //nbt number of node Bs in the system
    // assim é para o sistema todo
    //int nbt=nbCell+nbFemtoCells;
    //
    //std::vector <BandwidthManager*> spectrums = RunFrequencyReuseTechniques (nbt, cluster, bandwidth);
    // aqui acaba o sistema todo


    //Criação de vectores diferentes para o eNB e para os HeNB
    // assim é para o eNB
    std::vector <BandwidthManager*> spectrums = RunFrequencyReuseTechniques (nbCell, cluster_enb, bandwidth_enb);
    // Assim para o HeNB
    std::vector <BandwidthManager*> zx = RunFrequencyReuseTechniques (femtoCellsInBuilding, cluster_henb, bandwidth_henb);
     //Junta os dois vectores
     spectrums.insert(spectrums.end(), zx.begin(), zx.end() );

     ///////////////////////////
   ////Bahram code end
       ///////////////////////////
     /////

 // vector <BandwidthManager*> spectrums = RunFrequencyReuseTechniques (nbCell, cluster, bandwidth); Updated by Bahram code

 // BandwidthManager* femto_spectrums = spectrums.at(0);
// vector <BandwidthManager*> femto_spectrums =
```

```
  RunFrequencyReuseTechniques (nbCell, cluster, bandwidth);






  //Create a set of a couple of channels
  vector <RadioChannel*> *dlChannels = new vector
<RadioChannel*>;
  vector <RadioChannel*> *ulChannels = new vector
<RadioChannel*>;
  for (int i= 0; i < nbCell + nbFemtoCells; i++)
    {
      RadioChannel *dlCh = new RadioChannel ();
      dlCh->SetChannelId (i);
      dlChannels->push_back (dlCh);

      RadioChannel *ulCh = new RadioChannel ();
      ulCh->SetChannelId (i);
      ulChannels->push_back (ulCh);
    }



  //create gNBs
  vector <GNodeB*> *gNBs = new vector <GNodeB*>;
  for (int i = 0; i < nbCell; i++)
    {
      GNodeB* gnb = new GNodeB (i, cells->at (i));
      gnb->GetPhy ()->SetDlChannel (dlChannels->at (i));
      gnb->GetPhy ()->SetUlChannel (ulChannels->at (i));

      gnb->SetDLScheduler (downlink_scheduler_type);

      gnb->GetPhy ()->SetBandwidthManager (spectrums.at (i));

      cout << "Created gnb, id " << gnb->GetIDNetworkNode()
                << ", cell id " << gnb->GetCell ()->GetIdCell
()
                <<", position: " << gnb->GetMobilityModel ()-
>GetAbsolutePosition ()->GetCoordinateX ()
                << " " << gnb->GetMobilityModel ()-
```

```
>GetAbsolutePosition ()->GetCoordinateY ()
                << ", channels id " << gnb->GetPhy ()->GetDlChannel ()->GetChannelId ()
                << gnb->GetPhy ()->GetUlChannel ()->GetChannelId ()  << endl;

      spectrums.at (i)->Print ();


      ulChannels->at (i)->AddDevice(gnb);


      nm->GetGNodeBContainer ()->push_back (gnb);
      gNBs->push_back (gnb);
    }
  //create Home gNBs
  vector <Femtocell*> *femtocells = nm->GetFemtoCellContainer();
  for (int i = nbCell; i < nbCell + nbFemtoCells; i++)
    {
      double HeNBdrop = (double) rand()/ (double) RAND_MAX;
      HeNodeB* gnb = new HeNodeB (i, femtocells->at (i-nbCell));
      gnb->GetPhy ()->SetDlChannel (dlChannels->at (i));
      gnb->GetPhy ()->SetUlChannel (ulChannels->at (i));
      gnb->GetPhy ()->SetBandwidthManager (spectrums.at (i));

      if (accessPolicy == 1)
        {
          gnb->GetMacEntity()->SetRestrictedAccessMode(false);
        }

      cout << "Created Home gnb, id " << gnb->GetIDNetworkNode()
                              << ", cell id " << gnb->GetCell ()->GetIdCell ()
                              <<", position: " << gnb->GetMobilityModel ()->GetAbsolutePosition ()->GetCoordinateX ()
                              << " " << gnb->GetMobilityModel ()->GetAbsolutePosition ()->GetCoordinateY ()
                              << ", channels id " << gnb-
```

```
>GetPhy ()->GetDlChannel ()->GetChannelId ()
                              << gnb->GetPhy ()->GetUlChannel
()->GetChannelId ();
      if ( HeNBdrop <= activityRatio )
              {
                gnb->SetDLScheduler
(downlink_scheduler_type);
                cout << ", active " << endl;
              }
      else
        {
          cout << ", inactive " << endl;
        }
      spectrums.at (i)->Print ();

      ulChannels->at (i)->AddDevice(gnb);

      nm->GetHomeGNodeBContainer()->push_back (gnb);

    }
  vector <HeNodeB*> *HeNBs = nm->GetHomeGNodeBContainer();

  int totalNbUE = nbCell*nbUE + nbFemtoCells*nbFemtoUE;
  int totalNbCell = nbCell + nbFemtoCells;

  //Define Application Container
  VoIP VoIPApplication[ nbVoIP*totalNbUE ];
  TraceBased VideoApplication[ nbVideo*totalNbUE ];
  InfiniteBuffer BEApplication[ nbBE*totalNbUE ];
  CBR CBRApplication[ nbCBR*totalNbUE ];
  int voipApplication = 0;
  int videoApplication = 0;
  int cbrApplication = 0;
  int beApplication = 0;
  int destinationPort = 101;
  int applicationID = 0;

  //Create GW
  Gateway *gw = new Gateway ();
  nm->GetGatewayContainer ()->push_back (gw);


  // Users in MACRO CELL
```

```
  //nbUE is the number of users that are into each cell at the beginning of the simulation
  int idUE = totalNbCell;
  for (int j = 0; j < nbCell; j++)
    {

      //users are distributed uniformly into a cell
      vector<CartesianCoordinates*> *positions = GetUniformUsersDistribution (j, nbUE);

      //Create UEs
      for (int i = 0; i < nbUE; i++)
        {
          //ue's random position
          double posX = positions->at (idUE - totalNbCell)->GetCoordinateX ();
          double posY = positions->at (idUE - totalNbCell)->GetCoordinateY ();
          double speedDirection = (double)(rand() %360) * ((2*M_PI)/360);;

          UserEquipment* ue = new UserEquipment (idUE,
                                                 posX, posY, speed, speedDirection,
                                                 cells->at (j),
                                                 gNBs->at (j),
                                                 0, //HO deactivated!
                                                 Mobility::CONSTANT_POSITION);

          cout << "Created UE - id " << idUE << " position " << posX << " " << posY
                    << ", cell " <<  ue->GetCell ()->GetIdCell ()
                    << ", target gnb " << ue->GetTargetNode ()->GetIDNetworkNode () << endl;

          ue->GetPhy ()->SetDlChannel (gNBs->at (j)->GetPhy ()->GetDlChannel ());
          ue->GetPhy ()->SetUlChannel (gNBs->at (j)->GetPhy
```

```
()->GetUlChannel ());

          ue->SetIndoorFlag(false);

          FullbandCqiManager *cqiManager = new FullbandCqiManager ();
          cqiManager->SetCqiReportingMode (CqiManager::PERIODIC);
          cqiManager->SetReportingInterval (1);
          cqiManager->SetDevice (ue);
          ue->SetCqiManager (cqiManager);

          nm->GetUserEquipmentContainer ()->push_back (ue);

          // register ue to the gnb
          gNBs->at (j)->RegisterUserEquipment (ue);
          // define the channel realizations
          for (int k = 0; k < nbCell; k++)
            {
              ChannelRealization* c_dl = new ChannelRealization (gNBs->at (k), ue, ChannelRealization::CHANNEL_MODEL_MACROCELL_URBAN);
              gNBs->at (k)->GetPhy ()->GetDlChannel ()->GetPropagationLossModel ()->AddChannelRealization (c_dl);
              ChannelRealization* c_ul = new ChannelRealization (ue, gNBs->at (k), ChannelRealization::CHANNEL_MODEL_MACROCELL_URBAN);
              gNBs->at (k)->GetPhy ()->GetUlChannel ()->GetPropagationLossModel ()->AddChannelRealization (c_ul);
            }
          for (int k = 0; k < nbFemtoCells; k++)
            {
//              ChannelRealization* c_dl = new ChannelRealization (HeNBs->at (k), ue, ChannelRealization::CHANNEL_MODEL_FEMTOCELL_URBAN);
//              HeNBs->at (k)->GetPhy ()->GetDlChannel ()->GetPropagationLossModel ()->AddChannelRealization (c_dl);
//              ChannelRealization* c_ul = new ChannelRealization (ue, HeNBs->at (k), ChannelRealization::CHANNEL_MODEL_FEMTOCELL_URBAN);
//              HeNBs->at (k)->GetPhy ()->GetUlChannel ()->GetPropagationLossModel ()->AddChannelRealization (c_ul);
//
```

```


              ChannelRealization* c_dl = new ChannelRealization (HeNBs->at (k), ue, ChannelRealization::CHANNEL_MODEL_WINNER_DOWNLINK);
                      HeNBs->at (k)->GetPhy ()->GetDlChannel ()->GetPropagationLossModel ()->AddChannelRealization (c_dl);
                      ChannelRealization* c_ul = new ChannelRealization (ue, HeNBs->at (k), ChannelRealization::CHANNEL_MODEL_WINNER_DOWNLINK);
                      HeNBs->at (k)->GetPhy ()->GetUlChannel ()->GetPropagationLossModel ()->AddChannelRealization (c_ul);

            }
          idUE++;
        }
    }



  // Users in FEMTO CELLS
  //nbUE is the number of users that are into each cell at the beginning of the simulation
  //idUE = nbCell*nbUE;
  for (int j = 0; j < nbFemtoCells; j++)
    {
      int idCell = j + nbCell;
      vector<CartesianCoordinates*> *positions = GetUniformUsersDistributionInFemtoCell (idCell, nbFemtoUE);

      //Create UEs
      for (int i = 0; i < nbFemtoUE; i++)
        {
          //ue's random position
          double posX = positions->at (i)->GetCoordinateX ();
          double posY = positions->at (i)->GetCoordinateY ();
          double speedDirection = (double)(rand() %360) * ((2*M_PI)/360);;

          UserEquipment* ue = new UserEquipment (idUE,
                                                 posX, posY, speed, speedDirection,
                                                 femtocells-
```

```
>at (j),
                                                    HeNBs->at (j),
                                                    0, //HO deactivated!
                                                    Mobility::CONSTANT_POSITION);

          cout << "Created UE in femto-cell - id " << idUE << " position " << posX << " " << posY
                    << ", cell " <<  ue->GetCell ()->GetIdCell ()
                    << ", target gnb " << ue->GetTargetNode ()->GetIDNetworkNode () << endl;

          ue->GetPhy ()->SetDlChannel (HeNBs->at (j)->GetPhy ()->GetDlChannel ());
          ue->GetPhy ()->SetUlChannel (HeNBs->at (j)->GetPhy ()->GetUlChannel ());

          ue->SetIndoorFlag(true);

          if (accessPolicy == 1)
            {
              // adding Users to the closed subscriber group
              HeNBs->at(j)->GetMacEntity()->AddSubscribedUser(ue);
            }

          FullbandCqiManager *cqiManager = new FullbandCqiManager ();
          cqiManager->SetCqiReportingMode (CqiManager::PERIODIC);
          cqiManager->SetReportingInterval (1);
          cqiManager->SetDevice (ue);
          ue->SetCqiManager (cqiManager);

          nm->GetUserEquipmentContainer ()->push_back (ue);

          // register ue to the gnb
          HeNBs->at (j)->RegisterUserEquipment (ue);
          // define the channel realizations
          for (int k = 0; k < nbCell; k++)
```

```
            {
              ChannelRealization* c_dl = new ChannelRealization (gNBs->at (k), ue, ChannelRealization::CHANNEL_MODEL_MACROCELL_URBAN);
              gNBs->at (k)->GetPhy ()->GetDlChannel ()->GetPropagationLossModel ()->AddChannelRealization (c_dl);
              ChannelRealization* c_ul = new ChannelRealization (ue, gNBs->at (k), ChannelRealization::CHANNEL_MODEL_MACROCELL_URBAN);
              gNBs->at (k)->GetPhy ()->GetUlChannel ()->GetPropagationLossModel ()->AddChannelRealization (c_ul);
            }
          for (int k = 0; k < nbFemtoCells; k++)
            {
//              ChannelRealization* c_dl = new ChannelRealization (HeNBs->at (k), ue, ChannelRealization::CHANNEL_MODEL_FEMTOCELL_URBAN);
//              HeNBs->at (k)->GetPhy ()->GetDlChannel ()->GetPropagationLossModel ()->AddChannelRealization (c_dl);
//              ChannelRealization* c_ul = new ChannelRealization (ue, HeNBs->at (k), ChannelRealization::CHANNEL_MODEL_FEMTOCELL_URBAN);
//              HeNBs->at (k)->GetPhy ()->GetUlChannel ()->GetPropagationLossModel ()->AddChannelRealization (c_ul);
//
//

              ChannelRealization* c_dl = new ChannelRealization (HeNBs->at (k), ue, ChannelRealization::CHANNEL_MODEL_WINNER_DOWNLINK);   // Updated by Bahram

               HeNBs->at (k)->GetPhy ()->GetDlChannel ()->GetPropagationLossModel ()->AddChannelRealization (c_dl);
               ChannelRealization* c_ul = new ChannelRealization (ue, HeNBs->at (k), ChannelRealization::CHANNEL_MODEL_WINNER_DOWNLINK);  // Updated by Bahram
               HeNBs->at (k)->GetPhy ()->GetUlChannel ()->GetPropagationLossModel ()->AddChannelRealization (c_ul);



```

```
          }
        idUE++;
      }
  }

  for (auto ue : *nm->GetUserEquipmentContainer ())
    {
      // CREATE DOWNLINK APPLICATION FOR THIS UE
      double start_time = 0.1; // + GetRandomVariable (5.);
      double duration_time = start_time + flow_duration;
      // *** voip application
      for (int j = 0; j < nbVoIP; j++)
        {
          // create application
          VoIPApplication[voipApplication].SetSource (gw);
          VoIPApplication[voipApplication].SetDestination (ue);
          VoIPApplication[voipApplication].SetApplicationID (applicationID);
VoIPApplication[voipApplication].SetStartTime(start_time);
VoIPApplication[voipApplication].SetStopTime(duration_time);

          // create qos parameters
          if (downlink_scheduler_type == GNodeB::DLScheduler_TYPE_FLS)
            {
              QoSForFLS *qos = new QoSForFLS ();
              qos->SetMaxDelay (maxDelay);
              if (maxDelay == 0.1)
                {
                  cout << "Target Delay = 0.1 s, M = 9" << endl;
                  qos->SetNbOfCoefficients (9);
                }
              else if (maxDelay == 0.08)
```

```
                {
                  cout << "Target Delay = 0.08 s, M = 7" << endl;
                  qos->SetNbOfCoefficients (7);
                }
              else if (maxDelay == 0.06)
                {
                  cout << "Target Delay = 0.06 s, M = 5" << endl;
                  qos->SetNbOfCoefficients (5);
                }
              else if (maxDelay == 0.04)
                {
                  cout << "Target Delay = 0.04 s, M = 3" << endl;
                  qos->SetNbOfCoefficients (3);
                }
              else
                {
                  cout << "ERROR: target delay is not available"<< endl;
                  return;
                }

              VoIPApplication[voipApplication].SetQoSParameters (qos);
            }
          else if (downlink_scheduler_type == GNodeB::DLScheduler_TYPE_EXP)
            {
              QoSForEXP *qos = new QoSForEXP ();
              qos->SetMaxDelay (maxDelay);
              VoIPApplication[voipApplication].SetQoSParameters (qos);
            }
          else if (downlink_scheduler_type == GNodeB::DLScheduler_TYPE_MLWDF)
            {
              QoSForM_LWDF *qos = new QoSForM_LWDF ();
              qos->SetMaxDelay (maxDelay);
              VoIPApplication[voipApplication].SetQoSParameters (qos);
            }
```

```
          else
            {
              QoSParameters *qos = new QoSParameters ();
              qos->SetMaxDelay (maxDelay);
              VoIPApplication[voipApplication].SetQoSParameters (qos);
            }


          //create classifier parameters
          ClassifierParameters *cp = new ClassifierParameters (gw->GetIDNetworkNode(),
              ue->GetIDNetworkNode(),
              0,
              destinationPort,
              TransportProtocol::TRANSPORT_PROTOCOL_TYPE_UDP);
          VoIPApplication[voipApplication].SetClassifierParameters (cp);

          cout << "CREATED VOIP APPLICATION, ID " << applicationID << endl;

          //update counter
          destinationPort++;
          applicationID++;
          voipApplication++;
        }


      // *** video application
      for (int j = 0; j < nbVideo; j++)
        {
          // create application
          VideoApplication[videoApplication].SetSource (gw);
          VideoApplication[videoApplication].SetDestination (ue);
          VideoApplication[videoApplication].SetApplicationID (applicationID);
          VideoApplication[videoApplication].SetStartTime(start_time);
```

```
VideoApplication[videoApplication].SetStopTime(duration_time);

          switch (videoBitRate)
            {
            case 128:
              {
VideoApplication[videoApplication].LoadInternalTrace(&foreman_h264_128k);
//VideoApplication[videoApplication].LoadInternalTrace(&highway_h264_128k);
//VideoApplication[videoApplication].LoadInternalTrace(&mobile_h264_128k);
                cout << "  selected video @ 128k"<< endl;
                break;
              }
            case 242:
              {
VideoApplication[videoApplication].LoadInternalTrace(&foreman_h264_242k);
                cout << "  selected video @ 242k"<< endl;
                break;
              }
            case 440:
              {
VideoApplication[videoApplication].LoadInternalTrace(&foreman_h264_440k);
                cout << "  selected video @ 440k"<< endl;
                break;
              }
            default:
              {
                cout << "  Unsupported video bitrate!"<< endl;
                exit(1);
              }
            }
```

```

// create qos parameters
if (downlink_scheduler_type == GNodeB::DLScheduler_TYPE_FLS)
  {
    QoSForFLS *qos = new QoSForFLS ();
    qos->SetMaxDelay (maxDelay);
    if (maxDelay == 0.1)
      {
        cout << "Target Delay = 0.1 s, M = 9" << endl;
        qos->SetNbOfCoefficients (9);
      }
    else if (maxDelay == 0.08)
      {
        cout << "Target Delay = 0.08 s, M = 7" << endl;
        qos->SetNbOfCoefficients (7);
      }
    else if (maxDelay == 0.06)
      {
        cout << "Target Delay = 0.06 s, M = 5" << endl;
        qos->SetNbOfCoefficients (5);
      }
    else if (maxDelay == 0.04)
      {
        cout << "Target Delay = 0.04 s, M = 3" << endl;
        qos->SetNbOfCoefficients (3);
      }
    else
      {
        cout << "ERROR: target delay is not available"<< endl;
        return;
      }

    VideoApplication[videoApplication].SetQoSParameters (qos);
  }
else if (downlink_scheduler_type == GNodeB::DLScheduler_TYPE_EXP)
```

```
            {
              QoSForEXP *qos = new QoSForEXP ();
              qos->SetMaxDelay (maxDelay);
VideoApplication[videoApplication].SetQoSParameters (qos);
            }
          else if (downlink_scheduler_type == GNodeB::DLScheduler_TYPE_MLWDF)
            {
              QoSForM_LWDF *qos = new QoSForM_LWDF ();
              qos->SetMaxDelay (maxDelay);
VideoApplication[videoApplication].SetQoSParameters (qos);
            }
          else
            {
              QoSParameters *qos = new QoSParameters ();
              qos->SetMaxDelay (maxDelay);
VideoApplication[videoApplication].SetQoSParameters (qos);
            }


          //create classifier parameters
          ClassifierParameters *cp = new ClassifierParameters (gw->GetIDNetworkNode(),
              ue->GetIDNetworkNode(),
              0,
              destinationPort,
TransportProtocol::TRANSPORT_PROTOCOL_TYPE_UDP);
VideoApplication[videoApplication].SetClassifierParameters (cp);

          cout << "CREATED VIDEO APPLICATION, ID " << applicationID << endl;

          //update counter
          destinationPort++;
          applicationID++;
          videoApplication++;
        }
```

```

    // *** be application
    for (int j = 0; j < nbBE; j++)
      {
        // create application
        BEApplication[beApplication].SetSource (gw);
        BEApplication[beApplication].SetDestination (ue);
        BEApplication[beApplication].SetApplicationID (applicationID);
        BEApplication[beApplication].SetStartTime(start_time);
        BEApplication[beApplication].SetStopTime(duration_time);


        // create qos parameters
        QoSParameters *qosParameters = new QoSParameters ();
        BEApplication[beApplication].SetQoSParameters (qosParameters);


        //create classifier parameters
        ClassifierParameters *cp = new ClassifierParameters (gw->GetIDNetworkNode(),
            ue->GetIDNetworkNode(),
            0,
            destinationPort,
            TransportProtocol::TRANSPORT_PROTOCOL_TYPE_UDP);
        BEApplication[beApplication].SetClassifierParameters (cp);

        cout << "CREATED BE APPLICATION, ID " << applicationID << endl;

        //update counter
        destinationPort++;
        applicationID++;
        beApplication++;
      }

    // *** cbr application
```

```
      for (int j = 0; j < nbCBR; j++)
        {
          // create application
          CBRApplication[cbrApplication].SetSource (gw);
          CBRApplication[cbrApplication].SetDestination (ue);
          CBRApplication[cbrApplication].SetApplicationID (applicationID);
          CBRApplication[cbrApplication].SetStartTime(start_time);
          CBRApplication[cbrApplication].SetStopTime(duration_time);
          CBRApplication[cbrApplication].SetInterval (0.04);
          CBRApplication[cbrApplication].SetSize (5);

          // create qos parameters
          QoSParameters *qosParameters = new QoSParameters ();
          qosParameters->SetMaxDelay (maxDelay);

          CBRApplication[cbrApplication].SetQoSParameters (qosParameters);


          //create classifier parameters
          ClassifierParameters *cp = new ClassifierParameters (gw->GetIDNetworkNode(),
              ue->GetIDNetworkNode(),
              0,
              destinationPort,
              TransportProtocol::TRANSPORT_PROTOCOL_TYPE_UDP);
          CBRApplication[cbrApplication].SetClassifierParameters (cp);

          cout << "CREATED CBR APPLICATION, ID " << applicationID << endl;

          //update counter
          destinationPort++;
          applicationID++;
          cbrApplication++;
        }

```

```


    }


  simulator->SetStop(duration);
  simulator->Run ();

}

```

```
/* -*- Mode:C++; c-file-style:"gnu"; indent-tabs-mode:nil; -*- */
/*
 * Copyright (c) 2020 TELEMATICS LAB, Politecnico di Bari
 *
 * This file is part of 5G-air-simulator
 *
 * 5G-air-simulator is free software; you can redistribute it and/or modify
 * it under the terms of the GNU General Public License version 3 as
 * published by the Free Software Foundation;
 *
 * 5G-air-simulator is distributed in the hope that it will be useful,
 * but WITHOUT ANY WARRANTY; without even the implied warranty of
 * MERCHANTABILITY or FITNESS FOR A PARTICULAR PURPOSE.  See the
 * GNU General Public License for more details.
 *
 * You should have received a copy of the GNU General Public License
 * along with 5G-air-simulator; if not, see <http://www.gnu.org/licenses/>.
 *
 * Author: Francesco Capozzi <f.capozzi@poliba.it>
 * Updated by: Bahram khan <bahram.khan@lx.it.pt>
 */

#include "henb-phy.h"

HenbPhy::HenbPhy()
{
  SetTxPower(0); //dBm
  //SetTxPower(10); //dBm
 // SetTxPower(20); //dBm
}


HeNodeB*
HenbPhy::GetDevice(void)
{
```

```
  Phy* phy = (Phy*)this;
  return (HeNodeB*)phy->GetDevice();
}

```

```
/* -*- Mode:C++; c-file-style:"gnu"; indent-tabs-mode:nil; -*- */
/*
 * Copyright (c) 2020 TELEMATICS LAB, Politecnico di Bari
 *
 * This file is part of 5G-air-simulator
 *
 * 5G-air-simulator is free software; you can redistribute it and/or modify
 * it under the terms of the GNU General Public License version 3 as
 * published by the Free Software Foundation;
 *
 * 5G-air-simulator is distributed in the hope that it will be useful,
 * but WITHOUT ANY WARRANTY; without even the implied warranty of
 * MERCHANTABILITY or FITNESS FOR A PARTICULAR PURPOSE.  See the
 * GNU General Public License for more details.
 *
 * You should have received a copy of the GNU General Public License
 * along with 5G-air-simulator; if not, see <http://www.gnu.org/licenses/>.
 *
 * Author: Francesco Capozzi <f.capozzi@poliba.it>
 * Updated by: Bahram khan <bahram.khan@lx.it.pt>
 */

#ifndef USERSDISTRIBTION_H_
#define USERSDISTRIBTION_H_

#include "../core/cartesianCoodrdinates/CartesianCoordinates.h"
#include "CellPosition.h"
#include "../componentManagers/NetworkManager.h"

#include <vector>
#include <iostream>

#include <cmath>
#include <random>
```

```cpp
#include <chrono>

static CartesianCoordinates*
GetCartesianCoordinatesFromPolar (double r, double angle)
{
  double x = r * cos (angle);
  double y = r * sin (angle);

  CartesianCoordinates *coordinates = new CartesianCoordinates ();
  coordinates->SetCoordinates(x,y);
  return coordinates;
}

static vector<CartesianCoordinates*>*
GetUniformUsersDistribution (int idCell, int nbUE)
{
    NetworkManager * networkManager = NetworkManager::Init();
        vector<CartesianCoordinates*> *vectorOfCoordinates = new vector<CartesianCoordinates*>;

        Cell *cell = networkManager->GetCellByID(idCell);

        double radii = (cell->GetRadius()*1000)*0.8;

        CartesianCoordinates *cellCoordinates = cell->GetCellCenterPosition();
        double r; double angle;

        for (int i = 0; i < nbUE; i++)
        {
            // Updates in the Simulator to present a near random distribution of users in the eNB doi={10.1109/VTCFall.2018.8690935}
            unsigned seed = std::chrono::system_clock::now().time_since_epoch().count();
            std::mt19937 rng_mt(seed);
            std::uniform_real_distribution<double> dist_double(0.0, 1.0);
            std::uniform_real_distribution<double> theta_double(0.0, 360.0);

            double radius=dist_double(rng_mt);
```

```
            double th=theta_double(rng_mt);

            double angle = 2*M_PI*th/360;
            double r1 = sqrt(radius);
            double r = radii*r1;


            CartesianCoordinates *newCoordinates = GetCartesianCoordinatesFromPolar (r, angle);

            //Compute absoluteCoordinates
            newCoordinates->SetCoordinateX (cellCoordinates->GetCoordinateX () + newCoordinates->GetCoordinateX ());
            newCoordinates->SetCoordinateY (cellCoordinates->GetCoordinateY () + newCoordinates->GetCoordinateY ());

            vectorOfCoordinates->push_back(newCoordinates);
        }

  return vectorOfCoordinates;
}

static vector<CartesianCoordinates*>*
GetUniformUsersDistributionInFemtoCell (int idCell, int nbUE)
{
  NetworkManager * networkManager = NetworkManager::Init();
  vector<CartesianCoordinates*> *vectorOfCoordinates = new vector<CartesianCoordinates*>;

  Femtocell *cell = networkManager->GetFemtoCellByID(idCell);

  double sidehome = cell->GetSide();
  //double side = cell->GetSide();

  CartesianCoordinates *cellCoordinates = cell->GetCellCenterPosition();
  double r;
  double angle;

  for (int i = 0; i < nbUE; i++)
    {
      /*
      r = (double)(rand() %(int)side);
```

```
    angle = (double)(rand() %360) * ((2*M_PI)/360);

     CartesianCoordinates *newCoordinates = GetCartesianCoordinatesFromPolar (r, angle);

     //Compute absoluteCoordinates
     newCoordinates->SetCoordinateX (cellCoordinates->GetCoordinateX () + newCoordinates->GetCoordinateX ());
     newCoordinates->SetCoordinateY (cellCoordinates->GetCoordinateY () + newCoordinates->GetCoordinateY ());

     vectorOfCoordinates->push_back(newCoordinates);

     */


     //r = (double)(rand() %(int)side);
         //angle = (double)(rand() %360) * ((2*3.14)/360);




             unsigned seed = std::chrono::system_clock::now().time_since_epoch().count();
             std::mt19937 rng_mt(seed);
             std::uniform_real_distribution<double> distx_double(0.0, 1);
             std::uniform_real_distribution<double> disty_double(0.0, 1);

             double xa=distx_double(rng_mt);
             double ya=disty_double(rng_mt);

             //double xb = sqrt(xa);
             //double yb = sqrt(ya);

             double x = sidehome*xa-(sidehome/2);
             double y = sidehome*ya-(sidehome/2);

             //double angle = 2*M_PI*th/360;
             //double r1 = sqrt(radius);
             //double r = (sqrt (2*sidehome*sidehome))/2*r1;

```

```
                //CartesianCoordinates *coordinates = new CartesianCoordinates ();
                // coordinates->SetCoordinates(x,y);
                 //return coordinates;

            //CartesianCoordinates *newCoordinates = GetCartesianCoordinatesFromPolar (r, angle);
              CartesianCoordinates *newCoordinates = new CartesianCoordinates ();
              newCoordinates->SetCoordinates(x,y);
            //Compute absoluteCoordinates
            newCoordinates->SetCoordinateX (cellCoordinates->GetCoordinateX () + newCoordinates->GetCoordinateX ());
            newCoordinates->SetCoordinateY (cellCoordinates->GetCoordinateY () + newCoordinates->GetCoordinateY ());

            vectorOfCoordinates->push_back(newCoordinates);



    }

  return vectorOfCoordinates;
}


#endif /* USERSDISTRIBTION_H_ */

```

```
/* -*- Mode:C++; c-file-style:"gnu"; indent-tabs-mode:nil; -*- */
/*
 * Copyright (c) 2020 TELEMATICS LAB, Politecnico di Bari
 *
 * This file is part of 5G-air-simulator
 *
 * 5G-air-simulator is free software; you can redistribute it and/or modify
 * it under the terms of the GNU General Public License version 3 as
 * published by the Free Software Foundation;
 *
 * 5G-air-simulator is distributed in the hope that it will be useful,
 * but WITHOUT ANY WARRANTY; without even the implied warranty of
 * MERCHANTABILITY or FITNESS FOR A PARTICULAR PURPOSE.  See the
 * GNU General Public License for more details.
 *
 * You should have received a copy of the GNU General Public License
 * along with 5G-air-simulator; if not, see <http://www.gnu.org/licenses/>.
 *
 * Author: Francesco Capozzi <f.capozzi@poliba.it>
 * Updated by: Bahram khan <bahram.khan@lx.it.pt>
 */


#ifndef FREQUENCY_REUSE_HELPER_H_
#define FREQUENCY_REUSE_HELPER_H_

#include <stdint.h>
#include "stdlib.h"
#include <math.h>
#include "../core/spectrum/bandwidth-manager.h"
#include "../componentManagers/FrameManager.h"

/*

Number of supported non-overlapping channels in each
```

```
frequency band and bandwidth.

operative band      bandwidth          Channel bandwidth (MHz)
                                       1.4 3   5   10  15  20

1                       60             –   –   12  6   4   3
2                       60             42  20  12  6   [4] [3]
3                       75             53  23  15  7   [5] [3]
...

XXX: now is supported only the 1-th operative sub-band
*/

static vector <BandwidthManager*>
RunFrequencyReuseTechniques(int nodes, int cluster, double bandwidth)
{
  vector <BandwidthManager*> spectrum;

  int operativeSubBands;
  int cluster1[37] = {0,0,0,0,0,0,0,0,0,0,0,0,0,0,0,0,0,0,0,0,0,0,0,0,0,0,0,0,0,0,0,0,0,0,0,0,0};
  int cluster2[37] = {0,1,0,1,0,1,0,1,0,1,0,1,0,1,0,1,0,1,0,1,0,1,0,1,0,1,0,1,0,1,0,1,0,1,0,1,0};
  int cluster3[37] = {0,1,2,1,2,1,2,2,0,1,0,2,0,1,0,2,0,1,0,0,1,2,0,2,1,0,1,2,0,2,1,0,1,2,0,2,1};
  int cluster4[37] = {0,1,2,3,1,2,3,0,3,0,1,0,2,0,3,0,1,0,2,1,2,1,2,3,2,3,1,3,1,2,1,2,3,2,3,1,3};
  int cluster7[37] = {0,1,2,3,4,5,6,5,4,6,5,1,6,2,1,3,2,4,3,6,0,3,1,0,4,2,0,5,3,0,6,4,0,1,5,0,2};
  if (bandwidth == 1.4)
    {
      operativeSubBands = 6;
    }
```

```
  else if (bandwidth == 3)
    {
      operativeSubBands = 15;
    }
  else if (bandwidth == 5)
    {
      operativeSubBands = 25;
    }
  else if (bandwidth == 10)
    {
      operativeSubBands = 50;
    }
  else if (bandwidth == 15)
    {
      operativeSubBands = 75;
    }
  else if (bandwidth == 20)
    {
      operativeSubBands = 100;
    }
  else
    {
      cout << "ERROR: unsupported/invalid bandwidth: " << bandwidth << endl;
    }

  int* cluster_p;
  if (cluster == 1)
    {
      cluster_p = cluster1;
    }
  if (cluster == 2)
    {
      cluster_p = cluster2;
    }
  else if (cluster == 3)
    {
      cluster_p = cluster3;
    }
  else if (cluster == 4)
    {
      cluster_p = cluster4;
    }
```

```
  else if (cluster == 7)
    {
      cluster_p = cluster7;
    }
  else
    {
      cout << "ERROR: unsupported/invalid frequency reuse factor: " << cluster << endl;
    }

  for (int i = 0; i < nodes; i++)
    {
      int offset = cluster_p[i] * operativeSubBands;

      BandwidthManager *s = new BandwidthManager (bandwidth, bandwidth, offset, offset);
      spectrum.push_back (s);
    }

  return spectrum;
}



#endif /* FREQUENCY_REUSE_HELPER_H_ */

```

# Appendix D

# Input To And Out Put From 5G Air Simulator

## D.1 Source Code for Femto-cell Scenario

## D.2 Input to the Simulator

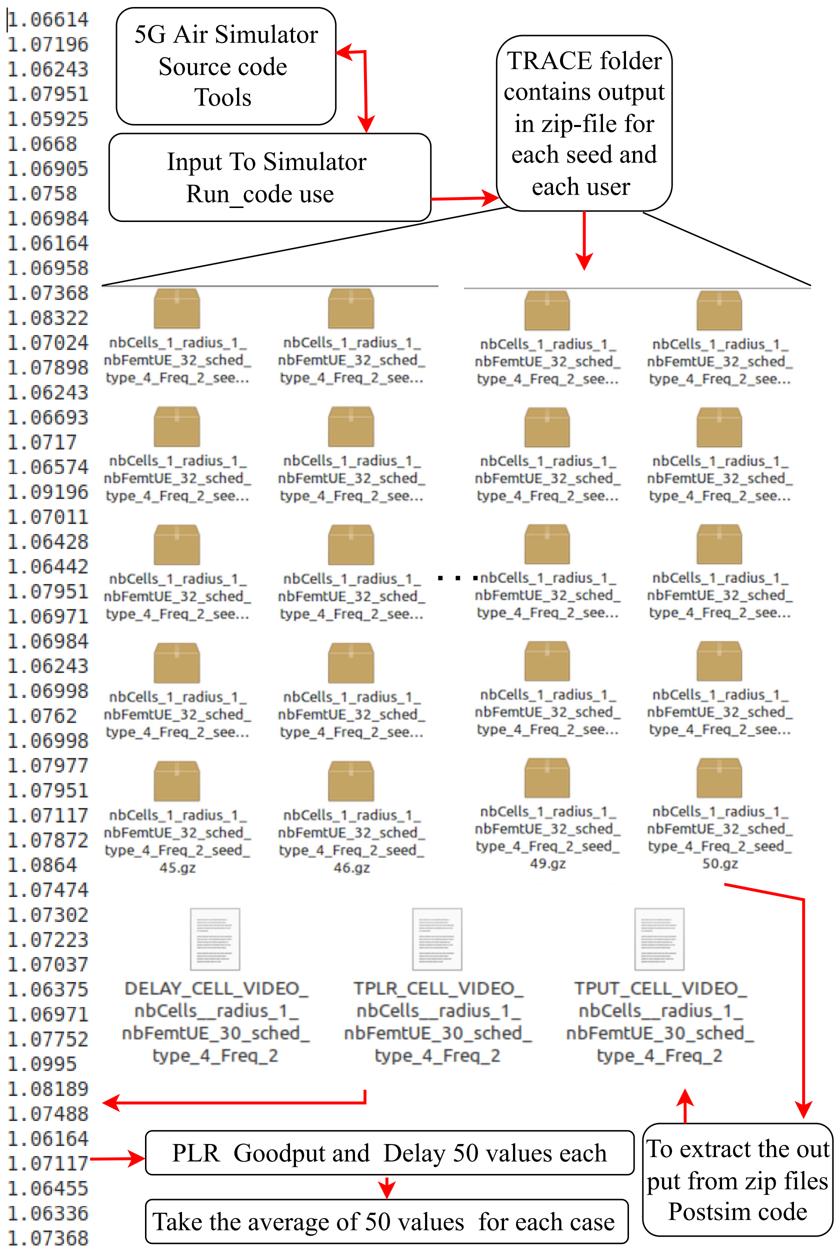


Figure D.1: Simulation approach to obtain the required output (PLR, goodput and delay) for analysis.

### D.2.1 To Set the Parameters To The Simulator

In this part of the code, we set the input to the simulator to obtain our result. When we give the information, the simulation start and run n number of seed. In our case, we consider the following parameters with input seed 50 and we update the following code according to our scenario. It meant that simulations ran for 50 number of seeds for each user. For example, if we take users 30 to 37, the simulator will produce 50 simulations for 30, 31, 32, 33, 34, 35, and 36 in the trace folders.

RUN="./5G-air-simulator" Run the simulator
SCENARIO= SingleCellWithFemto Name of the scenario
nCell= 1 Number of Macro cell
radius= 1 Radius of Macro cell
NbBuildings=1 Numbers of building
BuildingType= 0 Type of building defines how much number of Femto- cell inside the building there is possibligty of 25 and 40
NbUE= 0 Number of users in Macro cell
NbVoIP=0
NbVideo=1
NbBE= 0

Sched: 1-> M-LWDF, 2-> FLS Selected schedulers
Sched= 1 (2)
Frame_struct= 1
Speed= 3
AccessPolicy= 0
MaxDelay= 0.1
VideoBitRate= 440

Freq= 2 GHz
Freq_escrita= 2 GHz To set the folder name with frequency name
seedF= 50 Maximum seed
seedI= 1 Minimum seed
until [ $seedI - gt$seedF ]; do
For nbFemtoUE in 30 31 32 33 34 35 36 37 Number of users
do
Trace= "TRACE/nbCells_{$nCell$}_$radius$_{radius}_nbFemtUE_{$nbFemtoUE$}_$sched_type$

_{sched}_Freq_{$Freq\_escrita$}_$seed$_{seedI}" Name to the folder in the trace

Number of input parameters to the scenario $RUN ${SCENARIO} ${radius} ${nbBuildings}

${buildingType} ${activityRatio} ${nbUE} ${nbFemtoUE} ${nbVoIP}

${nbVideo} ${nbBE} ${nbCBR} ${sched} ${frame_struct} ${speed} ${accessPolicy} ${maxDelay} ${videoBitRate} > ${trace}

gzip $trace To make Zip file in the trace folder
done
seedI= (($seedI + 1)) ++ To the seed
done
./postsim.sh This is calling another code which calculate the average of the traces in the trace folder
echo SIMULATION FINISHED!

### D.2.2 To obtain the output (PLR, Good put and Delay)

With the help of the following code, one can get them out (PLR, Delay and Goodput) from the trace folder. In the trace folder, each user has 50 numbers of the folder (zip files). It is challenging to get the values direct.

RUN="./5G-air-simulator" Run the simulator
SCENARIO= SingleCellWithFemto Name of the scenario
nCell= 1 Number of Macro cell
radius= 1 Radius of Macro cell
NbBuildings=1 Numbers of building
BuildingType= 0 Type of building defines how much number of Femto- cell inside the building there is possibligty of 25 and 40
NbUE= 0 Number of users in Macro cell
NbVoIP=0
NbVideo=1
NbBE= 0

Sched: 1-> M-LWDF, 2-> FLS Selected schedulers
Sched= 1 (2)
Frame_struct= 1
Speed= 3
AccessPolicy= 0
MaxDelay= 0.1
VideoBitRate= 440

wall= 10 its is set to make different folder for different size of wall of the apartment
power= 0 Power of the home cell (Femto pico)

Freq= 2 GHz
Freq_escrita= 2 GHz To set the folder name with frequency name
seedF= 50 Maximum seed
seedI= 1 Minimum seed
until [ $seedI - gt$seedF ]; do
For nbFemtoUE in 30 31 32 33 34 35 36 37 Number of users
do

echo "POST SIM FOR $SCENARIO ${radius} ${nbBuildings} ${buildingType} $

{activityRatio} ${nbUE} ${nbFemtoUE} ${nbVoIP} ${nbVideo} ${nbBE} ${nbCBR} ${sched} ${frame

_struct} ${speed} ${accessPolicy} ${maxDelay} ${videoBitRate} " To get the results with defined parameters

FILE_IN= "TRACE/nbCells_$nCell_radius_${radius}_nbFemtUE_${nbFemtoUE}_type

_${sched}_Freq_${Freq_escrita}_seed_${seedI}"} Defining where is the trace folder

TPUT_CELL_AGGREGATE_VIDEO="OUTPUT/TPUT_CELL_VIDEO_nbCells_${nbCells}

_radius_${radius}_nbFemtUE_${nbFemtoUE}_sched_type_${sched}_Freq_${Freq_escrita}

_power_${power}_wall_${wall}" After calculations the good-put is saving in the OUTPUT folder with the above given name

DELAY_CELL_AGGREGATE_VIDEO="OUTPUT/DELAY_CELL_VIDEO_nbCells_${nbCells}

_radius_${radius}_nbFemtUE_${nbFemtoUE}_sched_type_${sched}_Freq_${Freq_escrita}

_power_${power}_wall_${wall}" After calculations the delay is saving in the OUTPUT folder with the above given name

TPLR_CELL_AGGREGATE_VIDEO="OUTPUT/TPLR_CELL_VIDEO_nbCells_${nbCells}_-

radius_${radius}_nbFemtUE_${nbFemtoUE}_sched_type_${sched}_Freq_${Freq_escrita}

_power_${power}_wall_${wall}" After calculations the PLR is saving in the OUTPUT folder with the above given name if [ -f $FILE_IN.gz ] If the file is zip files then

cd TRACE; unp nbCells_${nCell}_radius_${radius}_nbFemtUE_${nbFemtoUE}

_sched_type_${sched}_Freq_${Freq_escrita}_seed_${seedI}.gz; cd .. To unzip the files and get the directory

n= $(grep -c ”SIMULATOR_DEBUG:” ${FILE_IN})

if [ ”$n” = ”0” ] then

echo ”$FILE_IN” » simulate_again

else

./TOOLS/make_goodput.awk ./${FILE_IN} » $TPUT_CELL_AGGREGATE_VIDEO To use the tools and calculate the goodput

./TOOLS/make_plr.awk ./${FILE_IN} » $TPLR_CELL_AGGREGATE_VIDEO To use the tools and calculate the PLR

awk /RX/{arr[$2]+=$14; count[$2]++} END{for (x in arr)print arr[x]/count[x]} ./${FILE_-IN} »$DELAY_CELL_AGGREGATE_VIDEO To use the tools and calculate the delay

fi

rm ${FILE_IN}

```
fi

done

seedI=$(($seedI+1))

done

echo SIMULATION FINISHED!
```